

Development of Novel Dosage Forms to Repurpose the Drugs for Alzheimer's disease

A thesis

Submitted in total fulfilment of the requirements of the degree of

Doctor of Philosophy

Ankitkumar Yogeshbhai Parikh

B.Pharm, M.Pharm (Pharmaceutics)

Neuroregeneration Laboratory

Centre for Pharmaceutical Innovation and Development (CPID)

School of Pharmacy and Medical Sciences

Division of Health Sciences

University of South Australia

April 2017

Table of content

List of Figures ix
List of Tables xiv
List of Abbreviations xvi
Thesis Summary xx
Thesis Outline xxii
Declaration by Author xxiii
Acknowledgements xxiv
Publications xxv
Authorship Statement xxviii
1. Introduction 1
1.1 21st century and neurodegenerative disease 2
1.2 Dementia 3
1.3 Alzheimer's disease 3
1.3.1 Symptoms of AD 3
1.3.2 Journey of >100 years 4
1.3.3 Alzheimer's disease Statistic 5
1.3.3.1 Global Impact 5
1.3.3.2 Australian Statistics 5
1.3.4 Key mechanisms involved in Alzheimer's disease 6
1.3.4.1 Amyloid beta based mechanism 6
1.3.4.2 Tau-based Mechanism 7
1.3.4.3 Oxidative stress (OS) 8
1.3.4.4 Inflammation 9
1.3.4.5 Calcium homeostasis perturbation 9
1.3.4.6 Neurotransmission related mechanisms 10
1.3.4.7 Other Mechanisms 11
1.3.5 Current Standard of Care 12
1.3.6 Current research scenario for Alzheimer disease 14
1.4 Need of novel therapeutic option for AD 15
1.5 Edaravone (EDR) 16
1.5.1 Introduction of EDR 16
1.5.2 Mechanisms of Action 17

1.5.3 Marketed formulations 18
1.5.4 Therapeutic potential of EDR 19
1.5.5 EDR – As an Anti-Alzheimer Drug 23
1.5.6 Safety and toxicity studies in Animal and Human 25
1.5.6.1 Animals 25
1.5.6.2 Human 26
1.5.7 Problems associated with drug development 27
1.6 Curcumin (CUR) 27
1.6.1 Introduction for CUR 27
1.6.2 Chemistry of CUR 28
1.6.3 Therapeutic efficacy 28
1.6.4 CUR for Alzheimer disease 29
1.6.4.1 Inhibition of Aβ aggregation 29
1.6.4.2 Inhibition of BACE1 30
1.6.4.3 Inhibition of anticholinesterase (AChE) activity 30
1.6.4.4 Anti-oxidative properties 30
1.6.4.5 Inhibition of inflammation 30
1.6.5 Safety 31
1.6.6 Problems associated with drug development 31
1.6.6.1 Solubility 32
1.6.6.2 Stability 33
1.6.6.3 Metabolism 33
1.6.6.4 Bioavailability 33
1.6.7 Marketed CUR products 35
1.7 Need of development of novel formulations for EDR and CUR 36
1.7.1 Pre-formulation 37
1.7.2 Formulation strategies 41
1.7.2.1 Co-solvent based formulation 42
1.7.2.2 Lipid-based formulation 42
1.7.2.3 Solid dispersion (SD) based formulation 45
1.8 Hypothesis, aim, and significance 46
1.8.1 Rationale and Hypothesis 46
1.8.2 Aim and Objective 47
1.8.2.1 EDR drug 47
1.8.2.2 CUR Drug 47

1.8.3 Outcome and significance 48
2. Development of a Novel Oral Delivery System of Edaravone for Enhancing Bioavailability 49
3. Novel Lipid-based Nanosystem of Edaravone: Development, Optimization, Characterization, and In-vitro/In-vivo Evaluation 62
3.1 Abstract 63
3.2 Introduction 64
3.3 Materials and Methods 66
3.3.1 Materials 66
3.3.2 Formulation development of L-NLNS formulation 67
3.3.2.1 Selection of oil 67
3.3.2.2 Selection of surfactant 67
3.3.2.3 Selection of co-surfactant 68
3.3.2.4 Construction of ternary phase diagrams 68
3.3.2.5 In-vitro characterization of L-NLNS 69
3.3.3 Formulation development of solid NLNS (S-NLNS) formulation 70
3.3.3.1 Preparation of S-NLNS 70
3.3.3.2 Optimization of concentration of solid carriers 71
3.3.3.3 In-vitro characterization of S-NLNS formulation 71
3.3.4 In-vitro release test 72
3.3.5 Pharmacokinetic study 73
3.3.6 Statistical analysis 73
3.4 Results and discussion 73
3.4.1 Formulation development of L-NLNS 73
3.4.1.1 Selection of oil 73
3.4.1.2 Selection of surfactant 76
3.4.1.3 Selection of co-surfactant 79
3.4.1.4 Construction of ternary phase diagrams 80
3.4.1.5 In-vitro characterization of L-NLNS formulation 82
3.4.2 Formulation development and characterization of S-NLNS Formulation 85
3.4.2.1 Selection and optimization of concentration of solid carriers 85
3.4.2.2 In-vitro characterization of S-NLNS formulation 86
3.4.3 In-vitro release test 89
3.4.4 Pharmacokinetic study 91
3.5 Conclusions 93

4. Novel Edaravone Formulation Based on Self Nanomicelization Solid Dispersion Strategy for Enhancement of Oral Bioavailability and Reversal of Cognitive Deficits in Alzheimer's Disease Models. 97
4.1 Abstract 98
4.2 Introduction 99
4.3 Materials & Method 101
4.3.1 Materials 101
4.3.2 Formulation, Development, and optimization of NEF 102
4.3.2.1 Selection of a suitable carrier for the development of NEF 102
4.3.2.2 Preparation of SNMSD using solvent evaporation technique (SE) 102
4.3.2.3 Kinetic Solubility Study 102
4.3.2.4 Characterization of NEF 103
4.3.3 Investigating drug-polymer interaction with advance characterisation 103
4.3.3.1 Differential Scanning Calorimetry (DSC) 103
4.3.3.2 X-ray diffraction (XRD) study 103
4.3.3.3 Scanning electron microscopy (SEM) 103
4.3.3.4 Fourier transform infrared spectroscopy (FTIR) 104
4.3.3.5 ^{1}H NMR Study 104
4.3.4 Assessment of self-nanomicellising properties of NEF 104
4.3.4.1 Preparation of EDR loaded micelles solution of NEF 104
4.3.4.2 Characterization of EDR loaded micelles 104
4.3.4.3 Stability Study 104
4.3.5 Physical stability study of NEF as per ICH guideline 105
4.3.6 In-vitro permeation and metabolism study of NEF 105
4.3.7 Dissolution Study 105
4.3.8 Pharmacokinetic Study 106
4.3.9 Behaviour Tests 106
4.3.9.1 Suitability of drinking water to supply NEF 106
4.3.9.2 Animals 106
4.3.9.3 Measurement of water and food consumption 108
4.3.9.4 Open field test 108
4.3.9.5 NORT 108
4.3.9.6 Y-Maze test 109
4.3.9.7 MWM test 109
4.3.10 Long term toxicity assessment of NEF 110

4.3.10.1 Body weight....110
4.3.10.2 Water and food consumption....110
4.3.10.3 General behavior and mortality....110
4.3.10.4 Haematological Parameters....110
4.3.10.5 Coagulation Parameters....110
4.3.10.6 Serum Biochemistry....111
4.3.10.7 Organ weight....111
4.3.10.8 Histopathology....111
4.3.11 Statistical Analysis....111
4.4 Results and Discussion....112
4.4.1 Formulation, Development, and Optimisation of NEF....112
4.4.1.1 Selection of suitable carrier for the development of NEF....112
4.4.1.2 Kinetic Solubility....113
4.4.1.3 Characterisation of NEF....114
4.4.2 Investigating drug-polymer interaction with advanced characterisation....114
4.4.2.1 DSC study....114
4.4.2.2 XRD study....116
4.4.2.3 SEM Study....116
4.4.2.4 FTIR and ^{1}HNMR study....116
4.4.3 Assessment of self-nanomicellising properties of NEF....117
4.4.4 Stability study of NEF as per ICH guideline....118
4.4.5 In-vitro metabolism and permeation study....118
4.4.6 In-vitro drug dissolution....119
4.4.7 Pharmacokinetic study....121
4.4.8 Behaviour tests....122
4.4.8.1 Open field test....123
4.4.8.2 NORT....125
4.4.8.3 Y-maze test....126
4.4.8.4 MWM Test....127
4.4.9 Assessment of long-term repeated dose toxicity....130
4.4.9.1 Haematological parameter....132
4.4.9.2 Coagulation parameters....133
4.4.9.3 Blood electrolyte parameters....133
4.4.9.4 Biochemical parameters....134
4.4.9.5 Organ weight....135

4.4.9.6 Histopathology.....135
4.5 Conclusions.....136
5. Novel Self Nanomicellizing Solid Dispersion Curcumin Formulation for Oral Administration: Development, Optimization, and Assessment in Alzheimer's Disease Models 141
5.1 Abstract.....142
5.2 Introduction.....143
5.3 Materials and Methods.....146
5.3.1 Materials.....146
5.3.2 Analytical methods for CUR.....147
5.3.2.1 High-Performance liquid chromatography (HPLC) method.....147
5.3.2.2 Liquid chromatography-tandem mass spectrometry (LC/MS/MS) method 147
5.3.3 Selection of a suitable carrier for the development of NCF.....147
5.3.3.1 Solubility parameter (SP) analysis.....147
5.3.3.2 Miscibility study.....148
5.3.3.3 Kinetic Solubility.....148
5.3.3.4 Chemical Stability Study.....148
5.3.4 Formulation development and optimization of NCF.....149
5.3.4.1 Method of Preparation.....149
5.3.4.2 Concentration of Polymer.....149
5.3.5 Characterization of NCF.....149
5.3.5.1 Loading ability and efficiency.....149
5.3.5.2 Comparison of solubility of physical mixture (PM) and NCF in simulated body fluids 149
5.3.5.3 Determination of interaction between SOL and CUR in NCF.....149
5.3.6 Preparation and Characterization of self-micellizing properties of NCF.....151
5.3.6.1 Preparation of CUR loaded micellar solution using NCF.....151
5.3.6.2 Determination of particle size, poly-dispersity index (PDI) and Zeta potential 151
5.3.6.3 TEM analysis.....151
5.3.6.4 Analysis of photo physical properties.....151
5.3.6.5 Stability Study.....151
5.3.7 Stability study of NCF as per ICH guideline.....152
5.3.8 In-vitro release study.....152
5.3.9 Improvement in permeability.....152

5.3.10 Pharmacokinetic study 152
5.3.10.1 Animals 152
5.3.10.2 Dosing and sampling 152
5.3.10.3 Sample preparation 153
5.3.10.4 Pharmacokinetic Parameters 153
5.3.11 Behavioral tests with mouse models of Alzheimer disease 153
5.3.11.1 Animals 153
5.3.11.2 Stability of NCF in drinking water supplied to animals 153
5.3.11.3 Average water and food consumption 154
5.3.11.4 Experimental design 154
5.3.11.5 Open field test 155
5.3.11.6 NORT 155
5.3.11.7 Y-Maze test 155
5.3.11.8 Morris water maze test 156
5.3.12 Assessment of long-term repeated dose toxicity 156
5.3.12.1 Body Weight 156
5.3.12.2 Water and food consumption 156
5.3.12.3 General behavior and mortality 156
5.3.12.4 Haematological parameters 157
5.3.12.5 Coagulation parameters 157
5.3.12.6 Serum biochemistry 157
5.3.12.7 Organs weight 158
5.3.12.8 Histopathology 158
5.3.13 Statistical analysis 158
5.4 Results and Discussion 158
5.4.1 Selection of suitable carrier for the development of NCF 158
5.4.1.1 Solubility parameter (SP) analysis 159
5.4.1.2 Miscibility Study 159
5.4.1.3 Kinetic solubility 160
5.4.1.4 Chemical stability study 162
5.4.2 Formulation development and optimization of NCF 163
5.4.2.1 Method of preparation 163
5.4.2.2 Concentration of polymer 163
5.4.3 Characterization of NCF 164
5.4.3.1 Loading ability and efficiency 164

5.4.3.2 Comparison of Solubility of PM and NCF in simulated body fluids 164
5.4.3.3 Determination of interaction between SOL and CUR in NCF 164
5.4.4 Characterization of self-micellizing properties of NCF 167
5.4.5 Stability study of NCF as per ICH guideline 169
5.4.6 In-vitro release test 169
5.4.7 Improvement in permeability 170
5.4.8 Pharmacokinetic study 170
5.4.9 Behavioral tests with AD mice model 172
5.4.9.1 Open field test 173
5.4.9.2 NORT 174
5.4.9.3 Y-maze test 176
5.4.9.4 MWM test 177
5.4.10 Assessment of long-term repeated dose toxicity 179
5.5 Conclusions 184
6. Summary and Future Directions 192
6.1 Summary 193
6.1.1 Novel Oral Delivery System (NODS) of EDR (Chapter 2) 194
6.1.2 NLNS of EDR (Chapter 3) 194
6.1.3 NEF (Chapter 4) 195
6.1.4 NCF (Chapter 5) 196
6.2 Future Directions 196
6.2.1 Mechanism study 197
6.2.1.1 Do NEF and NCF reduce the amyloid burden in the brain and blood of AD mice? 197
6.2.1.2 Do NEF and NCF reduce the activation of inflammation in the brain of AD mice? 197
6.2.1.3 Do NEF and NCF reduce Tau phosphorylation and neurofibrillary tangles? 197
6.2.1.4 Do NEF and NCF inhibit expression of BACE1 and presenilin in vivo? 198
6.2.2 Clinical Studies 198
6.2.2.1 Phase I 198
6.2.2.2 Phase II: 198
7. References 200

List of Figures

Figure 1.1 Medical research in 21st century....2
Figure 1.2 Various key mechanisms involved in pathogenesis of AD [19, 22] 6
Figure 1.3 Oxidative stress and Alzheimer disease [29]....8
Figure 1.4 Inflammation and Alzheimer disease [44] 9
Figure 1.5 AGE/RAGE signaling Cascade and Alzheimer disease [47]....10
Figure 1.6 Various establish and ongoing research efforts as therapeutic strategies for Alzheimer disease [19] 15
Figure 1.7 EDR (3-methyl-1-phenyl-2-pyrazolin-5-one, left) and its two tautomers; 3-hydroxypyrozole isoform (center) and 1, 2-dihydro-pyrazol-3-one (right). Molecular Formula $C_{10}H_{10}N_2O$ and Molecular Weight174.1992 g/mol [80, 90]....17
Figure 1.8 Hypothetical mechanism of EDR as radical scavenger [87] 18
Figure 1.9 Schematic diagram depicting how EDR acts to break the vicious cycles which propagate the pathogenesis of Alzheimer's' disease driven by Amyloid beta (Aβ). EDR reduces oxidative stress (OS) by scavenging reactive oxygen species (ROS) induced by Aβ and inflammation. EDR can directly interact with Aβ and reduces its fibrillization and aggregation; EDR can reduce the expression of BACE1 expression and reduce Abeta production; EDR can inhibit phosphorylation of GSK3beta and Tau and can block tauopathy. 24
Figure 1.10 Curcuminoid's (Diferuloylmethane, desmethoxycurcumin, bisdemethoxycurcumin) therapeutic effects on different body systems associated diseases [227]. 29
Figure 1.11 Problems associated with the use of CUR including poor solubility, poor stability at physiological, alkaline condition or in the presence of light, extensive metabolism and poor bioavailability. CUR has β-diketone chain, displays a keto-enol tautomerism. Trans-6-(40-hydroxy-30-methoxyphenyl)-2, 4-dioxo-5-hexenal, ferulic aldehyde, ferulic acid, feruloyl methane, and vanillin are the major degradants of CUR [253, 254]. 32
Figure 1.12 Different approaches utilized to improve curcumin physicochemical properties and pharmacokinetics 34
Figure 3.1 Inhibitory effect of various surfactants on glucuronidation of EDR in a microsomal incubation assay (mean ± S.D., n = 3). ***P <0.001 and ****P <0.0001 for LBS: CR40: T1000 (1:0.8:0.2) compared to others. One-way ANOVA and Sidak's multiple comparisons test Data for Borneol and LBS were adopted from the earlier report. LBS: Labrasol®, T1000: D -α-Tocopherol polyethylene glycol 1000 succinate, CR40: Cremophor® RH 40. 78

Figure 3.2 Construction of ternary phase diagram with the system of CapryolTM PGMC as oil, Cremophor® RH 40: Labrasol®: TPGS 1000 (1:0.8:0.2) as a surfactant and Transcutol® P as a co-surfactant explored self-emulsifying region (A), obtained self-emulsifying region.....82
Figure 3.3 The effect of formulation ingredients of L-NLNS on permeability and metabolism of EDR during transportation across everted sacs of rat small intestine. The amount in percentage of EDR (A) and (B) on serosal side of everted sac at various time interval, molar ratio between EDR-G and EDR (C), and transfer rate of EDR in the serosal side of rat everted gut sacs (D) (mean ± S.D., n = 3). *P <0.05, **P<0.01, ***P<0.001 and ****P <0.0001. One-way ANOVA and Sidak's multiple comparisons test. Data for EDR suspension and Borneol were adopted from the earlier report.....85
Figure 3.4 Overlay of the DSC patterns (A), and PXRD patterns (B) of EDR, Aerosil® 200, a Physical mixture of EDR and Aerosil® 200 and S-NLNS. SEM images (C) of EDR, Aerosil® 200 and S-NLNS. TEM image (D) of microemulsion formed after dilution of S-NLNS in water. Data of DSC, PXRD, and SEM for EDR were adopted from the earlier report. EDR: Edaravone and A: Aerosil 200.....88
Figure 3.5 *In-vitro* release profile of EDR suspension, L-NLNS, and S-NLNS in various dissolution media SGF (A) and SIF (B) (mean ± S.D., n = 3).....90
Figure 3.6 Plasma concentration-time curves for the EDR suspension, L-NLNS and S-NLNS (30 mg/kg) in SD rats after oral administrations (mean ± S.D., n = 6). Data for EDR suspension was adopted from the earlier report.....92
Figure 4.1 Formulation development and optimization of NEF. Miscibility study of EDR with various polymers (A), Optimisation of EDR to SOL ratio for the development of NEF (B) and solubility assessment of EDR, PM and NEF in SGF (pH 1.2) and SIF (pH 6.8 and 7.4) (C) (mean ± S.D., n = 3).....113
Figure 4.2 Advanced characterisation of SOL-based NEF. DSC thermographs (A) and X-ray diffractograms (B) of EDR, SOL, PM and NEF, SEM photomicrographs of EDR (C), SOL (D) and NEF (E), FTIR spectra of EDR (F), SOL (G), PM (H) and NEF (I), ^{1}H NMR spectra of EDR (J) and NEF (K), TEM image of micellar solution of NEF (L), and stability assessment of NEF as per ICH guideline (M) (mean ± S.D., n = 3). DSC, XRD and SEM data of EDR were adopted from the earlier report [342]. The results of DSC, XRD, SEM and FTIR of SOL were used as a control for other projects.....115
Figure 4.3 The role of SOL on permeability and metabolism of EDR. Inhibitory effect of SOL (1%) on EDR glucuronidation in a microsomal incubation assay (A), the amount in percentage of EDR (B) and (C) on serosal side at predetermined time interval, molar ratio between EDR-

G and EDR (D), and transfer rate of EDR in the serosal side (E) (mean ± S.D., n = 3). *P <0.05, **P<0.01 and ***P<0.001. One-way ANOVA and Tukey's test or Unpaired t-test (two-tailed). The data of free EDR and Borneol were adopted from the earlier report [342].....119
Figure 4.4 *In-vitro* dissolution study of EDR and NEF in SGF and SIF(A), and plasma profile verses time curve for the EDR suspension and NEF (LD, MD, and HD) in SD rats after oral administrations (B) (mean ± S.D., n = 6). The pharmacokinetic data of EDR suspension was adopted from the earlier report [342].....120
Figure 4.5 Results of the open field test. Total distance traveled (A), number of rearing (B), Time spent in central zone (C), number of grooming (D), number of urination (E) and number of defecation (F). *P < 0.05, **P < 0.01, ***P < 0.001, and ****P < 0.0001 (One-way ANOVA, Tukey' s test) (mean ± SEM).....125
Figure 4.6 The results of NORT. Recognition index in the phase of familiarization (A) and the test phase (B), discrimination index in the test phase (C). ****P < 0.0001 (one-way ANOVA, Tukey's test) (mean ± SEM).....126
Figure 4.7 The behavioral performances of Tg mice in Y-maze test. % Alternation (A) and numbers of entries in each arm (B) and the spontaneous alternation test, % of total entry in novel arm compared to other arms (C), total number of entry to the novel arm (D) and time (%) (E) in the novel arm test. *P < 0.05, **P < 0.01, ***P < 0.001, and ****P < 0.0001 (one-way ANOVA, Tukey's test) (mean ± SEM) 127
Figure 4.8 The performances of Tg mice in MWM test. Path length (cm) to the platform (A), swim speed (cm/s) during platform trials and probe test (B), escape latency (s) during platform trials and distance travelled on each day of training (C), Number of annulus crossings in probe trial (D), Comparison of time spent in target zone (Q3) (First bar) where platform was located compared to average of all other zones (o.a.) (Second bar) (E). *P < 0.05 and **P < 0.01 (two-way or one-way ANOVA, Tukey's test) (mean ± SEM).....129
Figure 4.9 Photomicrographs of the sections of the tissues of Tg mice 136
Figure 5.1 Selection of suitable carrier for formulation development and optimization of NCF. Miscibility study of CUR within different polymers (A), chemical stability of CUR in blank buffers (B), buffers containing PVP K30 (C) and 10% (w/v) SOL (D), Solubility of SDs prepared by MM and SE techniques (E), with various CUR and SOL ratios (F), and with optimised ratio compared to PM (G) in SGF (pH 1.2), SIF (pH 6.8 and 7.4) (mean ± S.D., n = 3). 160
Figure 5.2 *In-vitro* characterization of NCF. DSC thermographs (A) and X-ray diffractograms (B) of CUR, SOL, PM and NCF, SEM photomicrographs of CUR (C), SOL (D) and NCF (E),

FTIR spectra of CUR (F), SOL (G), PM (H) and NCF (I), ^{1}H NMR spectra of CUR (J) and NCF (K), Mean particle size of micellar solution of NCF measured by particle size analyzer (L), Transmission electron micrograph images of micellar solution of NCF, (M) UV absorbance spectra of crude CUR (N) and NCF (O). 165
Figure 5.3 Stability profile of NCF at pH dependent stability study (A) and thermal stability as per ICH guideline (B) (mean ± S.D., n = 3), dissolution profiles of crude CUR and NCF in SGF (1.2 pH) and SIF (6.8 pH) (mean ± S.D., n = 3) (C), cumulative absorption of crude CUR and NCF during transportation across everted sacs of rat small intestine (mean ± S.D., n = 3) (D), CUR plasma concentrations upon oral administration of CUR suspension (150 µg/g), PM (47 µg/g) and NCF (47 µg/g) (mean ± S.D., n = 6) (E).....168
Figure 5.4 NCF improves the behavioral performances of APPSwe/PS1deE9 mice in open filed test. Total distance traveled (A), number of rearing (B), Time spent in central zone (C), number of grooming (D), number of urination (E) and number of defecation (F). *P < 0.05, **P < 0.01, ***P < 0.001, and ****P < 0.0001 (One-way ANOVA, Tukey's test) (mean ± SEM).....174
Figure 5.5 NCF improves the behavioral performances of APPSwe/PS1deE9 mice in NORT. The recognition index was calculated as the ratio of time spent exploring to the one object over the total time spent for exploring both objects. The discrimination index was based on the equation [DI = (T_N – T_F)/ (T_N + T_F)] where time spent to explore the novel object (T_N) and familiar object (T_F) [438]. Recognition index in the phase of familiarization (A) and the test phase (B), discrimination index in the test phase (C). ***P < 0.001 and ****P < 0.0001 (one-way ANOVA, Tukey's test) (mean ± SEM).....175
Figure 5.6 NCF improves the behavioral performances of APPSwe/PS1deE9 mice in Y-maze test. % Alternation (A) and numbers of entries in each arm (B) and in the spontaneous alternation test, % of total entry in novel arm compared to other arms (C), time (%) (D) and total number of entry to the novel arm (E) in the novel arm test. *P < 0.05, **P < 0.01, ***P < 0.001, and ****P < 0.0001 (one-way ANOVA, Tukey's test) (mean ± SEM). 177
Figure 5.7 NCF improves the behavioral performances of APPSwe/PS1deE9 mice in MWM test. Path length (cm) to the platform on the first day's trial were analysed (A), swim speed (cm/s) calculated by the equation velocity = distance/time during platform trials and probe test (B), escape latency (s) during platform trials and distance travelled on the each day of training (C), Number of crossings over the annulus of the platform in probe trial (D), Comparison of time spent in target zone (Q3) where platform was located compared to average of all other zones (o.a.) (E). *P < 0.05, **P < 0.01, and ***P < 0.001 (two-way or one-way ANOVA, Tukey's test) (mean ± SEM).....178

Figure 5.8 Qualitative histopathological evaluation and micrographs of tissues of APPSwe/PS1deE9 mice.....182
Figure 6.1 A flow chart of the design and trial outlines. 199

Note: Figures contained within published papers are not included in the above list.

List of Tables

Table 1.1 Currently approved drugs for Alzheimer's disease [12].....13
Table 1.2 Available Marketed Formulations 19
Table 1.3 Application of EDR in various diseases 20
Table 1.4 Current CUR products in the market. 35
Table 1.5 Various Preformulation study parameters with their importance in development of unique dosage form for any drug [283] 38
Table 1.6 Market formulations based on SMEDDS strategy [291].....44
Table 1.7 Marketed formulations based on Solid dispersion based strategy [315] 46
Table 3.1 Solubility of EDR in selected ingredients (mean ± S.D., n = 3).....74
Table 3.2 Assessment of emulsification ability of surfactants and co-surfactants (mean ± S.D., n = 3).....78
Table 3.3 Evaluation of the self-emulsifying ability of L-NLNS and S-NLNS in different dilution mediums (mean ± S.D., n = 3).....84
Table 3.4 Optimisation of Aerosil® 200 concentration for S-NLNS based on flow properties (mean ± S.D., n = 3).....86
Table 3.5 Results of release kinetics according to various kinetic models including First order, Zero order, Hixson–Crowell, Higuchi-matrix, and Korsmeyer–Peppas 90
Table 3.6 Pharmacokinetic parameters obtained by Phoenix WinNonlin software (mean ± S.D., n = 6). Unpaired Student's t-test for two groups. Data for EDR suspension was adopted from the earlier report 92
Table 4.1 Experimental design for behavioral tests with mouse models of Alzheimer disease 107
Table 4.2 Results of release kinetics of EDR and NEF in SGF and SIF, respectively.....120
Table 4.3 Pharmacokinetic parameters of EDR suspension and NEF with LD, MD, and HD obtained by Phoenix WinNonlin software (mean ± S.D., n = 6) 122
Table 4.4 Measurement of food and water consumption and body weight of Tg mice (mean ± S.D. n = 5).....131
Table 4.5 Analysis of Haematological and Coagulation parameters of Tg mice (mean ± S.D., n = 5).....132
Table 4.6 Analysis of biochemical parameters of Tg mice (mean ± S.D., n = 5).....133
Table 4.7 Analysis of organ weighs of Tg mice (mean ± S.D., n = 5) 135
Table 5.1 Kinetic solubility parameters of CUR and SDs (mean ± S.D., n = 3) 161

Table 5.2 The rate constant and half-lives of CUR in blank buffers of pH 1.2, 6.8 and 7.4, buffers with 10% (w/v) PVP K30 and 10% (w/v) SOL (mean ± S.D., n = 3).....162
Table 5.3 Results of release kinetics of crude CUR and NCF in SGF (pH 1.2) and SIF (pH 6.8) according to various kinetic models including First order, Zero order, Hixson–Crowell, Higuchi-matrix, and Korsmeyer–Peppas 170
Table 5.4 Pharmacokinetic parameters of CUR suspension, PM and NCF obtained by Phoenix WinNonlin software Unpaired Student's t-test for two groups, (mean ± S.D., n = 6) 171
Table 5.5 Measurement of food and water consumption and body weight of APPSwe/PS1deE9 mice (mean ± S.D.) 180
Table 5.6 Haematological and Coagulation parameters of APPSwe/PS1deE9 mice after various treatment of 3 months (mean ± S.D., n = 5).....181
Table 5.7 Biochemical parameters of APPSwe/PS1deE9 mice after various treatment of 3 months (mean ± S.D., n = 5).....182
Table 5.8 Organ weights of APPSwe/PS1deE9 mice after various treatment of 3 months (mean ± S.D., n = 5).....183

Note: Tables contained within published papers are not included in the above list.

List of Abbreviations

Acronym	Full form
ALS	amyotrophic lateral sclerosis
APP	Amyloid Precursor Protein
AChEIs	Acetylcholinesterase inhibitors
AIS	Acute ischemic stroke
AR	Angle of repose
ANOVA	Analysis of variance
API	Active Pharmaceutical Ingredient
APTT	Activated partial thromboplastin time
ALT	Alanine aminotransferase
AST	Aspartate aminotransferase
ALP	Alkaline phosphatase
AβPP	Amyloid beta protein precursor
BA	Bioavailability
BCS	Biopharmaceutics classification system
COX	Cytochrome C oxidase
CUR	Curcumin
CA	Cerebral aneurysms
CYP450	Cytochrome P450
CMC	Critical micelle concentration
DMSO	Dimethyl Sulphoxide
DSC	Differential scanning calorimetry
DNP	Donepezil
%DL	% Drug loading
ER	endoplasmic reticulum
%EE	% Entrapment efficiency
Egr1	Early growth response 1
FTD	Front-temporal dementia
FTIR	Fourier transform infrared spectroscopy
GIT	Gastrointestinal Tract

GRAS	Generally recognised as safe
GGT	Gamma-glutamyl transferase
HD	Huntington disease
HNE	4-hydroxynonenal
HCY	homocysteine
HR	Hausner's ratio
H	Hour
HSP	Hanson solubility parameter
HGB	Haemoglobin
HCT	Hematocrit
5HT	5-hydroxytriptamine
HPβCD	Hydroxyl propyl beta cyclodextrin
ICH	International Conference on Harmonisation
IBD	Inflammatory Bowel Disease
IM	Intestinal metaplasia
IND	Investigational New Drug Application
JMHW	Japanese Ministry of Health & welfare
LH	Luteinizing hormone
L-NLNS	Liquid NLNS
LBD	Lewy body dementia
MAM	Mitochondria-associated ER membranes
mg	Milligram
min	Minute
mL	Millilitre
MTT	3-(4,5 – dimethyl -2-thiozolyl)-2,5-diphenyltetrazolium bromide
MM	Melt mixing
MWM	Morrison water maze test
MCV	Mean corpuscular volume
MCH	Mean corpuscular hemoglobin
MCHC	Mean corpuscular haemoglobin concentration
MPV	Mean platelet volume

NO	Nitric oxide
NMR	Nuclear magnetic resonance
NCF	Novel curcumin formulation
NMDAR	NMDA-receptor antagonist
NF-κB	nuclear factor-kappa B
NTP	National Toxicology Program
NLNS	Novel Lipid-based Nanosystem
NMP	N-methyl-2-pyrrolidone
NEF	Novel Edaravone formulation
NORT	Novel objective recognition test
nm	Nanometer
OS	Oxidative stress
PP2A	Phosphatase 2A
PBS	Phosphate buffer Saline
PEG	Polyethylene Glycol
Pgp	P-glycoprotein
PD	Pharmacodynamics
PK	Pharmacokinetic
PTFE	Polytetrafluoro Ethylene
PVDF	Polyvinylidene difluoride
PDI	Polydispersity index
PLT	Platelet
PCT	Platelet haematocrit
PDW	Platelet distribution width
PT	Prothrombin time
PS1	presenilin-1
PS2	presenilin-2
ROS	Reactive oxygen species
RT	Room Temperature
RBC	Red blood cells
RPM	Rotation per minute

RA	Rheumatoid Arthritis
SEDDS	Self-Emulsifying drug delivery system
SMEDDS	Self-Emulsifying / Micro emulsifying drug delivery systems
SNMSD	Self-nanomicellizing solid dispersion
S-NLNS	Solid NLNS
SD	Standard deviation
SEM	Standard error
SP	Solubility Parameter
SEM	Scanning Electron Microscopy
SMSD	Self-micellizing solid dispersion
SD	Solid dispersion
SOL	Soluplus
SBF	Simulated biological fluid
SIF	Simulated intestinal fluid
SGF	Simulated gastric fluid
SE	Solvent evaporation
TgAD	transgenic AD
TEM	Transmission Electron Microscopy
Tg	Glass Transition Temperature
UGT	uridine 5′-diphospho-glucuronosyl-transferase
US-FDA	United States Food and Drug Administration
USP NF	United State Pharmacopoeia National Formulary
UV	Ultra Violet
VCM	Vancomycin Hydrochloride
VD	Vascular dementia
w/w	Weight by weight
w/v	Weight by volume
WBC	White blood cells
XRD	X-ray Diffraction

Note: Abbreviations contained within published papers are not included in the above list.

Thesis Summary

Developing a drug for Alzheimer's disease (AD) remains a holy grail and is one of the most challenging tasks for scientists and clinicians from more than 100 years. In spite of the wealth of knowledge that exists regarding AD, only a handful of options are currently available for its management. Recent multiple failures of phase II-III AD clinical trials call upon the need for the alternative strategies that targeting multiple pathways such as amyloid-beta, tau phosphorylation, oxidative stress, acetylcholinesterase activity and inflammation to halt the disease progression. Previously, Edaravone (EDR) and Curcumin (CUR) have been considered as one of the most promising currently available drugs in the market due to their proven therapeutic activity against AD by targeting multiple key pathways of the disease pathogenesis. Regardless of their broad pharmacological activity and safety, poor oral bioavailability (BA) is the main obstacle to their potential use. The purpose of the current research was to reposition EDR and CUR for AD by developing novel oral delivery systems of EDR and CUR to enhance their oral bioavailability. Due to limited attention towards defining its physicochemical characteristics and unfavorable oral pharmacokinetic profile of EDR, the pre-formulation study was conducted as an initial step. Based on the preformulation profile, the strategies including co-solvency (chapter 2), lipid-based (chapter 3) and self-micellizing solid dispersion (chapter 4) were investigated to enhance its oral BA. Novel Oral Delivery System (NODS) of EDR based on co-solvency and pH modification technology showed 5.71 fold enhancement of oral BA by improving solubility, metabolism, and permeability. To take an additional advantage of superior drug loading, facilitates transport through the intestinal lymphatic system, allowing enterocyte-based transport to enhance drug uptake, efflux, and deposition; Novel Lipid-based Nanosystem (NLNS) of EDR was considered for development. The Liquid-NLNS and Solid-NLNS presented 10.79 fold and 9.29 fold improvement of oral BA of EDR, respectively. A self-micellizing solid dispersion based Novel EDR Formulation (NEF) displayed >13 fold improvement in oral BA. Due to simplicity and economy of preparation, stability and superior oral bioavailability, NEF was explored to assess long-term (3 months) safety and efficacy on mice behaviors deficits (Open field, Novel objective recognition, Y-maze and Morris water maze tests) via oral administration with APP/PS1 AD mice models. The results indicate that the NEF is non-toxic up to 414 µM/kg and reversed the cognitive decline of APP/PS1 mice to the cognitive level of wild type normal aging mice and performed better than donepezil. For CUR, self-micellizing solid dispersion (chapter 5) was identified as a potential strategy to curb the issues which limit its oral BA including poor solubility, stability, and permeability. The

Soluplus® based novel CUR formulation (NCF) exhibited improved solubility, stability, permeability, and bioavailability (117-fold) as compared to crude CUR. With regards to *in-vivo* assessment of safety and efficacy, the results hold a promise as a therapeutic agent for AD with superior effectiveness and safety similar to NEF. The overall findings demonstrated a high potential for EDR and CUR to pave the way for clinical development for AD however further preclinical evaluation in non-human primates is warranted to ensure translation of the current findings.

Thesis Outline

Chapter	Name/Publication	Keywords/Sections
1	Introduction	Alzheimer disease, Edaravone Curcumin, Solid Dispersion, Self-microemulsifying drug delivery system, Co-solvent based drug delivery system.
2	Development of a Novel Oral Delivery System of Edaravone for Enhancing Bioavailability	Edaravone, Labrasol, Aqueous stability, Metabolism, Permeability, Oral Bioavailability
3	Novel Lipid-based Nanosystem of Edaravone: Development, Optimization, Characterization, and *In-vitro/In-vivo* Evaluation	Edaravone, Lipid-based Nanoformulations, Solubilisation, Glucuronidation, Permeability, Oral Bioavailability
4	Novel Edaravone Formulation based on self-nanomicellizing solid dispersion strategy for enhancement of oral bioavailability and reversal of cognitive deficits in Alzheimer's disease model	Edaravone, Soluplus, oral bioavailability, Dose-response relationship, APPSwe/PS1deE9 mice, Learning and Memory, safety assessment
5	Novel self-nanomicellizing solid dispersion Curcumin formulation for oral administration: Development, optimization and assessment in Alzheimer's disease model	Curcumin, Soluplus, oral bioavailability, APPSwe/PS1deE9 mice, Learning and memory, safety assessment
6	Summary and Future Perspectives	Thesis conclusion, critical analysis, and further research
7	References	

Declaration by Author

I declare that,

a) This thesis presents work carried out by myself and does not incorporate without acknowledgment any material previously submitted for a degree or diploma in any university;

b) To the best of my knowledge, it does not contain any materials previously published or written by someone else except where the references are made in the text; and all substantive contributions by others to work presented, including collaboratively authored publications, is clearly acknowledged.

c) I acknowledge that copyright of published works contained within this thesis (as listed below) resides with the copyright holders of those works.

- A. Parikh, K. Kathawala, C.C. Tan, S. Garg, X.F. Zhou, Development of a novel oral delivery system of edaravone for enhancing bioavailability, International journal of pharmaceutics, 515 (2016) 490-500.
- A. Parikh, Z. Shan, Y.Song, K. Kathawala, C.C. Tan, S. Garg, X.F. Zhou, A Novel Formulation of Curcumin for Alzheimer's disease (AD): *In-vitro* and *In-vivo* evaluation, Alzheimer's & Dementia: The Journal of the Alzheimer's Association, 12 (2016) 1024 (Abstract).
- S.S. Jiao, X.Q. Yao, Y.H. Liu, Q.H. Wang, F. Zeng, J.J. Lu, J. Liu, C. Zhu, L.L. Shen, C.H. Liu, Y.R. Wang, G.H. Zeng, A. Parikh, J. Chen, C.R. Liang, Y. Xiang, X.L. Bu, J. Deng, J. Li, J. Xu, Y.Q. Zeng, X. Xu, H.W. Xu, J.H. Zhong, H.D. Zhou, X.F. Zhou, Y.J. Wang, Edaravone alleviates Alzheimer's disease-type pathologies and cognitive deficits, Proceedings of the National Academy of Sciences of the United States of America, 112 (2015) 5225-5230.



Ankitkumar Yogeshbhai Parikh

Acknowledgements

I would like to take this opportunity to thank all the people who helped during my doctorate journey. First and foremost, I would like to thank my supervisors Prof. Xin-Fu Zhou and Prof. Sanjay Garg to give me a chance to work on the current research project. I would like to express my sincere gratitude and thanks for their exceptional guidance, motivation, helping in constructive scientific writing, and making me an independent and confident researcher during my candidature. Secondly, I would also like to say big thanks to lab managers Dr. May Song and Ms. Jenny Zhong for their constant motivation, timely support, and guidance for designing and presenting my research work at various national and international conferences.

I would like to say special thanks to the University of South Australia for providing me University President's Scholarship (UPS) to support my Ph.D. Big thanks to Fujian Kangshimei Co, China for funding my laboratory expenses and conference travel.

I would like to say great thanks to all my lab members for their good friendship, advice as and when needed, and collaborative work to generate good research outputs. I am incredibly grateful to all Reid animal house staff including Jayne Skinner, Alysha Servin, Jess Parken, Becky Nitsche, Alex Whittaker, and Ruth Brogan for their generous support in animal work. Furthermore, big thanks to Chintan Pansara and Carolyn Streckbein for reading all my drafted chapters and publications and provided me critical review and comments to complete my thesis.

I am highly obliged to Smitha, Helen, Jo-Anne, and Hattie for helping in all administration work throughout my candidature.

Last but not least, I would like to special thank my family members, without them, I could not have finished this journey. I am blessed to have a wonderful family including my parents, grandmother, wife, brothers and sister in-law, and in-laws. Thanks everyone for having faith in me and always standing beside me.

[redacted]

Ankitkumar Yogeshbhai Parikh

Publications

Research publication

- **A. Parikh**, K. Kathawala, C.C. Tan, S. Garg, X.F. Zhou, Development of a novel oral delivery system of edaravone for enhancing bioavailability, International journal of pharmaceutics, 515 (2016) 490-500.
- **A. Parikh**, Z. Shan, Y.Song, K. Kathawala, C.C. Tan, S. Garg, X.F. Zhou, A Novel Formulation of Curcumin for Alzheimer's disease (AD): *In-vitro* and *In-vivo* evaluation, Alzheimer's & Dementia: The Journal of the Alzheimer's Association, 12 (2016) 1024 (Abstract).
- S.S. Jiao, X.Q. Yao, Y.H. Liu, Q.H. Wang, F. Zeng, J.J. Lu, J. Liu, C. Zhu, L.L. Shen, C.H. Liu, Y.R. Wang, G.H. Zeng, **A. Parikh**, J. Chen, C.R. Liang, Y. Xiang, X.L. Bu, J. Deng, J. Li, J. Xu, Y.Q. Zeng, X. Xu, H.W. Xu, J.H. Zhong, H.D. Zhou, X.F. Zhou, Y.J. Wang, Edaravone alleviates Alzheimer's disease-type pathologies and cognitive deficits, Proceedings of the National Academy of Sciences of the United States of America, 112 (2015) 5225-5230.
- **A. Parikh**, K. Kathawala, C.C. Tan, S. Garg, X.F. Zhou, Novel Lipid-based Nanosystem of Edaravone: Development, Optimisation, Characterization and *In-vitro/In-vivo* evaluation. (Manuscript submitted to Drug Delivery).
- **A. Parikh**, K. Kathawala, Z. Shan, C. Chen, J. Li, C. C. Tan, S. Garg, X. F. Zhou. Self-micellizing Solid Dispersion-based Novel Edaravone Formulation for oral Administration: Development, Optimization, and *In-vitro/In-vivo* assessment of safety and efficacy in Alzheimer's Mice Models. (Manuscript submitted to ACS Nano).
- **A. Parikh**, K. Kathawala, Z. Shan, C. Chen, J. Li, C. C. Tan, Y. Song, X. F. Zhou, S. Garg. Self-micellizing Solid Dispersion-based Novel Curcumin Formulation for oral Administration: Development, Optimization, and *In-vitro/In-vivo* assessment of safety and efficacy in Alzheimer's Mice Models. (Manuscript submitted to Journal of Controlled Release).

Book Chapter

- **A. Parikh*,** C. M. Day*, Y.Song, S. Garg, Nanotechnology and Nature's Miracle Compound- Curcumin, accepted in NanoBioMedicine Series print by Studium Press Publications LLC, Chicago, USA. (*contributed equally to this work.)

Patents

- X.F. Zhou**, A. Parikh**, S. Garg, Novel pharmaceutical oral formulation of Curcumin drug, Patent application No.: 201610267974.5, Company name: Fujian Tiantai PTY LTD, China, Filed date: April 2016.
- X.F. Zhou**, A. Parikh**, S. Garg, Novel pharmaceutical oral formulation of Edaravone drug, Patent application No.: 200610149832.9, Company name: Fujian Tiantai PTY LTD, China, Filed date: March 2016.

Conference Presentation

- **A. Parikh**, Z. Shan, Y. Song, K. Kathawala, C. C. Tan, S. Garg, X. F. Zhou (2016), A Novel Formulation of Curcumin for Alzheimer's Disease (AD): *In-vitro* and *In-vivo* Evaluation, Poster presentation at "Alzheimer's Association International Conference 2016 (AAIC 2016)", Toronto, Canada.
- **A. Parikh**, K. Kathawala, Y. Song, C. C. Tan, Z. Shan, X. F. Zhou, S. Garg (2016), Development of Novel Curcumin Formulation (NCF) for Cancer and Alzheimer Disease (AD), Poster presentation at "The 43rd Annual Meeting & Exposition of the Controlled Release Society", Washington, USA.
- **A. Parikh**, K. Kathawala, Y. Song, C. C. Tan, Z. Shan, X. F. Zhou, S. Garg (2016), Development of Novel Curcumin Nanomicelle (CNM) as a potential drug delivery system for Alzheimer Disease (AD), Oral presentation at "ASMR SA Annual Scientific Meeting 2016", Adelaide, Australia.
- **A. Parikh**, K. Kathawala, X. F. Zhou, S. Garg (2015), Solubility and stability improvement of Curcumin using solid dispersion approach, Oral presentation at "APSA-ASCEPT Joint Scientific Meeting 2015", Hobart, Australia.
- **A. Parikh**, K. Kathawala, X. F. Zhou, S. Garg (2015), Selection of pharmaceutical vehicles for the development of liquid dosage form of Omeprazole, Poster presentation at "APSA-ASCEPT Joint Scientific Meeting 2015", Hobart, Australia.
- **A. Parikh**, S. Garg, X. F. Zhou (2015), Development of Edaravone drug for Alzheimer disease (AD) "a disease of 21st century": Edging closer to Therapy, Oral presentation at "3rd Bi-Annual PMB Symposium 2015", Adelaide, Australia.
- **A. Parikh**, X. F. Zhou, J. Liu, Y.J. Wang (2015), Edaravone in Alzheimer's disease: Encouraging early *In-vitro* results of interaction with Amyloid Beta, Oral presentation

at “ASMR SA Annual Scientific Meeting 2015”, Adelaide, Australia.

- **A. Parikh**, M. Patel, R. Patel, V. Patel, H. Patel, J. Shah, T. Patel (2014), Formulation, optimization and characterization of lipid nanoparticles (LNP) of Clioquinol (CQ) for Alzheimer's disease, Poster presentation at “5th FIP Pharmaceutical Sciences World Congress”, Melbourne, Australia.

Authorship Statement

Chapter 2

Title of Paper	Development of a Novel Oral Delivery System of Edaravone for Enhancing Bioavailability			
Publication Status	Published	~~Accepted for Publication~~	~~Submitted for Publication~~	~~Publication style Manuscript~~
Publication Detail	International Journal of Pharmaceutics, 515 (2016) 490-500			

Author's Contribution

By signing the statement of authorship, each author certifies that their stated contribution to the publication is accurate and the permission is granted to be included in candidate's thesis.

Name of the Principal Author (Candidate)	Ankit Parikh		
Contribution to the Paper	Conception, Experimental design, and performance, Data analysis and interpretation, Manuscript write up		
Signature	[redacted]	Date	01 APR 2017

Name of Co-Author	Krishna Kathawala		
Contribution to the Paper	Experimental design and Performance, Manuscript Preparation		
Signature	[redacted]	Date	01 APR 2017

Name of Co-Author	Chun Chaun Tan		
Contribution to the Paper	Experimental Performance, Manuscript Preparation		
Signature	[redacted]	Date	01 APR 2017

Name of Co-Author	Sanjay Garg		
Contribution to the Paper	Supervision, Experimental design, Manuscript editing and reviewing		
Signature	[redacted]	Date	01 APR 2017

Name of Co-Author	Xin-Fu Zhou		
Contribution to the Paper	Supervision, Experimental design and Performance, Manuscript editing and reviewing		
Signature	[redacted]	Date	01 APR 2017

Chapter 3

Title of Paper	Novel Lipid-based Nanosystem of Edaravone: Development, Optimization, Characterization, and *In-vitro/In-vivo* Evaluation			
Publication Status	~~Published~~	~~Accepted for Publication~~	Submitted for Publication	~~Publication style Manuscript~~
Publication Detail	Drug Delivery			

Author's Contribution

By signing the statement of authorship, each author certifies that their stated contribution to the publication is accurate and the permission is granted to be included in candidate's thesis.

Name of the Principal Author (Candidate)	Ankit Parikh		
Contribution to the Paper	Conception, Experimental design, and performance, Data analysis and interpretation, Manuscript write up		
Signature	[redacted]	Date	01 APR 2017

Name of Co-Author	Krishna Kathawala		
Contribution to the Paper	Experimental design and Performance, Manuscript Preparation		
Signature	[redacted]	Date	01 APR 2017

Name of Co-Author	Chun Chaun Tan		
Contribution to the Paper	Experimental Performance, Manuscript Preparation		
Signature	[redacted]	Date	01 APR 2017

Name of Co-Author	Sanjay Garg		
Contribution to the Paper	Supervision, Experimental design, Manuscript editing and reviewing		
Signature	[redacted]	Date	01 APR 2017

Name of Co-Author	Xin-Fu Zhou		
Contribution to the Paper	Supervision, Experimental design and Performance, Manuscript editing and reviewing		
Signature	[redacted]	Date	01 APR 2017

Chapter 4

Title of Paper	Self-micellizing Solid Dispersion-based Novel Edaravone Formulation for Oral Administration: Development, Optimization, and *In-vitro/In-vivo* assessment of safety and efficacy in Alzheimer's Mice Models			
Publication Status	~~Published~~	~~Accepted for Publication~~	Submitted for Publication	~~Publication style Manuscript~~
Publication Detail	ACS Nano			

Author's Contribution

By signing the statement of authorship, each author certifies that their stated contribution to the publication is accurate and the permission is granted to be included in candidate's thesis.

Name of the Principal Author (Candidate)	Ankit Parikh		
Contribution to the Paper	Conception, Experimental design, and performance, Data analysis and interpretation, Manuscript write up		
Signature	[redacted]	Date	01 APR 2017

Name of Co-Author	Krishna Kathawala		
Contribution to the Paper	Experimental design and Performance, Manuscript Preparation		
Signature	[redacted]	Date	01 APR 2017

Name of Co-Author	Zhengnan Shan		
Contribution to the Paper	Experimental design and Performance, Data analysis and interpretation		
Signature	[redacted]	Date	01 APR 2017

Name of Co-Author	Chi Chen		
Contribution to the Paper	Experimental design and Performance, Data analysis and interpretation		
Signature	[redacted]	Date	01 APR 2017

Name of Co-Author	Jintao Li		
Contribution to the Paper	Experimental design and Performance, Data analysis and interpretation		
Signature	[redacted]	Date	01 APR 2017

Name of Co-Author	Chun Chaun Tan		
Contribution to the Paper	Experimental Performance, Manuscript Preparation		
Signature	[redacted]	Date	01 APR 2017

Name of Co-Author	Xia Cao		
Contribution to the Paper	Experimental design and Performance, Data analysis and interpretation		
Signature	[redacted]	Date	01 APR 2017

Name of Co-Author	Sanjay Garg		
Contribution to the Paper	Supervision, Experimental design, Manuscript editing and reviewing		
Signature	[redacted]	Date	01 APR 2017

Name of Co-Author	Xin-Fu Zhou		
Contribution to the Paper	Supervision, Experimental design and Performance, Manuscript editing and reviewing		
Signature	[redacted]	Date	01 APR 2017

Chapter 5

Title of Paper	Self-micellizing Solid Dispersion-based Novel Curcumin Formulation for Oral Administration: Development, Optimization, and *In-vitro/In-vivo* assessment of safety and efficacy in Alzheimer's Mice Models			
Publication Status	~~Published~~	~~Accepted for Publication~~	Submitted for Publication	~~Publication style Manuscript~~
Publication Detail	Journal of Controlled Release			

Author's Contribution

By signing the statement of authorship, each author certifies that their stated contribution to the publication is accurate and the permission is granted to be included in candidate's thesis.

Name of the Principal Author (Candidate)	Ankit Parikh		
Contribution to the Paper	Conception, Experimental design, and performance, Data analysis and interpretation, Manuscript write up		
Signature	[redacted]	Date	01 APR 2017

Name of Co-Author	Krishna Kathawala		
Contribution to the Paper	Experimental design and Performance, Manuscript Preparation		
Signature	[redacted]	Date	01 APR 2017

Name of Co-Author	Zhengnan Shan		
Contribution to the Paper	Experimental design and Performance, Data analysis and interpretation		
Signature	[redacted]	Date	01 APR 2017

Name of Co-Author	Chi Chen		
Contribution to the Paper	Experimental design and Performance, Data analysis and interpretation		
Signature	[redacted]	Date	01 APR 2017

Name of Co-Author	Jintao Li		
Contribution to the Paper	Experimental design and Performance, Data analysis and interpretation		
Signature	[redacted]	Date	01 APR 2017

Name of Co-Author	Chun Chaun Tan		
Contribution to the Paper	Experimental Performance, Manuscript Preparation		
Signature	[redacted]	Date	01 APR 2017

Name of Co-Author	Yunmei Song		
Contribution to the Paper	Conception, Experimental design, and Performance, Data analysis and interpretation		
Signature	[redacted]	Date	01 APR 2017

Name of Co-Author	Xia Cao		
Contribution to the Paper	Experimental design and Performance, Data analysis and interpretation		
Signature	[redacted]	Date	01 APR 2017

Name of Co-Author	Sanjay Garg		
Contribution to the Paper	Supervision, Experimental design, Manuscript editing and reviewing		
Signature	[redacted]	Date	01 APR 2017

Name of Co-Author	Xin-Fu Zhou		
Contribution to the Paper	Supervision, Experimental design and Performance, Manuscript editing and reviewing		
Signature	[redacted]	Date	01 APR 2017

1. Introduction

1.1 21st century and neurodegenerative disease

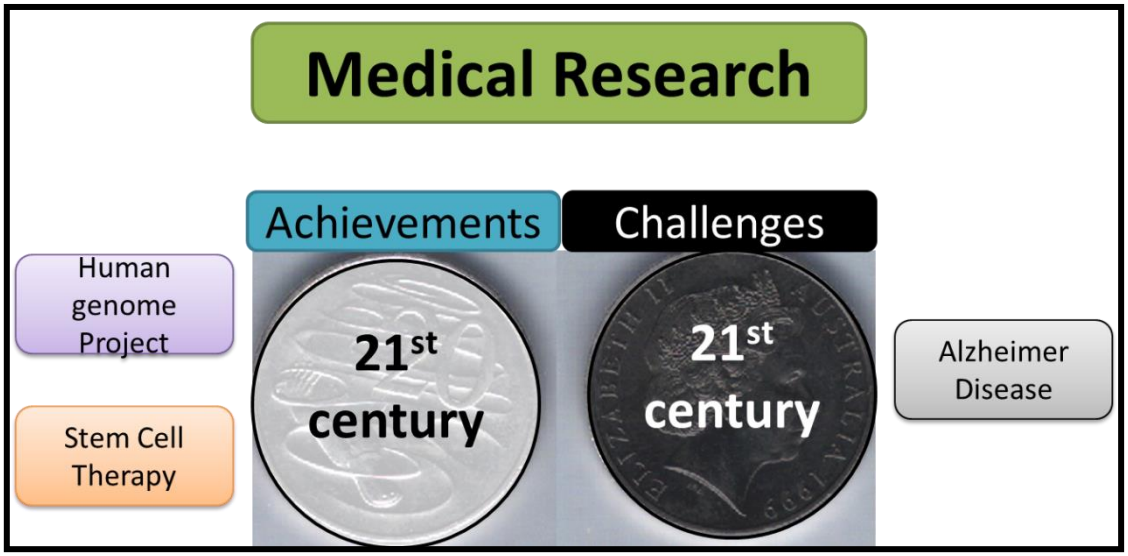

Figure 1.1 Medical research in 21st century

Medical research has always been on the forefront to combat dreadful diseases and provide human beings with longevity and a good quality of life. The 21st century has observed unprecedented advancement in medical technology like successfully finishing of human genome project with the order of 3 billion letters database to identify a single gene responsible for any diseases [1]. Addtionally, the research based on stem cell achived enormous success for the treatment of heart repair and eye diseases (Fig. 1.1) [2, 3]. Such discoveries are helping in increasing the life expectancy to a level that was never expected before. Though 21st century has seen some extraordinary advancement in the world of innovation & technology, the zeal for attaining excellence in itself has never quenched. With the increasing life expectancy, an epidemic of so-called diseases of aging has erupted. So, the impact of these modern technologies on society has been undoubtedly beneficial, but some might argue with some challenges, one being an increasing rate of Alzheimer disease (AD), a neurodegenerative disease amongst many.

Neurodegenerative diseases which impair cognitive functions, intellectual skills, physical movements, feelings, psychological phenomena are one of the greatest health challenges faced by people in today's world. They are believed to be the fourth largest cause of death after coronary & cardiac diseases, malignancies & tumors and paralysis [4]. More than 10 million people in the world are suffering from neurodegenerative disorders every year. This number is soon predicted to grow by over 20% in the coming decade as there is a significant rise in aging population that have high longevity due to medical science advancement and its ease of

availability [5]. In addition to causing short and long-term impairments and disabilities, they also cause an emotional, social and financial burden to the patients, families, and friends. Examples of neurodegenerative diseases include Alzheimer Disease, Parkinsonism, Lewy body dementia (LBD), Vascular dementia (VD) front temporal dementia (FTD), amyotrophic lateral sclerosis (ALS), Huntington disease(HD), spinocerebellar ataxia and prion diseases [6].

Among neurodegenerative diseases, AD is the most generalized and progressive form of dementia with unknown root causes that gradually leads to severe incapacitation in doing daily chores, finally worsening towards death. In spite of extensive research resulting in the best characterization of the disease, efficient management strategies still allude the healthcare system, resulting in a virtual pandemic and being labeled as “the disease of 21st century” [7]. Early identification of the disease, research into effective treatment options development and strategies to curb associated socioeconomic, as well as psychosocial issues, are suggested as possible measures to control the disease and are probably the most important task at the hands of modern neuroscience [8].

1.2 Dementia

It is described in the World Health Organisation’s (WHO) International Classification of Diseases as: “A syndrome due to disease of the brain, usually of a chronic or progressive nature, in which there is disturbance of multiple higher cortical functions, including memory, thinking, orientation, comprehension, calculation, learning capacity, language, and judgement. Consciousness is not clouded". Dementia is a syndrome affecting people worldwide due to the aging of the population. The cognitive impairment is usually escorted and sometimes led by changes in emotional and societal conduct or motivation [9, 10].

1.3 Alzheimer’s disease

Alzheimer Disease (AD) is a chronic, progressive neurodegenerative disease linked with Aβ plaques and phosphorylated Tau in the brain, especially the hippocampus. It comprises of almost 70% of all cases of dementia [11, 12].

1.3.1 Symptoms of AD

AD can affect an individual in several ways depending on the occurrence, and its severity manifested. The most common symptom (which usually appears first) is a gradual progressive decline in the formation and retention of new memory because of the first neurons affected by AD are functioning in memory formation. As other neurons are affected and start malfunction

and die, other symptoms start showing up and individuals start experiencing several issues related to the daily routine.

Common symptoms associated with Alzheimer's disease are mentioned below [13].

- Memory loss, initially short term, but eventually affecting long-term memory as well, disrupting everyday chores
- Difficulty in scheduling
- Decreased problem unraveling capacity and normal decision making.
- Trouble in doing routine or familiar work at home, workplace or leisure
- Loss of orientation to time and place
- Difficulty in grasping visual images and spatial relationships.
- Inability in speaking, learning and writing new words or phrases.
- Complications in handling things and inability to retrace things already done.
- Lower attentiveness.
- Lack of judgment power.
- Alterations in attitude and behavior

1.3.2 Journey of >100 years

Alois Alzheimer described a clinicopathological entity of neurological origin in a patient Auguste Deter, with the symptoms temporary amnesia, mixed visions, false dreams, unreal perceptions, delusions and died at an early age of 55, during a meeting of the Society of Southwest German Psychiatrists for the first time in 1906. It was named 'Alzheimer's disease' by Emil Kraeplin in 1910 [14].

Even after a century, the cure or even effective treatment to retard the progress of the disease still alludes us. But, current research in AD yields multiple pathways involved in the pathogenesis of the disease which could provide the breakthrough in finalizing treatment strategies for AD [15].

1.3.3 Alzheimer's disease Statistic

1.3.3.1 Global Impact

Currently, 46.8 million people in the world live with dementia, a figure which is projected to rise to 131.5 million by the year 2050 [16, 17]. In US alone 5.4 million cases of dementia has been noted to which almost 10 million more cases would add once the baby boom generation reaches the age 65. [13, 18]. By 2050, the prevalence of AD is expected to rise to 13.8 million cases, with a new case every 33 seconds in the US [13, 18]. It is expected that by the year 2050, one of every 85 people in the world will be suffering from AD [19]. A new case of AD is noted every 7 and 66 seconds in the world and the US, respectively [18]. Only 20-50% of those who have dementia are identified and provided care, even in developed countries [16]. AD is sixth overall and fifth among the list of prominent causes of death in people >65 years in the US. In the last decade, death rates due to stroke, heart disease, and prostate cancer reduced by 23%, 14%, and 11% respectively, whereas deaths due to AD increased by 71% [18]. Projected deaths in people living with AD in the year 2016 is 700 thousand in the US alone, many of whom die because of AD complications [13, 18]. The cost of care for patients with dementia is around 818 billion US dollars worldwide and 236 billion US dollars in the US alone every year [17, 18, 20]. Dementia has an economic impact which is only bettered by 18 countries' economy in the whole world [16].

1.3.3.2 Australian Statistics

In Australians 65 and above, dementia contributes the most to the disability, overtaking stroke, cancer, and depression and third leading cause overall [10, 16]. In Australia, the second foremost root of death is dementia. Prevalence of dementia has crossed 400,000 in Australia and is expected to rise above 500,000 in less than a decade and reach 1,100,000 by the year 2056 [17]. 1700 new cases of dementia are registered in Australia every week, and it is expected to rise to 4550 by the year 2056 [17]. Almost 26 thousand people in Australia suffer from what is known as early onset dementia. One in every ten people >65 years of age has dementia and one in every three people >85 years of age. Care of dementia patients demands a workforce of 1.2 million people in Australia [16]. Australia expects a shortage of > 150,000 paid and unpaid caregivers for people with dementia by the year 2029. Dementia is expected to become the third largest health and residential aged care spending within 20 years, costing approx. 1% of the gross domestic production of Australia and highest by the year 2060, amounting almost 11% of total healthcare spending [16].

1.3.4 Key mechanisms involved in Alzheimer's disease

AD has a complex pathogenesis with multiple pathways having an effect on the development and progression of the disease [21]. Two main pathological changes seen in patients with Alzheimer's disease are extracellular deposition of Aβ peptides forming neuritic plaques and neurofibrillary tangles formed by the intracellular deposition of hyperphosphorylated Tau protein. Various key mechanisms associated with Alzheimer disease are discussed in Fig. 1.2.

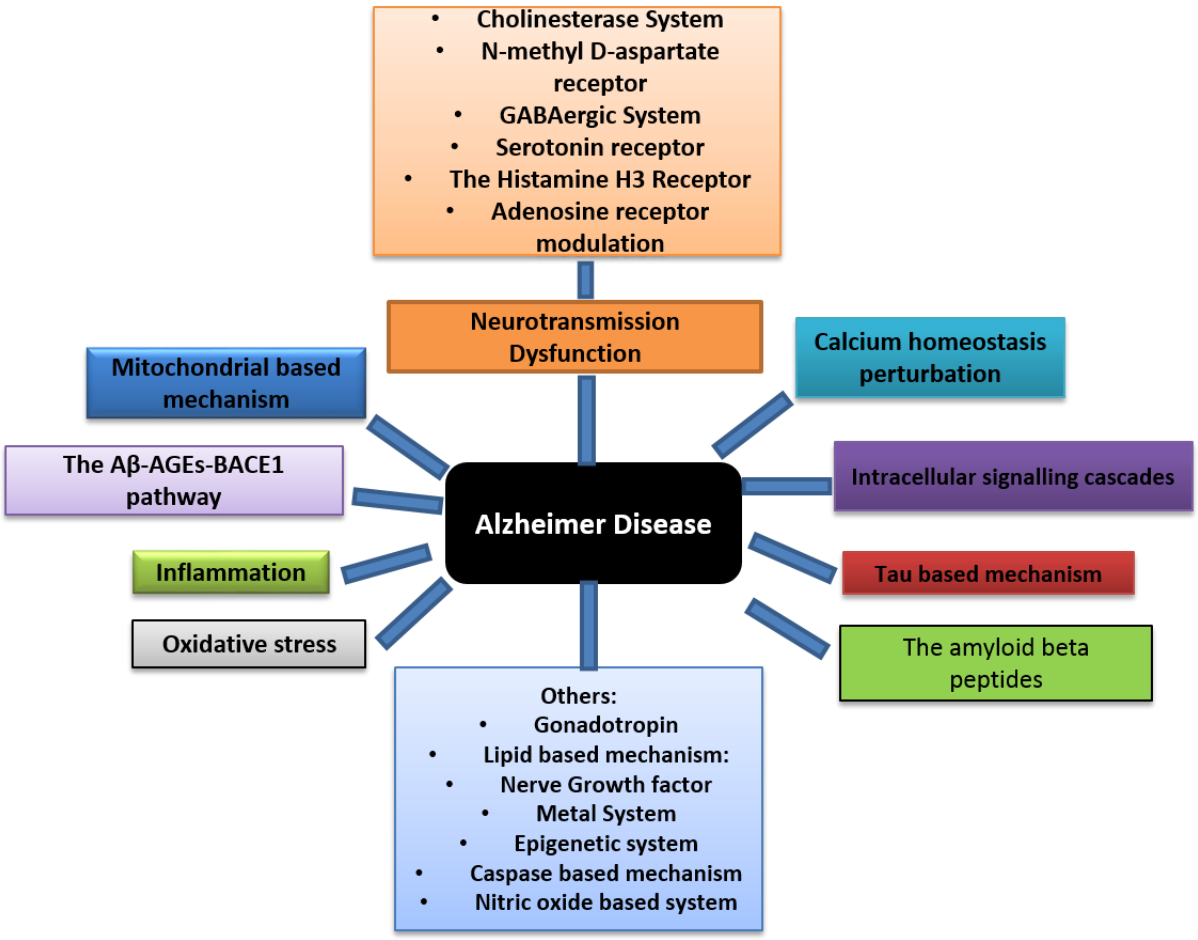

Figure 1.2 Various key mechanisms involved in pathogenesis of AD [19, 22]

1.3.4.1 Amyloid beta based mechanism

According to amyloid cascade hypothesis, Aβ formation is the key event in the initiation of AD, leading to senile plaque formation and consequent hyperphosphorylation of tau, ultimately resulting in the formation of neurofibrillary tangles. Amyloid Precursor Protein (APP), an important molecule involved in the pathogenesis of AD, is a type I mammalian transmembrane protein cleaved by two proteolytic pathways- non-amyloidogenic and amyloidogenic pathway [11].

In the non-amyloidogenic pathway, α-secretase cleaves APP at lys16-leu17 bond within Aβ region to produce a large extracellular fragment known as sAPPa and C83 fragment. C83 is further processed by γ-secretase to generate p3, a small 3 kDa peptide. sAPPa has been documented having several neuroprotective properties [11].

In amyloidogenic pathway, β-secretase cleaves APP to generate soluble APPb (sAPPb) and a fragment of 99 amino acids (C99) which is bound to the cellular membrane. C99 undergoes further hydrolysis to produce Aβ peptide with a varying length of the polypeptide chain of amino acids (Aβ1-40 and Aβ1-42)[11].

1.3.4.2 Tau-based Mechanism

Another hallmark of AD is neurofibrillary tangles, produced by the intracellular aggregation of hyperphosphorylated Tau protein. Tau hyperphosphorylation leads to unstable microtubules via helical filament pairing of hyperphosphorylated Tau protein, which in turn impairs axonal transport resulting in neuronal death. These pathological changes usually begin in the entorhinal/hippocampal region and then spread to other regions of the brain [11].

- **Aβ *-GSK3β-Tau pathway:*** Aβ also activates the up streaming kinases GSK3β and CDK5 which phosphorylate Tau, also leading to hyperphosphorylation of Tau which causes aggregation. These two kinases have become drug development targets for AD [22, 23]. A recent study showed that GSK3β signaling also regulated BACE1 expression and increased Aβ production [24]. Phosphatase 2A (PP2A) is the key enzyme that dephosphorylates Tau, thereby maintaining a balance in its activity. The expression of PP2A is decreased in AD brain [25, 26]. Aβ in the AD brain down-regulates PP2A, shifting the balance towards Tau hyperphosphorylation [25]. It also aggregated NFT disrupt axonal transport, which leads to more Aβ production in the degenerated axon [27, 28].

1.3.4.3 Oxidative stress (OS)

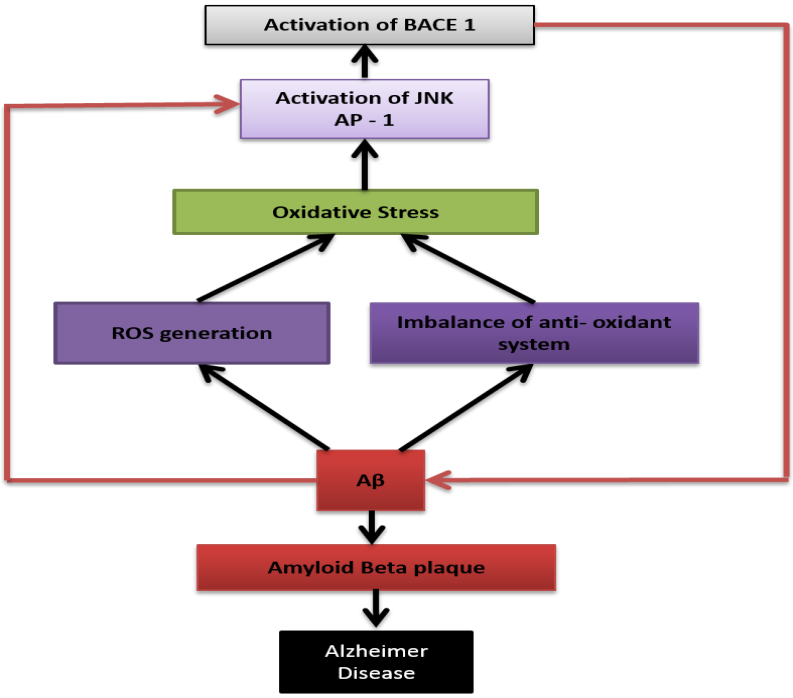

Figure 1.3 Oxidative stress and Alzheimer disease [29]

Oxidative stress-BACE1-Aβ cycle: Aging is the most common risk factor for AD. In a sporadic variant of AD, a positive feedback loop giving rise to Aβ overproduction is usually responsible. The oxidants and resultant lipid peroxidation product 4-hydroxynonenal (HNE) increases the expression of BACE1 and presenilin 1 [29-31]. As demonstrated in experimental studies, the BACE1 expression is significantly associated with increased oxidative markers in brain tissue of cases with sporadic AD [32]. Accumulation of Aβ is accompanied by accumulation of metal ions (e.g. copper, zinc, and iron) as these ions interact with Aβ [33, 34]. Aβ enhances oxidation, which is responsible for the generation of reactive oxygen species (ROS) and free radicals causing an increase in OS within cells [33-35]. Oxidative stress is shown to accelerate with age and is implicated in the pathogenesis of AD [36-38], causing damage to DNA structure and functioning, membrane destabilization and ultimately cell death [38]. It has been already shown in research that Aβ and OS are correlated, and increased Aβ increases the oxidative stress [39-41], and vice versa [30, 42]. Aβ and oxidative stress both are presumed to act on JNK, which in turn activates the transcription factor responsible for expression of substances implicated in the pathogenesis of AD such as BACE1 and presenilin1, AP1 [43], thus finishing the Aβ-JNK-BACE1 cycle. Traumatic brain injury is also implicated to have the similar mechanism via BACE1 activation by oxidative stress and by nuclear factor

kappa-B (NF-κB) transcription factor activation. Three different mechanisms are implicated which can contribute to AD pathogenesis: oxidative stress and the activation of the JNK pathway; HIF-1 transcription factor activation which in turn acts on BACE1 promoter directly or indirectly by activating NF-κB and RAGE; and increased intracellular calcium causing activation of calpain and cdk5 (Fig.1.3) [21].

1.3.4.4 Inflammation

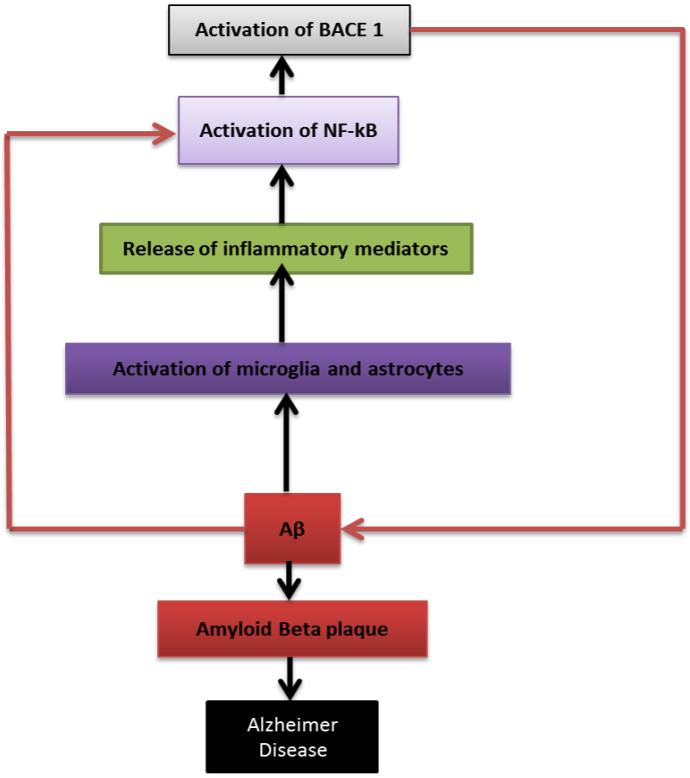

Figure 1.4 Inflammation and Alzheimer disease [44]

The* Aβ *-inflammation-NF-kB pathway: With strong proinflammatory properties, Aβ activates inflammatory cells of central nervous system, microglia, and astrocytes leading to release of proinflammatory cytokines. The cytokines, as well as proinflammatory properties of Aβ, activates NF-kB and increase inflammation [21]. NF-kB binds BACE1 gene promoter to increase the production of APP and Aβ (Fig. 1.4) [44, 45]. It leads to neurodegeneration leads to loss of memory [21]. Currently, anti-inflammatory drugs are being explored as a potential treatment option for AD [46].

1.3.4.5 Calcium homeostasis perturbation

The Aβ-calcium signalling-BACE1 pathway: Aβ is proposed to increase intracellular calcium by three different mechanisms: 1) Membrane receptors or ion channels activation; 2)

increased membrane permeability, and 3) calcium channel deregulation, which is in part explained by mutations in presenilins. Increased calcium causes activation of not only calpain/cdk5/STAT3 pathway but also NFAT1. Both STAT3 and NFAT1 increases expression of BACE1, which is responsible for the production of Aβ peptides, thus forming a positive feedback loop [47].

The Aβ-AGEs-BACE1 pathway Aβ peptides activate RAGE as well as AGEs generated in Diabetes Mellitus or events of oxidative stress such as hypoxia or inflammation. RAGE activation causes increased expression of BACE1 via activation of NF-κB and NFAT1. Also, AGEs can cause activation of BACE1 directly by producing oxidative stress. BACE1 generates Aβ peptides production which further increases RAGE activation (Fig. 1.5) [47].

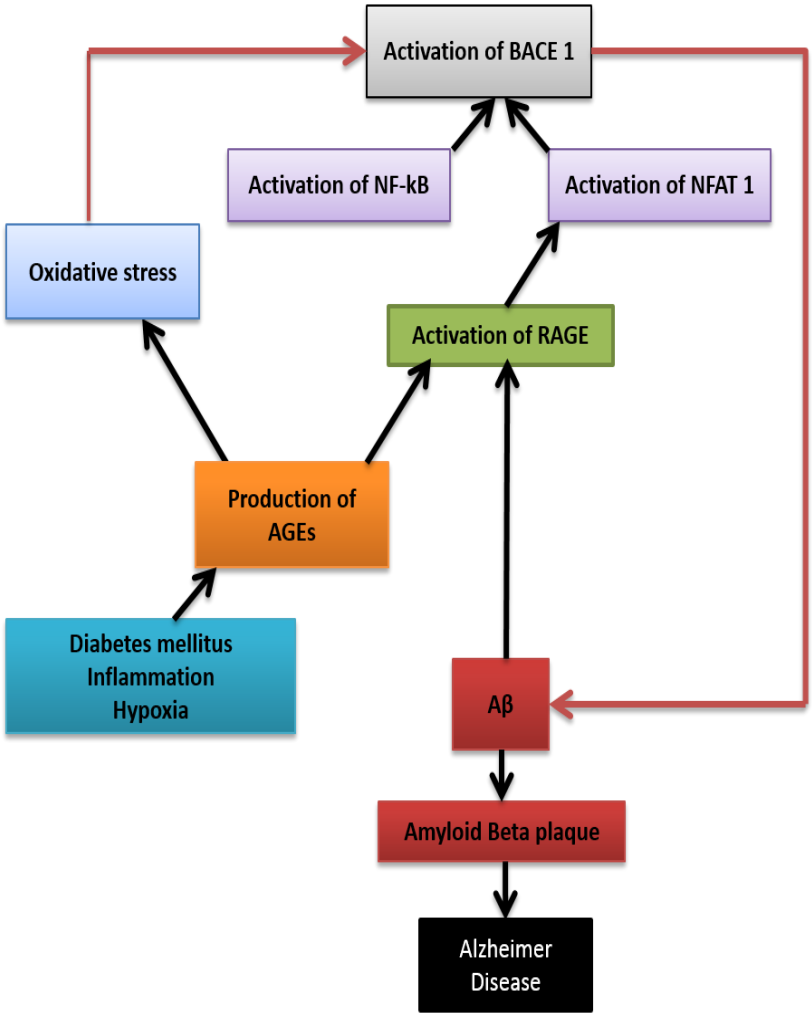

Figure 1.5 AGE/RAGE signaling Cascade and Alzheimer disease [47]

1.3.4.6 Neurotransmission related mechanisms

- **Cholinesterase System:** Decrease in activity of choline acetyltransferase and uptake of choline lead to reduced acetylcholine synthesis in AD [48].

- **N-methyl-D-aspartate receptor (NMDA):** Defects in glutamate cycle cause increased NMDA receptor activation and resultant excitotoxicity which further activates production of Aβ [49].
- **GABAergic System:** Changes in this neurotransmitter system was suggested to contribute to the neurobiology causing depression and impaired cognitive function in AD [50].
- **Serotonin receptor modulation:** Both decreased levels of 5-hydroxytryptamine (5-HT) receptors and 5-HT positive neuron density are significantly reduced in brains with AD [17].
- **Histamine H3 Receptor:** In AD, H3 receptor activation causes inhibition of histamine release in the brain which further decreases the levels of other neurotransmitters such as acetylcholine, GABA, dopamine and noradrenaline [18].
- **Adenosine receptor modulation:** Adenosine type 2A plays an important part in neuronal function modulation, suggesting a possible effect on neuronal systems leading to cognitive defects seen in AD [5].

1.3.4.7 Other Mechanisms

- **Mitochondrial based mechanism:** In AD, presenilin-1 (PS1), presenilin-2 (PS2), and gamma-secretase activity process the amyloid precursor protein (APP) to generate Aβ. They are situated in mitochondria-associated ER membranes (MAM), allows transportation of biochemicals across the membrane [51]. Imbalance and accumulation of Aβ in the mitochondria causes mitochondrial oxidative stress which impairs the electron transport chain and causes increased ROS levels [52, 53]. In the AD brain, the number of mitochondria in the synapses and axons are reduced, and their morphology and functions are abnormal [54, 55]. Accumulation of Aβ and amyloid precursor protein (APP) result in a reduction in key enzymes such as cytochrome C oxidase (COX), pyruvate dehydrogenase, Cu/Zn-superoxide dismutase (SOD) and manganese SOD [56-58]. Reduction of COX in the mitochondria increases ROS production depletes energy stores and disrupts energy metabolism. Mitochondrial ROS and OS cause tau hyper phosphorylation, leading to accumulation of NTF in neurons [59].
- **Intracellular signaling cascades**: Both cAMP signalling and nitric oxide/cGMP/cGMP-dependent protein kinase/cAMP responsive element-binding protein cascade are associated with synaptic loss and impaired memory in AD [4].

- **Gonadotropin**: In AD, changes in gonadotropins after a certain age are implicated in the causation of AD. Luteinizing hormone (LH) is expected to have effects in the disease process, and its concentration is rising with aging [60].
- **Lipid-based mechanism:** Lipid peroxidation involves a cascade of reactions in which production of free radicals occurs selectively in the lipid components of cellular membranes. Polyunsaturated fatty acids readily undergo lipid peroxidation chain reactions, which, in turn, lead to the formation of highly reactive electrophilic aldehydes [61].
- **Nerve Growth Factor:** The effects of nerve growth factor are seen by downstream antiapoptotic factors activation, proapoptotic pathway inhibition and stimulation of ERK/MAP kinase and CREB pathways. In AD, levels of NGF are decreased leading to increased neuronal deaths and progression of AD [62].
- **Metal chelation**: There is a change in the normal homeostasis of metal ions in AD with abnormally high activities of redox-active metals, most significantly Iron, in brain areas affected by AD. Metal ions are assumed to play an integral role in aggregation and metabolism of Aβ [63, 64].
- **Epigenetic system**: In AD, high homocysteine (HCY) levels, low vitamin B12, and folate levels are observed in the blood which may be associated with amyloid-beta overproduction and accumulation, which in turn leads to progression of AD. It may be a result of the loss of epigenetic control in the gene expression involved in the processing of AβPP (amyloid-beta protein precursor) [65].
- **Caspase based mechanism**: Caspase, proteases of the cysteine family, cleaved amyloid precursor protein (APPcc) and SET levels (inhibitor 2 of phosphatase 2A (I2PP2A) are elevated in the cytoplasm of the neurons in the brains of Alzheimer Disease (AD). Translocation of SET in the cytoplasm of a neuron can lead to hyperphosphorylation of Tau [66].
- **Nitric oxide-based system:** Nitric oxide (NO) dependent oxidative stress may lead to mitochondrial structural changes and may cause DNA damage in cases of AD [67].

1.3.5 Current Standard of Care

Drugs that are currently approved for the treatment of inabilities caused by cognitive deterioration in AD are based on the mechanism of Acetylcholinesterase inhibitors (AChEIs) and NMDA-receptor (NMDAR) antagonist. AChEIs is the key class of drugs used in the appropriate treatment of AD. Tacrine was the first AChEI which was acceptable by the US

Food and Drug Administration (FDA) for the clinical management of AD, discontinued later due to side effect like hepatotoxicity. Donepezil, Galantamine, and Rivastigmine are second generation AchEIs which can be preferred as a second choice. AChEIs are associated with gastrointestinal adverse effects like nausea and vomiting that most commonly lead to discontinuation of treatment. Tacrine and physostigmine have low oral BA. One more alternative to the treatment of AD is believed to be achieved by blocking of glutamatergic neurotransmission. An additional therapeutic approach is based on blocking glutamatergic neurotransmission through NMDA receptors which may responsible for neuron loss observed in AD. Memantine is a non-competitive NMDAR antagonist with a moderate affinity that appears to be able to protect neurons without interference with physiological NMDAR activation [11].

Both cholinesterase inhibitors and Memantine have shown valuable output regarding benefits and optimization in clinical trials on cognitive functions, functional results, and behavioral changes. However, cost effectiveness of cholinesterase inhibitors has been questioned as there are only a few patients who benefit from it. Both Memantine and cholinesterase inhibitors are recommended to be taken together since a combination of both works well [15]. The detail of currently approved drugs is mentioned in Table 1.1.

Table 1.1 Currently approved drugs for Alzheimer's disease [12]

Name	**Brand Name**	**Company**	**Type of formulation**	**Dose**	**Year of approval**	**Stage of Alzheimer disease**
Donepezil Hydrochloride	ARICEPT®	Pfizer	Film-coated tablet	5, 10 and 23 mg	1996	Mild to moderate Alzheimer
			Orally disintegrating tablet	5 and 10 mg		
Galantamine Hydrobromide	RAZADYNE®	Janssen, Ortho-McNeil Pharmaceutical,	Immediate release tablet	4, 8 and 12 mg	2001	Mild to moderate Alzheimer's
			Extended release capsule	8, 16 and 24 mg		

		Sanochemia Pharmazeutika, Shire Pharmaceuticals, Takeda Pharmaceutical Company	Oral solution	4 mg/mL		
Memantine Hydrochloride	NAMENDA	Forest Labs LLC	Tablet	5 and 10 mg	2003	Moderate to severe Alzheimer's
			Oral solution	2 mg/mL		
			Extended release capsule	7, 14, 21 and 28 mg		
Rivastigmine Tartrate	EXELON®	Novartis Pharmaceuticals	Capsule	1.5, 3, 4.5, and 6 mg	2000	All stages of Alzheimer's
			Oral solution	2 mg/mL		
			Transdermal patch	4.6, 9.5 and 13.3 mg/24 h		
Donepezil and Memantine	NAMZARIC	Allergan	Capsule	14 and 28 mg memantine and 10 mg donepezil	2014	Moderate to severe Alzheimer's

1.3.6 Current research scenario for Alzheimer disease

Fig. 1.6 shows the current research scenario which are examined used as a treatment for Alzheimer's disease and ongoing research.

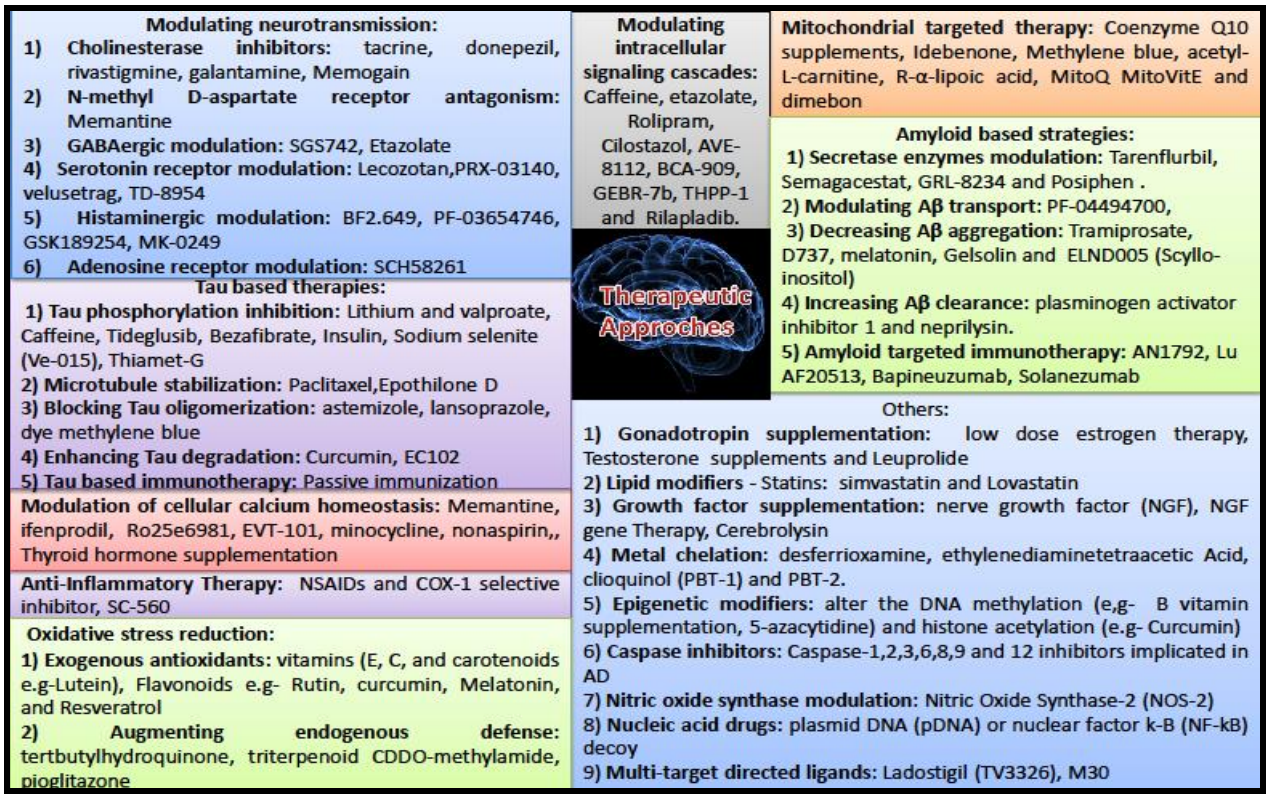

Figure 1.6 Various establish and ongoing research efforts as therapeutic strategies for Alzheimer disease [19]

1.4 Need of novel therapeutic option for AD

In spite of the wealth of knowledge that exists regarding AD, the only handful of options are available currently for its management. Despite the evidence of the multifactorial nature of AD and the involvement of several different mechanisms, because of the immense popularity of the amyloid cascade hypothesis, to date, most of the therapeutic efforts have been focused on inhibition and removal of Aβ plaques. However, none of these treatments have so far shown any improvement or even reduction in the rate of cognitive impairment in clinical studies [12]. The pathophysiology of AD involves disturbances and imbalances occurring in a variety of mechanisms [19]. Various vicious cycles are linked, and their interactions propagate deterioration in the pathogenesis of AD [47]. If these vicious cycles govern the pathogenesis of sporadic AD, it is conceivable that only targeting Aβ or tau by immunotherapy or by using inhibitors of BACE1 and presenilin may not break the cycles which cross-activate each other. The treatment of AD patients along with inhibition of neurodegeneration will also require neural regeneration. After all, the AD brain suffers from failed neurogenesis, a very marked loss of neuronal and synaptic plasticity, and these deficits even precede concluded to Aβ and

tau pathologies [12]. It is imperative to discover novel drugs targeting multiple key pathways in the pathogenesis of AD [68].

Results from failures of current clinical trials acclaim that targeting numerous critical pathways of the AD pathogenesis is essential to halt the disease progress. Number of studies and our previous study shows that EDA and CUR have a potential of hindering Aβ aggregation and declining Aβ-induced oxidation *in-vitro*. Before or after the onset of Aβ deposition, EDA and CUR noticeably reduces Aβ deposition, improves oxidative stress, decreases the downstream pathologies in conjunction with Tau hyperphosphorylation, glial activation, neuroinflammation, neuronal loss, synaptic dysfunction and also prevent the impairment of behavioral deficits of APP/PS1 mice [69-71].

1.5 Edaravone (EDR)

1.5.1 Introduction of EDR

EDR, also known as MCI-186 (5-Methyl-2-phenyl-2,4-dihydro-3H-pyrazol-3-one [72]; Fig. 1.7), is a strong and synthetic free oxygen radical scavenger that has an anti-oxidant action to reduce oxidative stress and inhibit lipid peroxidation [73] via both nonenzymatic lipid peroxidation and the lipoxygenase pathway [74]. But, besides these effects, EDR also exhibits beneficial action in inflammation, matrix metalloproteinases, nitric oxide production and apoptotic cell death [75]. Mitsubishi Tanabe Pharma Corporation (Osaka, Japan) developed EDR and introduced as Radicut in 2001 to be the first neurovascular protective drug in the world [76]. It was approved by Japanese Ministry of Health and Welfare (JMHW) in 2001 for the treatment of patients with acute ischemic stroke (AIS) [77, 78]. Since then, EDR is not only used commonly to treat AIS [79] but also being used to treat other ROS-related diseases [80] such as cardiovascular diseases and stroke [79]. EDR is very common and extensively prescribed in Japan, India, and China [81] for various treatments. Furthermore, an orphan designation for the undisclosed oral formulation of EDR developed by Netherlands-based company Treeway, was granted for amyotrophic lateral sclerosis (ALS) by regulatory agencies including European Medicines Agency (2014) [82] and U.S. Food and Drug Administration (USFDA) (2015) [83]. Subsequently, Radicut® has been approved in Japan for ALS treatment from 2015 [77]. A longer toxicity study with EDR over a 26-week period confirmed its safety with at 10 mg/kg iv in rats and 30 mg/kg iv in dogs [84].

EDR is designed to be a phenol-like compound which is responsible for their anti-oxidant property [85]. Phenols quench free radicals by donating one hydrogen ion to the free radical

and convert into a radical. However, the electron in the phenol are stabilized by the aromatic ring via resonance electron delocalization and become less active [86]. But due to the toxic and corrosive properties of phenols, they are not applicable for pharmaceutical usage even though they have exhibited radical scavenger action and have proven to be potent antioxidants [85]. On the other hand, EDR is shown similar anti-oxidant and free radical scavenging effects due to its aromatic hydroxyl group [85]. However, in contrary to phenols, EDR does not have any toxicity effects of phenols. Therefore, EDR is preferential over phenols.

EDR is categorized into three different tautomeric forms; the amine form, keto form, and enol form as mentioned in Figure 1.7 and the aromatic hydroxyl group is produced via keto-enol tautomerization [80, 85]. According to Watanabe et al., EDR has a pK_a value of 7.0, hence roughly 50% of EDR ionized and exist in anionic form at physiological pH [80]. Anionic form of EDR is the more reactive form that may readily react with ROS in the brain to bring about the anti-oxidant effects [87]. The advantages of EDR over other free radical scavengers such as Idebenone, Baicalein, and catechins (flavocoxid) is access to the brain via blood brain barrier. It is a lipophilic molecule with low molecular weight and solubility property in both water and lipid [80, 88]. Therefore, it can readily cross the blood-brain barrier to act at the target site in the brain [89]. According to Tabrizchi, the relative ratio of plasma to cerebral spinal fluid levels of EDR is estimated to be between 50 and 65% [84]. These properties may be the reason for the neuroprotective actions of EDR in cerebral infarction when other anti-oxidants do not exhibit such effect [88].

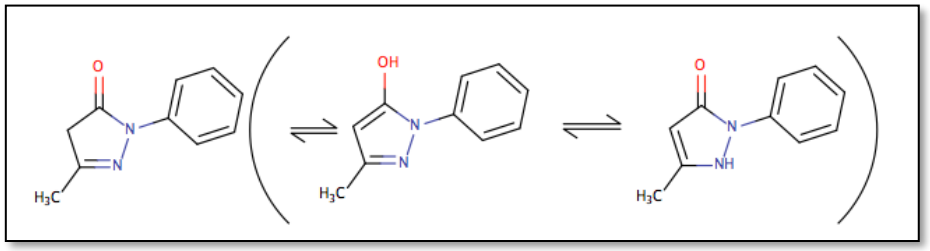

Figure 1.7 EDR (3-methyl-1-phenyl-2-pyrazolin-5-one, left) and its two tautomers; 3-hydroxypyrozole isoform (center) and 1, 2-dihydro-pyrazol-3-one (right). Molecular Formula C10H10N2O and Molecular Weight 174.1992 g/mol [80, 90]

1.5.2 Mechanisms of Action

According to Yamamoto *et al.* and Watanabe *et al.*, EDR shows radical scavenging efficacy which can lower the increased levels of hydroxyl radicals and superoxide radicals [90, 91] thereby protects cells against oxidative stress. The free radical scvenger activity is due to its

interaction and quenching the hydroxyl radicals and hydroxyl radical-dependent lipid peroxidation [87, 92]. It breaks the chain of lipid oxidation by transferring an electron to peroxyl radical from an EDR anion (Fig. 1.8). A study of the radical scavenging activity of EDR carried out by Higashi *et al.* showed that EDR activity increased as pH increased [93]. It is most likely because the anionic form of EDR is much more reactive in comparison to its nonionic form [94]. Since EDR has a pKa value of 7.0 [80], as pH increases, more EDR will exist in its anionic form at the physiological condition. Therefore, the rate of oxidation of EDR has a positive correlation with pH. The hypothetical mechanism of EDR as radical scavenger is mentioned in Fig. 1.8. It includes four steps. Step 1: EDR compound converts into EDR anion. Step 2: In the presence of radical, EDR anion transfers an electron to the radical (X) and forms a radical-derived anion (X^-) and EDR radical. it is also the reaction that breaks the lipid peroxidation chain reaction. Step 3: EDR radical transforms into EDR peroxyl radical by reacting with oxygen. Step 4: EDR peroxyl radical eventually become 4, 5-Dione. Step 5: 4, 5-dione yields OPB via hydrolysis and BPOH whereby its formation is equilibrated with 4, 5-dione and EDR [87].

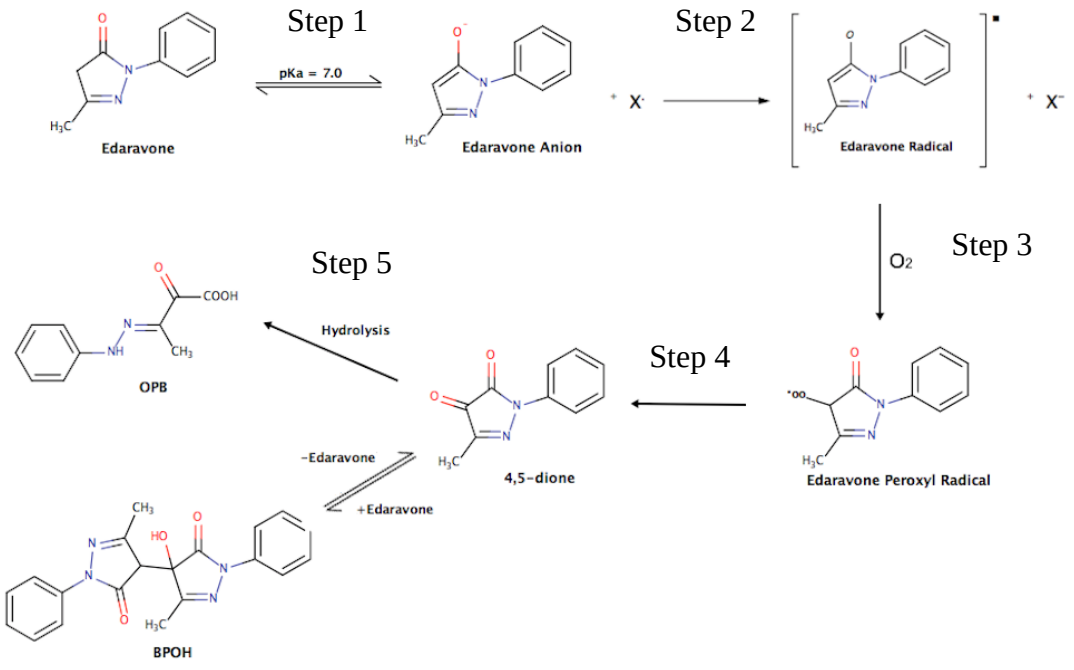

Figure 1.8 Hypothetical mechanism of EDR as radical scavenger [87]

1.5.3 Marketed formulations

EDR is one of the most powerful drugs not only for Neurodegenerative diseases but also for cardiovascular diseases, liver associated diseases, colitis, rheumatoid Arthritis, and lung Injury

as discussed in therapeutic uses section. Despite its research popularity, the clinical application of the drug is restricted by the unavailability of the typical formulation to achieve efficient therapeutic output except the only available parental formulation. It is because of the solubility and stability issues with EDR [95, 96]. The existing formulations of EDR in the market are injectable EDR ampoules and Radicut Bag [97] available and used in Asian countries. A list of nine manufactures across Asia is mentioned in Table 1.2.

Table 1.2 Available Marketed Formulations

Sr. no.	Company	Brand Name	Country	References
1	Jiwa Bio-Pharm Holdings	Jiwa Youmin	Hong Kong	[98]
2	Simcere	Bicun and Yidasheng	China	[99]
3	Sun Pharmaceutical Industries Ltd.	Aravon	India	[100]
4	Unichem Laboratories Ltd	Edvo	India	[101]
5	UCB India Ltd.	Fraseda	India	[102]
6	Piramal Healthcare	Nuravon	India	[103]
7	Intas Pharmaceuticals Pvt. Ltd.	Edarabid	India	[104]
8	Ranbaxy Laboratories Ltd.	Carevon	India	[105]
9	Mitsubishi-Tokyo Pharmaceuticals	Radicut	Japan	[106]

1.5.4 Therapeutic potential of EDR

EDR has been proven to be effective in preventing and treating a variety of diseases. The proven therapeutic efficacy of EDR in different diseases is mentioned in Table 1.3.

Table 1.3 Application of EDR in various diseases

Name of Disease	**Key Mechanism Responsible for the Disease**	**Pharmacological effects of EDR**	**References**
Stroke and Cerebral Ischemia	Free radical damages proteins and DNA via lipid peroxidation contribute to the Ischemic brain damage.	Free radical scavenging and antioxidant actions.	[81, 107-112]
Liver associated diseases	Oxidative stress-induced acute liver injury.	Free radical scavenging and antioxidant actions to eliminate intra-hepatocellular superoxide species thus, reduce membrane lipid peroxidation and to inhibit the production of inflammatory cytokines.	[113-124]
Cerebral Aneurysms	Reactive oxygen species (ROS) leads to inflammation, and chronic inflammation in arterial walls may be the factor of Cerebral Aneurysms.	Free radical scavenging and antioxidant actions suppress inflammation-related gene expression in aneurysmal walls hence, inhibited CA formation.	[125]
Amyotrophic Lateral Sclerosis* (under phase III clinical trial)	Increase in the generation of free radicals and oxidative stress causes degeneration motor neurons.	Free radical scavenging effect eliminating free oxygen radicals and delay the progression of functional motor disturbances.	[126-128]
Bone marrow Damage	Bone marrow damage caused by free radical generated by irradiation	Antioxidant and radical scavenging actions prevent lipid peroxidation by reducing oxidative stress caused by irradiation.	[129]
Spinal Cord Injury	Free radicals generated by spinal cord injury often leads to secondary tissues injury which will cause deterioration	Antioxidant and radical scavenging actions reduce ROS especially in neuron after spinal cord injury. It helps to minimize the secondary neurological damage.	[130-134]

Colitis (IBD)	Increase of ROS contributes to colitis	Antioxidant and radical scavenging actions.	[135, 136]
Rheumatoid Arthritis (RA)	Oxidative stress and proinflammatory cytokines lead to rheumatoid arthritis. Besides, the inequality between apoptosis and proliferation of rheumatoid synovial cells is due to the activation of nuclear factor-kappa B (NF-κB).	Suppression of activated NF-κB.	[137-139]
Cardiovascular Disease	Inflammation leads to enhanced generation of ROS causes cardiovascular diseases	Anti-oxidative function reduces oxidative and endoplasmic reticulum (ER) stress.	[76, 79, 93, 140-144]
Renal Toxicity	Cisplatin generates free radicals which lead to associated nephrotoxicity	Free radical scavengers or antioxidants actions reduce oxidative stress.	[145-152]
Traumatic Brain Injury	The mechanical trauma induces immediate tissue loss subsequent cascade of reactions like pro-inflammatory reactions and oxidative stress which further cause secondary brain damage.	Antioxidative action reduces neuronal death and improves neurological function by minimized oxidative stress and inflammatory response through decreasing the rate of generation of free radicals after brain injury.	[153-157]
Diabetes	Diabetes increases oxidative and endoplasmic reticulum stress which leads to the brain Ischemic Reperfusion (I/R) damage.	Scavenging free radicals action reduces immune destruction of islet β cells by interrupting the apoptotic pathways caused by ER stress.	[158-161]
Parkinson Disease	Free radicals contribute to cell death in Parkinson.	Minimized oxidative stress and apoptosis in Neuro2a cells.	[162-164]
Retinal Damage	Imbalance of ROS metabolism induces oxidative stress which leads to retinal damage.	Free radical scavenging function inhibits neuronal cell death induced by oxygen-glucose	[90, 165]

		deprivation stress and Retinal ganglion cell death induced by N-methyl-D-aspartate.	
Epilepsy	Oxygen free radical species is the factor of the development of seizures and also caused seizure-induced neuronal degeneration.	Anti-oxidant effect prevents epilepsy in human.	[166, 167]
Lung Injury	Bleomycin enhances the generation of ROS that leads to apoptosis and increases collagen production which involves in causing lung injury.	Free radical scavenging effect reduces the generation of ROS and prevention of acute lung injury.	[168-173]
Ovarian Ischemia and perfusion Damage	Torsion induces the increase of neutrophil adhesion in ovarian venous endothelium which leads to ROS production and causes Ovarian Ischemia and perfusion Damage.	EDR anti-oxidant action treats ischemic events and reduces oxidative stress induced by ovarian torsion.	[174]
Extensive Burn Injury	Extensive burn injury leads to the production of free radicals and follows by massive fluid resuscitation.	EDR eliminate free radical precursors and their metabolites.	[175]
Osteonecrosis	Patients who are taking too much steroid induces excessive production of ROS which leads to a variety of pathological conditions including vascular injury and cell apoptosis which is implicated in Osteonecrosis.	Reduce the lipid peroxidative and minimized oxidative DNA damage by the anti-oxidant effect.	[176]
Hearing Loss/ Inner Ear Barotrauma/	Free radicals in the ear are responsible for the ischemic damage.Iron–	EDR is a free radical scavenger with cochlear function against	[177-183]

Cisplatin-induced ototoxicity	antibiotic complexes generate free radicals which cause the injurious to the inner ear.	tobramycin-induced ototoxicity.	
Facial Palsy	Ischemia around the geniculate ganglion promote free radical production and increase ROS which induces tissue damage in the facial nerve.	EDR as free radical scavenger minimized the generation of ROS protects against the development of mild to moderate facial palsy.	[184]
I/R injury to skeletal muscles	I/R produces free radicals leading to lipid peroxidation and damage to skeletal muscle.	EDR with free radical scavenging and antioxidant effects inhibit lipid peroxidation of the myocyte in skeletal muscle and reduce oxidative stress which decreases dependent edema and inflammatory infiltration.	[74]
Streptomycin-induced vestibulotoxicity	Antibiotic complexes, producing free radicals	Antioxidant and free radical scavenging action.	[185]

1.5.5 EDR – As an Anti-Alzheimer Drug

Lipid oxidation is increased in Alzheimer's disease. EDR can suppress copper and endothelial cell-induced lipid oxidation of low-density lipoprotein and enhances the expression of neuroprotective eNOS in endothelial cells [186]. Previously, it was reported that EDR reduces the infarction volume of the brain, induced by ischemic reperfusion injury and inhibited neuronal apoptosis by suppressing gene expression in the Fas/FasL signaling pathway [187]. In a recent report, EDR inhibits mitochondria-dependent apoptosis, attenuating cytochrome c release and suppressing the activation of caspase-3 [188]. In aged rats with reperfusion brain injury, EDR can increase the level of glutathione peroxidase, reduce apoptosis and infarct size and inhibit the JNK-c-Jun pathway [189]. The benefits have been demonstrated in other disease models such as amyotrophic lateral sclerosis (ALS) and Parkinson's disease [163, 190-192]. As oxidative stress plays a critical role in the pathogenesis of sporadic AD [34] (Fig. 1.9), it was preferred to test for against AD. EDR breaks vicious cycles in AD pathogenesis: As shown

in Fig. 1.9, Aβ plays central roles in AD pathogenesis. It also activates several vicious cycles propagating AD development and progression [21] (Fig.1.9)

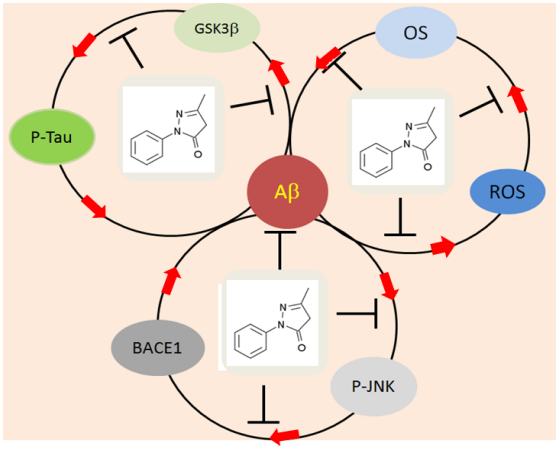

Figure 1.9 Schematic diagram depicting how EDR acts to break the vicious cycles which propagate the pathogenesis of Alzheimer's disease driven by Amyloid beta (Aβ). EDR reduces oxidative stress (OS) by scavenging reactive oxygen species (ROS) induced by Aβ and inflammation. EDR can directly interact with Aβ and reduces its fibrillization and aggregation; EDR can reduce the expression of BACE1 expression and reduce Aβ production; EDR can inhibit phosphorylation of GSK3beta and Tau and can block tauopathy.

- **Vicious cycle 1: Oxidative stress-BACE1-Aβ：** A positive feedback mechanism for Aβ overproduction operates in sporadic AD. The expression of BACE1 and presenilin 1 is increased by oxidants and by the lipid peroxidation product, 4-hydroxynonenal (HNE); BACE1 expression is significantly correlated with oxidative markers in the brain tissue of sporadic AD [32]. Both oxidative stress and Aβ activate the JNK pathway, which binds the AP1 transcription factor that regulates expression of BACE1 and presenilin1 [43]. Our data showed that EDR could break this vicious cycle by scavenging free radicals, reducing BACE1 expression and Aβ production [69].
- **Vicious cycle 2: Aβ-OS-ROS:** Aβ promotes oxidation of metal ions, which generate free radicals and reactive oxygen species (ROS) leading to OS within cells [33]. Oxidative stress and Aβ production are reciprocally regulated by each other; as such, Aβ induces OS [39-41], and OS increases the production of Aβ [30, 42]. EDR not only directly interacts with Aβ and suppresses its aggregation and fibrillization but also suppresses Aβ-induced OS and ROS, protect neurons from cell death and degeneration. Thus, EDR can break the vicious cycle of Aβ–induced vicious cycle and has strong therapeutic effect for AD [69].
- **Vicious cycle 3: *Aβ-GSK3b-Tau*:** Mitochondrial ROS and OS cause tau hyper phosphorylation [59], leading to accumulation of NTF in neurons. Aβ also activates the upstreaming kinases GSK3b and CDK5 which phosphorylate Tau, also leading to

hyperphosphorylation of Tau which causes aggregation. These two kinases have become drug development targets for AD [22, 23]. A recent study showed that GSK3b signaling also regulated BACE1 expression and increased Aβ production [24]. Phosphatase 2A (PP2A) is the key enzyme that dephosphorylates Tau, thereby maintaining a balance in its activity and the expression of PP2A is decreased in AD brain [25, 26]. Aβ in the AD brain down-regulates PP2A, shifting the balance towards Tau hyperphosphorylation [25]. Along with aggregated NFT, it disrupts axonal transport, which leads to more Aβ production in the degenerated axon [27, 28]. EDR can break this vicious cycle by reducing the phosphorylation of Tau at S262 and decreased that of GSK3b at S9 [69].

Moreover, the protective effect of EDR against AD-like insults in neuroblastoma N2a cells was reported by attenuating cytochrome c release, suppressing the activation of caspase-3 and decreasing the Bax/Bcl-2 ratio [193]. Also, its inhibitory effect on A-β-PP processing and enhancing non-amyloidogenic pathway for the regulation of Aβ production using human ‘‘Swedish’’ APP mutation APP695 (SY5Y-APP695swe) was shown [194]. Also, its efficacy in streptozotocin-induced and Aβ-induced rat models were demonstrated improvement against the cognitive dysfunction [195-197]. Additionally, its therapeutic potential in double transgenic (Tg) APPSwe/PS1deE9 (APP/PS1) mice after three months of treatment were revealed by targeting multiple pathologies such as Aβ, oxidative stress, Tau hyperphosphorylation, synaptic dysfunction, neuronal loss, neuroinflammation, glial activation and improvement of the behavioral deficits [69].

1.5.6 Safety and toxicity studies in Animal and Human

1.5.6.1 Animals

According to Iwase *et. al.,* in animal studies there are no significant adverse events accounted for 10 mg/kg IV in rats and 30 mg/kg IV EDR in dogs [198] and this result remained the same for 26 weeks long period toxicity study [199]. However, a toxic effect like increased urinary ketone bodies, bilirubin and urobilinogen, prolongation of prothrombin time and decreased liver weight have been observed in both rats and dogs in the long period (26 weeks) study with a higher dose of EDR (100 mg/kg IV) [199]. Following a higher dose (300 mg/kg iv) EDR administration, conditions such as ataxic gait and haemolytic anaemia were observed too[198]. The toxicity effects were similar in both rats and dogs [198, 199]. Besides that adverse effects like nictation, lacrimation, incomplete eyelid closures, loss of righting reflex and reduced food consumption have been observed in rats in a 30-day toxicity study with 100 mg/kg iv EDR

[84].

Reproductive toxicity studies including fertility and fetal development in rats have shown that there were not toxicity effect towards fertility at 20 mg/kg iv and no teratogenic effects even at 200 mg/kg [200]. However, in a study of the effects of EDR in organogenesis in rats revealed that live fetuses including both male and female have significantly lower weight at 300 mg/kg of EDR [201]. Another study utilized New Zealand rabbits suggested that the frequency of embryo or fetal death increases at 100 mg/kg of EDR but no toxic effects on fetal development and organogenesis at 20 mg/kg [202].

Iwase and his team also found out that EDR does not have any mutagenic or clastogenic actions [203], EDR also has negative result in genetic toxicity test with Ames test, CHL chromosome aberration test and mouse micronucleus test [204]. It has also been demonstrated that EDR does not cause any significant allergic reactions via active cutaneous anaphylaxis, active systemic anaphylaxis, delayed-type hypersensitivity and passive cutaneous anaphylaxis tests in rabbits, guinea pigs and mice [205].

LD_{50} of EDR following iv administration is 600 mg/kg (mice), 800 mg/kg (rat) and 600 mg/kg (dog), following oral administration is 1900 mg/kg (mice) and 2193 mg/kg (rat), while following sc administration is 691 mg/kg (mice) and 1101 mg/kg (rat) [206].

1.5.6.2 Human

According to Abe *et. al.*, in 36 weeks (12 weeks per-observation + 24 weeks treatment) double-blind, parallel-group, placebo-controlled study of efficacy and safety of EDR (clinical trial Phase II), there were not a significant inter-group difference in both adverse events and serious adverse event [207]. The adverse events observed in the study were constipation, dysphagia nasopharyngitis, muscular weakness, contusion, headache, insomnia, gait disturbance, eczema, and glucose present in urine [207]. Besides this adverse effects, Mitsubishi Tanabe Pharma Corporation stated that EDR might cause other clinically significant adverse reaction like acute renal failure (incident rate: 0.27%), nephrotic syndrome (incident rate: 0.02%), fulminant hepatitis (incident rate: unknown), hepatic dysfunction (incident rate: 0.25%), jaundice (incident rate: unknown), thrombocytopenia (incident rate: 0.08%), granulocytopenia (incident rate: unknown), disseminated intravascular coagulation (incident rate: 0.08%), acute lung injury (incident rate: unknown), and rhabdomyolysis (incident rate: unknown) [208]. There were approximately 4% of patients at 20 mg EDR dose and approximately 6% of patients at

60 mg EDR dose reported that have experienced side effects but no patients with 30 mg dose were reported with any side effects [209]. But Kikuchi mentioned that usually side effects would not be observed unless patients are elderly with renal impairment [79]. In another clinical phase II and III conducted by Watanabe *et. al.*, the results obtained were coincided with the results from Abe study whereby there were not serious safety issues observed in both phase II and III [210].

1.5.7 Problems associated with drug development

The oral route is the preferred route of administration for patients with chronic neurodegenerative diseases and doctors due to the ease of administration, flexibility in dose, improved quality of life, reduced the need for the hospital stay and low cost of treatment [211]. EDR is being explored extensively in research and has development prospects due to its proven safety and efficacy [76, 79, 212]. Its clinical application is still limited due to lack of oral formulation mainly due to poor oral bioavailability [96]. Poor solubility, stability, and dissolution have been reported as the reasons for this poor oral bioavailability [213]. Additionally, it has been categorised as the substrate for P-glycoprotein (Pgp), a transmembrane protein, which could increase its excretion and restrict its distribution and lead to poor permeability (Peff = 3.18 ± 0.0706*10^{-7} cm/s) [96]. EDR was categorized as a class IV drug as per Biopharmaceutics Classification System (BCS) [96]. Also, being a substrate of uridine 5′-diphospho-glucuronosyl-transferase (UGT) enzymes, it rapidly undergoes extensive metabolism [214, 215]. The reported absolute bioavailability of EDR was 5.23% [96]. Therefore, poor oral bioavailability (BA) could be a major challenge in enabling its oral use.

1.6 Curcumin (CUR)

1.6.1 Introduction for CUR

Natural plant products such as food and medicines are an integral part of human history. Many of these products have been successfully explored for development of drugs following modern scientific approaches. Turmeric (Curcumin Longa) is well known as the ‘golden spice’ with a history of over 4000 years of usage [216, 217]. CUR, an active ingredient isolated from turmeric, has also received serious attention in recent years for its health-related applications; indicated through its presence in over 3000 publications and 1700 patents in last 25 years [218, 219]. CUR is the natural antioxidant compound extracted from the rhizome of turmeric [220]. Regarding therapeutic value, it is the most important active ingredient present in turmeric, unlike others such as the less active demothoxycurcurmin or bisdemethoxycurcurmin [221, 222]., CUR is one of the most widely used herbal medicines specifically in Asian countries

[223]. Specifically, it has been used as a dye, a supplement, in food and cosmetic industries across the world [224, 225].

1.6.2 Chemistry of CUR

CUR is chemically 1, 7-bis-(4-hydroxy-3-methoxyphenyl)-hepta-1, 6-diene-3, 5-dione $C_{21}H_{20}O_6$ (Fig. 1.11) [219]. It has a molecular mass of 368.39 g/mol and is lipophilic. Structurally, comprises of two methoxy phenols attached to α & β-diketone [226, 227]. These phenolic and diketone functional groups possess the antioxidant property and, therefore, are responsible for the antioxidant activity of CUR [219, 228]. CUR's action as a Michael acceptor is due to keto-enol tautomerization (Fig. 1.11) [229]. Its solubility in polar solvents such as methanol, ethanol, and ethyl acetate is better than in aqueous solutions [230].

1.6.3 Therapeutic efficacy

CUR is one of the most bioactive molecules ever discovered from nature. Indeed, through its interaction with various intracellular and extracellular targets, CUR can affect different biological processes, including oxidative stress, inflammation, homeostasis, survival, and proliferation of cells [231]. The cells with irregular physiology, presenting in abnormal states could also be targeted by CUR [232]. CUR's lipophilic nature favors its permeability across physiological barriers, including the blood-brain barrier (BBB) [233].

The pharmacological effects of CUR against various diseases such as inflammation, neurological disorders, cancer, infectious diseases, as well as lifestyle associated diseases have also been reported [234]. Therefore, numerous *In-vitro*, animal and clinical studies have recommended its efficacy against a wide and diverse range of diseases (Fig. 1.10).

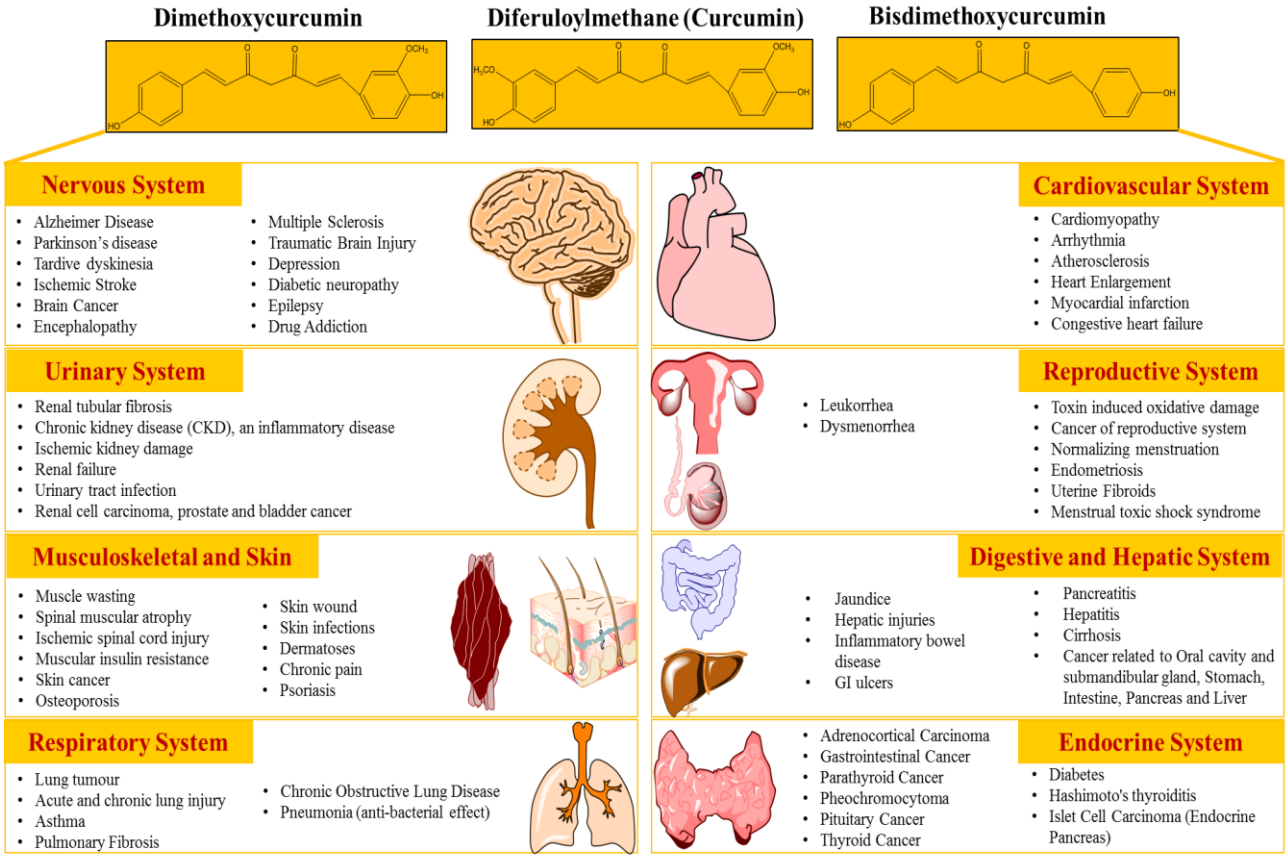

Figure 1.10 Curcuminoid's (Diferuloylmethane, desmethoxycurcumin, bisdemethoxycurcumin) therapeutic effects on different body systems associated diseases [227].

1.6.4 CUR for Alzheimer disease

Numerous *in-vitro* studies have been demonstrated the potential benefit of CUR on Alzheimer's disease. Various mechanisms have been proposed and examined based on the *in-vitro* and *in-vivo* studies, including inhibition of Aβ aggregation, and Aβ induced inflammation, inhibition of BACE1, inhibition of acetylcholinesterase activity, anti-oxidative properties, the effect on cholesterol metabolism, the effect on telomerase activity and chelating properties. A brief summary of potential effects of CUR on Alzheimer's disease pathophysiology is discussed below section.

1.6.4.1 Inhibition of Aβ aggregation

Aβ aggregation, especially aggregation of Aβ42 is currently the most targeted step in the pathophysiology of Alzheimer's disease for development of potential therapeutic strategies. It results in the formation of Aβ fibrils, known for their toxic effect on neurons. Also, some researchers have reported the role of Aβ oligomers in the neuronal toxicity seen in Alzheimer's disease. Nucleation-dependent polymerization model is used to represent the mechanism for

generation of Aβ fibrils as well as the development of Aβ oligomers. CUR also disaggregate the fibrillar Aβ40 and prevention of Aβ42 oligomer formation and toxicity in dose dependent manner between 0.1 and 1.0 μM [235, 236].

1.6.4.2 Inhibition of BACE1

Cleavage of APP by BACE1 is the critical step in the generation of Aβ. CUR has been shown to suppress Aβ induced BACE1 upregulation *in-vitro*, as well as suppression of APP and BACE1 mRNAs, which was enhanced with copper and manganese ions. CUR has also been shown to reduce Aβ-induced ROSs and Aβ structural changes towards β-sheets rich secondary structures [237, 238].

1.6.4.3 Inhibition of anticholinesterase (AChE) activity

CUR has been shown to impart effects on anticholinesterase enzyme similar to anticholinesterase inhibitors (AChE – inhibitors), currently the first line therapy for AD. Acting by inhibiting the breakdown of Acetylcholine, a dominant neurotransmitter, AChE -inhibitors have been shown to slow the progression of AD symptoms or even reduce the symptoms in the early phase. CUR demonstrated a dose-dependent inhibition of AChE in *in-vitro* and *ex-vivo* studies. Curcuminoids have been shown to reduce scopolamine-induced amnesia in rats [239, 240].

1.6.4.4 Anti-oxidative properties

CUR is proved to decrease the activity of a transcription factor AP-1, part of the expression pathway of amyloid. Curcuminoids have exhibited strong antioxidant properties, reducing the formation of free radicals. It decreases LDL oxidation and free radical generation associated with neurodegeneration. CUR significantly reduces lipid peroxidation and lipofuschin accumulation [241]. Animal studies have consistently shown that administration of CUR reduces infarct volume, reduces the neurological deficit and decreases cerebral edema in rats exposed to focal cerebral edema. Additionally, CUR protects brain mitochondria by neutralizing peroxynitrite, a strong oxidant [223].

1.6.4.5 Inhibition of inflammation

The studies have shown the role of inflammatory pathways in Alzheimer's disease pathology and the use of therapy with anti-inflammatory molecules in reducing the development and progression of AD. Early growth response – 1 (egr1) expression leading to increased cytokine

expression (TNF-∞ and IL-1b) and chemokine expression (MIP-1b, MCP-1, and IL-8) in monocytes. CUR is shown to inhibit egr-1 expression by the interaction of Ab40 or fibrillar Aβ42. Similarly, defective phagocytosis thought to be associated with down-regulation of MGAT3 and depressed transcription of TLR-3, bditTLR-4, TLR-5, bditTLR7, TLR8, TLR9, and TLR10, is shown to be enhanced by dimethoxy curcumin, resulting in increased MGAT3 and TLRs. It may suggest the role of dimethoxy curcumin in correcting immune defects, leading potentially to an immunotherapy approach to AD [242, 243].

1.6.5 Safety

CUR is listed as "Generally recognized as safe (GRAS)" by the US FDA. It has now been marketed as a supplement all over the world [244]. The safety of CUR was also confirmed by the National Toxicology Program (NTP); performed in rat and mouse studies for the duration of up to 2 years, with dose-escalating studies from 50 to 2600 mg/kg [245, 246]. A daily oral dose of 12 g was considered as safe and well tolerated, obtaining from phase I and II clinical trials [247]. It's safety has also been proved from the assessments in patients with oral leucoplakia, advanced pancreatic cancer, intestinal metaplasia (IM) of the gastric mucosa, multiple myeloma, Bowen disease of the skin relating to arsenic, rheumatoid arthritis, peptic ulcers, psoriasis, Dejerine-Sottas disease, uterine cervical dysplasia, Alzheimer's disease, type 2 diabetic nephropathy, bladder cancer, and lupus nephritis [234].

1.6.6 Problems associated with drug development

To accomplish desired therapeutic outcomes, it is necessary to achieve the required level of a drug at its target site [248]. The drug solubility and stability in biological fluids and physiological condition, metabolism, tissue distribution, permeability are significant factors affecting the achievement of the drug level needed to bring about therapeutic effects [249-251].

Regardless of proven efficacy and safety in multiple disease conditions through i*n-vitro* cell lines, animal and human trials, poor BA of CUR is considered as the major obstacle to its clinical development as a drug [252]. Moreover, the problems associated with the drug delivery of CUR include poor solubility, poor alkaline stability, photodegradation and extensive metabolism. These factors all account for CUR's poor BA (Fig. 1.11).

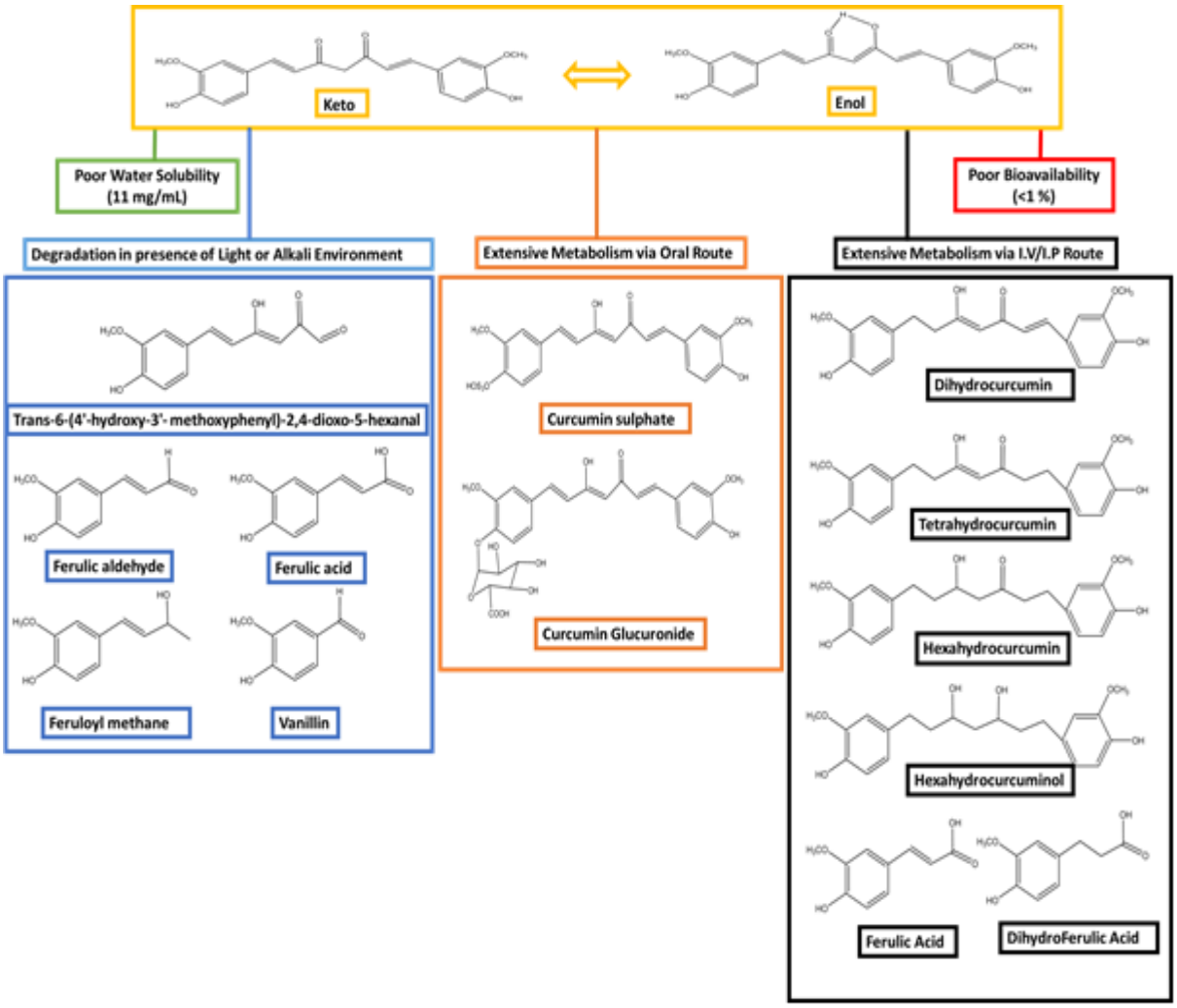

Figure 1.11 Problems associated with the use of CUR including poor solubility, poor stability at physiological, alkaline condition or in the presence of light, extensive metabolism and poor bioavailability. CUR has β-diketone chain, displays a keto-enol tautomerism. Trans-6-(40-hydroxy-30-methoxyphenyl)-2, 4-dioxo-5-hexenal, ferulic aldehyde, ferulic acid, feruloyl methane, and vanillin are the major degradants of CUR [253, 254].

1.6.6.1 Solubility

CUR is a lipophilic compound, practically insoluble in water. It was reported that the solubility of CUR in aqueous solution (pH 5.0) was only 11 ng/mL [255]. The lipophilic characteristic of CUR due to its log P value of 3.29, facilitates its permeability but rapid degradation at physiological condition together with an extensive metabolism, hampers its permeability [256]. According to the BCS class, CUR belongs to a class II drug as well as class IV [257].

1.6.6.2 Stability

The poor stability of CUR in an aqueous formulation, specifically at neutral to alkaline pH, could be considered the second major issue [258]. The phenolate ion formed in water has shown low stability at pH 7 and above, resulting in the formation of degradants (showed in Fig. 1.11) [259]. In neutral to basic environments, CUR undergoes rapid degradation, such as possessing over 90% degradation in 30 minutes at pH 7.2 [260]. CUR is relatively stable at acidic pH, showing less than 20% degradation within 1 hour, as its dissociation shifts to neutral forms and the conjugated diene structures [230]. CUR also showed poor stability in cell culture medium. However, in the addition of human blood, fetal calf serum or antioxidants such as ascorbic acid, the degradation of CUR is decreased [261]. In addition to this, CUR is also considered a light-sensitive drug. It is relatively stable at high temperature but suffers significant degradation in the presence of light, either in solution or at solid state [262]. The CUR sample prepared in transparent glassware showed 5% less CUR content, compared to formulations prepared in amber colored glassware [260].

1.6.6.3 Metabolism

The CUR metabolism depends on the route of administration as it goes for phase I metabolism based on reduction mechanism when administrated via parenteral routes For phase II metabolism, glucuronide and sulfates involved both in human and rodents [263]. The major metabolites with their chemical structures are shown in Fig. 1.11. Over 99% of CUR presented in its metabolite forms reveled from plasma hydrolysis study [264]. The liver is responsible for the extensive metabolism of CUR [265]. In detail, UDP-glucuronosyltransferase (UGT) is considered the prominent hepatic enzyme for CUR metabolism. Evidently, when CUR is co-administrated with the specific inhibitors for this enzyme, a significant improvement in its BA was obtained [266]. CUR or its metabolite were not detected in plasma or urine in a trial conducted on patients with colorectal cancer, during a period of 29 days with daily dosing of 440 – 2200 mg CUR, given orally [267]. In another study of 4-month duration, a concentration of 10 nM CUR and its metabolite was observed after 0.45 – 3.6 gm/day. However, there is no conclusion available on the comparative activity of CUR and its metabolite [252].

1.6.6.4 Bioavailability

In Sprague-Dawley rats, insignificant plasma level of CUR was reported after administrating an oral dosing of 1 g/kg; suggesting its poor BA [268]. After 50 minutes, a plasma level 15

ng/mL was detected following the same dose and route of administration. As 500 mg/kg dose, only 1% oral BA was obtained from rats' plasma [265]. Besides this, a C_{max} value of 6.6 µg/mL was achieved following an intravenous injection of 2 mg/kg dose [243]. Some studies also reported the high amount of CUR in serum compared to plasma [234]. For example, a 1.35±0.23 µg/mL serum availability of CUR was observed in rats after 2 g/kg oral CUR, after 0.83 hours [252]. Moreover, a 0.06 µg/mL serum level of CUR was achieved via oral route at 500 mg/kg dose, compared to that of 0.36 µg/mL following an intravenous administration of 10 mg/kg dose [269]. The BA observations suggest the superiority of a parenteral over oral for crude CUR.

In humans, a CUR plasma amount of 0.41-1.75 µM was determined after an hour, following an oral dosing of 4-8 g [270]. Likewise, an amount of 11.1 nM was also reported after 1 hour, post 3.6 g oral administration [271]. With 10 g and 12 g oral administrations, 50.5 ng/mL and 51.2 ng/mL CUR serum levels were detected respectively [268].

To overcome the obstacles in CUR delivery, numerous strategies have been proposed including the use of adjuvants, synthesis of CUR derivatives, and its analogues. However, nanotechnological approaches have emerged as the most prominent answer (Fig. 1.12).



Figure 1.12 Different approaches utilized to improve curcumin physicochemical properties and pharmacokinetics

1.6.7 Marketed CUR products

Table 1.4 Current CUR products in the market.

Delivery System	Name	Claim	Company	Country	References
Nano-micelle	MetaCUR®	277 fold improvement in absorption	RevGenetics	USA	[272]
Nano-micelle	NovaSOL® CUR	185 fold improvement in absorption	Molecular Health Technologies	USA	[273]
Liposome	Curcusome®	-	NanoLife Tonics	USA	[274]
Liposome	Optimal Liposomal CUR	-	Seeking Health	USA	[275]
Liposome	Liposomal Turmeric Complex	-	BioBalance	New Zealand	[276]
Liposome	Liposomal Structured CUR/Resveratrol	-	Empirical Labs	USA	[277]
Liposome	Liposomal CUR 16 fluid ounces	-	Healthy Items	USA	[278]
Phytosomes	Meriva®	31.5 fold improvement in absorption	Indena	Italy	[279]
Nanoparticles	Theracurmi®	27 fold improvement in BA	Theravalues	Japan	[280]
Nanoparticles	Nano Curcusorb®	40-60 fold improvement in BA	One Planet Nutrition	USA	[281]
Colloidal emulsion nanoparticles	Nano CUR Elixir	10 fold improvement in BA	Asia Botanicals Sdn. Bhd	Malaysia	[282]
SLN	Longvida®	65 fold improvement in BA	Verdure Sciences	USA	[283]
Nanoemulsion	Full Spectrum CUR 60 Liquid	185 fold improvement in BA	Solgar	USA	[284]

	Extract Softgels				
Nanocrystals	Curcuwin®	46 fold improvement in BA	Omniactive Health Technologies Ltd	USA	[285]
Gamma-CD	Cavadurmi®	40 fold improvement in BA	Wacker Chemie AG	Germany	[286]

1.7 Need of development of novel formulations for EDR and CUR

There are a number of drug candidates which target oxidative stress in clinical trials. These includes grape seeds-polyphenols, vitamin C, vitamin E, resveratrol, lutein, genistein, and melatonin. Based on the preclinical study in mouse models of AD, all these antioxidants have significant beneficial effects on either cognitive functions or amyloid metabolisms or significant disease-modifying effects [287, 288]. There is no doubt that these preclinical trials are necessary to facilitate the discovery of effective natural compounds for AD. However, none of these compounds has functions of targeting multiple pathways as EDR and CUR affecting all aspects of AD pathogenesis including amyloidogenesis, Tauopathy, synaptic degeneration and plasticity, cell death and ultimately cognitive functions [69-71].

For EDR, An intravenous infusion is the only commercially available formulation of EDR. Its clinical application is still limited due to lack of oral formulation mainly due to poor oral bioavailability. Several investigations based on complexation with (2-Hydroxypropyl)-β-cyclodextrin (HP-βCD) were reported to improve dissolution and permeability of EDR However, these investigational findings have not effectively translated to use for the clinical purpose.

For CUR, improvement in the solubility and dissolution of CUR are the only majorly focused area in improving oral BA compared to stability and permeability as per current trends in research. Low encapsulation efficiency, complicated preparation process, poor stability and degradation in the stomach are major factors in the failure of nanotechnology-based systems. The high molecular weight of cyclodextrin, slow process of complexation and the unstable condition of processing media limits its applicability.

The limited success at commercial scale was witnessed with EDR and CUR which motivate the need for re-formulation of EDR and CUR for repositioning of EDR and CUR for AD to achieve desired powerful disease modifying effects in a preclinical and clinical study.

There are two steps involved in the development of Formulation.

- Pre-Formulation
- Formulation Strategies

1.7.1 Pre-formulation

Drug research is a very complicated endeavor which includes several diverse disciplines united with a common goal of developing novel therapeutic agents. Due to growing complexity of drug substances, development of a quality drug product and a reproducible manufacturing process becomes more challenging and costly. The method should yield consistent, high-quality drug products that should not be affected by variation in the drug substance, excipients and raw materials [289, 290].

The role of preformulation data can be invaluable use in the discovery and development phases in Industry. For instance, in a chemistry team, pre-formulation testing provides ways and means to stabilize the chemical structure of that molecule by taking into consideration its solubility, permeability, and stability. For a biology group, pre-formulation studies that consider permeability, solubility and stability, are important tools that can be useful to idealize on optimal drug exposure for parameters. It includes pharmacokinetic & toxicological aspects. The team in analytical research gets a response from pre-formulation group on development of stability-indicating assays and get an idea of specifying drug properties. Pre-formulation studies can be of utmost help to the bulk production team on separate issues such as salt selection, purity of the polymorph and specifications that include properties like particle size. To choose an appropriate dosage form on the basis of pre-formulation studies is the primary responsibility of Formulation team. The study of parameters including solubility, permeability and stability is critical in selection of suitable excipients and processing conditions to achieve a fully efficient drug product. Pre-formulation studies are very much useful to the clinical research and evaluation team which are used in conjunction with data generated from preclinical animal studies to better understand the drug behavior and its actions achieved in humans through the maximum absorbed dose and the biopharmaceutics classification system (BCS) paradigms. It can hence be inferred that a very strong & productive preformulation team is mandatory where drug discovery is under consideration for having a highly efficient drug product as an output. In the long run, such type of expert pre-formulation team can be very useful in bringing down the attrition rates; time and cost for development of a new drug product, thus helping the globe become a better place to stay in through extensive research in fields of many other dreadful diseases [291].

To produce a well finished and effective drug product, implementation of all technical specifications and skilled labor is required. A combination of all physical, chemical and biological properties along with a wise choice of excipients & pharmaceutical drugs are needed for proper design and formulation of a dosage form. An ideal drug product and its ingredients are intended to possess properties like high stability, high-efficiency rate should be easy to administer and non-obnoxious, ease of handling and should not produce any immediate or prolonged side effects after being administered. Every dosage form possesses different physical and pharmaceutical properties [290].

Physicochemical studies have a vital role to play from a very early stage in the prediction of formulation issues and then deciding for the most favourable & efficient dosage form technology. At an early stage, physicochemical parameters evaluation has a noteworthy part of identification of formulation associated problem to develop a strategy for an unique formulation having all desired characteristic. Based on physicochemical drug properties, a suitable drug delivery approach can be selected or drug properties can be modified in terms of solubility, log P value, crystallinity, and hygroscopicity to achieve required criteria for a targeted delivery system. Physical properties such as particle size, crystalline structure and solubility are the ones responsible for having an effect on drug's parameters like dissolution and its systemic bioavailability. The secondary properties responsible are its physical appearance and melting point. Permeation capability of a drug is also key to produce a desired therapeutic response which depends on the drug's ability to pass through various biological membranes, through which it reaches its site of action and is thus included in the biological properties of the drug [290]. As a regulatory requirement, these drug substance properties should be emphasized in the pharmaceutical development section of Investigational New Drug (IND). It provides early insights to both industry and regulators. Such studies may also result in a reduction of development costs. Successful implementation of this process results in the generation of sufficient data to file an Investigation new drug application (IND) application [292]. The importance of various preformulation studies is discussed in Table 1.5.

Table 1.5 Various Preformulation study parameters with their importance in development of unique dosage form for any drug [283]

Preformulation study	Importance
Physical incompatibilities with Excipient	• To improve its manufacturability and to enhance the efficiency of any drug dose to be administered in an efficient manner and this type of interaction can affect

	therapeutic efficacy and its safety due to changes in chemical nature, stability, degradation and bioavailability at drug sites.
Biopharmaceutical aspects - absorption, distribution, metabolism and excretion	• May reduce the failure rate in clinical trials. • Compounds that are identified as poorly soluble, poor bioavailability and undergo extensive metabolism necessitates additional formulation efforts at the developmental stage
Drug solubility	• A direct relationship exists between solubility of a molecule and its dissolution rate. • Drug penetration through lipid membranes depends on how high the lipid coefficient of that molecule is, and it may thus be correlated with the partition coefficient value. • Absorption of a drug depends on the correct balance between these two opposite properties • A lack of solubility affects the ability of the drug to achieve efficacious and toxicologically relevant exposures in animals.
Drug stability	Five categories of stability issues have been considered by health care provider: • **Chemical**: Active pharmaceutical ingredient must be chemically inert and hence retain its chemical integrity and potency that is labeled, ensuring it's within the official standard limits as approved by government authority. • **Physical**: Active pharmaceutical ingredient must be maintained unique physical properties include appearance, content uniformity, dissolution, and so on as per the required standards.

	• **Microbiologic**: For sterile preparation, sterility must be maintaining throughout the shelf life of the product. • **Therapeutic**: The clinical therapeutic output must be unaffected. • **Toxicological**: The toxicological profile must be unaltered and remain under safety limit.
Hygroscopicity	• The moisture uptake rate varies for different drugs and excipients and is dependent on environmental conditions, and it often affects the stability of the Active pharmaceutical ingredient in final dosage form.
Bulk properties	• Knowledge of Bulk Properties like particle size and size distribution, flow properties and dissolution are key aspects which can affect the physicochemical features of final dosage form like Variations in the amount of biological activity can be attributed to the rate at which the drug becomes available to organism's site of action.
Melting Point	• The melting point of an active pharmaceutical ingredient has often effect on physicochemical features of final dosage form like dissolution, disintegration, friability. The drugs with low melting point often display plastic deformation which may produce an influence on flow and compressibility.
pKa/Dissociation Constants	• It indicates the extent of ionization of drug in various pH which helps in forecasting, solubility, and precipitation of drugs in the different biological fluid in the body.
Lipophilicity and partition coefficient	• The prerequisite step for any drug molecule to give a therapeutic response is to cross biological membrane which depends on lipid solubility and partition coefficient of the drug as membrane act as a lipid barrier.

Microscopic Examination	• The physical appearance of drug examine by Microscopy includes Particle size, shape, and crystal structure, have major impact on content uniformity, dissolution and bioavailability.

1.7.2 Formulation strategies

Deep understanding of the physicochemical characteristics of the molecules and early preclinical formulation assessment are key factors for a successful formulation development program [293]. Poor solubility and stability, dissolution, permeability, and metabolism profile could be considered as the major obstacles for an effective EDR and CUR therapy. Physicochemical property of drug molecules may be improved by various formulation technologies, resulted in enhancement of oral BA by formulating ideal drug delivery system [294]. To improve its physicochemical characteristic including solubility, stability, dissolution and permeability, the strategy of complexation with hydroxypropyl-β-cyclodextrin was studied [96, 213, 295, 296]. By improving solubility, dissolution, and permeability, hydroxypropyl-β-cyclodextrin based formulation showed 10.3-fold improvement in oral bioavailability. However, these investigational findings have not effectively translated to use for the clinical purpose. Therefore, the strategies including co-solvent based formulation, lipid based and solid dispersion based formulation with the polymer having self-nanomicellizing properties were finalized to investigate for enhancement of oral BA of EDR.

Similarly, poor aqueous solubility and stability, dissolution, and intestinal permeability were considered as contributing factors in poor oral BA of CUR. The limited success at commercial scale was witnessed with drug delivery approaches such as liposome, emulsion, complexation with cyclodextrin, nanosuspension, and nanoparticles. Low encapsulation efficiency, complicated preparation process, poor stability and degradation in the stomach are major factors in the failure of conventional nanotechnology-based systems [297]. The high molecular weight of cyclodextrin, slow process of complexation and the unstable condition of processing media limits its applicability [298]. Targeting multiple issues simultaneously such as solubility, stability, dissolution and permeability in one formulation could be a key step in the development of CUR loaded novel delivery system. Thus, self-nanomicellizing solid dispersion based formulation was decided to examine for enhancement of oral BA of CUR.

1.7.2.1 Co-solvent based formulation

Surfactant addition, Cosolvency, and pH adjustment are the most widely used approaches for solubilizing drug candidates with low aqueous solubility. It is also considered as a preferable one due to its inherent advantages like low cost, ease of self-administration, easy of manufacture and scale up and better safety profile [299]. It could be the individual or mixtures of water miscible surfactant often used to water which can dramatically change the solubility of drugs. The solubility could increase with the increment of surfactant amount. This process is called cosolvency as solubilizing agent used to increase solubility are also known as cosolvent. The cosolvents reduce water's ability to squeeze out hydrophobic compounds by rupturing water's self-association, thus increase the solubility. Moreover, it could supply as liquid dosage form, which has been proven to be easily swallowed and therefore of benefit to geriatric and pediatric patients as a delivery method [300].

Pharmaceutical excipients can improve the performance of an active compound and its use in pharmaceutical dosage [301]. For EDR, there is a need for a vehicle which can solubilize the desired quantity, modulate P-glycoprotein 1 (Pgp) efflux pump to improve the permeability and inhibit (UDP-glucuronosyltransferase (UGT) to reduce the metabolism. Labrasol, a water-miscible surfactant, has been used successfully to improve drug absorption by solubilisation and by modulating Pgp efflux pump for drugs such as vancomycin [302], low molecular weight heparin [303], gentamicin [304], and rifampicin [305]. Moreover, Labrasol is also proven as a UGT inhibitor excipient [306]. Labrasol has a carbon chain length of C8 to C10 and Hydrophilic-Lipophilic Balance (HLB) value of 14. It is obtained by the polyglycolysis of medium-chain triglycerides containing 30% fatty acids, 50% esters of polyethylene glycol and 20% free PEG 400. The coconut oil like medium chain triglycerides, caprylic/capric acid and PEG 400; and alcoholysis/esterification process are used to synthesize Labrasol [302, 303, 305, 307]. Labrasol has a proven its safety via oral administration with 22 g/kg of LD_{50} value in rats and a dose of 1 g/kg/day in dogs for 13 weeks [308]. Labrasol has been successfully used to formulate sparingly water-soluble Non-steroidal anti-inflammatory drugs (NSAIDs) piroxicam in Piroflam-Li (Germany). A soft gelatin capsule containing Labrasol as the solubilizing excipient is also reported from Sidmak Laboratories [309].

1.7.2.2 Lipid-based formulation

Lipid-based drug delivery include drug dissolved in a mixture of one or more lipophilic and hydrophilic surfactants and a cosurfactant. Lipid formulations remain in the dissolved state

throughout its transit in the GI tract. The absorption of the drug within a colloidal dispersion is enhanced since the drug dissolution step is partially evaded [310].

Lipid-based formulations are categorized based on their composition and properties.

- Type I - Non-dispersing systems
- Type II- Self-Emulsifying Drug delivery systems (SEDDS): non-water soluble component systems
- Type III-SMEDDS: water soluble component systems
- Type IV-dispersion systems: non-oil micellar Systems

Self-Emulsifying / Micro emulsifying drug delivery systems (SMEDDS) are isotropic mixtures of oil, hydrophilic surfactant, cosurfactant, and a solubilized drug. These formulations spontaneously form nano emulsion in the case of SMEDDS upon dilution with water. Surfactant concentration is very high in SMEDDS, therefore upon dilution, the drug molecule remain in oil droplets, or it forms a micellar solution. They get easily dispersed in GI tract. Wherein, gut motility of the stomach and small intestine offers the moderate agitation required for emulsification [311]. Rate and extent of absorption of the hydrophobic drugs are improved using SMEDDS whose absorption is dissolution rate limited. Moreover, There are several mechanisms proposed that SMEDDS can increase absorption which can be achieved due to retardation of gastric transit time, increase in effective drug solubility in the lumen, enterocyte-based drug transport, lymphatic transport of the drug and increase membrane permeability [312].

SMEDDS also offers salient features including enhanced oral bioavailability, reduction in dose, more consistent temporal profiles of drug absorption, selective targeting of drug toward specific absorption window in GI tract, protection of drug from the hostile environment in gut, control of delivery profiles, reduced variability including food effects, protective of sensitive drug substances, high drug payloads, can be autoclaved and also formulated in liquid or solid dosage forms.

The commercial success of liquid lipid-based nanoformulations is limited due to stability concern including the interaction of components with gelatine capsules, the interaction between the components and issues related to oxidation of the oil [313]. By converting liquid to solid lipid-based nanoformulations using solid adsorbents, it is possible to overcome issues including stability and handling problems. Various hydrophilic carriers including lactose, sorbitol, mannitol and hydrophobic carriers including colloidal silica, and dextran, were widely utilized [314, 315].

The selection of surfactants is the critical step as it plays a significant role in modifying metabolism and permeability profile by inhibiting Cytochrome P450 (CyP450), UGT enzymes and modulating Pgp efflux pump [306, 316, 317]. It which has been successfully utilized to enhance oral BA of drugs such as Exemestane [318], Coenzyme Q10 [319], Curcumin [266], and Fenofibrate [320]. The marketed formulations are mentioned in below-mentioned Table 1.6. Neoral, Norvir, and Fortovase are commercially successful products based on lipid-based nanoformulations strategy [321].

Table 1.6 Market formulations based on SMEDDS strategy [291]

Dosage form	**Brand Name**	**Drug**	**Innovator**
Soft gelatin capsule	Neoral	Cyclosporin	Novartis
	Norvir	Ritonavir	Abbott Laboratories
	Fortovase	Saquinavir	Roche
	Agenerase	Amprenavi	Glaxo Smithkline
	Convulex	Valproic Acid	Pharmacia
	Targretin	Bexarotene	Ligand
	Rocaltrol	Calcitriol	Roche
	Juvela	Tocopherol nicotinate	Eisai Co.
	Restandol	Testosterone undecanote	Organon Labs.
	Glakay	Menatetrenone	Eisai Co
	Epadel	Ethyl icosapentate	Mochida Pharmaceuticals
	Lipirex	Fenofibrate	Genus
Hard gelatin capsule	MXL	Morphine sulphate	Napp Pharmaceuticals
	Selbex	Teprenone	Eisai Co.
	Gengraf	Cyclosporin	Abbott Laboratories

1.7.2.3 Solid dispersion (SD) based formulation

"Solid dispersion" refers to the solid state dispersion of one or more active ingredient in an inert carrier or matrix. It can be prepared by melting (fusion), solvent, or the melting-solvent method. It is a system in which the drug is dispersed in the polymer matrix in either crystalline or amorphous form. The carrier gets dissolved when solid dispersion is exposed to aqueous media leading to drug release into smaller particles, which also increase the exposed surface area of the drug particle facilitating the improved rate of dissolution and bioavailability for the poorly water-soluble drug. [322].

Self-nanomicellizing solid dispersion (SNMSD) is the novel strategy which offers the advantage of the SD based strategy and nanotechnology as it forms Nano-sized micelles upon contact with an aqueous media [323]. It is also a mixture of active pharmaceutical ingredient (API) with a single or multiple pharmaceutical carriers which could generate nano-sized micelles. It improves the physicochemical profile of API like solubility, and dissolution by nanosizing, enhancing wettability, and polymorphic changes [324, 325]. Moreover, it could protect the drug against the degradation in a physiological condition. Additionally, it offers a superior loading ability, stability, simple manufacturing and scale-up process, economic, possibility of translating into the conventional oral solid dosage form such as tablets and capsule over other technologies [326]. Also, its potential for enhancing oral BA was proven with a number of drugs including Cyclosporine A [323], Valsartan [327], and 9-nitrocamptothecin [328]. The selection of the appropriate carrier as per the characteristics of the drug is the key step in achieving the desired outcome.

Few studies with limited success were reported based on CUR loaded SD with the polymers Gelucire® 50/13 [329], D-α-Tocopheryl Polyethylene Glycol 1000 Succinate [330] and Eudragit® E PO [331]. For EDR and CUR, there is a need for carrier which can offer protection in physiological conditions and enhancement of the intestinal permeability with improving solubility and dissolution. The polymer such as Soluplus® (SOL), forms the micelles by accommodating polyethylene glycol moiety at wall and vinyl acetate and vinyl caprolactam side chains inside the micelles above its critical micelle concentration (CMC) of 0.0007% w/v at 37°C [332]. SOL is a 4th generation novel amphiphilic polymer has successfully improved the BA of drugs having similar characteristics of CUR including Aprepitant [333], Carvedilol [334], Quercetin [335]. It is chemically Polyethyleneglycol–polyvinyl caprolactam– polyvinyl acetate grafted copolymer (PEG 6000/vinylcaprolactam/vinyl acetate copolymer, BASF,

Germany). It acts as a solubilizer by enhancing wettability and nanosizing, stabilizer by encapsulating the drug in micelles and reducing recrystallization rate of drugs; and permeability enhancer by modulating Pgp efflux pump [328, 332]. The marketed formulations are mentioned in Table 1.7.

Table 1.7 Marketed formulations based on Solid dispersion based strategy [315]

Dosage Form	Brand Name	Drug	Innovator
Capsule	Sproronox	Itraconazole	Janseen Pharmaceutica
	Cesamet	Nabilone	Lilly
	Gris-PEG	Griseofulvin	Novartis
	Kaletra	Lopinavir and ritonavir	Abbot Laboratories
Tablet	Isoptin SRE-240	Verapamil	Abbot Laboratories
	Intelence	Etravirine	Janseen Therapeutics
	Certican	Everolimus	Novartis
	Afeditab	Nifedipine	Actavis
	Rezulin	Piogliatazone and Metformine Hcl	Pfizer
	fenoglide	fenofibrate	Salix

1.8 Hypothesis, aim, and significance

1.8.1 Rationale and Hypothesis

On the basis of generated preliminary data at our laboratory and extensive literature review shows that EDR and CUR directly have a powerful disease modifying effect via i) acts on amyloid β-protein (Aβ) by inhibiting its aggregation and promoting its disaggregation; ii) halts the progression of amyloid plaques and enhances memory and learning; iii) suppresses Aβ production by inhibiting BACE1 expression; iv) inhibits Aβ -induced increases in reactive oxidative species (ROS); and, v) inhibits Aβ -induced Tau phosphorylation. Regardless of its cutting-edge pharmacological activity and safety, poor oral bioavailability (BA) is the major obstacle to their potential use. To reposition EDR and CUR for AD and to achieve desired pharmacological outcome in a preclinical and clinical study, it is necessary to develop a novel formulation to curb the issues that limit in achieving desired concentration at a target site. Thus, the purpose of the current research was to reposition of EDR and CUR for AD by developing novel oral delivery systems of EDR and CUR to enhance their oral bioavailability. Due to limited attention towards defining its physicochemical characteristics and unfavorable oral pharmacokinetic profile of EDR, the pre-formulation study was conducted as an initial step. Based on preformulation profile, the strategies including co-solvency (chapter 2), lipid-based

(chapter 3) and self-nanomicellizing solid dispersion (SNMSD) (chapter 4) were investigated to enhance its oral BA.

For CUR, an extensive literature has been already reported regarding the preformulation profile of CUR, and poor aqueous solubility and stability, and permeability are designated as limiting factors for poor oral BA. Targeting multiple issues simultaneously such as solubility, stability, dissolution and permeability in one formulation could be a key step in the development of CUR loaded novel delivery system. SNMSD is the only novel strategy which offers the advantage of the SD based strategy and nanotechnology as it forms nanosized micelles upon contact with an aqueous media to improve solubility, stability, dissolution and permeability simultaneously. Therefore, SNMSD (chapter 5) was identified as a potential strategy to curb the issues which limit its oral BA. Moreover, to rapidly move this drug into clinical trials, several key questions needed to be addressed such as

- Can an oral formulation achieve a therapeutic bioavailability of the drug?
- Can the novel formulation rescue AD-like memory deficits?
- Is novel oral formulation produce any chronic toxicity?
- What is the optimal dosage for oral formulation for the best efficacy with least toxicity?

I hypothesize that separate novel oral formulation of EDR and CUR would alleviate their limiting physicochemical factors with enhancement of oral BA, well tolerated and ameliorates the AD-like memory deficits transgenic AD mice model (TgAD) (APPS/PS1).

1.8.2 Aim and Objective

1.8.2.1 EDR drug

- To perform Preformulation study (Chapter 1).
- To develop and characterize novel oral EDR formulation based on co-solvent, lipid, and self-nanomicellizing solid dispersion strategies (Chapter 2, 3 and 4).
- To determine safety and efficacy of selected novel oral EDR formulation in dose dependent manner in AD mice model with long-term exposure (3 months) via the oral route (Chapter 4).

1.8.2.2 CUR Drug

- To develop and characterize novel CUR formulation based on self-nanomicellizing solid dispersion strategies (Chapter 5).

- To determine safety and efficacy of selected novel oral CUR formulation in AD mice model with long-term exposure (3 months) via the oral route (Chapter 5).

1.8.3 Outcome and significance

Developing a drug for AD remains a holy grail and is one of the most challenging tasks for scientists and clinicians from more than 100 years. Despite the wealth of knowledge available about AD, only a limited of options are currently accessible. Recent repetitive failures of phase II-III AD clinical trials call upon the need for the efficient use of therapeutic agents targeting multiple pathways. EDR and CUR are potential drugs for Alzheimer's disease as it acts on multiple pathways of AD pathogenesis like breaking the key signals leading to vicious cycles in AD pathology, thus improving learning and memory and able to arrest Neurodegeneration with stimulating Neuroregeneration. Preformulation study of EDR will provide information required to develop oral drug delivery system ideal for AD treatment, which in turn will reduce time and cost measures for developing the treatment protocols and decreases the attrition rate. The Pharmacokinetic and bioavailability study of the oral formulation will give an idea of the fraction of an administered dose of unchanged drug that reaches to the systemic circulation to predict the therapeutic response. A preclinical trial on an AD model is also essential to prove its effectiveness before any clinical trials regarding safety and efficacy for AD disease. My dissertation project has been designed to develop EDR and CUR therapy for Alzheimer Disease with a foolproof strategy which will bring drugs with formulation directly into clinical trials and, if successful; it can be translated into early registration of a valuable therapy for AD.

2. Development of a Novel Oral Delivery System of Edaravone for Enhancing Bioavailability

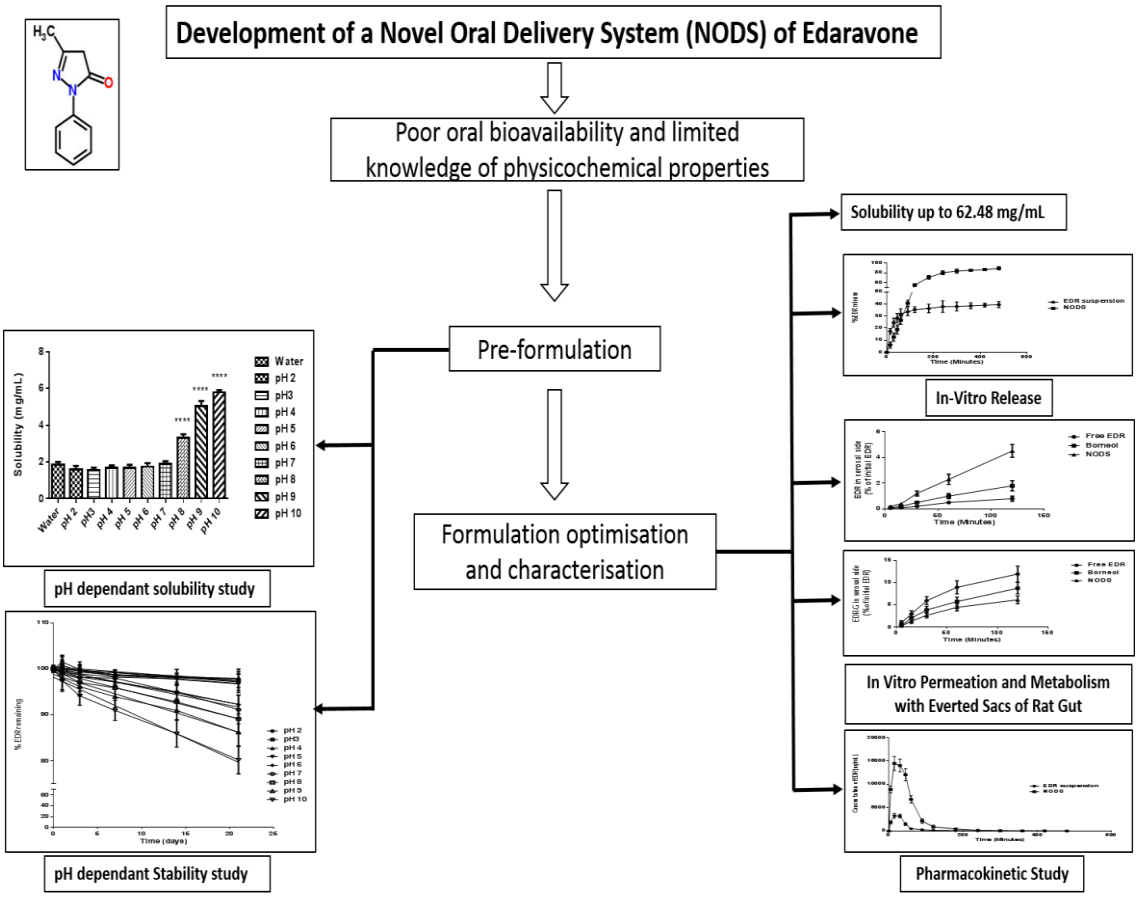

Graphical Abstract

International Journal of Pharmaceutics 515 (2016) 490–500

Contents lists available at ScienceDirect

International Journal of Pharmaceutics

journal homepage: www.elsevier.com/locate/ijpharm

Development of a novel oral delivery system of edaravone for enhancing bioavailability

Ankit Parikh, Krishna Kathawala, Chun Chuan Tan, Sanjay Garg*, Xin-Fu Zhou*

School of Pharmacy and Medical Sciences, University of South Australia, Adelaide, SA 5000, Australia

ARTICLE INFO

Article history:
Received 19 September 2016
Received in revised form 14 October 2016
Accepted 23 October 2016
Available online 24 October 2016

Chemical compounds:
Edaravone (PubChem CID: 4021)
Borneol (PubChem CID: 1201518)
Labrasol

Keywords:
Edaravone
Labrasol
Aqueous stability
Metabolism
Permeability
Oral bioavailability

ABSTRACT

Edaravone (EDR), a strong free radical scavenger, is known for its promising therapeutic potential in oxidative stress (OS) associated diseases, however poor oral bioavailability is the major obstacle in its potential use. Oral liquid dosage form is the most preferred delivery method in paediatric, geriatric and specialised therapies. The present research discusses the development of a Novel Oral Delivery System (NODS) of EDR to enhance oral bioavailability. From preformulation study, solubility, and stability were identified as key challenges and the requirement of an acidic environment and protection against oxidation were found to be critical. The NODS made up of a mixture of Labrasol (LBS) and an acidic aqueous system, was optimized on the basis of solubility and stability study. It can be stored ≤40 °C for at least one month. Drug release from NODS was slow, sustained and significantly better as compared to suspension. The significant reduction in metabolism and improvement in permeability across the small intestine were observed with NODS compared to free EDR. The oral pharmacokinetic study showed 571% relative bioavailability with NODS compared to EDR suspension. From the results obtained, NODS is a promising candidate for use in OS associated diseases.

© 2016 Elsevier B.V. All rights reserved.

1. Introduction

Oxidative stress (OS) due to an overload of free radicals, is one of the main factors that is involved in the pathogenesis of diseases such as neurological disorders, cardiovascular diseases and cancer (Essick and Sam, 2010; Reuter et al., 2010). A strong free oxygen radical scavenger, like edaravone (EDR) (3-methyl-1-phenyl-2-pyrazolin-5-one, MCI-186,) was shown as a potential therapeutic candidate for diseases associated with OS (Kikuchi et al., 2012, 2013). In 2001, Radicut®, an aqueous based parenteral preparation of having 1.5 mg/mL of EDR developed by Mitsubishi Tanabe Pharma Corporation (Japan), was first approved to treat patients of acute ischemic stroke (AIS) in Japan (Anonymous, 2015a; Lapchak, 2010). Furthermore, orphan designation for undisclosed oral formulation of EDR developed by Netherlands based company Treeway, was granted for amyotrophic lateral sclerosis (ALS) by regulatory agencies including European Medicines Agency (2014), (Anonymous, 2015d) and U.S. Food and Drug Administration (USFDA), (2015), (Anonymous, 2015b). Subsequently, Radicut® has been approved in Japan for ALS treatment from 2015 (Anonymous, 2015a). In addition, its therapeutic potential for Alzheimer's disease has been recently revealed (Jiao et al., 2015).

EDR is being explored extensively in research and has development prospects due to its proven safety and efficacy (Kikuchi et al., 2012, 2013, 2011). Its clinical application is still limited due to lack of oral formulation mainly due to poor oral bioavailability (Rong et al., 2014). Poor solubility, stability and dissolution have been reported as the reasons for this poor oral bioavailability (Zeng et al., 2011). Additionally, it has been categorised as the substrate for P-glycoprotein (Pgp), a transmembrane protein, which could increase its excretion and restrict its distribution and lead to poor permeability (*Peff* = 3.18 ± 0.0706 10^{-7} cm/s) (Rong et al., 2014). EDR was categorised as a class IV drug as per Biopharmaceutics Classification System (BCS) (Rong et al., 2014). Also, being a substrate of uridine 5′-diphospho-glucuronosyl-transferase (UGT) enzymes, it rapidly undergoes extensive metabolism (Li et al., 2012; Ma et al., 2012). The reported absolute bioavailability of EDR was 5.23% (Rong et al., 2014). To improve its physico-chemical characteristic including solubility, stability, dissolution and permeability, the strategy of complexation with hydroxypropyl-β-cyclodextrin was studied (Zeng et al., 2011; Rong et al., 2014; Sato et al., 2009, 2010). By improving solubility, dissolution and permeability, hydroxypropyl-β-cyclodextrin based formulation

* Corresponding authors.
E-mail addresses: Sanjay.garg@unisa.edu.au (S. Garg), xin-fu.zhou@unisa.edu.au (X.-F. Zhou).

http://dx.doi.org/10.1016/j.ijpharm.2016.10.052
0378-5173/© 2016 Elsevier B.V. All rights reserved.

showed 10.3-fold improvement in oral bioavailability. No information on liquid formulation for oral administration has been reported.

An intravenous infusion is the only commercially available formulation of EDR (Rong et al., 2014). The most preferred in terms of patient compliance is oral route (Shahiwala, 2011). The liquid dosage form has proven to be easily swallowed and therefore of benefit to geriatric and paediatric patients as a delivery method (Liu et al., 2014). For successful liquid formulation, solubility and stability are the two key factors to be considered (Niazi, 2009; Strickley, 2004). The effect of pH on solubility and stability of EDR was not assessed. Similarly, the influence of temperature, light, oxygen, initial concentration of EDR and plasma on the stability of EDR has not been evaluated. Hence, pre-formulation profile needs to be established for the development of Novel Oral Delivery System (NODS) of EDR.

Pharmaceutical excipients can improve the performance of an active compound and its use in pharmaceutical dosage (Fatouros et al., 2007). For NODS of EDR, there is a need for a vehicle which can solubilise the desired quantity, modulate Pgp efflux pump to improve the permeability and inhibit UGT to reduce the metabolism. LBS, a water-miscible surfactant, has been used successfully to improve drug absorption by solubilisation and modulating Pgp efflux pump for drugs such as vancomycin (Rama Prasad et al., 2003a,b), low molecular weight heparin (Rama Prasad et al., 2004), gentamicin (Rama Prasad et al., 2003a,b), and rifampicin (Ma et al., 2011). Moreover, LBS is also proven as a UGT inhibitory excipient (Zhou et al., 2015). LBS has been successfully used to formulate sparingly water-soluble Non-steroidal anti-inflammatory drugs (NSAIDs) piroxicam in Piroflam-Li (Germany). A soft gelatin capsule containing LBS as the solubilising excipient is also reported from Sidmak Laboratories (Strickley, 2004).

The objective of the present research was to develop the NODS of EDR for improvement of oral bioavailability and enhancement of patient compliance. The preformulation profile was established to identify suitable conditions for NODS. The selection of pharmaceutical ingredients and its ratio for NODS was optimised based on solubility and stability study. *In-vitro* performance of NODS was evaluated for protection against extensive metabolism and for permeability enhancement through the small Intestine. The *in-vivo* oral bioavailability of NODS compared to suspension was investigated in adult rats.

2. Materials and methods

2.1. Materials

EDR was purchased from Aladdin Industrial Corporation (Shanghai, China). LBS was gifted by Trapeze Associates Pty Ltd, Gattefosse (Clayton, VIC, Australia). Hydrogen peroxide, octanol, potassium pyrophosphate, Tyrode's solution, ascorbic acid, sodium carboxy methylcellulose, DMSO, conc. HCL, di-sodium hydrogen phosphate, citric acid, perchloric acid, formic acid, uridine-diphosphateglucuronic acid trisodium salt (UDPGA), alamethicin, and D-glucaric acid 1, 4-lactone were purchased from Sigma Aldrich (Sydney, NSW, Australia). Acetic Acid, phosphoric acid, sucrose, magnesium chloride, and sodium hydroxide pellets, were purchased from Chem Supply (Adelaide, SA, Australia) Boric acid was obtained from Optigen Scientific (Adelaide, SA, Australia) and Saline from Pfizer (West Ryde, NSW, Australia). Human Plasma was obtained from BioreclamationIVT (Westbury, New York, USA). Fresh blood samples were collected from 10 to 12 week old male Sprague-Dawley rats and the plasma was extracted. Pierce BCA Protein Assay Kit was purchased from Thermo Fisher Scientific, Australia. Millipore Ultra-Pure Water System was utilised as a source of MilliQ water (Millipore Australia). All the mobile phase components were of HPLC grade. All other chemicals and reagents were of analytical grade.

2.2. Analytical methods

2.2.1. HPLC method

The analytical method from the Japanese Pharmacopeia was used with minor modification (Komiyama, 2012). The samples were analysed using a HPLC system (Shimadzu, Kyoto, Japan) with an Ultraviolet–visible spectrophotometer as a detector (model: SPD-20A), an online degasser (model: DGU-20A3), a system controller (model: CBM-20A), an auto sampler (SIL-20AHT), a pump (LC20AD) and a LC solution Chromopac data processor at the wavelength of 240 nm. A Waters Symmetry^{TM} C18 (3.9*150 mm) (part no WAT046980) analytical column and the mobile phase consisting of methanol, milliQ water and acetic acid in the ratio of 100:100:1 (v/v/v) were used. The flow rate was maintained at the rate of 1 ml/min and sample injection volume was 20 μl. The mean regression equation for EDR for the concentration range of 10–180 $\mu g ml^{-1}$ was $y = 106299x - 355277$ ($r = 0.9999$, $n = 10$), where x and y represent the concentration and the peak area of EDR, respectively.

2.2.2. LC/MS/MS method

The samples were analysed by using a Quadrapole LC/MS/MS (Shimadzu, Kyoto, Japan) system fitted with API 3000 mass spectrometer, LC system having an online degasser (model: DGU-20A3), a system controller (model: CBM-20A), a pump (LC20AD) and an auto sampler (SIL-20AHT); and an Analyst 1.6.2 data processor. The concentration of EDR was estimated by using a reported LC/MS/MS method in literature with minor modification (Ma et al., 2012). The extracts were reconstituted in methanol: water mixture (50:50). The chromatographic separation was carried out by using a phenomenex lura C18 (50 mm × 3 mm × 3 μm) column. The gradient method was used containing mobile phase A (MPA) (5% methanol + 95% water + 0.1% formic acid) and B (MPB) (95% methanol + 5% water + 0.1% formic acid) with the program from 15% MPB initially to 70% MPB in 7.5 min, set to 100% for further 0.5 min, followed by 15% for 2 min. The flow rate and injection volume were 0.2 ml/min and 15 μl respectively with total run time of 10 min. The electro spray ionization (ESI) with negative mode was utilized for mass spectrometry. To gain the desired performance, the optimisation of parameters was carried out with the ionization source. The specific transition of EDR (175.1/133.1) and phenazone (189.1/147.1) (as an internal standard) from precursor ion to ion transition (m/z) were analysed in the multiple reaction monitoring mode. Zero air and nitrogen gas were applied as the source gas and both curtain and collision gas, respectively. The calibration curve was plotted based on the peak areas obtained from the known concentration of the drug and the internal standard. The linearity was observed between the concentrations of 10 to 500 ng/mL.

2.2.3. Determination of EDR glucuronide metabolites (EDR-G)

It has been reported that by the heat-acid treatment, nearly 100% EDR glucuronide is hydrolysed, and EDR was found stable against heat-acid treatment (Mizuno et al., 2007). The hydrolysis using 3N HCL was performed as reported in the literature (Mizuno et al., 2007). The EDR glucuronide concentration was estimated by deducting the EDR concentration from the heat-acid treated EDR (i.e. sum of the EDR and its glucuronide conjugate).

2.2.4. Drug extraction from plasma

To determine the concentration of the EDR in plasma, the plasma (120 μl) was added to 1 ml of McIlvaine buffer of pH 5.4 and extracted by using a dichloromethane-*n*-pentane in the ratio of

3:7 v/v. After separating the organic layer by centrifugation for 3000 RPM for 20 min, it was evaporated under a stream of nitrogen at room temperature (Mizuno et al., 2007). The mixture of water and methanol (50:50) was used to reconstitute the residue.

2.3. Preformulation study

2.3.1. Solubility profile

The aqueous solubility of EDR based on pH was conducted between pH 2–10 by using universal buffer (pH 2–8) and alkaline borate buffer systems (pH 9–10) and compared with milliQ water. The universal buffer solutions were prepared using boric acid, citric acid and phosphoric acid. The pH of final solution was adjusted by using 0.2 M NaOH (Wang et al., 2015). The alkaline borate buffer was prepared as per United States Pharmacopeia guidelines. An excess amount of EDR was added to the glass vials containing 2 ml of vehicle which was covered with aluminium foil and sealed with paraffin film to protect against light and moisture. A mechanical shaker (Model: so4036, Axyos Technologies, Brisbane, Australia) was used for 24 h at room temperature (25 °C). The samples were filtered through 0.45-μm polyvinyl difluoride (PVDF) syringe filters. The filtrate was diluted with mobile phase followed by analysing using UV-HPLC method. All solubility studies were performed in triplicate (Zhang et al., 2014).

2.3.2. Stability study

All stability studies were carried out with 500 μg/mL EDR solution for 21 days in triplicate. The influence of pH on the stability of EDR, was studied between pH 2–10. (Robinson et al., 2015). The EDR solution (2 ml) was prepared in glass vials and covered with aluminium foil and sealed with paraffin film. The samples were stored at 25 °C. Thermal stability was assessed by incubating an aqueous solution to various stability conditions including 4 °C, 25 °C/60% RH, and 40 °C/75% RH (Kuehl et al., 2006). Stability to oxidation was assessed by exposing a solution of EDR in 0.03%, and 3% hydrogen peroxide (H_2O_2) (Blessy et al., 2013). For photo stability, the drug solution was stored in KBF ICH 720 (E2) – constant climate chamber as per ICH recommendation (Group, 1996). The concentration dependent stability was conducted at 50, 100, 500, and 1000 μg/mL (Kuehl et al., 2006). The samples were collected at desired time points, filtered and analysed using UV-HPLC method.

2.3.3. Stability study in human and rat plasma

The 100 μl of EDR solution in water (100 μg/mL) was mixed with the blank rat/human plasma (5 ml) and incubated at 37 °C. The samples were collected at 0, 5, 15, 30, 45, 60, 90, 120, 180, 240, 300, 360, 420, 480, and 1440 min and immediately transferred to ice bath. Later, the extraction was carried out by previously mentioned method in Section 2.2.4. The determination of drug concentration was carried out by LC/MS/MS method (Gualdesi et al., 2014).

2.3.4. Log Po/w determination

The Log Po/w of EDR was determined by using a reported protocol in literature with minor modification (Zhang et al., 2014). The octanol:aqueous solutions (milliQ water, and phosphate-buffered saline (PBS) of pH 7.4 in the ratio of 1:2 (V/V) were prepared. The mixture of the above prepared solutions were stored at room temperature for 24 h for pre-saturation. The known amount of EDR was added to the above solutions and were rotated continuously on a mechanical shaker (Axyos Technologies, Brisbane, Australia) for 120 h at room temperature (25 °C). An aliquot from the aqueous phase was collected and the concentration of EDR was determined by UV-HPLC method. Based on the known distribution of the EDR in the aqueous phase, the concentration of EDR in the octanol phase was determined. A log $P_{o/w}$ value was determined as a logarithmic ratio of EDR in octanol phase to that of the aqueous phase. The ChemBioDraw® Ultra 14 from PerkinElmer was used to determine the calculated $logP_{o/w}$ ($cLog_{o/w}$). All measurements were carried out in triplicate.

2.4. Formulation development

2.4.1. In-vitro *glucuronidation assay*

To evaluate the effect of LBS on the metabolism of EDR, *In-vitro* glucuronidation assay was performed with rat liver microsomes (Pranav Patel and Panchal, 2014; Zhou et al., 2015). The differential centrifugation method was used to prepare rat liver microsomes. After 12 h of fasting of male wistar rat, fresh liver was collected and rinse with cold saline. The homogenisation (Model: Precellys 24 homogenizer, Bertin Technology) of liver was carried out in sucrose solution (0.25 M) (1:4 w/w). After centrifugation (Model: Centrifuge 5415 R, Eppendorf) of homogenates at 9×10^3 relative centrifugal force (RCF) for 0.33 h at 4 °C the supernatant was collected. To separate cytosol and microsomes, ultracentrifugation (Model: Optima™ L-80 XP Ultracentrifuge, Beckman Coulter) was performed at 1.05×10^5 RCF for 1 h at 4 °C. The potassium pyrophosphate buffer (pH 7.4) was used to wash the microsomes followed by ultracentrifugation. The concentration of microsomes was determined by the Thermo Scientific Pierce Bicinchoninic acid (BCA) protein assay kit as per the supplier's instruction. Briefly, 25 μl of standard (20–2000 μg/mL) or unknown samples was pipetted into Thermo Scientific™ Pierce 96-well plate. 200 μl of working reagent (50:1, BCA Reagent A:B) was added to each wells followed by incubating plate at 37 °C for 30 min. The absorbance was measured at 570 nm by using plate reader (VICTOR³ 1420 Multilabel Coulter, PerkinElmer, Massachusetts, USA) (Anonymous, 2015c).

For *in-vitro* glucuronidation assay, the solution containing microsomes (200 μg/mL), 0.95 mg/mL magnesium chloride, 24.94 μg/mL alamethicin, 1.05 mg/mL D-glucaric acid 1,4-lactone, 10.44 μg/mL EDR and its equivalent formulation, was kept in an incubator at 37 °C for 5 min. By adding 2 mM UDPGA, the enzymatic reaction was commenced and continued for 15 min at 37 °C. The cold methanol (400 μl) was mixed with the solution to stop the reaction and to precipitate proteins. Proteins were removed by centrifugation at 1.5×10^5 RCF for 0.16 h at 4 °C. The LC/MS/MS was used to quantify the concentration of EDR and its metabolite EDR glucuronide as mentioned in Sections 2.2.2 and 2.2.3. Borneol was considered as a control at 100 μg/mL.

2.4.2. Study design and sample preparation

The selected aqueous buffer system (0.05 M Citric acid, pH 4) and LBS were mixed volumetrically to form mixtures containing 0, 10, 20, 30, 40, 50, 60, 70, 80, 90, and 100% of LBS. Briefly, an excess amount of EDR was added in 5 ml of vehicle in tightly closed test tube and put in a mechanical shaker for 48 h. The samples were collected at desired time points, filtered and analysed with UV-HPLC. All solubility studies were carried out in triplicate (Yeh et al., 2009).

2.4.3. Physico-chemical characterization of formulation

The selected composition with 3% w/v EDR concentration was assessed against potential for change in pH and precipitation after dilution of 1:10 with MilliQ water (Liang, 2014). The finalised formulation was stored at 4 °C, 25 °C/60% RH, and 40 °C/75% RH. Nitrogen purging was conducted to remove the oxygen from vial before sealed. Samples were collected at various time intervals and filtered through 0.45-mm PVDF syringe filter. The analysis of the samples was performed on UV-HPLC. All studies were carried out in triplicate (Liang, 2014).

2.4.4. In-vitro *release study*

The dialysis bag method was used. EDR solution (30 mg/mL concentration, 1 ml) either in novel liquid formulation or in suspension formulation (0.5% sodium carboxymethyl cellulose) was filled in the dialysis bag (Liu et al., 2011). The dialysis bag with formulation was placed in a glass beaker on magnetic stirrer containing 100 ml of milliQ water at 37 °C and 100 rpm. The samples were collected at scheduled time intervals, filtered and analysed using UV-HPLC. The sink condition was maintained by replacing equal amount of blank buffer after collecting each samples. The study was performed in triplicate.

2.4.5. In-vitro *permeation and metabolism study (Pranav Patel and Panchal, 2014; Zhou et al., 2015)*

Male Sprague Dawley rats (300 ± 25 g) were fasted overnight and sacrificed. The small intestines were removed between 50 mm from the stomach to the ileocecal junction. It was washed with cold Tyrode's solution. The Tyrode solution (1 l) was prepared using 8 g sodium chloride, 0.2 g potassium chloride, 95.20 mg magnesium chloride, 200 mg calcium chloride, 28.4 mg disodium hydrogen phosphate, 1 g sodium bicarbonate and 0.99 g D-glucose. The small part of the intestine was ligated to the glass rod on one end firmly tied with silk and second end kept open to insert the solution. Total 2 ml of Tyrode's solution was added into each sac. After filling the solution, the sac was firmly tied with silk and put in to a beaker having 40 ml Tyrode's solution and a test sample. Borneol was used as a positive control at 200 μg/mL concentration. The whole system was continuously supplied with the mixture of O_2 and CO_2 (95%/5%). The initial concentration of EDR was 50 μg/mL in each test. A 200 μl sample was collected from both sides i.e. serosal side (inside) and mucosal side (beaker) at different time points (5, 10, 20, 30, 60, 90, and 120 min) and were further analysed by previously developed LC–MS/MS method.

2.4.6. Pharmacokinetic study (Rong et al., 2014)

The male Sprague Dawley rats (300 ± 25 g) were procured from the laboratory animal services (University of Adelaide, Adelaide, Australia), and the animal experiment was evaluated and approved by the University of South Australia (Australia). As the rats need to be acclimatised with the available environment, food, and water, we procured them a week ahead. Before performing a surgery, the rats were anaesthetized. On the neck part and the area closer to the jugular vein, a longitudinal cut was made. The catheter was filled with 20 units/mL solution of heparin saline and inserted into the jugular vein with the tip in the right ventricle. The catheter was fixed in place by sewing the muscles around the stopper. Another end of this catheter was led out of skin between two ears by passing underneath the skin of the neck part. Finally, the catheter was filled with 500 units/mL solution of heparin saline and plugged into the free end of the catheter. After surgery, the rats were kept individually (in different cages) in order to attain better recovery. Before administering the drug, the animals were fasted for 12 h and had with free access to water. A required amount of EDR was added into 0.5% sodium carboxymethylcellulose solution to prepare the suspension followed by vortexing for approximately 10 min to get homogeneity. Two groups of rats were orally administrated EDR suspension and NODS at an equivalent dose of 30 mg/kg EDR. At the predetermined time interval of 0, 5, 15, 30, 45, 60, 90, 12, 180, 240, 300, 360, 420, and 480 min, a 0.2 ml blood sample was collected and flushing of the catheter was done with an equal amount of the heparin saline solution. The plasma was extracted from the blood samples by centrifugation at 5000 rpm for 15 min at 4 °C and stored at −80 °C until analysis. The analysis for EDR was performed by using LC–MS/MS as mentioned above.

The various pharmacokinetic parameters including maximum plasma concentration (C_{max}), time to achieve maximum plasma concentration (T_{max}), elimination half-life ($t_{1/2}$), area under the concentration–time curve (AUC), and relative bioavailability were determined. Relative bioavailability is defined as a measurement of the bioavailability of EDR suspension B (estimated as AUC) in comparison with NODS of EDR following an oral administration. F_{rel} (%) is calculated by the formula $[(AUC_A \times Dose_B)/(Dose_A \times AUC_B)]$ (John et al., 2013).

2.5. Statistical analysis

Statistical analysis was performed using GraphPad Prism 6. All values were indicated as Mean ± standard deviation (SD). The statistical analysis of data was performed by using Student's *t*-test for two groups, and one-way and two way analysis of variance (ANOVA) for multiple groups. A p value < 0.05 was considered as a significant difference for data analysis.

3. Results and discussion

In the last three decades, researchers over the world have recognised the extraordinary therapeutic potential of EDR for its free radical scavenger activity (Kikuchi et al., 2012, 2011; Tabrizchi, 2000). The limited attention towards defining its physicochemical characteristics and unfavourable oral pharmacokinetic profile creates major obstacles to assess its therapeutic value for various OS associated diseases at the clinical stage. The pre-formulation study to determine the unrevealed physicochemical properties was considered as an initial step for the drug development of EDR.

3.1. Preformulation study

3.1.1. Solubility profile

The water solubility of EDR was found 1.85 ± 0.15 mg/mL. The solubility in aqueous buffers were 1.58–5.80 mg/mL and depended on the pH of the solution pH > 7 at 25 °C (Fig. 1). A significant enhancement of solubility was observed from pH 8 to 10 compared to water solubility ($P < 0.001$) while from pH 2 to 7, there was no considerable difference observed. We have used solubility in water as a control. The phenol like structure of EDR and weak acidic nature having pKa value of 7 allows its ionisation in the basic environment (Higashi et al., 2006; Yoshida et al., 2006). The solubility of the drug could be dependent on the ability to dissociate into ions when subjected to the pH of the aqueous solution (Beringer, 2006). This could be one of the reasons for high solubility above pH 8 because increment in the solubility is dependent on the higher degree of ionization compared to neutral and acidic pH (Zhang et al., 2014). Observations in neutral and acidic environments showed low solubility compared to a basic

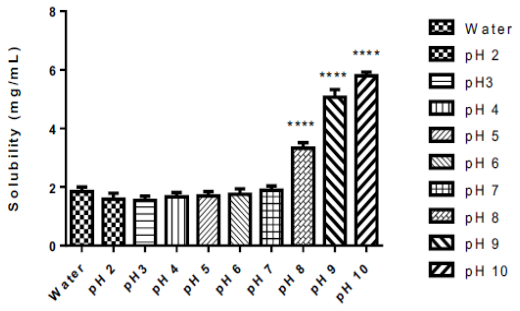

Fig. 1. pH-solubility profile of EDR at various pH in different buffer solutions (mean ± S.D., n = 3). ****$P < 0.0001$ compared to control (Water). One-way ANOVA and Sidak's multiple comparisons test.

environment. So, use of a basic environment could be an option to increase the solubility of EDR in an aqueous solution.

3.1.2. Stability study

To define the stability profile of the drug molecule is considered a mandatory requirement as per the Food and Drug Administration (FDA) and International Conference on Harmonisation (ICH) guidelines (ICH Q1AR2) for registration as a drug. It can influence its safety and efficacy. As per the guideline, the stability study should be conducted for a duration of 6 months (intermediate and accelerated) and 12 months (long term) respectively (Group, 2003). The forced degradation study could be done within a short period of time (a few weeks) and gives an indication of stability in various environmental conditions similar to intermediate, accelerated and long term studies. The determination of a stability profile could help to decide the suitable conditions for the pharmaceutical dosage form (Blessy et al., 2013). Since we would like to develop an oral liquid formulation of EDR, we have used conditions like different pH, temperatures, presence of light and oxygen and effect of initial concentration.

The process of the breakdown of a compound in presence of water is called Hydrolysis. It is considered as one of the most common reactions involved in the degradation process. The range of pH from acidic to basic using different buffer conditions could trigger the process of hydrolysis (Blessy et al., 2013). We have used a universal buffer system (pH 2–8) containing citric acid, boric acid and phosphoric acid (Wang et al., 2015); and alkaline borate buffer system (pH 9–10) (Robinson et al., 2015) to cover the broad range of pH 2–10.

The result of the effect of hydrolysis on EDR was presented in Fig. 2A. EDR was found to be relatively stable from pH 2 to 4 for 21 days as the degradation was <3% which is not statistically significant compared to day 0 sample preparation. At pH 5, there was no significant degradation observed up to 14 days at room temperature and nearly 4% ($p < 0.05$) until 21 days. The significant degradation was seen after day 7 at pH 6 and 7 ($p < 0.01$ on day 14 and $p < 0.0001$ on day 21), after day 3 at pH 8 ($p < 0.05$ on day 7, $p < 0.0001$ on day 14 and 21), after day 1 at pH 9 ($p < 0.05$ on day 3, $p < 0.001$ on day 7, $p < 0.0001$ on day 14 and 21), and 10 ($p < 0.001$ on day 3, $p < 0.0001$ on day 7, 14 and 21) respectively. Two-way ANOVA analysis by using Sidak's multiple comparisons test was performed. In acidic conditions (pH 2–6), EDR was found to be relatively stable with <8% degradation within 21 days compared to <10% in neutral conditions (pH 7) and ≤20% in basic conditions (pH 8–10) (Robinson et al., 2015). EDR seems to degrade rapidly due to basic hydrolysis which was already reported with drug having phenolic structure (Beringer, 2006; Friedman and Jurgens, 2000). It can be ionised in basic conditions and undergoes rapid degradation. Acidic conditions could be preferable for NODS.

The stability study was conducted on EDR with conditions like 4 °C, 25 °C/60%RH, room temperature, 40 °C/75% RH in order to assess the effect of thermal stress conditions as recommended by ICH guideline. The effect of temperature on EDR was not significant as shown in Fig. 2B as <3% degradation was observed at all conditions. The photo stability of EDR was also conducted by exposing EDR to light. Photo oxidation of the drug could happen in presence of light via free radical mechanism (Blessy et al., 2013). EDR showed <3% degradation up to day 21 which was not statistically significant compared to day 0. Two-way ANOVA analysis by using Tukey's multiple comparisons test was conducted.

The oxidative degradation of the drug is also considered as a major concern due to electron transfer leads in the formation of reactive anions and cations (Hovorka and Schoneich, 2001). To define the stability profile of EDR in presence of oxygen, hydrogen peroxide (H_2O_2) was used as an oxidizing agent at 0.03% and 3% concentration at room temperature (Zhang et al., 2014). With 0.03% concentration of H_2O_2, the significant degradation was observed after day 3 with more than 3% degradation ($p < 0.05$ on day 7, $p < 0.01$ on day 14 and $p < 0.0001$ on day 21) to nearly 12% degradation until day 21 as showed in Fig. 2C. In presence of 3% H_2O_2, EDR suffered significant degradation with >7% on day 1 to

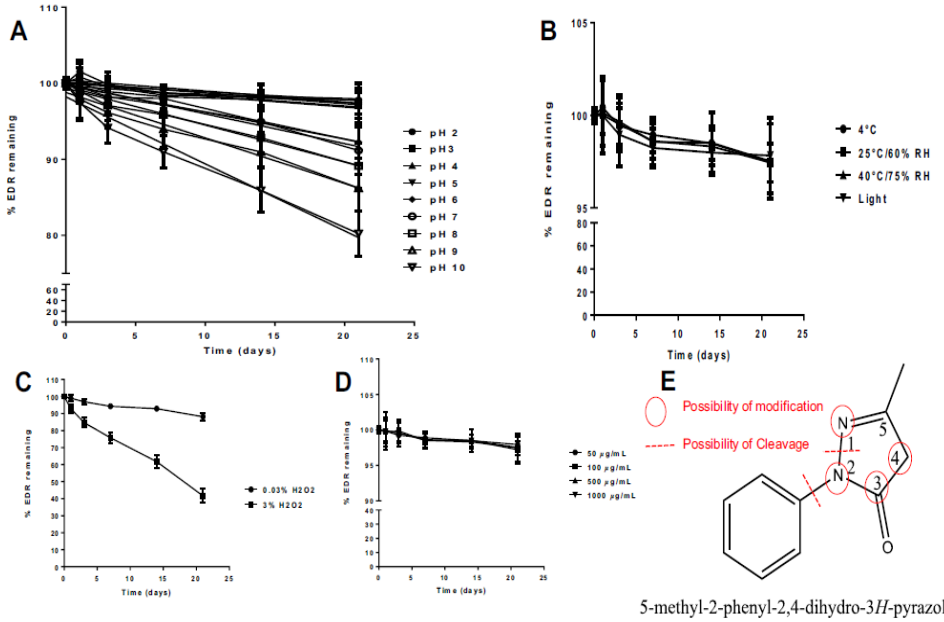

Fig. 2. Stability profile of EDR at different pH dependent stability study (A), Thermal and Light stability study (B), Oxidative stability study (C), Concentration dependent stability study (D), chemical structure of EDR with possible modifications due to Hydrolytic degradation and oxidative degradation (E) (mean ± S.D., n = 3).

nearly 60% till day 21 ($p < 0.01$ on day 1, $p < 0.0001$ on day 3, 7, 14, and 21). Two-way ANOVA analysis by using Sidak's multiple comparisons test was performed. As EDR has a phenol like structure, it is susceptible to oxidation via electron transfer (Harjivan et al., 2014). Hence, it can be inferred that protection against oxidation is critical for the development of NODS.

The drug like Imexon showed concentration dependent stability as it acts as a catalyst for its own degradation (Kuehl et al., 2006). To evaluate the effect of initial concentration of EDR, different concentrations from 50 to 1000 μg/mL were prepared. The data represented in Fig. 2D, revealed the negligible effect of initial concentration in solution on stability of EDR. Less than 3% degradation was observed until day 21 in all cases, which was not statistically significant compared to day 0. Two-way ANOVA analysis by using Sidak's multiple comparisons test was performed.

EDR is susceptible to alkaline hydrolysis degradation and oxidative degradation. The modification of EDR chemical structure (Fig. 2E) could be occurred due to a reaction with water (Hydrolysis) and presence of an oxygen with electron transfer mechanism (Oxidative) (Hovorka and Schoneich, 2001; Blessy et al., 2013). The cleavage of chemical bonds at position 1 and 2 of pyrazole ring might be resulted into ring opening due to attack of nucleophile. The modification at position 3 and 4 could explain from the proposed mechanism of EDR's free radical scavenger activity (Watanabe et al., 2008).

Poor oral bioavailability of EDR with rapid clearance was reported but the clear mechanism behind it still remains unexplored (Li et al., 2012; Rong et al., 2014). In our experiment, nearly 30% and 50% degradation of EDR in 24 h were observed in human and rat plasma, respectively (Fig. 3). A significant difference in degradation of EDR in human plasma was observed compared to rat plasma after 30 min. Two-way ANOVA analysis by using Sidak's multiple comparisons test was performed. Based on the data, half-life of several hours could be expected. However, half-life of 1.41 h was reported (Rong et al., 2014). Results suggest that other mechanisms like rapid metabolism in liver, and substrate for Pgp might have a major contribution compared to instability in plasma for quick clearance from the body

3.1.3. Log $P_{o/w}$ determination

The absorption of drug depends on its permeability across the biological membrane after dissolution. The prediction of drug permeability is generally determined based on Log Po/w study at the initial stage of drug development. Octanol has lipophilicity similar to that of biological membranes. Log Po/w value of drug determines its ability to partition in to the biological membranes (Fan et al., 2015; Zhang et al., 2014). The partition coefficient value of EDR in water, and PBS (pH 7.4) were 1.20, and 1.10, respectively. The value is comparable to log P (1.16) determined by Chembio-draw ultra 13.0 (developed by PerkinElmer Inc.). The lipophilic nature of EDR was confirmed which could facilitate permeability. In contrast, Rong et al. reported that EDR had poor permeability ($Peff = 3.18 \pm 0.0706\ 10-7$ cm/s). EDR belongs to a class of Pgp substrate which could be the potential reason for its poor permeability (Rong et al., 2014).

3.2. Formulation development

The encouraging therapeutic potential of EDR against various OS associated disorders such as AIS, ALS and Alzheimer disease, will surely lead to a rise in the market share of EDR at a global scale. From our study and literature review, poor aqueous solubility and stability, rapid and extensive metabolism, and poor permeability could be considered as the major obstacles for an effective EDR therapy. The requirement of an acidic environment and protection against oxidation should also be considered as critical factors for the development of oral formulation of EDR.

The NODS based on co-solvent strategy is considered as the most preferable one due to its inherent advantages like low cost, ease of self-administration, easy of manufacture and scale up and better safety profile (Panigrahi, 2012). The acidic aqueous preparation with appropriate co-solvent was considered as an ideal choice for EDR. From literature review, LBS has been selected for study as a co-solvent for EDR as it could improve the oral bioavailability directly or indirectly facilitating solubilisation, protection against rapid and extensive metabolism as well as improving permeability. LBS has a carbon chain length of C8–C10 and Hydrophilic-Lipophilic Balance (HLB) value of 14. It is obtained by the polyglycolysis of medium-chain triglycerides containing 30% fatty acids, 50% esters of polyethylene glycol and 20% free PEG 400. The coconut oil like medium chain triglycerides, caprylic/capric acid and PEG 400; and alcoholysis/esterification process are used to synthesize LBS (Koga et al., 2006; Ma et al., 2011; Rama Prasad et al., 2004, 2003a,b). LBS has a proven its safety via oral

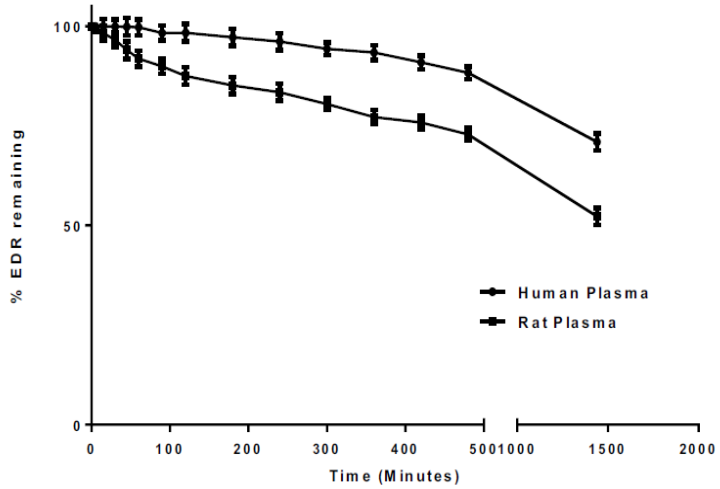

Fig. 3. Human and Rat plasma stability study of EDR (mean ± S.D., n = 3).

administration with 22 g/kg of LD_{50} value in rats and a dose of 1 g/kg/day in dogs for 13 weeks (Shah et al., 2014).

3.2.1. Inhibition of EDR glucuronidation by LBS

LBS as a UGT inhibitory excipient, has showed inhibitory effect on resveratrol glucuronidation (Zhou et al., 2015). The extensive metabolism of EDR via glucuronidation was reported in the literature (Ma et al., 2012). The effect on metabolism of EDR was assessed in the presence of LBS compared with borneol as a positive control on glucuronidation in rat liver microsomes. There was a significant inhibition on glucuronidation observed in the presence of LBS (88.78%) compared to borneol (37.56%) as shown in Fig. 4. The chemical structure of EDR and its glucuronide metabolite are mentioned in Fig. S1. Considering the significant inhibitory effect of LBS on EDR's metabolism, the NODS based on LBS as a co-solvent was selected for further development.

3.2.2. Selection of the composition

The enhancement of solubility of EDR was studied followed by performing a stability study to optimise the ratio of acidic aqueous solution and LBS. Table 1 shows the enhancement of solubility in terms of enhancement factor of EDR in a co-solvent system based on the increment in proportion of LBS. The solubility of EDR in LBS was 62.48 mg/mL. The probable reasons of the enhancement of solubility by LBS could be direct co-solvent effect and micelle formation (Ito et al., 2005; Panigrahi, 2012; Strickley, 2004).

3.2.3. Physico-chemical characterization of NODS

The stability of liquid formulation is always considered a major concern for the development as a market formulation (Niazi, 2009). It was assessed for 1 month as per ICH guideline and evaluated by comparing the drug content, pH and appearance from day 0 (Garg et al., 2007; Liang, 2014). As shown in Fig. 5, no statistically significant difference was observed in EDR content at various storage conditions for 1 month. There was no significant difference in pH of the NODS or precipitation observed until 1 month. Two-way ANOVA analysis by using Sidak's multiple comparisons test was performed.

3.2.4. In-vitro *release study*

The release study was carried out to evaluate the effect of formulation ingredients of NODS on release of EDR compared to suspension. The release of EDR from NODS and suspension are shown in Fig. 6 as a function of time. The burst release was observed in the case of suspension as about 80% cumulative amount compared to 30% within 60 min. The sustained release was observed from NODS suggesting a high affinity between EDR and LBS. LBS has a polyethylene glycol chain which could restrict the release of the drug after micellization (Zhou et al., 2015). At 480 min, EDR was released nearly 90% from NODS compared to 40% from EDR suspension. The significant difference was also observed at all time points except 60 and 90 min ($p < 0.001$). Two-way ANOVA analysis by using Sidak's multiple comparisons test was performed.

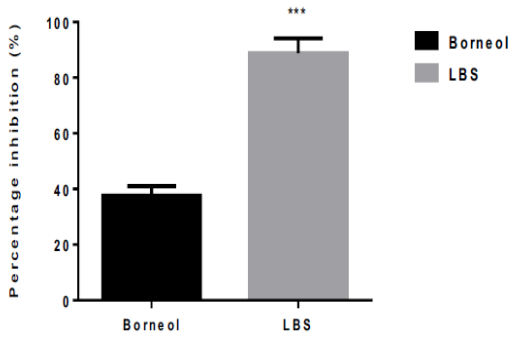

Fig. 4. Inhibitory effect of LBS (1%) on EDR glucuronidation in a microsomal incubation assay (mean ± S.D., n = 3). ***P < 0.001compared to control (Borneol). Unpaired *t*-test (two-tailed).

3.2.5. In-vitro *permeation and metabolism of EDA across the rat small intestine*

The effect of formulation ingredients on EDR permeability and metabolism during permeation across the small intestine was assessed. NODS showed 5 and 2.5 fold higher amount of EDR transferred within 2 h compared to free EDA and with Borneol, respectively (Fig. 7A). NODS and Borneol showed nearly 50% and 74% amount of EDR-G on serosal side compared to free EDR (Fig. 7B). The extensive glucuronidation of EDR was observed during the permeation of EDR. The molar ratio of EDR-G to EDR was 28% and 56% with NODS and Borneol, respectively compared to free EDR (Fig. 7C). The presence of LBS could be the reason for the desired outcome of NODS due to its significant inhibitory effect on glucuronidation. The transfer rate of EDR was 3.73 and 1.41 fold higher with NODS compared to free EDR and Borneol (Fig. 7D). LBS showed an inhibitory effect on Pgp efflux (Lin et al., 2007). It showed the significant role of Pgp efflux inhibitor in improvement of bioavailability of EDR (Rong et al., 2014). An increase in the permeability could be due to the synergistic effect on glucuronidation as well as Pgp efflux effect of LBS.

3.2.6. Pharmacokinetic study

The plasma profile of EDR with time for EDR suspension and NODS are shown in Fig. 8. Various pharmacokinetic parameters were obtained from Phoenix WinNonlin software are presented in Table 2. A significant difference was observed in the pharmacokinetic parameters including C_{max}, $t_{1/2}$, $AUC_{0\text{-}t}$, $AUC_{0\text{-}\infty}$, F0-t (%) and F0-∞ (%). The statistical analysis was performed with two-tailed unpaired *t*-test. The C_{max} value of NODS was 4.41 fold higher than the EDR suspension but no difference in t_{max} value for both formulations was noted. The $t_{1/2}$ value was increased by 1.30 fold in case of NODS compared to EDR suspension. The long $t_{1/2}$ value might be explained by the fact that LBS has an ability to form micelles and EDR could be entrapped into the micelles. The sustained release from NODS was also observed in *in-vitro* drug release study which could be responsible for long plasma half-life of NODS *in-vivo*. The enhancement of oral bioavailability of NODS was 5.75 fold compared to EDR suspension.

A characteristic melting point peak at 128.39 °C in Differential Scanning Calorimetry (DSC) analysis (Fig. S2), sharp numerous distinct peaks in X-ray powder diffraction (XRD) analysis (Fig. S3) and irregular shaped crystals in Scanning Electron Microscopy (SEM) analysis (Fig. S4) study confirmed the crystalline nature of EDR. Due to crystalline nature, the solubility of EDR in suspension formulation was 1.89 mg/mL and additional EDR would be present in solid undissolved form. In case of NODS, EDR was completely solubilised which could be potential reason for enhancing oral bioavailability. The reduction in metabolism and improved permeability in G.I tract might serve to justify the favourable outcome. In conclusion, NODS looks to be a promising candidate for clinical development in the near future.

4. Conclusions

To enable the clinical assessment for various OS associated diseases, the suitable oral liquid formulation of EDR may be considered as a very important. From the preformulation study and based on the available resources; poor solubility, stability,

Table 1
Solubility profile of EDR in Aqueous buffer-LBS mixture (mean ± S.D., n = 3).

Aqueous buffer (%V/V)	LBS (%V/V)	Solubility of EDR (mg/mL) (Mean ± S.D., n = 3)	Enhancement factor[a]
100	0	1.65 ± 0.19	1
90	10	7.18 ± 1.05	4.35
80	20	15.21 ± 1.52	9.22
70	30	21.24 ± 2.85	12.87
60	40	27.28 ± 2.56	16.54
50	50	33.31 ± 1.89	20.19
40	60	39.34 ± 2.74	23.85
30	70	44.38 ± 2.48	26.90
20	80	50.41 ± 1.56	30.56
10	90	55.54 ± 1.11	33.67
0	100	62.48 ± 1.84	37.87

[a] Enhancement factor: the ratio is calculated by EDR solubility in 1 ml of water and LBS mixture/EDR solubility in 1 ml of water.

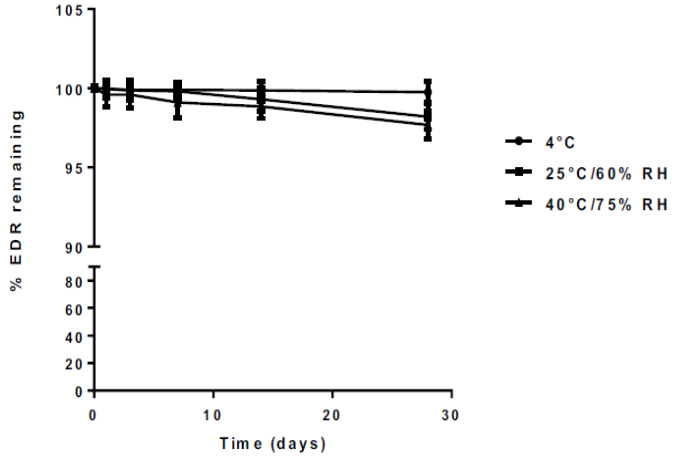

Fig. 5. Stability study of NODS as per ICH guideline (mean ± S.D., n = 3).

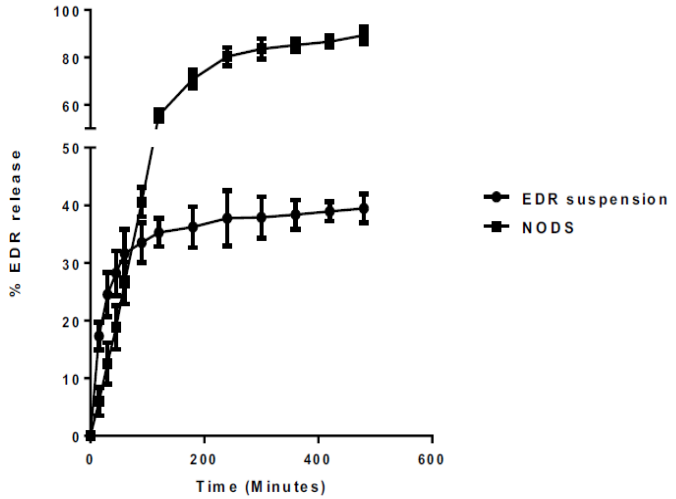

Fig. 6. In-vitro release of EDR from EDR suspension or NODS (mean ± S.D., n = 3).

permeability across the GI tract and extensive metabolism; were determined as the potential obstacles that lead to the poor oral bioavailability. The NODS based on LBS and aqueous buffer system having pH 4 was developed based on solubility and stability study. From the *in-vitro* study, LBS showed a significant improvement in the metabolism of EDR as well as intestinal absorption. The beneficial effect of LBS might be due to its inhibitory activity on UGT enzyme and Pgp efflux transporter. The 5.7 fold improvement

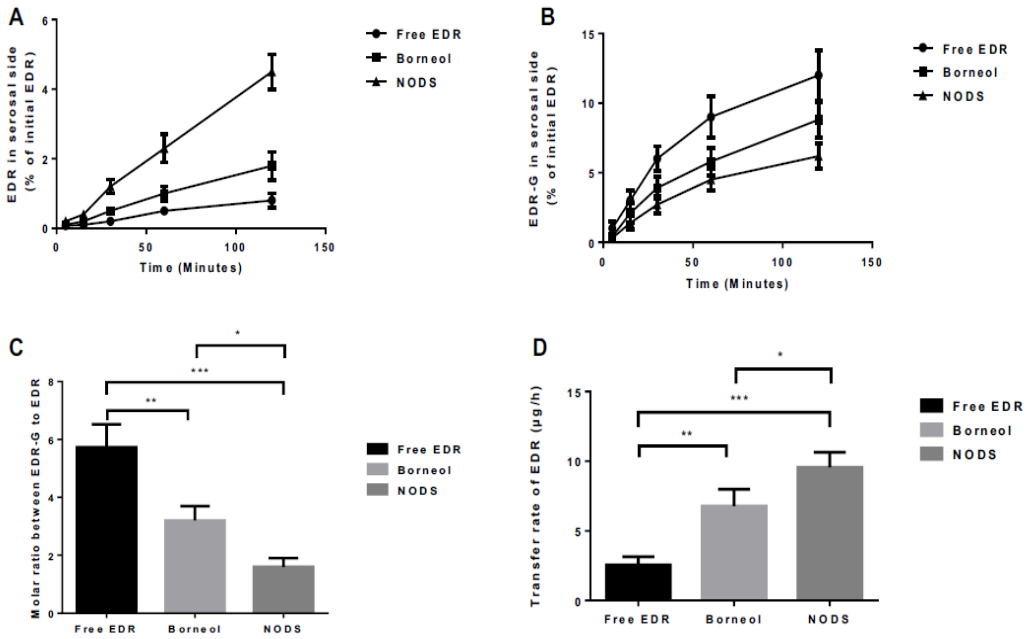

Fig. 7. The effect of formulation ingredients on permeability and metabolism of EDR during transportation across everted sacs of rat small intestine. The amount in percentage of EDR (A) and (B) on serosal side of everted sac at various time interval, molar ratio between EDR-G and EDR (C), and transfer rate of EDR in the serosal side of rat everted gut sacs (D) (mean ± S.D., n = 3). *P < 0.05, **P < 0.01 and ***P < 0.001. One-way ANOVA and Sidak's multiple comparisons test.

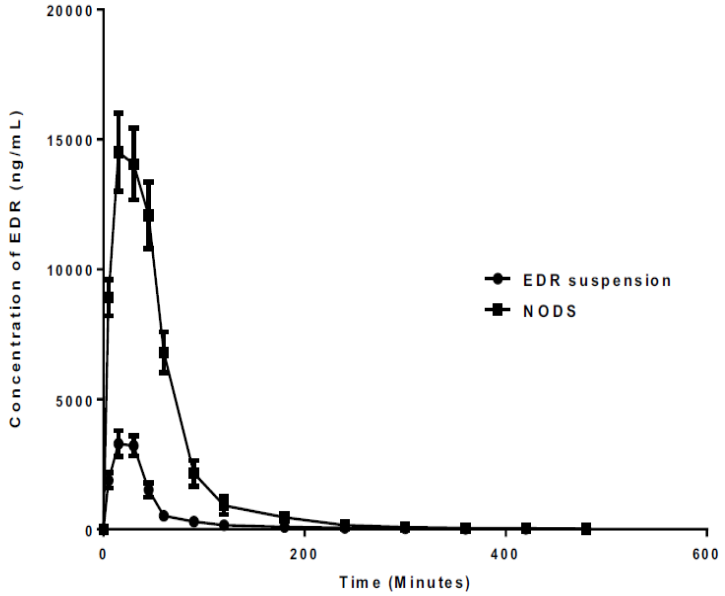

Fig. 8. Plasma concentration-time curves for the EDR suspension and NODS (30 mg/kg) in SD rats after oral administrations (mean ± S.D., n = 6).

in the oral bioavailability might be due to a combination of improvement in solubility, stability, intestinal permeability and reduction of extensive metabolism. This study reveals the importance of selecting appropriate formulation ingredients which provides an ultimate solution to overcome the obstacles for the clinical development of potential therapeutic agent like EDR.

Conflict of interest

Ankit Parikh, Xin-Fu Zhou and Sanjay Garg are named inventors on Chinese patent 201610149832.9. Fujian Kangshimei Co, China owns the intellectual property. All other co-authors declares no conflict of interest.

Table 2
Pharmacokinetic parameters obtained by Phoenix WinNonlin software (mean ± S.D., n = 6).

Parameters	EDR suspension	NODS	P Value
C_{max} (ng/mL)	3290.42 ± 507.41	14510.63 ± 1507.41	<0.0001
T_{max} (mins)	15.19 ± 1.45	15.52 ± 2.42	NS
$t_{1/2}$(mins)	58.31 ± 3.52	75.98 ± 6.53	<0.001
$AUC_{0\text{-}t}$ (ng min/mL)	164185 ± 15264	943885 ± 95211	<0.0001
$AUC_{0\text{-}\infty}$ (ng min/mL)	165281 ± 16525	944726 ± 96241	<0.0001
$F_{0\text{-}t}$ (%)	100	574.89 ± 18.72	<0.0001
$F_{0\text{-}\infty}$ (%)	100	571.58 ± 25.53	<0.0001

NS: Non-significant.

Author contribution

Xin-Fu Zhou (XFZ) conceived the project, Ankit Parikh (AP), Krishna Kathawala (KK), XFZ and Sanjay Garg (SG) designed the study, AP, KK, Chun Chuan Tan (CT), XFZ performed the research, AP, KK, CT, XFZ and SG analysed the data; AP, KK, XFZ, SG wrote the paper.

Acknowledgements

The authors would like to acknowledge the financial support from Fujian Kangshimei Co, China, and a special grant from University of South Australia to Xin-Fu Zhou for the present research. Ankit Parikh is grateful for the University President's Scholarships (UPS) to support his PhD study. Chun Chuan Tan is also grateful for Vacation Research Scholarships from University of South Australia. Xin-Fu Zhou is supported by an NHMRC fellowship. Dr Mingfeng Yu, a Postdoctoral research fellow and Stephen Philip, a PhD candidate, from School of Pharmacy and Medical Sciences, UniSA, are acknowledged for proposing degradation mechanism. Mike Hempstead from Trapeze Associates Pty Ltd is gratefully acknowledged for providing the gratis sample of LBS. Carolyn Streckbein and Jasmine Karanjia are acknowledged for revising the language. The animal welfare officer, Alex Whittaker and the animal ethics officer, Ruth Brogan and Reid animal house staff members including Jayne Skinner, Alysha Servin, Jess Parken, and Becky Nitschke from University of South Australia are acknowledged for their generous support in animal work.

Appendix A. Supplementary data

Supplementary data associated with this article can be found, in the online version, at http://dx.doi.org/10.1016/j.ijpharm.2016.10.052.

References

Anonymous, 2015a. Information for Approved Products. Pharmaceuticals and Medical Devices Agency, Tokyo, Japan.
Anonymous, 2015b. Orphan Drug Designations and Approvals. U.S. Food and Drug Administration, Maryland, USA.
Anonymous, 2015c. Pierce BCA Protein Assay Kit. Thermo Fisher Scientific, Illinois, USA, pp. 1–8.
Anonymous, 2015d. Public Summary of Opinion on Orphan Designation: Edaravone for the Treatment of Amyotrophic Lateral Sclerosis. European Medicines Agency, London, United Kingdom.
Beringer, J.P.R.a.P., 2006. Remington: The Science and Practice of Pharmacy, 21 ed. Lippincott Williams & Wilkins, USA.
Blessy, M., Prajesh, R.D.P., Prajapati, N., Agrawal, Y.K., 2013. Development of forced degradation and stability indicating studies of drugs—a review. J. Pharm. Anal. 4, 159–165.
Essick, E.E., Sam, F., 2010. Oxidative stress and autophagy in cardiac disease, neurological disorders, aging and cancer. Oxid. Med. Cell. Longev. 3, 168–177.
Fan, Y., Yang, M., Wang, Y., Li, Y., Zhou, Y., Chen, X., Shan, L., Wei, J., Gao, C., 2015. Preformulation characterization and in vivo absorption in beagle dogs of JFD, a novel anti-obesity drug for oral delivery. Drug Dev. Ind. Pharm. 41, 801–811.
Fatouros, D.G., Karpf, D.M., Nielsen, F.S., Mullertz, A., 2007. Clinical studies with oral lipid based formulations of poorly soluble compounds. Ther. Clin. Risk Manage. 3, 591–604.
Friedman, M., Jurgens, H.S., 2000. Effect of pH on the stability of plant phenolic compounds. J. Agric. Food Chem. 48, 2101–2110.
Garg, M., Dutta, T., Jain, N.K., 2007. Stability study of stavudine-loaded O-palmitoyl-anchored carbohydrate-coated liposomes. AAPS PharmSciTech 8 (Article 38).
Group, I.E.W., 1996. Stability Testing: Photostability Testing of New Drug Substances and Products Q1bb. ICH Harmonised Tripartite Guideline p. 12.
Group, I.E.W, 2003. Stability Testing of New Drug Substances and Products Q1a(R2). ICH Harmonised Tripartite Guideline, Switzerland p. 18.
Gualdesi, M.S., Ravetti, S., Raviolo, M.A., Brinon, M.C., 2014. Preformulation studies of novel 5′-O-carbonates of lamivudine with biological activity: solubility and stability assays. Drug Dev. Ind. Pharm. 40, 1246–1252.
Harjivan, S.G., Wanke, R., Ferreira da Silva, J.L., Marques, M.M., Antunes, A.M., 2014. The phenolic metabolites of the anti-HIV drug efavirenz: evidence for distinct reactivities upon oxidation with Fremy's salt. Eur. J. Med. Chem. 74, 7–11.
Higashi, Y., Jitsuiki, D., Chayama, K., Yoshizumi, M., 2006. Edaravone (3-methyl-1-phenyl-2-pyrazolin-5-one), a novel free radical scavenger, for treatment of cardiovascular diseases. Recent Pat. Cardiovasc. Drug Discov. 1, 85–93.
Hovorka, S., Schoneich, C., 2001. Oxidative degradation of pharmaceuticals: theory, mechanisms and inhibition. J. Pharm. Sci. 90, 253–269.
Ito, Y., Kusawake, T., Ishida, M., Tawa, R., Shibata, N., Takada, K., 2005. Oral solid gentamicin preparation using emulsifier and adsorbent. J. Control. Release 105, 23–31.
Jiao, S.S., Yao, X.Q., Liu, Y.H., Wang, Q.H., Zeng, F., Lu, J.J., Liu, J., Zhu, C., Shen, L.L., Liu, C.H., Wang, Y.R., Zeng, G.H., Parikh, A., Chen, J., Liang, C.R., Xiang, Y., Bu, X.L., Deng, J., Li, J., Xu, J., Zeng, Y.Q., Xu, X., Xu, H.W., Zhong, J.H., Zhou, H.D., Zhou, X.F., Wang, Y.J., 2015. Edaravone alleviates Alzheimer's disease-type pathologies and cognitive deficits. Proc. Natl. Acad. Sci. U. S. A. 112, 5225–5230.
John, M.K., Xie, H., Bell, E.C., Liang, D., 2013. Development and pharmacokinetic evaluation of a curcumin co-solvent formulation. Anticancer Res. 33, 4285–4291.
Kikuchi, K., Uchikado, H., Miyagi, N., Morimoto, Y., Ito, T., Tancharoen, S., Miura, N., Miyata, K., Sakamoto, R., Kikuchi, C., Iida, N., Shiomi, N., Kuramoto, T., Kawahara, K., 2011. Beyond neurological disease: new targets for edaravone. Int. J. Mol. Med. 28, 899–906 (Review).
Kikuchi, K., Takeshige, N., Miura, N., Morimoto, Y., Ito, T., Tancharoen, S., Miyata, K., Kikuchi, C., Iida, N., Uchikado, H., Miyagi, N., Shiomi, N., Kuramoto, T., Maruyama, I., Morioka, M., Kawahara, K.I., 2012. Beyond free radical scavenging: beneficial effects of edaravone (Radicut) in various diseases (Review). Exp. Ther. Med. 3, 3–8.
Kikuchi, K., Tancharoen, S., Takeshige, N., Yoshitomi, M., Morioka, M., Murai, Y., Tanaka, E., 2013. The efficacy of edaravone (radicut), a free radical scavenger, for cardiovascular disease. Int. J. Mol. Sci. 14, 13909–13930.
Koga, K., Kusawake, Y., Ito, Y., Sugioka, N., Shibata, N., Takada, K., 2006. Enhancing mechanism of Labrasol on intestinal membrane permeability of the hydrophilic drug gentamicin sulfate. Eur. J. Pharm. Biopharm. 64, 82–91.
Komiyama, Y., 2012. The Ministry of Health, Labour and Welfare Ministerial Notification No. 519. In: The Minister of Health, L.a.W.o.J. (Ed.), The Minister of Health, Labour and Welfare, Japan p. 301.
Kuehl, P.J., Hoye, W.L., Myrdal, P.B., 2006. Preformulation studies on imexon. Drug Dev. Ind. Pharm. 32, 687–697.
Lapchak, P.A., 2010. A critical assessment of edaravone acute ischemic stroke efficacy trials: is edaravone an effective neuroprotective therapy? Expert Opin. Pharmacother. 11, 1753–1763.
Li, H., Xu, K., Wang, Y., Zhang, H., Li, T., Meng, L., Gong, X., Zhang, H., Ou, N., Ruan, J., 2012. Phase I clinical study of edaravone in healthy Chinese volunteers: safety and pharmacokinetics of single or multiple intravenous infusions. Drugs R&D 12, 65–70.
Liang, J.J.a.D., 2014. Oral liquid formulation of etravirine for enhanced bioavailability. Bioequivalence Bioavailab. 6, 7.
Lin, Y., Shen, Q., Katsumi, H., Okada, N., Fujita, T., Jiang, X., Yamamoto, A., 2007. Effects of Labrasol and other pharmaceutical excipients on the intestinal transport and absorption of rhodamine123 a P-glycoprotein substrate, in rats. Biol. Pharm. Bull. 30, 1301–1307.
Liu, Z., Liu, D., Wang, L., Zhang, J., Zhang, N., 2011. Docetaxel-loaded pluronic p123 polymeric micelles: in vitro and in vivo evaluation. Int. J. Mol. Sci. 12, 1684–1696.
Liu, F., Ranmal, S., Batchelor, H.K., Orlu-Gul, M., Ernest, T.B., Thomas, I.W., Flanagan, T., Tuleu, C., 2014. Patient-centred pharmaceutical design to improve acceptability of medicines: similarities and differences in paediatric and geriatric populations. Drugs 74, 1871–1889.
Ma, L., Wei, Y., Zhou, Y., Ma, X., Wu, X., 2011. Effects of Pluronic F68 and Labrasol on the intestinal absorption and pharmacokinetics of rifampicin in rats. Arch. Pharm. Res. 34, 1939–1943.
Ma, L., Sun, J., Peng, Y., Zhang, R., Shao, F., Hu, X., Zhu, J., Wang, X., Cheng, X., Zhu, Y., Wan, P., Feng, D., Wu, H., Wang, G., 2012. Glucuronidation of edaravone by human liver and kidney microsomes: biphasic kinetics and identification of UGT1A9 as the major UDP-glucuronosyltransferase isoform. Drug Metab. Dispos. 40, 734–741.
Mizuno, N., Takahashi, T., Kusuhara, H., Schuetz, J.D., Niwa, T., Sugiyama, Y., 2007. Evaluation of the role of breast cancer resistance protein (BCRP/ABCG2) and multidrug resistance-associated protein 4 (MRP4/ABCC4) in the urinary excretion of sulfate and glucuronide metabolites of edaravone (MCI-186; 3-methyl-1-phenyl-2-pyrazolin-5-one). Drug Metab. Dispos. 35, 2045–2052.

Niazi, S.K., 2009. Handbook of Pharmaceutical Manufacturing Formulations Liquid Products. In: Zollo, S. (Ed.), Informa Healthcare, USA p. 400.
Panigrahi, A.K.N.a.P.P., 2012. Solubility enhancement of etoricoxib by cosolvency approach. ISRN Phys. Chem. 2012, 5.
Pranav Patel, T.M., Panchal, Shital, 2014. Preparation, evaluation and comparison of lipid based drug delivery systems of tacrolimus. Int. J. Pharm. Pharm. Sci. 6, 4.
Rama Prasad, Y.V., Eaimtrakarn, S., Ishida, M., Kusawake, Y., Tawa, R., Yoshikawa, Y., Shibata, N., Takada, K., 2003a. Evaluation of oral formulations of gentamicin containing labrasol in beagle dogs. Int. J. Pharm. 268, 13–21.
Rama Prasad, Y.V., Sudarat Eaimtrakarn, S.P.P., Ishida, Makoto, Yoshikawa, Yukako, Shibata, Nobuhito, Takada, Kanji, 2003b. Enhanced intestinal absorption of vancomycin with Labrasol and D-a-tocopheryl PEG 1000 succinate in rats. Int. J. Pharm. 250, 10.
Rama Prasad, Y.V., Minamimoto, T., Yoshikawa, Y., Shibata, N., Mori, S., Matsuura, A., Takada, K., 2004. In situ intestinal absorption studies on low molecular weight heparin in rats using Labrasol as absorption enhancer. Int. J. Pharm. 271, 225–232.
Reuter, S., Gupta, S.C., Chaturvedi, M.M., Aggarwal, B.B., 2010. Oxidative stress, inflammation, and cancer: how are they linked? Free Radic. Biol. Med. 49, 1603–1616.
Robinson, K., Mock, C., Liang, D., 2015. Pre-formulation studies of resveratrol. Drug Dev. Ind. Pharm. 41, 1464–1469.
Rong, W.T., Lu, Y.P., Tao, Q., Guo, M., Lu, Y., Ren, Y., Yu, S.Q., 2014. Hydroxypropyl-sulfobutyl-beta-cyclodextrin improves the oral bioavailability of edaravone by modulating drug efflux pump of enterocytes. J. Pharm. Sci. 103, 730–742.
Sato, T., Mizuno, K., Ishii, F., 2009. A novel administration route for edaravone: I. Effects of metabolic inhibitors on skin permeability of edaravone. Int. J. Pharm. 372, 33–38.
Sato, T., Mizuno, K., Ishii, F., 2010. A novel administration route of edaravone–II: mucosal absorption of edaravone from edaravone/hydroxypropyl-beta-cyclodextrin complex solution including L-cysteine and sodium hydrogen sulfite. Pharmacology 85, 88–94.
Shah, S.M., Jain, A.S., Kaushik, R., Nagarsenker, M.S., Nerurkar, M.J., 2014. Preclinical formulations: insight, strategies, and practical considerations. AAPS PharmSciTech 15, 1307–1323.
Shahiwala, A., 2011. Formulation approaches in enhancement of patient compliance to oral drug therapy. Expert Opin. Drug Deliv. 8, 1521–1529.
Strickley, R.G., 2004. Solubilizing excipients in oral and injectable formulations. Pharm. Res. 21, 30.
Tabrizchi, R., 2000. Edaravone mitsubishi-Tokyo. Curr. Opin. Investig. Drugs 1, 347–354.
Wang, W., Song, Y., Petrovski, K., Eats, P., Trott, D.J., Wong, H.S., Page, S.W., Perry, J., Garg, S., 2015. Development of intramammary delivery systems containing lasalocid for the treatment of bovine mastitis: impact of solubility improvement on safety, efficacy, and milk distribution in dairy cattle. Drug Des. Dev. Therapy 9, 631–642.
Watanabe, T., Tahara, M., Todo, S., 2008. The novel antioxidant edaravone: from bench to bedside. Cardiovasc. Ther. 26, 101–114.
Yeh, M.K., Chang, L.C., Chiou, A.H., 2009. Improving tenoxicam solubility and bioavailability by cosolvent system. AAPS PharmSciTech 10, 166–171.
Yoshida, H., Yanai, H., Namiki, Y., Fukatsu-Sasaki, K., Furutani, N., Tada, N., 2006. Neuroprotective effects of edaravone: a novel free radical scavenger in cerebrovascular injury. CNS Drug Rev. 12, 9–20.
Zeng, Jian, Chengliang Zhou, Y.R., Yu, Shuqin, Chen, Wen-Hua, 2011. Preparation and physicochemical characteristics of the complex of edaravone with hydroxypropyl-b-cyclodextrin. Carbohydr. Polym. 83, 5.
Zhang, W., Parniak, M.A., Mitsuya, H., Sarafianos, S.G., Graebing, P.W., Rohan, L.C., 2014. Preformulation studies of EFdA, a novel nucleoside reverse transcriptase inhibitor for HIV prevention. Drug Dev. Ind. Pharm. 40, 1101–1111.
Zhou, J., Zhou, M., Yang, F.F., Liu, C.Y., Pan, R.L., Chang, Q., Liu, X.M., Liao, Y.H., 2015. Involvement of the inhibition of intestinal glucuronidation in enhancing the oral bioavailability of resveratrol by labrasol containing nanoemulsions. Mol. Pharm. 12, 1084–1095.

Supplementary Information

Development of a Novel Oral Delivery System of Edaravone for Enhancing Bioavailability

Author information

Ankit Parikh, Krishna Kathawala, Chun Chuan Tan, Sanjay Garg*, Xin-Fu Zhou*,

School of Pharmacy and Medical Sciences, University of South Australia, Adelaide, SA 5000, Australia.

*Corresponding author-

E-mail address: xin-fu.zhou@unisa.edu.au; Sanjay.garg@unisa.edu.au;

Phone: +61-8830 22329; +61-883021575

Fax: +61 8830 21087; +61 8830 22389

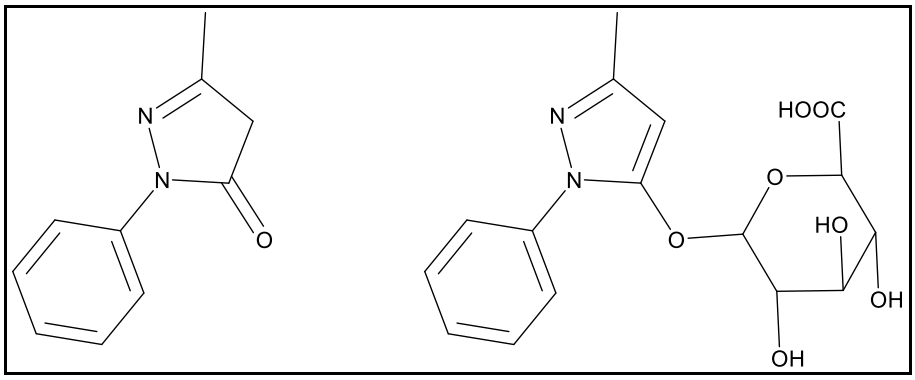

Figure S1 Structure of EDR (3-methyl-1-phenyl-2-pyrazolin-5-one) (A) and its glucuronide (B)

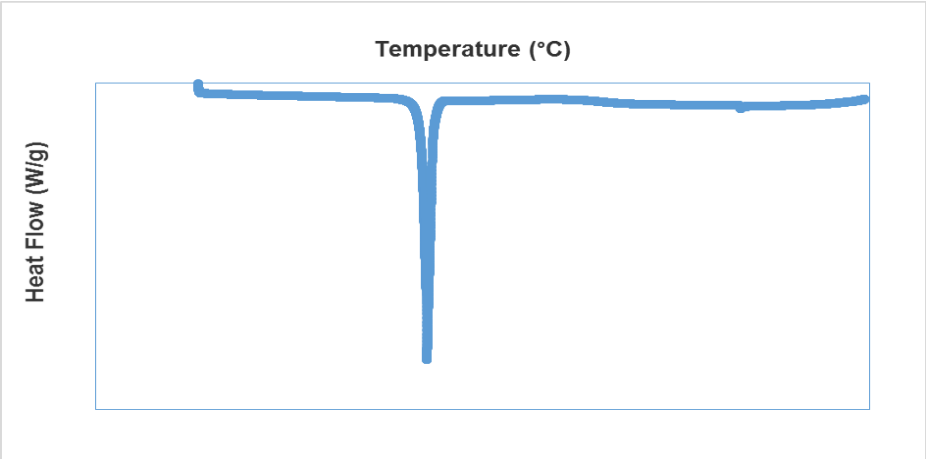

Figure S2 Differential scanning calorimetry (DSC) pattern of EDR

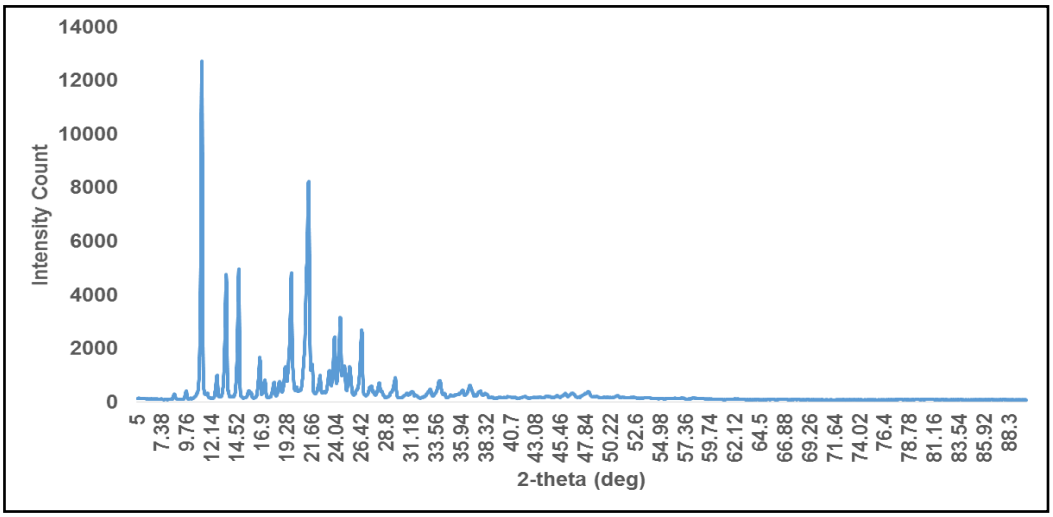

Figure S3 X-ray powder diffraction (XRD) pattern of EDR

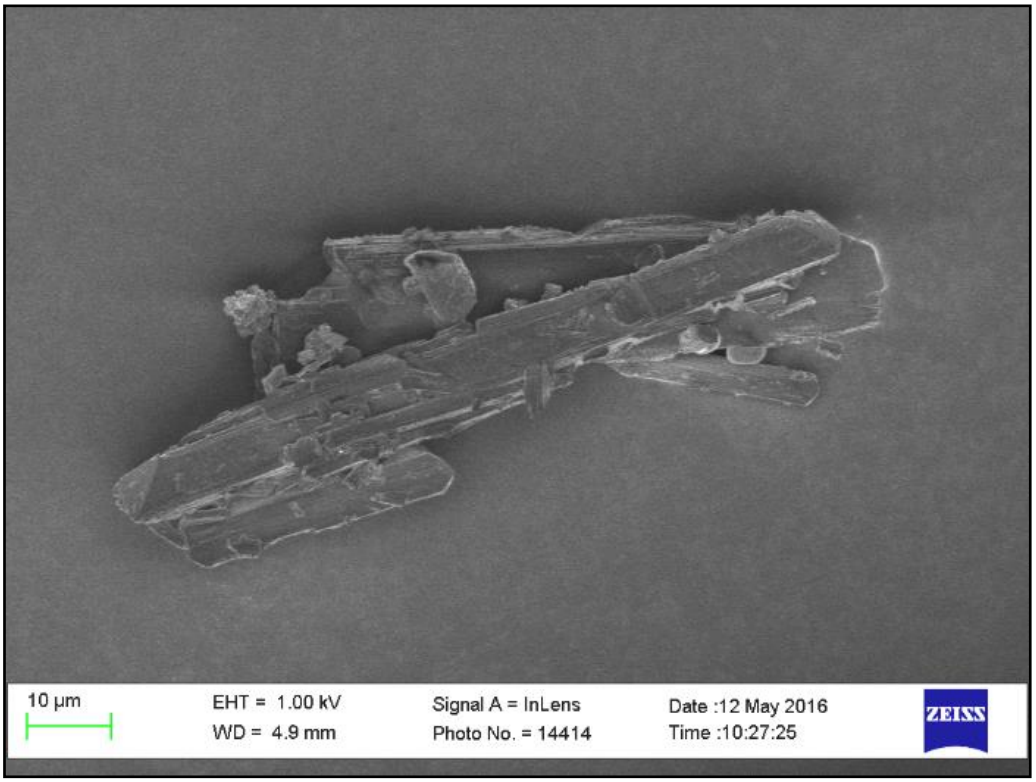

Figure S4 Scanning Electron Microscopy (SEM) photomicrograph of EDR

3. Novel Lipid-based Nanosystem of Edaravone: Development, Optimization, Characterization, and *In-vitro/In-vivo* Evaluation

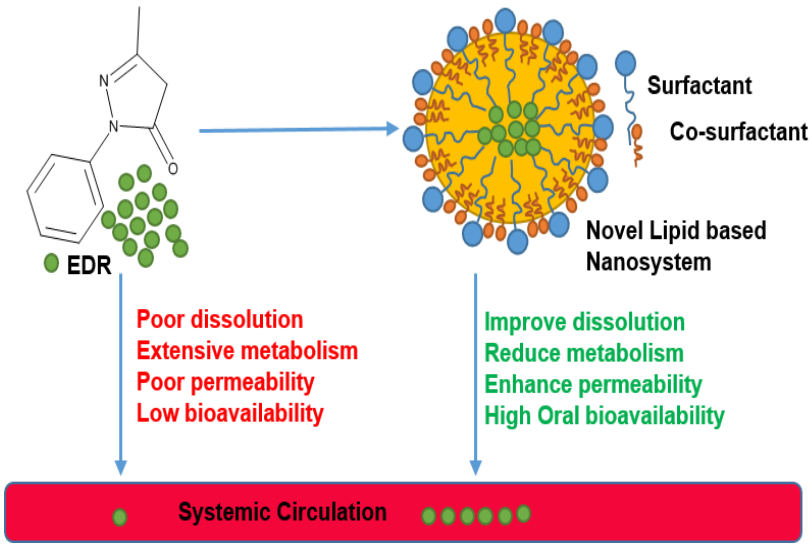

Graphical Abstract

3.1 Abstract

Edaravone (EDR) is a well-recognised lipophilic free radical scavenger for diseases including neurodegenerative disease, cardiovascular disease, and cancer. However, its oral use is restricted due to poor oral bioavailability (BA). The aim of present research was to enable its oral use by developing a Novel Lipid-based Nanosystem (NLNS). The components of NLNS including oil, surfactants, and co-surfactants were selected based on their potential to maximize the solubilisation in gastrointestinal (GI) fluids, reduce its glucuronidation and improve transmembrane permeability. The Liquid NLNS (L-NLNS) with Capryol™ PGMC (Oil), Cremophor® RH 40: Labrasol®: TPGS 1000 (1:0.8:0.2) (Surfactant) and Transcutol P® (Co-surfactant) were optimised to form microemulsion having droplet size (16.25 nm), polydispersity index (PDI, 0.039), % Transmittance (99.85%) and self-emulsification time (32 s). It significantly improved the drug loading as well as metabolism and permeability of EDR during its transport across the GI tract. To overcome the possible drawbacks of L-NLNS, Aerosil® 200 was used to formulate Solid NLNS (S-NLNS), and its concentration was optimized based on flow properties. S-NLNS possessed all quality attributes of L-NLNS confirmed by solid-state characterization, morphology, reconstitution ability and stability study. The dissolution rate of EDR was significantly enhanced with L-NLNS and S-NLNS in simulated gastric fluid (SGF), and simulated intestinal fluid (SIF) compared to EDR suspension. The Pharmacokinetic study revealed significant improvement in relative BA, $C_{max,}$ and $t_{1/2}$ with L-NLNS and S-NLNS against EDR suspension. An appropriate selection of the components of NLNS could enable effective oral delivery of challenging therapeutics that are conventionally used by the parenteral administration.

Keywords: Edaravone, lipid-based nanoformulations, solubilisation, glucuronidation, permeability, oral bioavailability

Chemical compounds: Edaravone (PubChem CID: 4021), Borneol (PubChem CID: 1201518), Capryol™ PGMC, Cremophor® RH 40, Labrasol®, D -α-Tocopherol polyethylene glycol succinate (TPGS 1000), Transcutol P®

3.2 Introduction

Free radicals contribute significantly to the pathogenesis of a variety of diseases associated with the organs including brain, heart, lung, liver, pancreas, intestine and kidney [212, 336, 337]. Modulators of free radicals showed promising therapeutic efficacy in *in-vitro* and *in-vivo* studies but found limited success in clinical trials attributable to achieving a sub therapeutic level at the target site [76, 338]. Edaravone (EDR), a free radicle scavenger (3-methyl-1-phenyl-2-pyrazolin-5-one, MCI 186), showed its ability to diffuse into the most organs including brain, removed hydrogen radicals and displayed protective effects [76, 212]. Radicut®, a parenteral preparation developed and marketed by Mitsubishi Tanabe Pharma Corporation, established global attention by receiving approval as a first neuroprotective drug in Japan for the treatment of acute ischemic stroke (AIS) [78]. Additionally, EDR showed significant pharmacological efficacy in the incurable diseases like Amyotrophic lateral sclerosis (ALS) and Alzheimer diseases [69, 126].

A liquid solution for intravenous infusion is the only EDR preparation available in the current market [78]. It's approved dosage regimen for AIS is one ampoule (30 mg of EDR) diluted with physiological saline and administered intravenously over 30 min twice a day for up to 14 days [339]. There is no oral formulation of EDR commercially available even though its therapeutic efficacy against diseases like Alzheimer and Cerebral aneurysm reported via oral administration in animals [69, 340]. The oral route is the preferred route of administration for patients with chronic neurodegenerative diseases and doctors due to the ease of administration, flexibility in dose, improved quality of life, reduced the need for the hospital stay and low cost of treatment [211]. Poor oral bioavailability (BA) could be a major challenge in enabling its oral use.

EDR is a lipophilic molecule having the low molecular weight of 174.2 g/mol with pka value of 7 [341]. It belongs to Biopharmaceutics Classification System (BCS) class IV drug due to poor solubility (1.85 mg/mL) and permeability (P_{eff} = 3.18 ± 0.0706 10^{-7} cm/s) [96]. The poor oral BA (F_{abs} 5.23) could be attributed to poor aqueous solubility, stability, permeability across the gastrointestinal tract (GIT) and extensive glucuronidation (phase II metabolism) due to the substrate for P-glycoprotein (Pgp) efflux pump and uridine 5′-diphospho-glucuronosyl-transferase (UGT) enzymes, respectively [96, 214]. Several investigations based on complexation with (2-Hydroxypropyl)-β-cyclodextrin (HP-βCD) were reported to improve dissolution and permeability of EDR [95, 96]. However, these investigational findings have

not effectively translated to use for the clinical purpose. A Novel Oral Delivery System (NODS) of EDR based on co-solvency and pH modification technology, showed 5.71 fold enhancement of oral BA by improving solubility, metabolism, and permeability [342]. To take additional advantage of superior drug loading, facilitates transport through the intestinal lymphatic system, allowing enterocyte-based transport to enhance drug uptake, efflux, and deposition; Novel Lipid-based Nanosystem (NLNS) of EDR was considered to develop [343, 344].

NLNS is based on a strategy called "lipid-based nanoformulations" specifically Self-microemulsifying drug delivery system (SMEDDS). SMEDDS has been successfully utilized to enhance oral BA of drugs such as Exemestane [318], Coenzyme Q10 [319], Curcumin (CUR) [266], and Fenofibrate [320]. It is an isotropic mixture of oil, surfactant, and co-surfactants, which forms microemulsion having droplet size <100 nm after dilution with gentle stirring. Improvement of oral BA with lipid-based nanoformulations strategy is be owing to either individual or a combination of various factors, including greater solubilization, stabilization, and modifying permeability and metabolism profile [310]. By producing nanosized droplets, it facilitates rapid dissolution and absorption [312]. Moreover, it also protects the drug from Gastrointestinal (GI) environment as almost 100% drug could be entrapped in the microemulsion [311]. Also, due to the presence of oil, nano-sized droplets could diffuse via lymphatic circulation which bypasses first pass metabolism [345]. The selection of surfactants is the critical step as it plays a significant role in modifying metabolism and permeability profile by inhibiting Cytochrome P450, UGT enzymes and modulating Pgp efflux pump [306, 316, 317]. Sandimmune, Neoral, Norvir, and Fortovase are commercially successful products based on lipid-based nanoformulations strategy [321].

The commercial success of liquid lipid-based nanoformulations is limited due to stability concern including the interaction of components with gelatin capsules, the interaction between the components and issues related to oxidation of the oil [313]. By converting liquid to solid lipid-based nanoformulations using solid adsorbents, it is possible to overcome issues including stability and handling problems. Various hydrophilic carriers including lactose, sorbitol, mannitol and hydrophobic carriers including colloidal silica and dextran; were widely utilized [314, 315]. To the best of our knowledge, there is no lipid-based nanoformulations based strategy applied to enhance oral BA of EDR.

In the present research, NLNS was assessed to enable effective oral delivery of EDR. The initial screening of surfactants was conducted based on the ability of inhibition of EDR glucuronidation. Solubility and emulsification studies were performed to finalize oil, surfactant, and co-surfactant for the development of Liquid NLNS (L-NLNS). Ternary phase diagram was constructed to optimize the concentration of each component of L-NLNS based on criteria such as droplet size (<100 nm), polydispersity index (PDI, <0.1), % Transmittance (>99%) and self-emulsification time (<120 s). *In-vitro* characterization of Liquid L-NLNS including drug loading, determination of drug content, thermodynamic stability and its reconstitution ability in GI fluids. Moreover, its *in-vitro* effect on metabolism and permeability of EDR across the everted sacs of rat gut were evaluated. Solid NLNS (S-NLNS) was developed with Aerosil® 200 and further optimized based on its flow properties. Also, Differential scanning calorimetry (DSC), X-ray diffraction (XRD), scanning electron microscopy (SEM), transmission electron microscopy (TEM) and dissolution studies were conducted for further characterisation. The stability of the S-NLNS formulation was evaluated in various simulated GI fluids and after dilution to different folds. Additionally, an *in-vivo* performance of L-NLNS and S-NLNS was studied with pharmacokinetic study in rats against EDR suspension.

3.3 Materials and Methods

3.3.1 Materials

EDR was obtained from Aladdin Industrial Corporation (Shanghai, China). Capryol™ PGMC, Labrasol®, Transcutol P®, Capryol™ 90, Peceol™, Labrafil® M1944cs, Lauroglycol™ FCC, Labrafac™ PG, Labrafil® M2115, Lauroglycol™ 90, Labrafac™ Lipophile WL 1349 were received as gratis samples from Trapeze Associates Pty Ltd, a representative of Gattefosse in Australia and New Zealand (Victoria, Australia). The samples of Captex® 355, Captex® 300, Capmul® MCM C8, Capmul® MCM EP, Capmul® PG 8, Capmul® PG 12 were received from Abitec Corporation (Wisconsin, USA). Acetic Acid, Phosphoric acid, sucrose, magnesium chloride, sodium hydroxide pellets, Glycerol, polysorbate 20, and polysorbate 80 were purchased from Chem Supply (South Australia, Australia). Corn oil, Cotton seed oil, Oleic acid, N-methyl-2-pyrrolidone (NMP), Propylene glycol, poly (ethylene glycol) 300 (PEG 300), PEG 400, 1,3-Propanediol, potassium pyrophosphate, Tyrode's solution, ascorbic acid, sodium carboxymethylcellulose, DMSO, concentrated HCL, di-sodium hydrogen phosphate, citric acid, perchloric acid, formic acid, uridine diphosphate glucuronic acid trisodium salt

(UDPGA), alamethicin, and D-glucaric acid 1, 4-lactone were purchased from Sigma-Aldrich (New South Wales, Australia). Cremophor® RH 40 and Cremophor® EL were obtained from BASF (Ludwigshafen, Germany), TPGS 1000 from Connell Bros Company Australasia Pty Ltd (Victoria, Australia), Miglyol® 812 from IOI Oleo GmbH (Hamburg, Germany), peanut oil was purchased from PCCA (Texas, USA); sunflower oil from Goodman Fielder (New South Wales, Australia); castor oil from Wille Laboratory (Queensland, Australia); Triethanolamine from BDH Chemicals (Victoria, Australia); Caprylic triglyceride from Goldschmidt Chem Corporation (Victoria, Australia); Aerosil® 200 from Evonik Industries AG (Hanau, Germany), Ethanol from Ajax fine chem (New South Wales, Australia), and Pierce BCA Protein Assay Kit from Thermo Fisher Scientific (Victoria, Australia). Water was purified by a MilliQ water purification system (Millipore Ultra-Pure Water System; Millipore Australia). All the HPLC grade mobile phase components were procured from Merck (Victoria, Australia).

3.3.2 Formulation development of L-NLNS formulation

3.3.2.1 Selection of oil

The selection of oil was carried out by saturated solubility study. An excess amount of EDR was added to the different vehicles (1 ml of each) in glass vials and shaken continuously on a mechanical shaker (Model: so4036, Axyos Technologies, Brisbane, Australia) for 24 h at room temperature. The resultant mixtures were centrifuged (Model: Centrifuge 5415 R, Eppendorf) at 13000 Revolutions per minute (RPM) for 10 min. The supernatant was further diluted with methanol or petroleum ether and mobile phase. The determination of EDR solubility was analyzed by previously reported Ultraviolet-Visible (UV) Spectrophotometers detector - High-Performance liquid chromatography (HPLC) method after suitable dilution with methanol or petroleum ether and mobile phase [342].

3.3.2.2 Selection of surfactant

The selection of surfactant was performed in 3 steps including *In-vitro* glucuronidation assay (step 1), solubility as mentioned in the section 3.3.2.1 (step 2), and emulsification ability (step 3).

***In-vitro* glucuronidation assay**

In-vitro glucuronidation assay was carried out to examine the influence of different surfactants on the metabolism of EDR as described previously [342]. The level of EDR and EDR

glucuronide (EDR-G) metabolite were determined with established extraction and analytical LC/MS/MS method [342].

Emulsification study

Screening of the selected surfactants was finalized based on their emulsification ability [312, 346]. A 0.5 g of Capryol™ PGMC was mixed with the same amount of different surfactants and vortexed for about 2 min. The resultant mixture was warmed nearly 50°C for 1 min. The final mixture (500 mg) was then diluted with water (500 mL) to obtain a dispersion with gentle shaking. All the mixtures were kept for 2 hrs to equilibrate and evaluated by measuring droplet size, and PDI using Malvern Zetasizer Nano ZS (Model ZEN3600), and % transmittance using UV-Visible Spectrophotometers (Thermo Scientific™ Evolution™ 201) at 638 nm. The emulsification time was also used as a parameter to determine the self-emulsification ability of the respective surfactants.

3.3.2.3 Selection of co-surfactant

The selection of co-surfactant was carried out in 2 steps including from solubility as mentioned in the section 3.3.2.1 (step 1) and emulsification study 3.3.2.2 (step 2).

Emulsification study

The selection of co-surfactant was finalized based on their emulsification ability [346]. A 0.3 g of the selected surfactant was mixed with 0.2 g of different co-surfactants followed by an addition of 0.5 g of the oily phase. Droplet size, PDI, % transmittance and self-emulsification time were observed.

3.3.2.4 Construction of ternary phase diagrams

To identify the self-emulsification region, a ternary phase diagram was plotted for the different ratios of an oil Capryol™ PGMC, surfactants Cremophor® RH 40: Labrasol®: TPGS 1000 in the ratio of 1:0.8:0.2, and a co-surfactant Transcutol P® using Chemix® School Software, trial version 3.6 (Oslo, Norway) [347]. In this mixture, the concentration of an oil, surfactant, and co-surfactant was varied from 0-70% (w/w), 30–80% (w/w) and 0–30% (w/w), respectively. Initially, the concentration of oil, surfactant, and co-surfactant was altered in the order of 10%, and selection criteria were droplet size (<100 nm) and PDI (<0.1) [310, 348]. Later, the selected range of concentration oil, surfactant, and co-surfactant were further altered in the order of 5% and selection criteria were as kept as follow: droplet size (<100 nm), PDI (<0.1), % transmittance (>99%) and self-emulsification time (<120 s) [346, 349]. This particular region

was considered as a self microemulsifiying region in the plotted pseudo ternary phase diagram. The selection of L-NLNS was conducted based on formulation with maximum oil concentration and minimum surfactant concentration and ability to produce microemulsion with having quality attributes mentioned above after dilution.

3.3.2.5 *In-vitro* characterization of L-NLNS

Globule size, PDI and zeta potential

500 mg of L-NLNS was diluted with 500 ml of water and mixed by gentle hand shaking to obtain a homogenous dispersion [350]. Droplet size, zeta potential, and PDI of the resultant microemulsion was measured using Malvern Zetasizer.

% Transmission test and self-emulsification time

900 mg of the L-NLNS was added drop by drop to the dissolution flask containing 900 ml of required aqueous media in United States Pharmacopeia (USP) paddle type II Sotax Dissolution Apparatus (Victoria, Australia) dissolution apparatus at 37°C and 75 RPM [351]. % Transmittance against water and Self-emulsification time were determined using UV-Visible Spectrophotometers at 638 nm and visual observation, respectively.

Drug loading ability

The maximum drug loading of EDR was determined based on the solubility protocol described in the selection of oil section. The stability of L-NLNS formulation was visually observed for 24 h.

Determination of drug content

500 mg of L-NLNS was diluted with methanol and vortexed for 15 min to extract the drug completely. The samples were then centrifuged for 10 min at 13,000 RPM. The supernatant was filtered through 0.45-µm polyvinyl difluoride (PVDF) syringe filters and further diluted with a suitable amount of mobile phase to analyze with previously developed UV-HPLC method.

Cloud point measurement

The cloud point is one of the important parameters to determine the reliability of the microemulsion-based formulation [352]. 500 mg of the L-NLNS was diluted with 500 ml distilled water and placed in a water bath (Ratek Instruments, Adelab scientific, South

Australia, Australia) with a slow rise in temperature. The cloud point was visually observed at the point where the solution becomes cloudy.

Thermodynamic stability study

The aim of this study was to check the stability of the L-NLNS against temperature and centrifugal force [353]. The test was performed in 3 steps including heating-cooling cycle, centrifugation, and a freeze-thaw cycle.

Step 1 (Heating cooling cycle): L-NLNS was gone through six heating-cooling cycles of storage at each temperature of 4°C and 45°C, for not less than 48 h and observed for precipitation.

Step 2 (Centrifugation): The formulation was further evaluated by centrifugation at 5000 RPM for 30 min and evaluated for phase separation.

Step 3 (Freeze-thaw cycle): In the last step of the freeze-thaw cycle, the formulation was stored for 48 h at each temperature -10°C and 25°C. The formulation was observed visually for precipitation, creaming, and cracking.

Reconstitution behaviour

The reconstitution study of the L-NLNS was carried out in water, simulated gastric fluid (SGF, pH 1.2) and simulated intestinal fluid (SIF, pH 6.8) [346]. The SGF and SIF were prepared as previously reported [354]. Briefly, 500 mg of L-NLNS was dispersed in 500 ml of aqueous media. The reconstituted behavior of L-NLNS was evaluated by measuring droplet size, PDI and emulsification time.

***In-vitro* evaluation of L-NLNS composition on metabolism and permeability of EDR**

In-vitro permeation and metabolism study was carried out as per our previous study [342].

3.3.3 Formulation development of solid NLNS (S-NLNS) formulation

3.3.3.1 Preparation of S-NLNS

The EDR loaded S-NLNS was adsorbed on Aerosil® 200 in a different ratio of L-NLNS to Aerosil® 200 (1:0.4, 1:0.6, 1:0.8 and 1:1) by physical mixing using a mortar and pestle [355]. The mixture was passed through 150 µm sieve to get uniformity and dried at room temperature. The resultant mixtures were evaluated for flow properties [314, 355]. The optimum

concentration of Aerosil® 200 was selected based on the standards mentioned in USP 35 (Table S1) [356].

3.3.3.2 Optimization of concentration of solid carriers

Flow characteristics of the S-NLNS formulations were determined to select the best concentration of solid carrier based on different parameters including the Carr's Index (CI), Hausner's Ratio (HR) and Angle of Repose (AR).

Carr's Index and Hausner's Ratio

The cylinder method was utilized to calculate the tapped density and bulk density. An accurately weighed S-NLNS was filled into the measuring cylinder, and the apparent volume was noted to determine the bulk density. The measuring cylinder was tapped for 100 times, and then the reduced volume was noted to calculate tapped density. The CI and HR were calculated by using the following equations.

$$\text{CI (\%)} = \frac{Tapped\ density - Bulk\ density}{Tapped\ density} * 100$$

$$\text{HR} = \frac{Tapped\ density}{Bulk\ density}$$

Angle of Repose

The static funnel method was used to determine the AR of S-NLNS. In brief, the sample was poured from the top of the funnel until the top of the pile touched to the tip at a specific height of 1.5 cm on a flat horizontal surface. The AR was calculated by using the formula, tan θ = height (h)/radius (r) where r is the radius of a pile of the powder.

3.3.3.3 *In-vitro* characterization of S-NLNS formulation

The determination of droplet size, PDI, drug content, %Transmittance and self-emulsification time were performed as described in the section 3.3.2.5 [346].

Solid state characterization

The solid state characterization of EDR, Aerosil® 200 and S-NLNS formulation was investigated by DSC, XRD, and SEM.

DSC study was conducted to evaluate the thermal characteristic of EDR, Aerosil® 200 as a solid carrier, and the S-NLNS [357]. The DSC was carried out by using TA Instruments Discovery DSC (Model 2920). The samples (2-4 mg) were placed and sealed in hermetic

aluminum pans. The measurement was executed over the temperature range from room temperature to 300 °C at a heating rate of 10 °C/min under nitrogen gas (50 ml/min).

The PXRD patterns of EDR, Aerosil® 200 and the S-NLNS, were recorded by using an X-ray diffraction instrument (PANalytical, Empyrean X-ray diffractometer) [332]. X-ray diffraction patterns were acquired using CuKα radiation (λ = 1.5418 Å) on an X-ray diffractometer operating at 40 kV and 40 mA between 2 to 90° 2θ at a step size of 0.013° with a fixed 0.25° divergence slit, 0.50° anti-scatter slit and scanning rate of 2° min^{-1}.

The external morphological characteristics of EDR, Aerosil® 200, and S-NLNS were studied by SEM [332]. The samples were mounted on a SEM stub with conductive double-sided adhesive. The ultra-high resolution secondary electron microscopy (Zeiss Microscopy Merlin with GEMINI II column) was used to study the surface characteristics. It equipped with a field emission gun was operated at 0.7 kV to acquire the secondary electron images.

TEM analysis upon reconstitution

The morphology of the microemulsion was analyzed using Cryo-TEM, wherein the copper grids were first dipped into a sample solution and immediately transferred into liquid nitrogen and allowed to stay in for 10 min [358]. The Copper grid was freeze dried and analyzed using transmission electron microscope using JEOL JEM-1010. S-NLNS of EDR (500 mg) was dispersed in 500 ml of water to generate the microemulsion.

Stability in simulated GI fluids (SGF)

The stability of formulation was carried out in water, SGF and SIF [346]. 500 mg of S-NLNS was dispersed into 500 ml of an aqueous media, incubated for 24 h further evaluated for droplet size, PDI, and drug precipitation.

Stability after dilution to different folds

S-NLNS was dispersed in the SGF at different folds (200, 400, 600, and 800) [346]. The samples were further evaluated for droplet size, PDI, and drug precipitation.

3.3.4 In-vitro release test

The *in-vitro* release was carried out with dialysis bag method by using USP dissolution apparatus type II (paddle) at 37°C and 75 RPM speed [359]. The EDR suspension, L-NLNS and S-NLNS formulation equivalent to 30 mg of EDR were filled in a dialysis bag (Cellu·Sep T4 12,000–14,000 MW, Seguin, TX, USA). The dialysis bag was sealed from both sides with

clamps and placed in the dissolution flask containing 900 ml of dissolution media including SGF and SIF. Samples (5mL) were collected at different time intervals of 5, 15, 30, 45, 60, 90, 120 min, respectively and replaced with fresh dissolution medium. The collected samples were further analyzed by previously developed UV-HPLC method after dilution with mobile phase. The release kinetic of EDR from suspension, L-NLNS and S-NLNS were determined by putting obtained data in various kinetic models including First order, Zero order, Hixson–Crowell, Higuchi-matrix, and Korsmeyer–Peppas [359-361]. The relevant correction coefficient was considered to select the best model. Moreover, the dissolution profiles of EDR suspension, L-NLNS, and S-NLNS in SGF and SIF were compared using similarity factor (f2) and dissimilarity factor (f1) approach. All calculations were performed based on the equations mentioned in Table S3. In general, f1 values 0–15 and f2 values 50–100 demonstration the similarity of the dissolution profiles [361].

3.3.5 Pharmacokinetic study

The approved protocol from the University of South Australia (Australia), was used as discussed previously using male Sprague-Dawley rats (300 ± 25 gm) [342]. Three groups of rats (n=6) were orally administered with EDR suspension, L-NLNS, and S-NLNS at an equivalent dose of 30 mg/kg. To extract EDR from the plasma matrix, a mixture of Mcllvaine buffer of pH 5.4 and dichloromethane-n-pentane (3:7 v/v) was used as described previously [342]. The EDR level was determined by previously developed LC/MS/MS method. The pharmacokinetic parameters were calculated using Phoenix WinNonlin software.

3.3.6 Statistical analysis

GraphPad Prism 6 was used for statistical analysis. All values were indicated as Mean ± standard deviation (SD). The statistical analysis of data was performed by using Student's t-test for two groups, one-way and two-way analysis of variance (ANOVA) for multiple groups. The mean differences were considered significantly valued in all experiments at $P < 0.01$.

3.4 Results and discussion

3.4.1 Formulation development of L-NLNS

3.4.1.1 Selection of oil

The selection of appropriate oil based on solubility study is critical to prevent precipitation of drug during storage and before undergoing in situ solubilization [346]. Table 3.1 shows the solubility profile of EDR in several natural and synthetic oils. Capryol^{TM} PGMC (34.63 ± 2.52

mg/mL) revealed the highest solubilization capacity among different oils followed by Capmul® MCM EP (24.08 ± 1.24 mg/mL) and Labrafil® M2125 (22.14 ± 1.51). The solubility of EDR was lower in natural oils compared to synthetic oils. The oils showed higher solubilization for EDR compared to water (1.85 mg/mL) might be owing to its lipophilic (log p: 1.2) nature [342]. In a case of the lipophilic drug, higher solubility in oils could increase drug loading and facilitates absorption through lymphatic route and therefore provide protection against the first pass metabolism [362]. Capryol™ PGMC is chemically propylene glycol monocaprylate having Hydrophilic-Lipophilic Balance value (HLB) of 6. The components of hard and gelatine capsule are compatible with Capryol™ PGMC. It conforms to US Pharmacopeia– National Formulary (USP-NF) standard for Human and Veterinary applications [363]. It was successfully used to enhance the oral BA of drugs including Fenofibrate [320] and Flutamide [364]. Capryol™ PGMC was selected as an oil for further development.

Table 3.1 Solubility of EDR in selected ingredients (mean ± S.D., n = 3)

Oil	**Solubility (mg/mL)**
Capryol™ PGMC	34.63 ± 2.52
Capryol™ 90	21.20 ± 1.45
Captex® 355	9.61 ± 1.41
Peceol™	6.91 ± 1.56
Peanut oil	7.38 ± 0.97
Sunflower oil	8.83 ± 1.46
Miglyol® 812	11.17 ± 2.92
Corn oil	6.31 ± 1.64
Caprylic triglyceride	8.10 ± 1.56
Cottonseed oil	3.37 ± 0.85
Castor oil	5.78 ± 1.63
Lauroglycol™ FCC	1.54 ± 0.32

Labrafac™ PG	1.77 ± 0.23
Captex® 300	7.74 ± 1.35
Labrafil® M2115	22.14 ± 1.57
Lauroglycol™ 90	18.02 ± 2.13
Labrafac™ Lipophile WL 1349	7.26 ± 1.52
Capmul® MCM C8	22.11 ± 2.56
Capmul® MCM EP	24.08 ± 1.24
Capmul® PG 8	18.17 ± 1.76
Capmul® PG 12	16.88 ± 2.36
Oleic Acid	7.37 ± 2.52
Surfactant	
Labrasol®	62.48 ± 5.56
Labrasol®: TPGS 1000 (4:1)	58.63 ± 4.74
Cremophor® RH 40	26.09 ± 3.11
Glycerol	9.92 ± 1.42
Polysorbate 20	14.65 ± 3.64
Cremophor® EL	9.95 ± 1.86
Polysorbate 80	8.29 ± 3.56
Triethanolamine	19.42 ± 3.26
Co-surfactant	
Transcutol P®	93.06 ± 6.21
Propane Diol	21.54 ± 2.26
Ethanol	70.28 ± 5.27

PEG 300	50.63 ± 4.63
Labrafil® M1944cs	9.55 ± 1.36
NMP	37.79 ± 3.67
PEG 400	6.40 ± 1.47
Propylene glycol	5.93 ± 1.63

3.4.1.2 Selection of surfactant

The role of surfactant in lipid-based nanoformulations is the most critical in modulating pharmacokinetic profile of drugs as a solubilizer, stabilizer, for inhibition of enzymes including UGT and cytochrome p450 for metabolism of drugs; and as a permeability enhancer [306, 365]. EDR is extensively metabolized and has an issue of poor permeability across GIT due to substrates of UGT enzyme and Pgp [96, 342]. Hence, the selection of appropriate surfactant for the development of L-NLNS could consider three steps including *in-vitro* glucuronidation assay, solubility, and emulsification ability test.

As a step 1, Labrasol®, Cremophor® RH 40 and TPGS 1000 were selected from the literature which showed a significant effect on UGT and Pgp, thereby improves oral BA of various drugs [306, 366, 367]. The inhibitory effect on the glucuronidation of EDR was assessed *in-vitro* for each surfactant with a well-established assay using rat liver microsomes. Labrasol® and Cremophor® RH 40 showed the superior inhibitory effect on EDR metabolism compared to Borneol (as a positive control) and TPGS 1000 which is good agreement with previous reports (Fig. 3.1) [342].

To avoid the precipitation of drug during the storage and formulate stable L-NLNS, the solubility of EDR with various surfactants as mentioned in the section 3.3.2.1 [312, 346]. Use of a combination of surfactants in the development of lipid-based nanoformulations is a popular approach for increasing solubility as well as dissolution [368, 369]. The highest solubility of EDR was observed in Labrasol® (62.48 mg/mL) followed by Cremophor® RH 40 (26.09 mg/mL) among all surfactants as showed in Table 3.1. The surfactants play a critical role in the spontaneous formation of stable and transparent microemulsion (Droplet size <100 nm and PDI < 0.2). The emulsification ability of surfactants as an individual or in combination were further studied with Capryol™ PGMC as an oil and evaluated based on the following criteria such as droplet size (<100 nm), PDI (near to zero), % T (near to 100%) and emulsification time

(<2 min) (step 3). The results are shown in Table 3.2. Labrasol® and Cremophor® RH 40 as individual surfactants were passed the criteria for emulsification time but failed for others and unable to generate microemulsion with desired characteristics. TPGS 1000 as a stabilizer, showed improvement of emulsification ability of labrasol® by decreasing droplet size and PDI, and increasing %Tranmittance but was unable to match the criteria. The combination of Cremophor® RH 40, Labrasol® and TPGS 1000 (1:0.8:0.2) successfully formed a microemulsion with desired characteristics. The selected combination was again assessed for inhibitory effect on EDR glucuronidation and solubility study. Labrasol® was considered as a control as it showed superior effects. No significant difference was observed compared to labrasol® in both studies (Fig. 3.1 and Table 3.1).

Cremophor® RH 40 is categorized as a Polyoxyethylene castor oil derivatives having a hydrophobic portion (glycerol polyethylene glycol oxystearate with fatty acid glycerol polyglycol esters) and hydrophilic constitute (polyethylene glycols and glycerol ethoxylate). It had HLB value of 14 – 16 and considered as a non-toxic and non-irritant for oral administration from acute (LD 50: >20 gm/kg/day), subacute and chronic toxicity studies [370]. It was successfully utilized for the development of lipid-based nanoformulation for a number of drugs to enhance oral BA including ritonavir [371] and seocalcitol [372]. Labrasol® is chemically Caprylocaproyl macrogol-8 glycerides having HLB value of 12. It is a mixture of monoesters, diesters, and triesters of glycerol and monoesters and diesters of polyethylene glycols with a mean relative molecular mass between 200 and 400. It is also proven as a relatively a non-toxic and non-irritant with LD 50 value >20 ml/kg/day [370]. A number of lipid-based nanoformulations with Labrasol® are reported to improve physicochemical characteristics and oral absorption of drugs such as Exemestane [318] and Coenzyme Q10 [319]. TPGS 1000 is chemically vitamin E polyethylene glycol 1000 succinate having a mixture of monoesterified polyethylene glycol 1000, the diesterified polyethylene glycol 1000, free polyethylene glycol 1000, and free tocopherol. It has HLB value 13.2. It is recognised as safe (GRAS) listed and also included in the FDA Inactive Ingredients Database [370]. The use of TPGS 1000 as a stabilizer was reported previously with lipid-based nanoformulations [211, 348]. The combination of Labrasol® and TPGS 1000 (1:0.25) was successfully improved intestinal absorption of Vancomycin hydrochloride (VCM) [367].

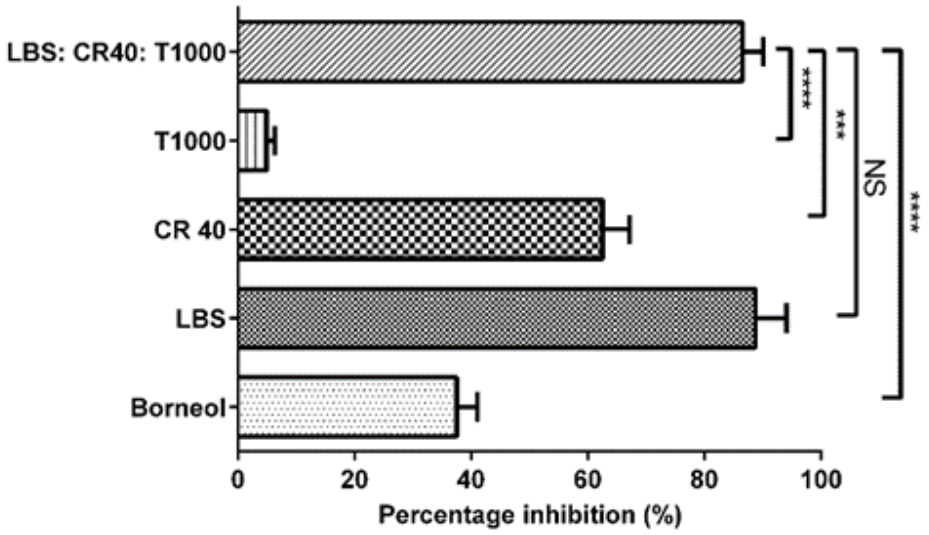

Figure 3.1 Inhibitory effect of various surfactants on glucuronidation of EDR in a microsomal incubation assay (mean ± S.D., n = 3). ***P <0.001 and ****P <0.0001 for LBS: CR40: T1000 (1:0.8:0.2) compared to others. One-way ANOVA and Sidak's multiple comparisons test Data for Borneol and LBS were adopted from the earlier report. LBS: Labrasol®, T1000: D -α-Tocopherol polyethylene glycol 1000 succinate, CR40: Cremophor® RH 40.

From inhibitory effect on EDR glucuronidation, solubility, emulsification, the potential of inhibitory effect on Pgp efflux and safety profile, a combination of Cremophor® RH 40, Labrasol® and TPGS 1000 (1:0.8:0.2) was selected as a surfactant.

Table 3.2 Assessment of emulsification ability of surfactants and co-surfactants (mean ± S.D., n = 3).

Screening of surfactants				
Surfactants	Droplet size (nm)	PDI	% Transmittance	Self-emulsification time
Labrasol®	282.52 ± 21.56	0.432 ± 0.141	68.51 ± 5.11	< 2 min
Labrasol®: TPGS 1000 (4:1)	198.41 ± 12.24	0.357 ± 0.092	79.41 ± 4.62	< 2 min

Cremophor® RH 40	92.34 ± 8.92	0.341 ± 0.094	94.62 ± 3.59	< 2 min
Cremophor® RH 40 : Labrasol® : TPGS 1000 (5:4:1)	69.51 ± 3.41	0.260 ± 0.064	98.21 ± 0.24	< 2 min

Screening of co-surfactants

Co-Surfactants	Droplet size (nm)	PDI	% Transmittance	Emulsification time
Transcutol P®	31.41 ± 2.51	0.174 ±0.025	99.08 ± 0.09	< 2 min
Ethanol	58.26 ± 6.78	0.414 ± 0.104	94.52 ± 0.94	< 2 min
PEG 300	98.83 ± 9.35	0.552 ± 0.162	91.84 ± 1.68	< 2 min

3.4.1.3 Selection of co-surfactant

To make stable L-NLNS and improve emulsification ability of selected surfactant, the selection of co-surfactant was carried out in 2 steps including solubility and emulsification study. The maximum saturated solubility of EDR was observed in Transcutol P® (93.06 mg/mL) among all co-surfactants (Table 3.1). From solubility study, Transcutol P®, ethanol and PEG 300 were selected for emulsification study. The appropriate co-surfactant with surfactant lowers the interfacial tension and forms a steady layer of oil–water interface [346]. The microemulsion with Ethanol and PEG 300, did not show desired characteristics. The significant decrease in droplet size from 69.51 nm to 31.41 nm and in PDI from 0.260 to 0.174 was observed in the case of Transcutol P®. Previously, Transcutol P® has been effectively utilized to improve emulsification of lipid-based nanoformulationshaving Labrasol® as a surfactant [315, 373]. The results confirmed the candidature of Transcutol P® as a co-surfactant. Chemically, it is diethylene glycol monoethyl ether. Its safety is also proven in various acute, subchronic and chronic toxicity studies with LD 50 value >5 g/kg/day [370]. From solubility, emulsification and proven safety profile, Transcutol P® was selected as a co-surfactant.

3.4.1.4 Construction of ternary phase diagrams

From studies mentioned above, Capryol™ PGMC was selected as oil, Cremophor® RH 40: Labrasol®: TPGS 1000 as a surfactant and Transcutol P® as a co-surfactant for the development of L-NLNS for EDR. It could spontaneously form an oil in water transparent microemulsion with gentle agitation after the dilution with aqueous media as it requires minimal requirement of free energy for emulsion formation [318]. The optimization of the concentration of each component is critical to the formation of stable microemulsion after dilution. To identify a self-microemulsification region and to select the appropriate amount of selected oil, surfactant and co-surfactant, Pseudoternary phase diagrams were constructed. The concentration of an oil 0-80 % (w/w), surfactant 20–80 % (w/w), and co-surfactant 0–30 % (w/w) was tried. Initially, total 24 formulations were prepared and evaluated by altering the oil, surfactant and co-surfactant concentration in the order of 10%. The criteria for the selection of range for oil, surfactant, and co-surfactants for further screening, were based on droplet size (<100 nm) and PDI (<0.1). The measurement of droplet size was considered as a crucial factor as nanosize droplets influence the dissolution of the drug by providing a large surface area, thus enhance the drug absorption. It also affects the stability of microemulsion [374]. The determination of PDI is used to understand the droplet size range in the system. The PDI value closer to zero indicates the uniformity in the size of droplets into the system. The PDI value of >0.3 indicates a heterogeneous dispersion while <0.1 designates homogenous dispersion [348].

The ternary phase diagram (Fig. 3.2A) was constructed based on the result of 24 trial formulations. Total 15 formulations are having a composition of oil (10-40 %), surfactant (40-80 %) and co-surfactant (0-30 %) were passed as per the acceptable criteria. In the absence of oil, the formulation made up with surfactant and co-surfactant were not able to form stable dispersion after dilution. A significant increase in the droplet size and PDI were witnessed with increasing concentration of an oil and decreasing concentration of surfactant and co-surfactant. The probable reasons for increasing the droplet size are an increment of bulk due to the high concentration of oil and an inability of reduction in interfacial tension at a lower concentration of surfactant [355]. The role of co-surfactant is critical with surfactant in forming a steady layer at the oil-water interface and preventing penetration of water in oil droplets. It could also play a significant role to solubilize the drug of required clinical dose [346].

The selected concentrations of oil (10-40 %), surfactant (40-80 %) and co-surfactant (0-30 %) were further assessed by varying each concentration in the order of 5%. Total 46 formulations

were tried to identify typical composition for L-NLNS (Fig. 3.2A). The criteria were set for the selection of typical composition for L-NLNS such as maximum oil content with minimum surfactant content, and for microemulsion after dilution having minimum droplet size (<100 nm), minimum PDI (<0.1), % Transmittance (>99%) and self-emulsification time (<120 s) [312, 346]. The concentration of oil is critical for a lipophilic drug like EDR as it could solubilize the drug and also facilitate the transport through lymphatic route and prevent its metabolism by protecting it from GI environment. It also affects the drug release and rate of absorption from GI tract. The concentration of surfactants was decided to keep minimum as its higher concentration could show unwanted toxicity and GI irritation [34]. Measurement of % Transmittance is the indicative of the clarity of microemulsion. The formulation with % Transmittance <99 % compared to water, confirms the formation of a microemulsion containing droplets of nanosize [37]. The determination of self-emulsification time is the assessment of the efficiency of emulsification after exposing to the aqueous media. The acceptable criteria of 120 s was set as per the previous literature [34].

The droplet size of microemulsion was decreased with decreasing the concentration of oil and increasing the concentration of surfactant and co-surfactant. The higher amount of surfactant and co-surfactant lowers the interfacial tension, thus increasing the penetration of water to disrupt oil-water interface resulting in decreased droplet size. The range of droplet size of trial formulations was 15.4 - 129.3 nm. The PDI was in the range of 0.035 - 0.297 for all formulations. The higher proportion of oil in the formulation made the variable size of droplets and resulted in the higher PDI. The concentration of surfactant and co-surfactant played a significant role in stabilization of interfacial tension to generate a system having uniform droplet size and minimum PDI. The self-emulsification time was increased from 20 s to 120 s with increasing the concentration of oil in the composition and decreasing the concentration of surfactant and co-surfactant. The formulation with a high proportion of oil required more time for emulsification while the higher amount of surfactant and co-surfactant lowered the emulsification time. The increasing droplet size and PDI showed significant decreasing % Transmittance. The increasing concentration of oil and decreasing concentration of surfactant and co- surfactant varied % transmittance in the range of 94.09 - 99.95. The self-microemulsifying region was plotted in Fig. 3.2B. Considering all the requirements, the L-NLNS with Capryol™ PGMC as oil, the mixture of Cremophor® RH 40, Labrasol® and TPGS 1000 (1:0.8:0.2) as a surfactant and Transcutol P® as a co-surfactant in the ratio of 30:25:25:20 % w/w was finalized.

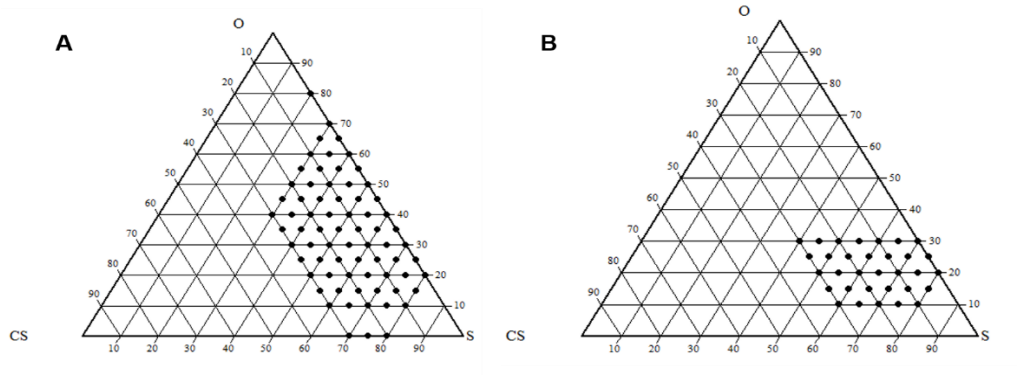

Figure 3.2 Construction of ternary phase diagram with the system of CapryolTM PGMC as oil, Cremophor® RH 40: Labrasol®: TPGS 1000 (1:0.8:0.2) as a surfactant and Transcutol® P as a co-surfactant explored self-emulsifying region (A), obtained self-emulsifying region.

3.4.1.5 *In-vitro* characterization of L-NLNS formulation

Droplet size, PDI, and %transmittance

The table displays the *in-vitro* characterization of the optimized L-NLNS. The optimized L-NLNS showed 16.25 nm droplet size, 0.039 PDI and 99.85% of transmittance after dilution with water which confirms its potential to form a clear uniform dispersion and to improve drug dissolution and absorption.

Self-emulsification time

The self-emulsification time for optimized L-NLNS was found to be 32 s which suggests a requirement of very low amount of free energy for emulsification, thus spontaneous formation of a microemulsion of desired qualities.

Zeta potential

Zeta potential is the crucial parameter in determining the stability of microemulsion formed after dilution with aqueous media. The stability of formed microemulsion depends on the electrostatic force of droplets. A decreasing electrostatic repulsive force could destabilize the microemulsion and result in phase separation. Increasing the electrostatic forces will prevent aggregation of droplets and stabilize the microemulsion [61]. The higher zeta potential compared to zero value indicates superior stability. L-NLNS showed zeta potential of -9.37 mV which designates stable microemulsion.

Drug loading ability

The maximum loading ability was found 6.45% w/w. There was no precipitation observed before and after dilution with water during the storage for 24 h at room temperature.

Determination of drug content

The loading efficiency was determined to understand the actual amount of EDR loaded in L-NLNS after preparation. L-NLNS showed 99.74% of drug content which confirmed the uniform distribution of the drug in the formulation.

Cloud point measurement

The determination of the cloud point is the temperature at which irreversible phase separation, as well as dehydration of surfactants, results in the sudden appearance of cloudiness. Hence, it is critical to determine the integrity of microemulsion as a function of temperature [352]. The ideal cloud point should be more than 37 °C, a physiological temperature to avoid phase separation in physiological condition [375]. The cloud point of finalized L-NLNS was found to be 72 ˚C suggesting its suitability for oral administration.

Thermodynamic stability study

The thermodynamic stability is the unique advantage of microemulsion-based formulation over simple suspension and emulsion-based formulations [376]. The thermodynamic stability of formulations was carried out to evaluate the effect of various stress conditions like temperature and centrifugal force. The optimized L-NLNS was found thermodynamically stable with no phase separation, precipitation, creaming and cracking.

Reconstitution ability of L-NLNS

After oral administration, L-NLNS would encounter dilution with GI fluids like SGF and SIF. Therefore, the reconstitution ability of L-NLNS was assessed by determining droplet size and PDI at various time intervals [346]. There were no phase separation or drug precipitation and significant difference perceived in droplet size and PDI after dilution with water, SGF and SIF up to 24 h (Table 3.3). The results revealed that the L-NLNS is the robust after dilution with all aqueous media.

Table 3.3 Evaluation of the self-emulsifying ability of L-NLNS and S-NLNS in different dilution mediums (mean ± S.D., n = 3)

Formulation	Media	0 h		6 h		24 h	
		Droplet size (nm)	PDI	Droplet size (nm)	PDI	Droplet size (nm)	PDI
L-NLNS	Water	16.25 ± 3.53	0.04 ±0.015	17.51 ± 2.32	0.04 ±0.013	18.82 ± 4.61	0.04 ±0.019
	SGF (pH 1.2)	18.48 ± 2.15	0.04 ± 0.014	17.09 ± 3.63	0.04 ± 0.019	19.68 ± 3.13	0.05 ± 0.015
	SIF (pH 6.8)	17.28 ± 2.84	0.04 ± 0.019	18.45 ± 3.25	0.05 ± 0.011	20.21 ± 3.96	0.05 ± 0.011
S-NLNS	Water	75.25 ± 4.57	0.07 ±0.01	75.56 ± 2.91	0.07 ±0.01	75.34 ± 3.12	0.07 ±0.01
	SGF (pH 1.2)	72.58 ± 3.13	0.07 ±0.01	73.51 ± 2.42	0.07 ±0.01	72.94 ± 4.56	0.07 ±0.01
	SIF (pH 6.8)	76.73 ± 2.94	0.07 ±0.01	76.45 ± 3.51	0.07 ±0.01	77.02 ± 2.49	0.07 ±0.01

***In-vitro* evaluation of L-NLNS composition on metabolism and permeability of EDR**

The extensive metabolism and poor permeability were considered as the major hurdle contributed to the poor oral BA of EDR [96, 342]. To evaluate the effect of formulation ingredients of L-NLNS on metabolism and transport from mucosal to serosal side, *in-vitro* permeability and metabolism assay were conducted with everted sac of rat gut. Two-way ANOVA analysis by using Sidak's multiple comparisons tests confirmed the significant effect of ingredients on metabolism as well as permeability. The L-NLNS showed the significantly higher amount of EDR transfer after 15 min compared to EDR suspension and in combination with Borneol (Fig. 3.3 A). The amount of EDR transferred with L-NLNS and Borneol were 7.63 fold ($p < 0.0001$) and 2.25 fold ($p < 0.0001$), respectively compared to EDR suspension after 120 min. EDR undergoes significant glucuronidation during the transport to the serosal

side from mucosal. For EDR-G, the significantly low amount was observed on the serosal side with L-NLNS compared to EDR suspension (1.96 fold) ($p < 0.0001$) and with Borneol (1.44 fold) ($p < 0.001$), which confirmed the significant effect on metabolism (Fig. 3.3 B). The molar ratio of EDR-G to EDR was found significantly low with L-NLNS compared to EDR suspension (3.82 fold) ($p < 0.001$) and with Borneol (2.13 fold) ($p < 0.05$) (Fig.3.3 C). Fig. 3.3 D shows the significant higher transfer rate (4.32 fold) of EDR with L-NLNS compared to EDR suspension (4.32 fold) ($p < 0.0001$) and with Borneol (1.63 fold) ($p < 0.001$). The results confirmed the potential of L-NLNS formulation for EDR to enhance the oral BA.

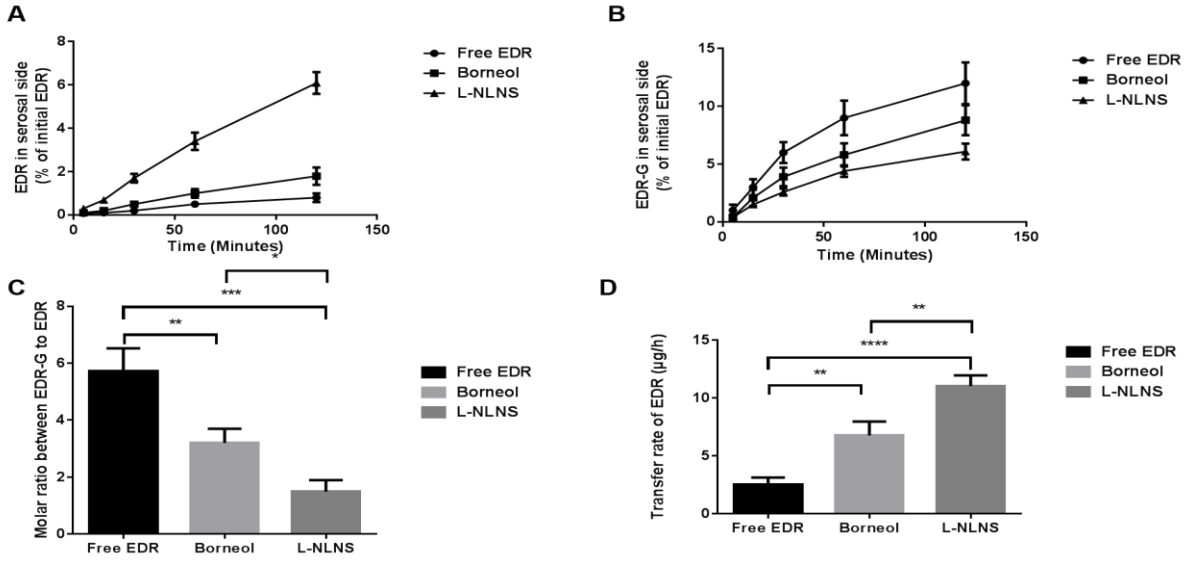

Figure 3.3 The effect of formulation ingredients of L-NLNS on permeability and metabolism of EDR during transportation across everted sacs of rat small intestine. The amount in percentage of EDR (A) and (B) on serosal side of everted sac at various time interval, molar ratio between EDR-G and EDR (C), and transfer rate of EDR in the serosal side of rat everted gut sacs (D) (mean ± S.D., n = 3). *P <0.05, **P<0.01, ***P<0.001 and ****P <0.0001. One-way ANOVA and Sidak's multiple comparisons test. Data for EDR suspension and Borneol were adopted from the earlier report.

3.4.2 Formulation development and characterization of S-NLNS Formulation

3.4.2.1 Selection and optimization of concentration of solid carriers

The possible drawbacks related to liquid lipid-based nanoformulation are poor stability, interaction with capsule material and low portability during the manufacturing. Solid lipid-based nanoformulation could offer the superior stability and patient compliance. Therefore various water-soluble carriers such as mannitol and lactose, and water-insoluble carriers including silicon dioxide were used previously to convert liquid to solid lipid-based nanoformulation [313]. The water-insoluble carrier was preferred over water-soluble carriers by reason of possible inadequacy related to water-soluble carriers such as significantly low oil

absorbing capacity and being relatively hygroscopic in nature which tends to recrystallize during the storage and deteriorate the quality features of liquid lipid-based nanoformulation [314]. Aerosil® 200 was chosen on account of its small droplet size (<10 µm), larger surface area (>200 m^2/g) and higher oil adsorbing capacity (255 mL/100 g) [314]. Additionally, it is widely used for pharmaceutical preparation for the oral and topical administration because of its proven safety profile with GRAS listing [370].

The optimization of the concentration of Aerosil® 200 was performed by evaluating the flow characteristics of the S- NLNS [314, 355]. The CI, HR, and AR were considered as evaluation parameters and standards as per USP to categories the flow of S-NLNS from very very poor to excellent [356]. The result of various S-NLNS based on a different ratio of L-NLNS to Aerosil® 200 is shown in Table 3.4. The flow of S-NLNS improved with increasing the concentration of Aerosil® 200 as CI, HI and AR were decreasing. With the ratio of L-NLNS to Aerosil® 200 (1:1), S-NLNS displayed excellent flow as per USP standard with CI (9.67), HR (1.11) and AR (27.19). Therefore it has been selected for further characterization.

Table 3.4 Optimisation of Aerosil® 200 concentration for S-NLNS based on flow properties (mean ± S.D., n = 3)

Ratio (L-NLNS: Aerosil® 200)	CI (%)	HR	AR	Flow character
1:0.4	45.83 ± 2.42	1.85 ± 0.07	66.68 ± 4.52	Very, very poor
1:0.6	31.57 ± 1.13	1.45 ± 0.04	47.32 ± 3.13	Poor
1:0.8	14.38 ± 1.92	1.17 ± 0.05	34.92 ± 3.20	Good
1:1	9.67 ± 1.10	1.11 ± 0.03	27.19 ± 2.82	Excellent

3.4.2.2 *In-vitro* characterization of S-NLNS formulation

Droplet size, PDI, %transmittance and Self-emulsification time

The characterization of S-NLNS was evaluated to assess the quality of microemulsion formation diluting with water. S-NLNS retained 98.56 % of EDR content and previously mentioned all quality attributes after dilution like droplet size (75.25 ± 4.57 nm), PDI (0.07 ±0.01), % Transmittance (99.48 ± 0.14) and self-emulsification time (38 ± 6).

Solid state characterization

The determination of the physical state of EDR in S-NLNS was considered as it could influence its performance *in-vitro* and *in-vivo* [314]. DSC, XRD and SEM analysis were performed for solid state characterisation of S-NLNS compared to EDR and Aerosil® 200.

The DSC thermograms of pure EDR, Aerosil® 200, a physical mixture of EDR and Aerosil® 200 and S-NLNS are revealed in Fig. 3.4 A. A sharp endothermic peak in case of EDR at 128.39 °C was indicated its highly crystalline nature. No endothermic peak was observed with Aerosil® 200, which could be due to amorphous nature. DSC curve for a physical mixture of EDR and Aerosil® 200 displayed a small endothermic peak of EDR compared to the pure drug, which could be as a result of dilution with Aerosil® 200. Interestingly, no endothermic peak of EDR appeared in the DSC spectra of S-NLNS. It might be explained as EDR could exist in a solubilized or amorphous form in S-NLNS compositions [377].

The internal physical state of EDR in the S-NLNS was further verified by XRD analysis. The XRD spectra of pure EDR, Aerosil® 200, a physical mixture of EDR and Aerosil® 200 and S-NLNS are shown in Fig. 3.4 B. The crystalline nature of EDR was reflected with several sharp and intense peaks. The low intense peaks of EDR were observed with a physical mixture of EDR, and Aerosil® 200 might be as a result of dilution with solid carriers. Aerosil® 200 did not show any peak because of amorphous in nature. The result of S-NLNS showed the absence of obvious peaks of EDR confirming the complete solubilisation of EDR in the composition of S-NLNS, the thorough conversion in an amorphous state from crystalline state or disordered, crystalline state in the S-NLNS [314].

The analysis of surface morphology by SEM images of pure EDR, Aerosil® 200 and S-NLNS are shown in Fig. 3.4 C. The rod-shaped structure of EDR confirmed the crystalline structure. The SEM image of Aerosil® 200 displayed aggregates of amorphous particles with a porous surface. Distinct crystalline particles of EDR were not observed in the case of S-NLNS suggesting complete adsorption of L-NLNS into the solid carriers [314].

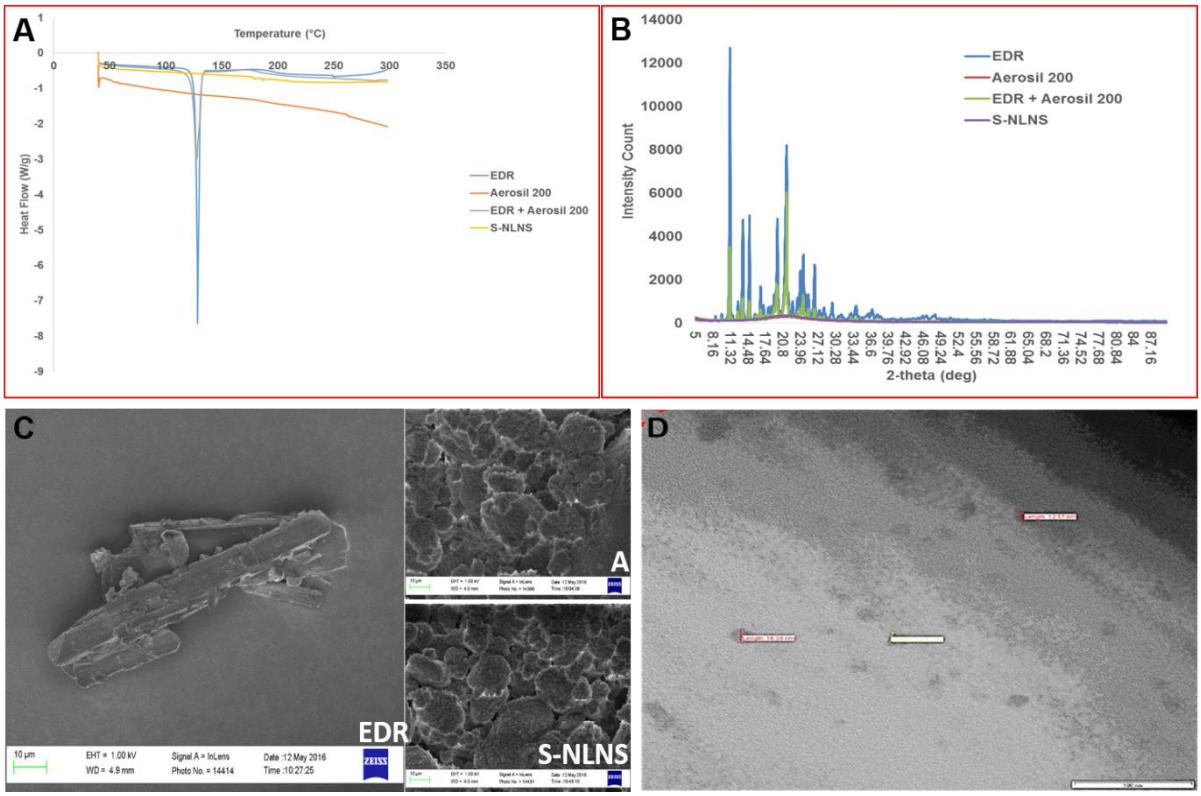

Figure 3.4 Overlay of the DSC patterns (A), and PXRD patterns (B) of EDR, Aerosil® 200, a Physical mixture of EDR and Aerosil® 200 and S-NLNS. SEM images (C) of EDR, Aerosil® 200 and S-NLNS. TEM image (D) of microemulsion formed after dilution of S-NLNS in water. Data of DSC, PXRD, and SEM for EDR were adopted from the earlier report. EDR: Edaravone and A: Aerosil 200

TEM analysis

The morphology of microemulsion after reconstituting of S-NLNS with water was examined with a transmission electron microscope (Fig. 3.4 D). The spherical shape, size (<100 nm) and Gaussian distribution were confirmed with TEM photography. The TEM results are consistent with the analysis of zeta sizer.

Stability in simulated GI fluids

The robustness of S-NLNS was confirmed as similar to L-NLNS with no significant difference in droplet size and PDI after dilution up to 24 hours (Table 3.3). S-NLNS revealed nearly 5 fold, and 1.4-1.75 fold more droplet size and PDI compared to L-NLNS, respectively after dilution with various aqueous media. An incomplete desorption of different components of S-NLNS on water-insoluble carriers could be likely reason for increasing droplet size and PDI and consistent with the previous report [314].

Stability after dilution to different folds

After an oral administration, S-NLNS undergoes variable dilution with GI fluids. Thus, the stability of microemulsion was determined after diluting with various dilutions of SGF [346]. There is no significant difference in droplet size and PDI of microemulsion formed from various dilution up to 24 hours as shown in Table 3.2. Additionally, no phase separation or drug precipitation was observed. All the quality attributes of L-NLNS were retained in S-NLNS after all dilutions.

3.4.3 In-vitro release test

After exposing formulation to the GI environment, the drug could be present in a free molecule, emulsion and/or micellar form. The standard dissolution testing could not mimic the *in-vivo* dissolution as it might not separate the free drug molecule to the entrapped drug molecule in emulsion droplet or micelles form. The additional dialysis bag method was utilized to compare the *in-vitro* release of EDR from EDR suspension, L-NLNS and S-NLNS in SGF and SIF [359]. The determination of equilibrium solubility of EDR in SGF and SIF was performed to check the possibility of a pH-dependent release of EDR as the pH-dependent solubility of EDR was reported from pH 2 to 10 [342]. Surprisingly, the superior solubility of EDR in SGF (8.26 ± 1.42 mg/mL) was observed compared to SIF (1.89 ± 0.51 mg/mL). The higher solubility in SGF could be explained due to the formation of salt as SGF is made up of hydrochloric acid which has a tendency to make salt with EDR. The results of EDR release from suspension, L-NLNS, and S-NLNS in SGF and SIF media are shown in Fig. 3.5A and 3.5B, respectively and analyzed by two-way ANOVA analysis using Sidak's multiple comparisons tests. In SGF, the EDR suspension demonstrated 86.45% and 100% drug release within 5 min and 15 min, respectively due to high solubility in SGF. The L-NLNS showed significant improvement in dissolution ($p < 0.05$) with 96.14% EDR release within 5 min followed by 100% in 15 min, whereas S-NLNS showed 83.42% EDR release in 5 min, 93.24% in 15 min and almost 100% in 30 min. There was a significant difference in dissolution profile of L-NLNS and S-NLNS observed at 5 min ($p < 0.001$) and 15 min ($p < 0.05$). In SIF, there was 85% drug release witnessed within 120 min with EDR suspension while 100% drug release within 15 and 30 min in case of L-NLNS and S-NLNS, respectively. The dissolution of EDR was significantly enhanced with L-NLNS and S-NLNS against EDR suspension at each time points ($p < 0.001$). The novel approach overcomes the hindrance to the drug release of EDR related to characteristics of dissolution media. It could improve the dissolution by providing higher surface area because of generating nano-sized droplets and increasing the solubilization of

EDR. There was the significant difference in dissolution profile in SGF and SIF of L-NLNS, and S-NLNS observed at 5 min ($p < 0.001$) and 15 min ($p < 0.05$). The possible reason could be hydrogen bonding between a silanol group and EDR [314].

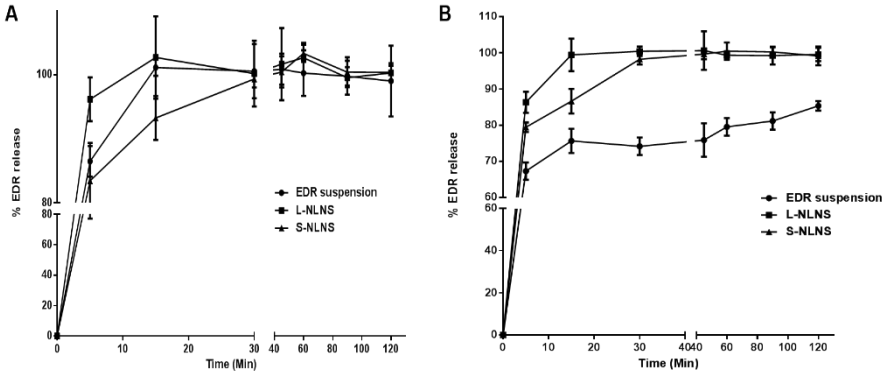

Figure 3.5 *In-vitro* release profile of EDR suspension, L-NLNS, and S-NLNS in various dissolution media SGF (A) and SIF (B) (mean ± S.D., n = 3)

The result of release kinetic of EDR from Suspension, L-NLNS, and S-NLNS are presented in Table 3.5. From suspension, the release kinetic of EDR follows Hixson–Crowell in SGF and Korsmeyer–Peppas model (following an anomalous transport with non-Fickian model) in SIF. It shows dissimilar release profile in SGF an SIF which confirmed the pH-dependent release (f2 value 27and f1 values 22). In a case of L-NLNS, EDR release fits in Hixson–Crowell model and finds similar (f2 value 69 and f1 values below 3) in SGF and SIF. The EDR release with S-NLNS follows the first order in SGF and SIF and similar release profile (f2 value 74 and f1 values below 2). L-NLNS and S-NLNS show similar release profile in SGF and SIF which confirms the pH-independent release of EDR in various dissolution media.

Table 3.5 Results of release kinetics according to various kinetic models including First order, Zero order, Hixson–Crowell, Higuchi-matrix, and Korsmeyer–Peppas

Formulation	Medium	First order	Zero order	Hixson–Crowell	Higuchi-matrix	Korsmeyer–Peppas
EDR suspension	SGF	0.987	0.7005	0.9948	0.9127	0.9234
	SIF	0.5591	0.3794	0.4886	0.6347	0.7859
L-NLNS	SGF	0.8302	0.6271	0.96	0.864	0.877
	SIF	0.9876	0.6963	0.991	0.9101	0.9209

S-NLNS	SGF	0.9578	0.5325	0.8166	0.8023	0.863
	SIF	0.9709	0.5177	0.8435	0.7771	0.8639

3.4.4 Pharmacokinetic study

The pharmacokinetic study of L-NLNS and S-NLNS were performed to evaluate the effect of formulation composition on oral absorption against EDR suspension. The plasma concentration-time profile and pharmacokinetic parameters estimated by using Phoenix WinNonlin software were showed with the comparison of the p-value in Fig. 3.6 and Table 3.6, respectively. Two-way ANOVA analysis by using Sidak's multiple comparisons tests was performed to analyze the improvement statistically between the groups. There is a significant enhancement of C_{max} and AUC with L-NLNS (10.79 fold) and S-NLNS (9.29 fold) than EDR suspension. S-NLNS revealed longer T_{max} whereas no significant difference was witnessed in EDR suspension and L-NLNS. L-NLNS and S-NLNS presented a marked improvement in $t_{1/2}$ value compared to EDR suspension. The relative BA, $C_{max,}$ and AUC of S-NLNS was slightly lower than the L-NLNS. The possibility of incomplete desorption of L-NLNS on Aerosil® 200 could be a potential reason for a slightly low C_{max} and AUC value of S-NLNS than S-NLNS. S-NLNS displayed longer $t_{1/2}$ value compared to L-NLNS as the slow release of liquid components from solid carriers showed in dissolution study could be responsible. The hydrogen bonding interaction between a silanol group of Aerosil® 200 and EDR could be another potential factor [314].

In our previous and current study, the crystalline nature of EDR was confirmed with DSC, XRD and SEM study [342]. The selected dose for the pharmacokinetic study was 30 mg/kg for EDR suspension, L-NLNS, and S-NLNS. The solubility of EDR in suspension was 1.89 mg/mL so additional EDR would be present in undissolved suspension form. In L-NLNS and S-NLNS, the dose of EDR was completely dissolved due to solubilization effect of the components of the novel system. Therefore, enhancement of solubility and dissolution would be potential reasons for enhancement of BA. The significant impact of its composition on metabolism and permeability of EDR as shown in the *in-vitro* assay could play a critical role in the enhancement of oral BA of EDR. The possible higher cellular uptake with microemulsion system could also contribute to the enhancement of intestinal absorption [211]. Cremophor® RH 40, Labrasol® and TPGS 1000 have an ability to modulate Pgp efflux pump [306, 366, 367]. Therefore, their combination could significantly inhibit its excretion through Pgp efflux and enhance EDR absorption. For EDR, modulation of Pgp efflux pump and inhibition on UGT

enzyme are the critical requirements [96, 342]. Thus, L-NLNS and S-NLNS with a combination of Cremophor® RH 40, Labrasol® and TPGS 1000, showed significant improvement in oral BA of EDR.

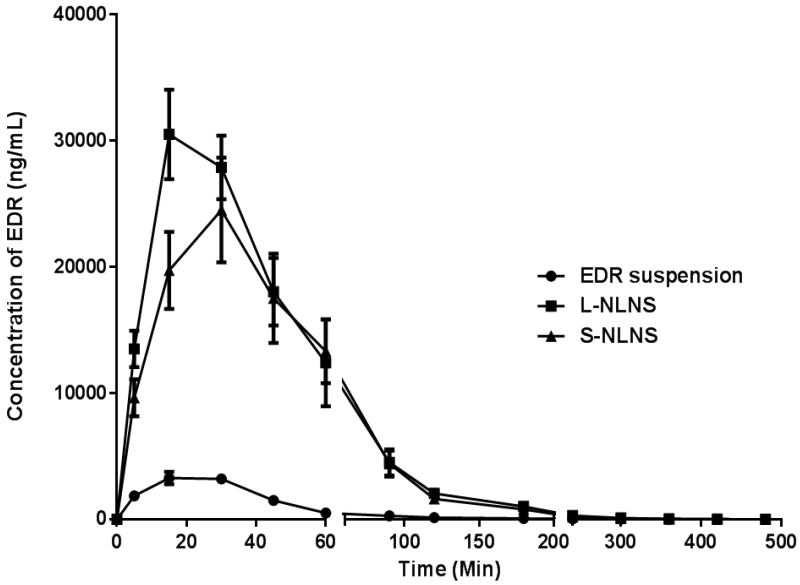

Figure 3.6 Plasma concentration-time curves for the EDR suspension, L-NLNS and S-NLNS (30 mg/kg) in SD rats after oral administrations (mean ± S.D., n = 6). Data for EDR suspension was adopted from the earlier report

Table 3.6 Pharmacokinetic parameters obtained by Phoenix WinNonlin software (mean ± S.D., n = 6). Unpaired Student's t-test for two groups. Data for EDR suspension was adopted from the earlier report

Parameters	EDR suspension	L-NLNS	S-NLNS	P Value[a]	P Value[b]	P Value[c]
C_{max} (ng/mL)	3290.42 ± 507.41	30525.13 ± 2014.5	24521.32 ± 3451.69	<0.0001	<0.0001	NS
T_{max} (min)	15.19 ± 1.45	12.52 ± 2.03	30.56 ± 5.29	NS	<0.01	<0.01
$t_{1/2}$(min)	58.31 ± 3.52	78.49 ± 2.53	85.12 ± 3.81	<0.001	<0.001	NS
AUC_{0-t} (ng·min/mL)	164185 ± 15264	1770750 ± 854244	1524862 ± 624240	<0.0001	<0.0001	NS

F_{0-t} (%)	100	1078.5 ± 155.9	±	928.75 ± 140.89	<0.0001	<0.0001	NS

NS: Non-significant

a: Comparison between EDR suspension and L-NLNS

b: Comparison between EDR suspension and S-NLNS

c: Comparison between L-NLNS and S-NLNS.

3.5 Conclusions

The present study reports the development of EDR loaded NLNS to enable its effective oral delivery by enhancing the oral BA. The selection of surfactant was considered as a critical step and performed based on the inhibitory effect on glucuronidation and having superior solubilization and emulsification ability. L-NLNS containing Capryol™ PGMC (30%), Cremophor® RH 40: Labrasol®: TPGS 1000 (1:0.8:0.2) (50%) and Transcutol P® (20%) successfully inhibited the metabolism and enhanced permeability across the rat gut. The S-NLNS formulated by using Aerosil® 200, retained all quality attributes of L-NLNS formulation and showed superior *in-vitro* dissolution compared to EDR suspension. The L-NLNS and S-NLNS showed excellent potential for further development of solid and liquid dosage form by enhancing 10.79 fold and 9.29-fold oral BA of EDR, respectively. This study revealed that the incorporation of appropriate ingredients for the NLNS offers enormous success in the clinical development of drugs having hurdles like poor oral BA.

Conflict of interest

Ankit Parikh, Xin-Fu Zhou, and Sanjay Garg are the named inventors on Chinese patent 201610149832.9. Fujian Kangshimei Co, China owns the intellectual property. There is no other potential conflict of interest relevant to this article.

Acknowledgements

Fujian Kangshimei Co, China and University of South Australia are acknowledged for the financial support for the present study. Ankit Parikh and Chun Chuan Tan are thankful to the University of South Australia for the University President's Scholarships (UPS) for PhD study and Summer Vacation Research Scholarships, respectively. Xin-Fu Zhou is grateful for the NHMRC fellowship. The authors would like to express their gratitude towards Prof. Harendra S. Parekh and Dr. Karnaker Tupally from School of Pharmacy, The University of Queensland,

for technical support in TEM analysis, Mike Hempstead from Trapeze Associates Pty Ltd. for gratis samples of Capryol™ PGMC, Labrasol®, Transcutol P®, Capryol™ 90, Labrafil® M1944cs, Lauroglycol™ FCC, Labrafac™ PG, Labrafil® M2115, Lauroglycol™ 90, and Labrafac™ Lipophile WL 1349; Abitec corporation for samples of Capmul® MCM C8, Capmul® MCM EP, Capmul® PG 8, Capmul® PG 12, Captex® 300 and Captex® 355; Carol Toft from Connell Bros Company Australasia Pty Ltd. for sample of TPGS 1000; Kartika Kasmuri for technical support, Carolyn Streckbein and Deep Pujara for revising the language; the animal welfare officer, Alex Whittaker and the animal ethics officer, Ruth Brogan; Reid animal house staff members including Jayne Skinner, Alysha Servin, Jess Parken, and Becky Nitschke from the University of South Australia for their support in *in-vivo* study.

Supplementary Information

Novel Lipid-based Nanosystem of Edaravone: Development, Optimization, Characterization and *In-vitro/In-vivo* Evaluation

Ankit Parikh, Krishna Kathawala, Chun Chuan Tan, Sanjay Garg*, Xin-Fu Zhou*

School of Pharmacy and Medical Sciences, University of South Australia, Adelaide, SA 5000, Australia.

*Corresponding author- E-mail address: xin-fu.zhou@unisa.edu.au; Sanjay.garg@unisa.edu.au;

Phone: +61-8830 22329; +61-883021575

Fax: +61 8830 21087; +61 8830 22389

Table S1 Scale of flow ability as per USP.

Flow character	CI	HR	AR
Excellent	≤10	1.00–1.11	25–30
Good	11–15	1.12–1.18	31–35
Fair	16–20	1.19–1.25	36–40
Passable	21–25	1.26–1.34	41–45
Poor	26–31	1.35–1.45	46–55
Very poor	32–37	1.46–1.59	56–65
Very, very poor	>38	>1.60	>66

Table S2 Effect of dilution on S-NLNS of EDR (mean ± S.D., n = 3).

Dilution	0 h		6 h		24 h	
	Droplet size (nm)	PDI	Droplet size (nm)	PDI	Droplet size (nm)	PDI
200	86.52 ± 4.57	0.07 ±0.01	87.78 ± 3.21	0.07 ±0.01	87.16 ± 4.82	0.07 ±0.01
400	82.84 ± 2.52	0.07 ±0.01	81.10 ± 3.58	0.07 ±0.01	82.61 ± 3.19	0.07 ±0.01
600	79.14 ± 1.91	0.07 ±0.01	79.58 ± 2.56	0.07 ±0.01	79.81 ± 2.99	0.07 ±0.01
800	76.63 ± 2.83	0.07 ±0.01	76.20 ± 4.81	0.07 ±0.01	76.16 ± 4.80	0.07 ±0.01

Table S3 Mathematical models used to describe drug dissolution curves.

Mathematical models to determine the release kinetic		
Model	Equation	Description
First order	$Q_t = \ln Q_0 + K_1 t$	Q_t: amount of drug dissolved in time t,
Zero order	$Q_t = Q_0 + K_0 t$	Q_0: initial amount of drug in the solution, t: time,

Hixson–Crowell	$Q^{1/3}{}_0 - Q^{1/3}t = K_C t$	Q_∞: amount of drug dissolved in time ∞.
Higuchi-matrix	$Q_t = K_H t^{1/2}$	K_1, K_0, K_C, K_H, K_K are the rate constants for first order, zero order, Hixson–Crowell, Higuchi-matrix and Korsmeyer–Peppas resepctively.
Korsmeyer–Peppas	$Q_t/Q_\infty = K_K t^n$	

Table S4 Release profiles comparison using Dissimilarity factor and Similarity factor.

Release profiles comparison		
Dissimilarity factor (f1)	$f_t = \frac{\sum_{j=1}^{n} \lvert R_j - T_j \rvert}{\sum_{j=1}^{n} R_j} \times 100$	n: sampling number,
Similarity factor (f2)	$f_2 = 50 \times \log\left\{ [1 + (1/n) \sum_{j=1}^{n} \lvert R_j - T_j \rvert^2]^{-0.5} \times 100 \right\}$	Rj and Tj: percent dissolved of the reference and test products at each time point j,

4. Novel Edaravone Formulation Based on Self Nanomicelization Solid Dispersion Strategy for Enhancement of Oral Bioavailability and Reversal of Cognitive Deficits in Alzheimer's Disease Models.

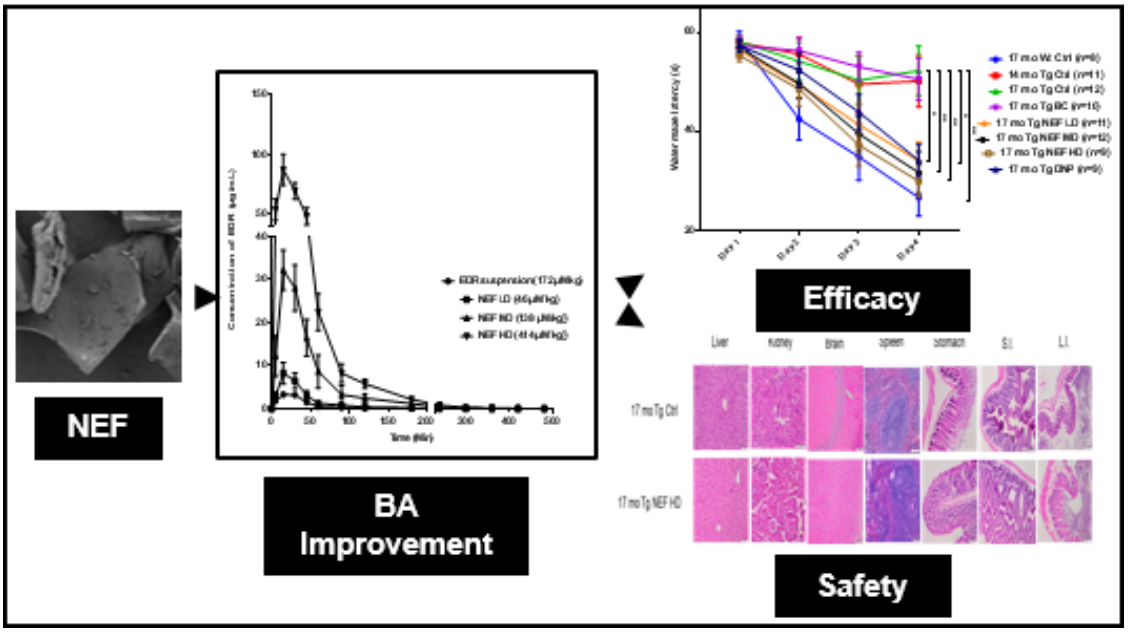

Graphical Abstract

4.1 Abstract

Alzheimer disease (AD) is a devastating neurodegenerative disorder that lacks any disease-modifying drug for the prevention and treatment. The drug development for this disease has become a holy grail as 99.6% failure rate is encountered in clinical trials. Edaravone, an approved free radical scavenger for ischemic stroke, is proved its potential against the AD by targeting multiple key pathologies including amyloid-beta, tau phosphorylation, oxidative stress, and neuroinflammation. The poor oral bioavailability (BA) could be a major hurdle for its clinical development. The novel Edaravone formulation (NEF) is developed using self-nano micellizing solid dispersion strategy to enhance the oral BA. From the screening of polymers based on their potential for improving the solubility, Soluplus® (SOL) was selected. NEF with EDR and SOL (1:5) resulted in the highest enhancement in aqueous solubility (17.53-fold) due to amorphization, hydrogen bonding interaction and micellization. Moreover, the NEF demonstrated significant improvement in intestinal permeability and dissolution profile of EDR. Furthermore, the oral BA of NEF showed 10.2, 16.1 and 14.8-fold enhancement compared to EDR suspension at 46, 138 and 414 µM/kg dose. Besides, our data confirms non-toxicity up to 414 µM/kg dose after 3 months and its potential to reverse AD-like cognitive deficits of APP/PS1 mice in dose-dependent manner. Therefore, NEF could be used as a potential candidate for the treatment of AD.

Keywords: Edaravone, Soluplus®, oral bioavailability, Dose-response relationship, APPSwe/PS1deE9 mice, Learning and memory, safety assessment

4.2 Introduction

Due to unprecedented advancement in medical technology to combat dreadful diseases and providing a high quality of life in the 21st century, the ageing population is increasing [378]. Alzheimer Disease (AD), the most common cause of dementia, is a chronic neurodegenerative disease linked with the progressive cognitive deficits specifically in elder community with a sufficient severity to compromise an individual's daily function [69]. It causes huge social and economic burden such as estimated cost of care for global patients of AD and dementia is equivalent to 1% global gross domestic product (GDP) [379]. Currently, 47 million global people are live with dementia and, a figure which is projected to rise to 74 million by the year 2030 [62]. Even after a century of its discovery, the effective therapy is still not available which could prevent, cure and even stop its progression [14]. The Amyloid-beta plaques and phosphorylated Tau neurofibrillary tangles are considered as primary hallmarks in the brain [11, 12]. The complexity of the disease is the main reason for several failures in clinical trials due to the involvement of multiple pathways in the development and progression of the disease such as oxidative stress, neuroinflammation, mitochondrial dysfunctions, glial activation, synaptic dysfunction, and neurotransmission-related mechanisms. Most mechanisms form vicious cycles to accelerate the disease progression. Thus, targeting multiple key pathways of the AD pathogenesis is the key for the successful therapeutic outcome [69, 380].

Edaravone (3-methyl-1-phenyl-2- pyrazolin-5-one, MCI-186, EDR) is a free radical scavenger, developed by Mitsubishi Tanabe Pharma Corporation (Japan). It has been approved for the treatment of acute cerebral infarction and amyotrophic lateral sclerosis (ALS) in Japan [342]. The protective effect of EDR against AD-like insults in neuroblastoma N2a cells was reported by attenuating cytochrome c release, suppressing the activation of caspase-3 and decreasing the Bax/Bcl-2 ratio [193]. Also, its inhibitory effect on amyloid-β precursor protein (APP) processing and enhancing non-amyloidogenic pathway for the regulation of Aβ production using human ''Swedish'' APP mutation APP695 (SY5Y-APP695swe) was shown [194]. Also, its efficacy in streptozotocin induced and Aβ-induced rat models were demonstrated improvement against the cognitive dysfunction [195-197]. Moreover, its therapeutic potential in double transgenic (Tg) APPSwe/PS1deE9 (APP/PS1) mice after 3 months of treatment were revealed by targeting multiple pathologies such as Aβ, oxidative stress, Tau hyperphosphorylation, synaptic dysfunction, neuronal loss, neuroinflammation, glial activation and improves the behavioral deficits [69]. The dose-dependent efficacy assessment of EDR is

yet to be explored as it showed dose dependent effect against cerebral arachidonate cascade [381], cardioembolic stroke [112] and neonatal hypoxic-ischemic encephalopathy [382].

The oral route of administration is the most preferred by patients considering their compliance and comfort. Accurate and flexible dosing, easy production, economic, higher stability are key reasons for most frequently use of oral route for drug administration [383]. EDR was proved orally active against the AD [69] and cerebral aneurysms [125]. However, the current approved and available form of EDR in the market is Radicut®, an intravenous infusion solution for parenteral administration. Rong et al. reported the poor absolute oral bioavailability (BA) (5.23%) of EDR. Besides, it was designated as class IV drug as per Biopharmaceutics Classification System (BCS) due to its poor aqueous solubility (1.85 ± 0.15 mg/mL) and permeability (Peff = 3.18 ± 0.0706*10^{-7}cm/s) [96, 342]. The poor oral BA was the key reason for the failure of a clinical trial of potential candidates against AD such as Curcumin [384, 385]. Therefore, there is a need of appropriate oral formulation to conduct the clinical trials for its safety and efficacy study at large scale for the development of EDR for the AD-like chronic disease. To improve oral BA of EDR, the complexation of EDR with Hydroxypropyl-Sulfobutyl-β-cyclodextrin showed promising results by displayed 10.3-fold improvement by improving its solubility, dissolution, and permeability [96]. However, its commercial potential was limited due to the high molecular weight of cyclodextrin, slow process of complexation and the unstable condition of processing media [298]. Moreover, Treeway, a biotech company, developed a unrevealed oral formulation of EDR to conduct clinical trials for amyotrophic lateral sclerosis (ALS), which received orphan designation from regulatory agencies including European Medicines Agency (2014) [82] and U.S. Food and Drug Administration (USFDA) (2015) [83]. Furthermore, the Novel Oral Delivery System (NODS) of EDR based on co-solvency and pH modification technology showed limited success by improving oral BA by 5.71-fold [342]. Hence, a novel oral formulation of EDR is necessary to establish which could offer superior oral BA compared to currently available alternatives and have commercialization potential. Self-nanomicellizing solid dispersion (SNMSD) strategy is the combination of widely accepted solid dispersions and nanomicelles strategies to improve the oral BA of challenging drugs. The dramatic improvement in oral BA of drugs including Curcumin [249, 330] and Ritonavir [386], belonging to BCS class IV using SNMSD strategy. Use of SNMSD strategy to enhance the oral BA of EDR is yet to be studied as per our knowledge. Thus, it was explored to develop Novel Edaravone Formulation (NEF).

AD is progressive and irreversible brain disease in which a steady decline in cognitive, behavioral and physical abilities are the key clinical manifestations. Memory loss is one of the key clinical manifestations of AD so the efficacy of any potential intervention candidate could be judged based on its ability to prevent or restore learning and memory ability [387]. Furthermore, progressive cognitive impairment is always accomplished with the progression of the pathogenesis of AD such as Aβ accumulation, downstream pathological events such as oxidative stress, tau hyperphosphorylation, glial activation, neuroinflammation, neuronal loss, and synaptic dysfunction [388]. The potential therapeutic candidates which significantly inhibit the downstream pathologies could improve the behavioral deficits of APP/PS1 mice [69]. Thus, the improvement in behavioral deficits was considered as a marker for the efficacy of NEF and evaluated by well accepted behavioral tests such as open field, novel objective recognition test (NORT), Y-maze and Morris water maze (MWM) tests [69, 389]. The information regarding the toxicity of EDR via oral administration and Soluplus® (SOL) based preparation are very limited which necessities the evaluation of safety assessment of NEF to provide guidance for clinical applications.

The work reported here aimed to develop NEF using SNMSD strategy and characterized its solubility, stability, dissolution, permeability, and BA. Moreover, its safety and efficacy in dose dependent manner with AD mice models such as Tg-AD mice (APP/PS1) was studied after long-term exposure (3 months) via the oral route.

4.3 Materials & Method

4.3.1 Materials

EDR was bought from Aladdin Industrial Corporation (Shanghai, China). SOL and CAVASOL® W7 HP PHARMA (hydroxypropyl- β-cyclodextrin) were gifted from BASF Australia Ltd and Chemiplas Australia Pty Ltd (Victoria, Australia), respectively. Potassium pyrophosphate, Tyrode's solution, ascorbic acid, sodium carboxymethylcellulose, Polyvinylpyrrolidone K 30 (PVPK30), Polyethylene glycol 4000 (PEG 4000), Poloxamer 188, Poloxamer 407, Concentrated HCL, perchloric acid, formic acid, disodium hydrogen phosphate, citric acid, uridine-diphosphate glucuronic acid trisodium salt (UDPGA), alamethicin, D-glucaric acid 1, 4-lactone and DMSO-d3 were purchased from Sigma-Aldrich (New South Wales, Australia). Acetic acid, phosphoric acid, sucrose, magnesium chloride, and sodium hydroxide pellets, were obtained from Chem Supply (South Australia, Australia), Boric acid from Optigen Scientific (South Australia, Australia), Saline from Pfizer (New South Wales, Australia) and Pierce BCA Protein Assay Kit from Thermo Fisher Scientific, Australia.

HPLC grade Ethanol and methanol were purchased from Merck (Melbourne, VIC, Australia). High purity (Milli-Q) water was used throughout the study. All other reagents were of analytical grade.

4.3.2 Formulation, Development, and optimization of NEF

4.3.2.1 Selection of a suitable carrier for the development of NEF

The carrier selection is performed based on the miscibility study as described previously [390]. The solutions of polymeric carriers including include SOL, hydroxypropyl- β-cyclodextrin, PVP K30, PEG 4000, poloxamer 407 and 188 were prepared at different concentrations including 2.5%, 5%, 7.5%, and 10% w/v using water. An excess amount of EDR was added to each polymeric solution in glass vials and allowed to shake in a mechanical shaker (Axyos Technologies) for 24 h with 150 revolutions per minute (rpm) at ambient temperature. Subsequently, each sample was filtered with 0.45 µm polyvinyl difluoride (PVDF) syringe filter and diluted with appropriate dilution by mobile phase. The analysis of samples was conducted using previously developed HPLC method with mobile phase consist of water, methanol and acetic acid (100:100:1) with 1 mL/min flow rate and 20 µL injection volume at 240 nm [342].

4.3.2.2 Preparation of SNMSD using solvent evaporation technique (SE)

SE method was used to prepare the SNMSDs of EDR and SOL, a selected polymer from miscibility study, as described by Wang et al. [391]. EDR and SOL at the ratio of 1:1, 1:2.5, 1:5, 1:7.5, 1:10, 1:12.5 and 1:15 were dissolved in an ethanol. Subsequently, the mixture was allowed to evaporate under the vacuum (500-600 mbar) using a rotatory evaporator at 55-60 °C. SNMSDs were then scraped using a spatula, pulverized in the mortar-pestle and passed through 250 µm sieve. All prepared SNMSDs were kept overnight in the desiccator for drying and stored in a refrigerator at 4 °C until use for further studies.

4.3.2.3 Kinetic Solubility Study

The selection of SNMSD as a NEF was based on the kinetic solubility study. SNMSDs or EDR were added in an excess amount to the 2 mL of simulated intestinal fluid (SIF) pH 6.8 in glass vials [332]. The solubility study was conducted as described in 4.3.2.1 and samples were collected at pre-determine time intervals.

4.3.2.4 Characterization of NEF

Comparison of solubility of NEF with crystalline EDR and physical mixture (PM)

To prepare PM, EDR, and SOL in the ratio of 1:5 was mixed using pestle-mortar until a homogeneous mixture obtained, and passed through 250 µm sieve [392]. The improvement of aqueous solubility of EDR with PM and NEF was investigated in simulated body fluids (SBF) such as simulated gastric fluid (SGF) pH 1.2, SIF pH 6.8 and pH 7.4 and water as mentioned in section 4.3.2.1 and compared with the EDR.

Loading ability and efficiency

The NEF equivalent to 1 mg of EDR was dissolved in the 1 mL of methanol. The solution was further analyzed by using previously developed HPLC method. The loading ability and loading efficiency were determined based on the weight ratio of EDR to SOL in NEF and the amount of EDR loaded in the NEF from the initial amount used for the preparation, respectively [331].

4.3.3 Investigating drug-polymer interaction with advance characterisation

4.3.3.1 Differential Scanning Calorimetry (DSC)

DSC analysis was carried out by using TA Instruments Discovery DSC (Model 2920). DSC was performed for the samples including EDR, SOL, PM and NEF. The samples (2-4 mg) was taken in the aluminum open crucible, and an empty crucible was used as a blank. Thermograms of each sample were recorded at the heating rate of 10°C/min, in the temperature range of 40 – 250 °C under the flow (50 mL/min) of nitrogen gas [332].

4.3.3.2 X-ray diffraction (XRD) study

X-ray diffraction patterns were recorded for the samples including EDR, SOL, PM and NEF to study the solid characteristics. The X-ray diffraction instrument (PANalytical, Empyrean X-ray diffractometer) was used, and diffractograms were taken by using CuKα radiation (λ = 1.5418 Å), 40 kV voltage, and 40 mA current. The scanning rate was 2°/min in the range of 2 to 50° 2θ [332].

4.3.3.3 Scanning electron microscopy (SEM)

Surface morphology was studied by using an instrument, Zeiss Microscopy Merlin with GEMINI II column. SEM study was carried out for the samples including EDR, SOL, and NEF. Each sample was mounted on the double-sided adhesive tape. The photomicrographs were obtained at the voltage of 0.7 kV and examined at the magnification of × 2000 [332].

4.3.3.4 Fourier transform infrared spectroscopy (FTIR)

FTIR spectroscopy was carried out using a conventional potassium bromide (KBr) pellet method and a PerkinElmer Spectrum 400 spectrometer. The study was performed for the samples including native EDR, SOL, PM and NEF. Briefly, 2-4 mg samples were mixed with 100-150 mg of KBr and made pellet using the pressure of 8 tonnes for 10-15 s. The KBr pellet was placed in the sample holder. FTIR spectra were obtained between the ranges of 400-4000 cm^{-1} at the scanning rate of 2 cm^{-1} [391].

4.3.3.5 ^{1}H NMR Study

Bruker AVANCE-III 500 was used to recording the ^{1}H NMR spectra at the frequency of 500 MHz, respectively. The samples including EDR and NEF were prepared by dissolving in DMSO-d_3 followed by transferring to thin 5 mm diameter tubes before measurement. The data analysis was performed by using Topspin 3.2 software [393].

4.3.4 Assessment of self-nanomicellising properties of NEF

4.3.4.1 Preparation of EDR loaded micelles solution of NEF

An accurate quantity of NEF (equivalent to 15 mg EDR) was dispersed in the 10 mL of water and kept on the magnetic stirrer for stirring at 500 rpm up to 3 h. The resultant mixture was then filtered through 0.45 µm PVDF filter to get homogeneous micellar solution [394].

4.3.4.2 Characterization of EDR loaded micelles

The Malvern Zetasizer Nano ZS was used to measure the particle size, poly-dispersity index (PDI), and zeta potential of the above prepared micellar solution based on the principle of photon correlation spectroscopy. In addition, A Philips CM100 Transmission Electron Microscope fitted with a SIS mega view ll CCD camera was used to determine morphological characteristics using transmission electron microscopy (TEM) analysis. Briefly, a tiny drop of micellar solution was kept on the copper grid followed by drying overnight and analyzed by Image analysis software.

4.3.4.3 Stability Study

Stability study of EDR loaded micelles was performed at various stability conditions including hydrolytic, thermal, photolytic, and oxidation up to 24 h [342]. Concisely, 2 mL of each solution was filled in the glass bottle and covered with aluminum foil to protect from light and kept at 25 °C. The solution was kept at various conditions which included 4 °C, 25 °C / 60

%RH, and 40 °C / 75 %RH in determining the stability against temperature. The solution was exposed to the two different concentration of H_2O_2 including 0.03 and 3% to assess the susceptibility to oxidation. The EDR micellar solution was kept in the KBF ICH 720 (E2) - constant climate chamber as per ICH guideline to determine the stability when exposed to light. The samples were pulled out at pre-determined time points and analyzed with HPLC.

4.3.5 Physical stability study of NEF as per ICH guideline

The stability study of NEF was carried out by evaluating % drug content and aqueous solubility up to 8 weeks as per ICH guideline [342]. The stability conditions include 4 °C, 25 °C/60 %RH, and 40 °C/75 %RH. The NEF was filled in the glass vials, sealed and stored in the stability chamber after covering with aluminium foil. The aliquots were collected at pre-determined time intervals and analyzed by HPLC method.

4.3.6 In-vitro permeation and metabolism study of NEF

In-vitro permeation and metabolism study was carried out as per our previous study [342]. Everted sacs of rat gut were prepared from male Wistar rats (180-200 g) to conduct the assay. Each sac was filled with 2 mL of Tyrode's solution having EDR concentration of (287.02 µmol) with or without Borneol (1.30 mmol) and NEF. The amount of EDR and EDR glucuronide metabolites (EDR-G) and the rate of permeation were determined and compared.

4.3.7 Dissolution Study

A dissolution study was performed for EDR and NEF by using USP type II (paddle) apparatus at 37°C and 50 RPM [249]. EDR and NEF were placed in the dissolution flask containing 900 mL of dissolution media including SGF (pH 1.2) and SIF (pH 6.8). At different time points of 5, 15, 30, 45, 60, 90, and 120 min, samples were collected and replaced with an equal volume of the dissolution media. The amount of the drug released at each time point was determined after dilution if required, by previously developed HPLC method. The results obtained from the HPLC analysis were fitted into the different release kinetic models including First order, Zero order, Hixon Crowell, Higuchi-matrix, and Korsmeyer-peppas to determine the release kinetic. In addition, the release profile of native EDR and NEF were compared by calculating the dissimilarity (f1) and similarity (f2) factors to understand the impact of pH on release. The formulas to determine the best suitable release kinetic model, and dissimilarity and similarity factors are mentioned in Table S1. Dissolution profiles are considered to be similar if the f1 and f2 values are <15 and 50-100, respectively.

4.3.8 Pharmacokinetic Study

The Animal study was carried out as per the previous report using the male Sprague – Dawley rats (300 ± 25 g) and the animal ethics was approved by animal ethics committee of the University of South Australia [342]. The dose dependent pharmacokinetic study of NEF was conducted and compared with the EDR suspension prepared using 0.5% sodium carboxymethylcellulose. Four groups of rats (n=6) were orally administered with EDR suspension of 172 µM/kg and NEF equivalent to 46, 138 and 414 µM/kg of EDR. EDR was extracted from the plasma by using the mixture of Mcllvaine buffer of pH 5.4 and dichloromethane-n-pentane (3:7 v/v) as mentioned in our study [342]. EDR concentration in each sample was measured using the LC-MS/MS method, and Phoenix WinNonlin software was used to calculate the pharmacokinetic parameters [342].

4.3.9 Behaviour Tests

4.3.9.1 Suitability of drinking water to supply NEF

The behavioral of animals could affect due to daily gavage or injection for 3 months. To supply with the drinking water is the best way to perform long-term safety and efficacy study. The acidic water (pH of 2.5 to 3.0) is supplied to the animals to prevent the spread of bacterial disease. Thus, stability study was conducted to investigate the suitability of drinking water supplied to animals to supply NEF formulation. To determine the stability of NEF in the total 300 mL of the formulation at the concentration equivalent to 0.27 (46 µM/kg), 0.82 (138 µM/kg) and 2.48 mM (414 µM/kg) of EDR using NEF were prepared and filled in the water bottles. These bottles were stored at room temperature in the animal house facility. The samples were collected at the predetermined time intervals and loaded in HPLC for further analysis after dilution and filtration.

4.3.9.2 Animals

APP/PS1 transgenic mice with C57BL/6 background was procured from Jackson Laboratory (Maine, United States). The animal ethics committee of the University of South Australia approved animal ethics for breeding procedures and the experiments. The breeding was done in the Reid animal facility of the University of South Australia. The standard conditions were maintained which includes standard light/dark cycles of 12 h each, the temperature of 22 ± 1°C, and humidity of 52 ± 2%. All the animals were assessed for their health, general behavior, and appearance to confirm the suitability for the whole experiment.

Table 4.1 Experimental design for behavioral tests with mouse models of Alzheimer disease

Groups	Treatment	Dose	APP/PS1 mice		
			Identity	Age (months)	Sample size (n)
Normal Control	Normal drinking Water	-	17 mo Wt Ctrl	17	8
Basal Control	Normal drinking Water	-	14 mo Tg Ctrl	14	11
Sham control	Normal drinking Water	-	17 mo Tg Ctrl	17	12
Blank control (B.C)	SOL	-	17 mo Tg BC	17	10
NEF Treated	NEF Low dose (LD)	46 µM/kg	17 mo Tg NEF LD	17	11
NEF Treated	NEF Medium dose (MD)	138 µM/kg	17 mo Tg NEF MD	17	12
NEF Treated	NEF High dose (HD)	414 µM/kg	17 mo Tg NEF HD	17	9
DNP	DNP	5.27 µM/kg	17 mo Tg DNP	17	9

The APP/PS1 (at the age of 14th months) was divided into total seven groups mentioned in Table 4.1. The group of 17 months old C57BL/6 mice supplied with normal drinking water was utilized as a positive control for the treatment groups of APP/PS1. The required amount of SOL and NEF were dissolved in drinking water, filtered and supplied to animals as per the requirement. For Donepezil (DNP), Aricept tablet (Pfizer, Auckland, New Zealand) was crushed using mortar and pestle and mixed with the required quantity of drinking water, filtered and supplied to the animals. Open field, Novel Objective Recognition Test (NORT), Y-maze and Morris Water Maze (MWM) tests were conducted to investigate the effect of 3 months of treatment of NEF on behavioral change the behavioral phenotype of APP/PS1 compared to the control groups. All behavioral tests were carried out in isolated behavior room in the Reid animal facility. To acclimate to the environment, animals were moved to the behavior room 1

h before initiating the test. ANY-maze video tracking software (Illinois, USA) and a digital camera were utilized to record the animals' behaviors as per the previous reports [69, 389, 395].

4.3.9.3 Measurement of water and food consumption

To determine the appropriate dosing, average water and food intake for animal were recorded. The animals were divided into the different groups and average water, and food consumption was documented up to 14 d before and after the addition of NEF to confirm the appropriate dosing. The initial amount and the amount left at the end of the day were recorded to get the amount consumed over a period.

4.3.9.4 Open field test

The white square open arena with an area of 40*40*40 cm was utilized for the test. Each animal was placed gently in the center of the arena and letting them move freely for the first 5 min. Each test lasts for about 10 min, and the arena was cleaned by using 70% ethanol and water respectively after each trial. In this test, a number of various conventional and ethological parameters were recorded during each session including 1) Spontaneous locomotor activity assessed by the entire distance covered and number of rearing; and 2) Anxious behaviour determined by the % time spent in the central arena, number of grooming, defecation and urination [395].

4.3.9.5 NORT

NORT test assesses the mice's ability to identify the novel object in the environment. The experiment was carried out in the same arena used in open field test. The test was carried out in the three different phases which include 1) Habituation; 2) Familiarisation; 3) Test phase. During habituation phase, each mouse was allowed to explore the whole arena without any objects. The mouse was then removed from the arena and put back into the holding cage. In the familiarization phase, the mouse was kept for some time in the open arena consisting of 2 identical objects (a + a). In the final testing phase, one of the identical objects was replaced with the novel object and the mouse was then kept in the white open arena composed of one identical and one novel object (a + b). In the 2nd and 3rd phase, the objects were kept in the opposite direction and 15 cm away from each other. Here, the time spent closure to the familiar object versus the time spent closure to the novel object on day 2 and 3 were recorded to generate the recognition and discrimination index [396]. The ratio of time spent exploring to the one object over the total time spent for exploring both objects was calculated as a recognition index.

The equation [DI = (TN − TF) / (TN + TF)] where time spent to explore the novel object (TN), and familiar object (TF) was used to calculate discrimination index.

4.3.9.6 Y-Maze test

Y-maze spontaneous alteration test was carried out to assess the willingness of mice to discover new environment. An immediate spatial working memory was evaluated by using a Y-shape maze composed of 3 opaque arms at the angle of 120° from each other as per the previous study [69]. The mouse was kept in the center of the opaque block and allowed to walk freely during 5 min session. The movement of each mouse on the opaque block was visually recorded. Alteration means successive entry to each arm when performed. The % alteration was calculated based on the actual alterations to possible alterations. For the novel arm exploration, the mouse was kept on any of the 2 arms and allowed to walk through the opaque block during the 5 min of the first session. In the second season, the mouse was allowed to explore all 3 arms and to discover a novel arm. A total number of entries in novel arm and the time spent on novel arm were recorded.

4.3.9.7 MWM test

A circular arena of 120 cm diameter and 45 cm height was used to carry out the MWM test as per the previous report [69, 395]. The test apparatus was filled up to the height of 30 cm with water having temperature of 23-25°C. The water was made cloudy using a nontoxic white dye before initiating the test. The MWM test pool was theoretically divided into the 4 different parts. In one of the four quadrants, a white platform of 7.5 cm diameter was placed, and others are marked by the testing quadrant with left, right, and opposite. The mice were allowed to freely swim in the pool for approximately 1 min so as to adjust themselves in the testing environment (Habituation phase). Here, the mice were trained in 2 phase known as a visible and hidden phase. In the visible phase, the platform was 0.5 cm above the water level while in the hidden phase, the platform was below 0.5 cm water level. Here, the training to find out a visible platform was given for 1 d (60 s/trial, 3 trials/d) and for the hidden platform, the training was given for 4 d (60 s/trial, 3 trials/d). The animals were allowed to swim from each quadrant except the quadrant closer to the platform during each trial for up to 60 s. Animals were led to the platform if they could not find it by themselves within 60 s and allowed to be there for 30 s. Moreover, the animals were allowed to be on the platform even if they find it in 60 s. The probe test (single trail of 60s) without a platform for each mouse was performed on last day of the study. The escape latency curve, swimming speed and path length (Habituation phase) in

platform trials, while a number of annulus crossing and time spent in target quadrant compared to all other quadrants were recorded.

4.3.10 Long term toxicity assessment of NEF

4.3.10.1 Body weight

Once the treatment was initiated, the weight of each mouse was documented on a daily basis for up to 2 weeks and then on a weekly basis.

4.3.10.2 Water and food consumption

The food and water consumption (g/d/10 g body weight) were noted down during the whole treatment period on a weekly basis.

4.3.10.3 General behavior and mortality

All the mice were monitored for any abnormal behavior and symptoms every day such as mortality or morbidity dull/ruffled coat, hunched posture, reluctant to move, dehydration by skin tent, diarrhea/abnormal bloating, changes in skin and fur, eyes and mucous membranes and behavior patterns [397]. The clinical record sheet for each group was maintained for every day record up to 3 months. The individual clinical record sheet was used for mice with abnormal behavior or symptoms for close monitoring. The weight loss of more than 10% was used as a standard for humane killing under veterinary advice.

4.3.10.4 Haematological Parameters

To investigate the different hematological parameters, the blood samples were collected in the $EDTAK_2$-coated vials after finishing the experiment. A fully automated 5-part differential hematology analyser (Sysmex XN550) was used for the analysis of haematological parameters such as white blood cells (WBC), red blood cells (RBC), hemoglobin (HGB), hematocrit (HCT), mean corpuscular volume (MCV), mean corpuscular hemoglobin (MCH), Mean corpuscular hemoglobin concentration (MCHC), platelets (PLT), mean platelet volume (MPV), platelet haematocrit (PCT), platelet distribution width (PDW), neutrophils, lymphocytes, monocytes, eosinophils and basophils [398].

4.3.10.5 Coagulation Parameters

Different coagulation parameters including prothrombin time (PT) and activated partial thromboplastin time (APTT) were measured manually using blood plasma. For PT estimation, the Innovin reagent was pre-heated at 37 °C using a water bath. 100 µL of plasma was taken

in the glass test tube. In the glass test tube with plasma, 200 µL of the previously heated Innivon reagent was added and the time for the fibrin strand formation was recorded. In the case of APTT determination, APTT reagent and 0.025 M calcium chloride were pre-heated at 37 °C. 100 µL of plasma sample was mixed with 100 µL of APTT reagent in the glass test tube. The resultant mixture was then incubated for 180 s (write the condition of incubation). In the above mixture, 100 µL of the calcium chloride was added and the time to start the fibrin strand formation (1st appearance of the fibrin) was documented at 37 °C. Analysis of each sample was performed in triplicate.

4.3.10.6 Serum Biochemistry

An automatic biochemistry meter (SELECRTA-E, Vital Scientific) was used to measure the different biochemical parameters such as alanine aminotransferase (ALT), aspartate aminotransferase (AST), alkaline phosphatase (ALP), Amylase, Lipase, gamma-glutamyl transferase (GGT), Sodium, Bicarbonate, Anion Gap, Potassium, Calcium, Sodium :Potassium ratio, Chloride, Inorganic Phosphorus, Calcium:Phosphorus ratio, Albumin, Total Protein, Globulin, Total Bilirubin, Creatinine, urea nitrogen, Glucose, and total cholesterol.

4.3.10.7 Organ weight

Each animal was sacrificed by carbon dioxide inhalation and perfused intracardially with cold phosphate-buffered saline (pH 7.4) after finishing the experiment. Different organs which include brain, stomach, small intestine (S.I), large intestines (L.I), liver, kidneys, spleen, and heart were collected and weighed individually.

4.3.10.8 Histopathology

The histopathological examination was performed on the all collected tissues including brain, stomach, S.I, L.I, liver, kidneys, spleen, heart, and lungs. The tissues were fixed in 10% formalin and subsequently dehydrated using the different volume of alcohol with the protocol described in Table S2 and Fully Enclosed Tissue Processor (Leica ASP300). The tissues were embedded in the paraffin (Leica EG 1160) before taking standard sections via Microm Microtome and histology water bath (Leica HI1210). The sections were then stained with hematoxylin-eosin dye and observed under the microscope (Olympus CX 41) [399].

4.3.11 Statistical Analysis

Mean, and standard deviation (SD) or mean and standard error (SEM) were used to express all values. The statistical analysis of data was conducted using GraphPad Prism 6 with Student's

t-test for two groups, one way and two-way analysis of variance (ANOVA) for multiple groups. The statistical analysis of data was performed by using Student's t-test for two groups, one-way and two-way analysis of variance (ANOVA) for multiple groups. P-values less than 0.05 were considered significant.

4.4 Results and Discussion

4.4.1 Formulation, Development, and Optimisation of NEF

Poor solubility, dissolution, metabolism, and permeability are determined as challenges resulted into poor oral BA of EDR [342]. SNMED strategy is the combination of solid dispersion and nanomicelles strategies which are the part of the most exciting area to curb the issues that restrict drug's absorption and displayed a potential for overall improvement in the BA. It is the system where drug molecule disperses in the polymeric carrier similar to solid dispersion based formulation [324, 325]. The role of polymeric carrier is critical for drug solubilisation, stabilization, improving dissolution, permeability, and absorption [249, 328]. Therefore, miscibility study was used to finalize the most suitable polymer for the development of NEF. Furthermore, the ratio of drug: carrier was chosen based on kinetic solubility study. Also, the solubility of optimized NEF was compared to a physical mixture of EDR and carrier with the similar amount used in NEF to evaluate the impact of presence on the polymeric carrier on solubility profile of EDR.

4.4.1.1 Selection of suitable carrier for the development of NEF

A number of carriers were short listed from the literature based on their potential to overcome the hurdles in development of Novel oral delivery systems such as PVP K30, SOL, PEG 4000, poloxamer 188 and poloxamer 407 [332, 391]. In addition to above polymers, hydroxypropyl-β-cyclodextrin (HP-β-CD) was considered as a control based on its proven ability of improving solubility and dissolution of EDR [95]. The reported aqueous solubility of EDR was 1.85 ± 0.15 mg/mL [342]. The increment in aqueous solubility of EDR was observed with increasing the polymer content % (w/v). The regression coefficient (R^2) value for PVP K30, SOL, PEG 4000, HP-β-CD, poloxamer 188 and poloxamer 407 are 0.997, 0.994, 0.951, 0.971, 0.917 and 0.989, respectively. The polymers such as PVP K30 and SOL suggests the best linear relationship in the enhancement of solubility with the polymer concentration compared to other polymers. Also, 10% SOL showed 4.67-fold improvement in aqueous solubility of EDR, whereas, with the same concentration of HP-β-CD, PVP K30, PEG 4000, poloxamer 188 and poloxamer 407 presented 3.49, 2.22, 1.73, 1.74 and 2.14-fold enhancement, respectively (Fig.

4.1A). The solubility enhancement of EDR with SOL is statistically significantly greater than HP-β-CD which justified the selection of SOL for the development of NEF.

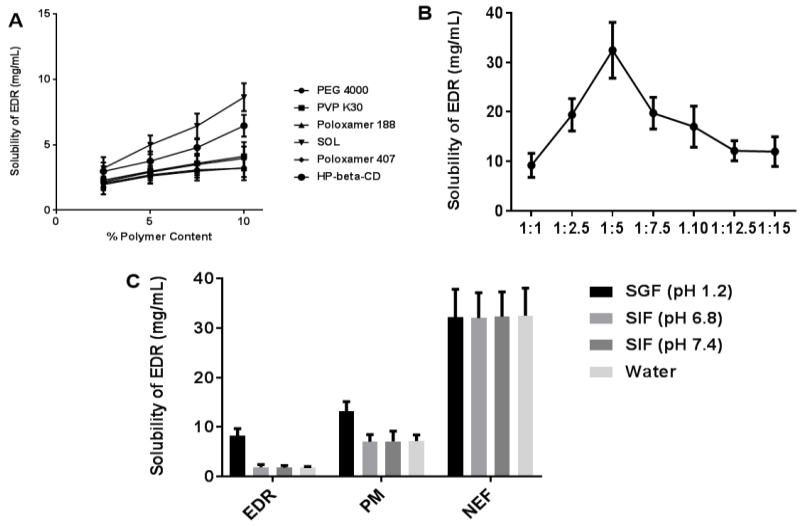

Figure 4.1 Formulation development and optimization of NEF. Miscibility study of EDR with various polymers (A), Optimisation of EDR to SOL ratio for the development of NEF (B) and solubility assessment of EDR, PM and NEF in SGF (pH 1.2) and SIF (pH 6.8 and 7.4) (C) (mean ± S.D., n = 3)

4.4.1.2 Kinetic Solubility

The ratio of EDR to SOL was optimized based on the kinetic solubility study. The maximum and equilibrium solubility and time for precipitation were determined for each ratio. The SD showing highest solubility without precipitation was considered for the development of NEF [332]. The crystalline EDR displayed equilibrium aqueous solubility and maximum solubility 1.85 ± 0.15 mg/mL [342] and 2.29 ± 0.32 mg/mL, respectively. Additionally, the precipitation was seen after 30 min which could be a reason for the difference in the values of maximum solubility and equilibrium solubility. With a good agreement to miscibility study, the solubility of EDR was significantly enhanced with increasing concentration of SOL in up to 1:5 EDR to SOL ratio. Almost 5 and 11-fold improvement in aqueous solubility was observed with SDs having 1:1 and 1:2.5 ratio, while the SD with 1:5 ratio showed highest solubility enhancement (17.5-fold) compared to all ratios used for the optimization study (Fig. 4.1B). Interestingly, lower solubility was detected with 1:7.5, 1:10, 1:12.5 and 1:15 ratio compared to 1:5 ratio but significantly higher in comparison with crystalline EDR with nearly 11, 9, 6.6, 6.5-fold, respectively. The decreasing solubility after certain drug to polymer ratio could be because of reaching beyond supersaturation stage which was also observed in the previous study with SOL, PEG 4000 and PVP K30 polymers [391]. No precipitation was noticed with all ratios,

suggesting the critical role of SOL as a precipitation inhibitors by maintaining supersaturation condition for desire period. The binary solid dispersion system of EDR and SOL with 1:5 ratio was considered as a NEF.

4.4.1.3 Characterisation of NEF

Comparison of Solubility of PM and NEF

There is a significant enhancement in aqueous solubility of EDR observed with PM (3.88-fold) and NEF (17.53-fold) (Fig. 4.1C). The NEF displayed 4.51-fold greater solubility improvement compared to PM. Partial amorphization could be a potential reason for the low solubility of EDR with PM compared to NEF [400]. The solubility of EDR in SGF (pH 1.2) was significantly greater (4.46-fold), while SIF (pH 6.8 and 7.4) showed an insignificant difference compared to solubility in water. The PM and NEF showed significant enhancement in solubility of EDR in all SBF. The exceptional performance of NEF was further investigated with advanced characterization study of NEF.

Loading ability and efficiency

The loading ability and efficiency of EDR were 16.52 ± 0.16 %w/w and 99.03 ± 0.42%. The EDR was almost completely encapsulated in SOL in NEF prepared by solvent evaporation technique without a significant loss during the manufacturing.

4.4.2 Investigating drug-polymer interaction with advanced characterisation

Change in solid state characteristics from crystalline to amorphous, hydrogen bonding interaction and micellization are perhaps potential reasons for dramatic improvement of EDR aqueous solubility with NEF. To evaluate our hypothesis, DSC, XRD and SEM studies were conducted to determine if any change happened in solid state characteristics of EDR and SOL in optimized NEF compared [332]. Also, the possibility of hydrogen bonding between EDR and SOL were assessed from FTIR and ^{1}HNMR analysis [331]. The micellization properties were studied by evaluating the aqueous solution of NEF for the parameters such as particle size, zeta potential and PDI by zetasizer and TEM analysis [335].

4.4.2.1 DSC study

The thermal behavior of EDR, SOL, PM and NEF were shown in Fig. 4.2 A. The characteristic melting endothermic peak at 128.39 °C were recorded with pure EDR which confirmed the crystalline nature of EDR used in the preparation of developing NEF. SOL did not display any thermal event due to amorphous nature of the polymer reported in the literature [401]. Less

intense endothermic peak was seen in the case of PM which might be due to the partial amorphization because of the force using in mixing during preparation with mortar and pestle or dilution effect of SOL. The disappearance of the sharp melting endothermal peak of EDR in the thermogram of NEF revealed the complete alteration of the solid state of EDR from crystalline to amorphous.

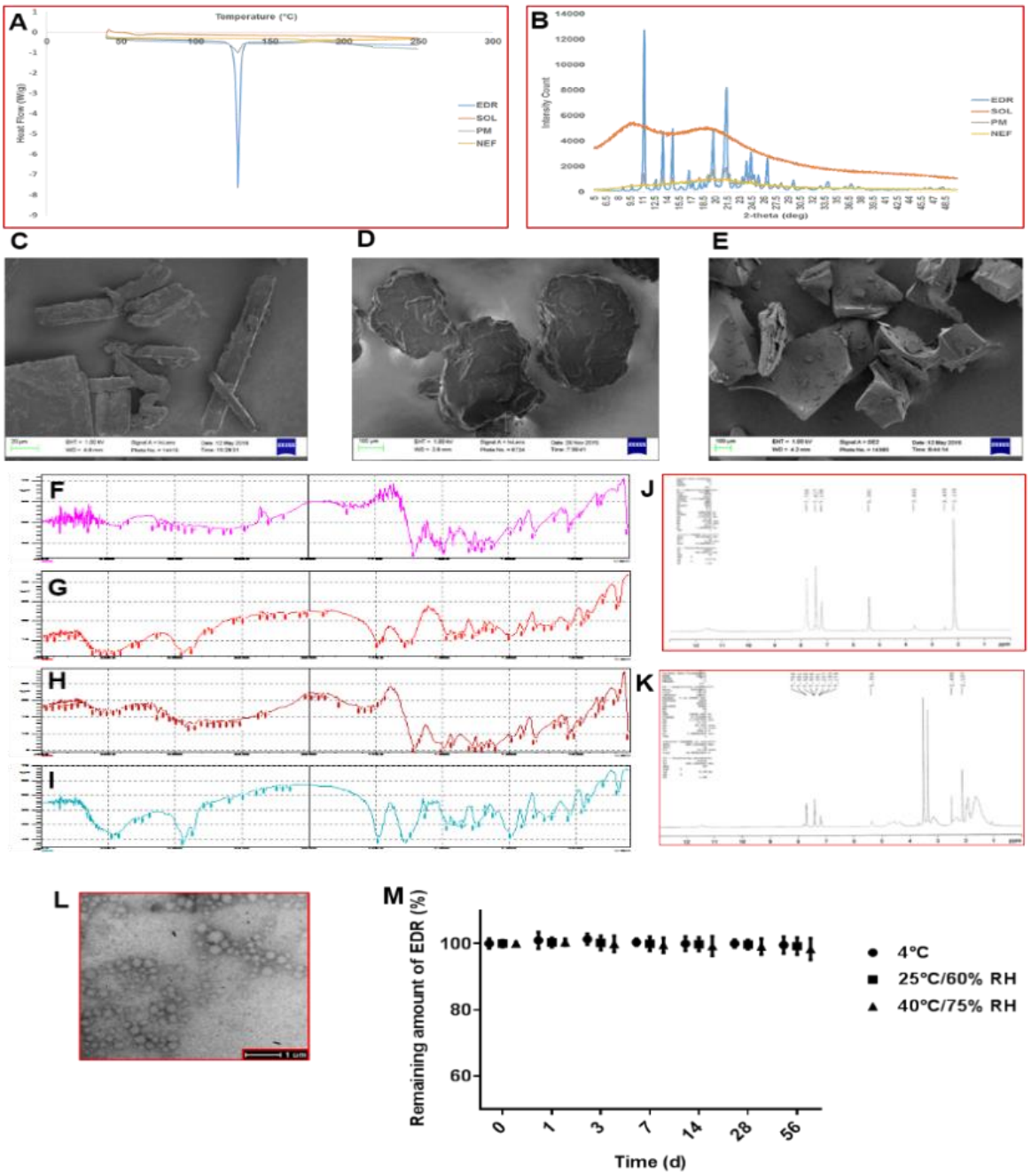

Figure 4.2 Advanced characterisation of SOL-based NEF. DSC thermographs (A) and X-ray diffractograms (B) of EDR, SOL, PM and NEF, SEM photomicrographs of EDR (C), SOL (D) and NEF (E), FTIR spectra of EDR (F), SOL (G), PM (H) and NEF (I), ^{1}H NMR spectra of EDR (J) and NEF (K), TEM image of micellar solution of NEF (L), and stability assessment of NEF as per ICH guideline (M) (mean ± S.D., n = 3). DSC, XRD and SEM data of EDR were adopted from the earlier

report [342]. The results of DSC, XRD, SEM and FTIR of SOL were used as a control for other projects

4.4.2.2 XRD study

The solid state characteristic of NEF was further confirmed with XRD study by comparing diffractograms of pure EDR, SOL, PM and NEF. Pure EDR showed sharp characteristics peaks at 11.2, 13.7, 14.7, 20.1 and 21.4 2θ assuring its crystalline nature, whereas amorphous nature of SOL was confirmed from its diffractogram without any characteristic peaks (Fig. 4.2 B). The decrease in intensity of all characteristic peaks of pure EDR in the diffractogram of PM verified the results of partial conversion to amorphous or dilution effect of SOL from DSC study (Fig. 4.2B). However, diffractogram of NEF exhibited clearly absent of all peaks of pure EDR, which indicated complete amorphization of EDR in NEF (Fig. 4.2B). The results of XRD analysis are a well agreement to the DSC study.

4.4.2.3 SEM Study

The SEM analysis was performed to determine the surface micrographs of pure EDR, SOL, and NEF. The large agglomerates particles with ordered size and shape were observed in the micrograph of pure EDR, which indicated its crystalline nature (Fig. 4.2C). Moreover, irregular-shaped particles were seen in the micrograph of SOL reveals its amorphous nature (Fig. 4.2D). Furthermore, the micrograph of NEF demonstrated particles with relatively rough surface and disordered shape, which specified the amorphous nature of EDR in NEF without any traces of crystalline EDR (Fig. 4.2E). The surface characteristics of NEF facilitates the quick and efficient dissolution of NEF upon the contact with aqueous fluids [402]. The confirmation of complete amorphization of EDR in NEF from SEM results is consistent with the results of DSC and XRD analysis.

4.4.2.4 FTIR and ^{1}HNMR study

The hydrogen bond interaction could be possible between EDR and SOL due to the presence of hydrogen donor and acceptor chemical groups in their chemical structure [342, 394]. Therefore, the interaction between EDR and SOL was investigated using FTIR and ^{1}HNMR. FTIR spectra of pure EDR, SOL, PM and NEF are displayed in Fig. 4.2F, 4.2G, 4.2H, and 4.2I, respectively. Pure EDR displayed peaks 3200-3600 cm^{-1} corresponding to N–H and O–H stretching, 1580-1627 cm^{-1} in regards to C=N stretching and 2850-3100 for aliphatic and aromatic C–H stretching. SOL displayed peaks representing O–H and aliphatic C–H stretching which were similar to EDR. The stretching corresponding to carbonyl group was additionally

observed at 1670-1820 cm^{-1} in SOL spectra. The shifting or broadening of peaks between 3200 and 3600 cm^{-1} were witnessed in FTIR spectra of NEF, which indicated the involvement of chemical groups present in EDR and SOL such as N–H and O–H in hydrogen bonding. Additionally, a similar observation was seen between 1670 and 1820 cm^{-1} that confirm participation of carbonyl group of SOL in hydrogen bonding. Shifting of chemical shifts were also observed in the results of ^{1}HNMR of NEF compared to pure EDR, which could be considered as a proof of hydrogen bonding interaction between the drugs and polymer as per the previously publications (Fig. 4.2J and 4.2K) [331]. SOL has both, each hydrogen donor as well as accepter group while EDR has two hydrogen donor groups. As the optimized ratio of EDR to SOL for NEF development is 1:5, five times more SOL molecules were present in the NEF which could facilitate six hydrogen bonding interaction. From the results of FTIR and NMR study, the strong hydrogen bonding interaction between EDR and SOL were confirmed. The formation of hydrogen bond between drug and polymer in preparation could restrict the solid state change from amorphous to crystalline during the storage and provide physical stability to the formulation [403]. Similar results have been reported previously in solid dispersion based preparations [331, 402].

4.4.3 Assessment of self-nanomicellising properties of NEF

SOL, a graft copolymer of poly (vinyl caprolactam)-poly (vinyl acetate)-poly (ethylene glycol), could form micelles over the concentration of 7.6 mg/L [335]. The micellar system of SOL showed dramatic improvement in oral BA of drugs such as quercetin [335] and cyclosporine A [394] and the therapeutic efficacy of drugs for examples doxorubicin [404], α-Lipoic Acid [405] and carvedilol [334]. Thus, the self-nanomicellising properties of NEF after dissolving NEF in aqueous media was investigated. The particle size is the most critical parameter as <100 nm could enhance cellular uptake of drugs and also facilitate the transport across the intestinal membrane by paracellular or transcellular routes [335]. The average particle diameter of 73.46 ± 3.15 nm, PDI 0.12 ± 0.04 and zeta potential -4.98 ± 1.56 mV were seen using zeta sizer. A TEM photograph of micelles of NEF revealed the spherical droplets with the good agreement of particle size measured by zeta sizer (Fig. 4.2L). Additionally, micellar formulation remained stable with and without 20-fold dilution with dissolution media such as SGF (pH 1.2) and SIF (pH 6.8) after 24 h. The narrow size distribution and higher zeta potential could justify the good stability of micelles in dissolution media.

Moreover, the uniform dispersion of NEF in various aqueous buffer systems from pH 2 to 8, SBF and water that confirmed complete encapsulation of EDR in micelles. The complete

encapsulation could provide protection to EDR against the degradation or metabolism in the presence of gastrointestinal contents [406]. Thus, the stability of EDR in micelles form at different pH, temperatures, in the presence of light and oxygen, and in SBF such as SGF (pH 1.2) and SIF (pH 6.8) were examined for one week. There was no significant degradation (<3% degradation) of EDR detected in all conditions, while, crude EDR showed dramatic degradation at alkaline conditions (pH 8-10) and in the presence of oxygen [342]. These results confirmed the complete amorphization, strong hydrogen bonding interaction, and micellization which made NEF as an excellent candidate for further development.

4.4.4 Stability study of NEF as per ICH guideline

No significant difference in % drug content and aqueous solubility of EDR were witnessed (Fig. 4.2M). Therefore, it might be stored at ≤ 40 °C for at least eight weeks. The strong hydrogen bond interaction between EDR and SOL could favor the physical stability of EDR in NEF and prevent the conversion of solid state from amorphous to crystalline [403].

4.4.5 In-vitro metabolism and permeation study

The extensive metabolism of EDR could be a significant contributor in its poor oral BA. The Labrasol based novel oral delivery system showed 5.71-fold improvement in oral BA of EDR due to the inhibitory effect of on glucuronidation and P-glycoprotein (Pgp) efflux of EDR during metabolism and permeability [342]. Based on such information, the impact of SOL on glucuronidation of EDR was studied in rat liver microsomes. The significant inhibitory effect of SOL (45.64 %) compared to Borneol (37.56%) was observed (Fig. 4.3A). The potential of SOL-based NEF was further tested on permeability and metabolism of EDR during permeation across the S.I with everted intestine sac technique. The inhibitory effect of SOL was also witnessed as NEF displayed 2.73-fold greater transfer amount of EDR compared to crude EDR and statistically significant compared to Borneol (Fig. 4.3B). Additionally, NEF displayed 41.67% and 15% less amount of EDR-G on the serosal side compared to crude EDR and Borneol, respectively (Fig. 4.3C). Moreover, it presented 59.9% and 44.2% fewer molar ratio of EDR-G to EDR compared to crude EDR and Borneol, respectively, which indicated a significant effect of SOL presence in NEF glucuronidation of EDR (Fig. 4.3D). There was 2.96-fold higher transfer rate detected of EDR from NEF while 2.65-fold greater with Borneol compared to crude EDR (Fig. 4.3E). The inhibitory effect of SOL on Pgp efflux and <100 nm of micelles generated from NEF could also enhance the permeability of EDR across the S.I [335]. The results confirmed the significant improvement of metabolism and permeability profile of EDR with NEF due to the inhibitory effect of SOL on glucuronidation.

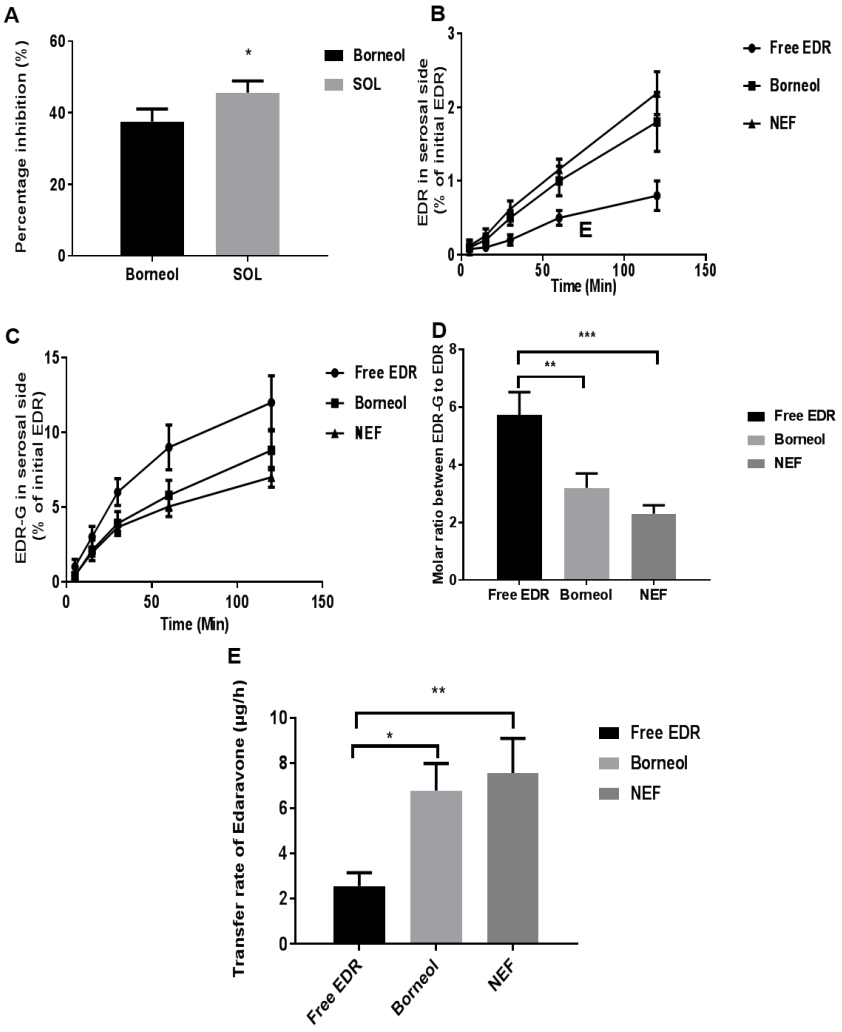

Figure 4.3 The role of SOL on permeability and metabolism of EDR. Inhibitory effect of SOL (1%) on EDR glucuronidation in a microsomal incubation assay (A), the amount in percentage of EDR (B) and (C) on serosal side at predetermined time interval, molar ratio between EDR-G and EDR (D), and transfer rate of EDR in the serosal side (E) (mean ± S.D., n = 3). *P <0.05, **P<0.01 and ***P<0.001. One-way ANOVA and Tukey's test or Unpaired t-test (two-tailed). The data of free EDR and Borneol were adopted from the earlier report [342]

4.4.6 In-vitro drug dissolution

The result of dissolution study of EDR and NEF is shown in Fig. 4.4A. EDR showed 100% release within 15 min in SGF compared to 85% release in 120 min in SIF, which indicated pH dependent release. It was further examined by comparing the dissolution profiles using f1 and f2 factors. The determined f2 value (similarity factor) and f1 value (dissimilarity factor) are 14 and 26, which confirmed the impact of pH of the media on EDR release. The solubility of EDR in SGF and SIF were determined as pH dependent solubility profile of EDR was reported previously. The EDR exhibited significantly higher solubility in SGF (8.26 ± 1.42 mg/mL) compared to SIF (1.89 ± 0.51 mg/mL). The greater solubility of EDR in SGF over SIF could

be the reason of the difference in dissolution profile in SGF and SIF. Moreover, crude EDR followed Hixson–Crowell, and Korsmeyer–Peppas release kinetic models in SGF and SIF, respectively (Table 4.2). Additionally, in SIF, it followed an anomalous transport (non-fickian) mechanism, which could be controlled by factors other than diffusion. The sedimentation and wetting of the EDR at interface could control the release of EDR in SIF.

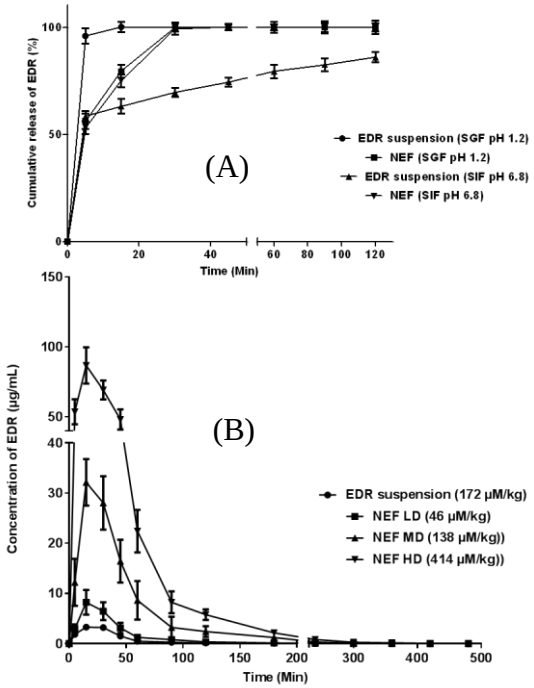

Figure 4.4 *In-vitro* dissolution study of EDR and NEF in SGF and SIF(A), and plasma profile verses time curve for the EDR suspension and NEF (LD, MD, and HD) in SD rats after oral administrations (B) (mean ± S.D., n = 6). The pharmacokinetic data of EDR suspension was adopted from the earlier report [342]

Table 4.2 Results of release kinetics of EDR and NEF in SGF and SIF, respectively

Formulation	Medium	First order	Zero order	Hixson–Crowell	Higuchi-matrix	Korsmeyer–Peppas
EDR	SGF	0.834	0.6077	0.9216	0.8501	0.8636
	SIF	0.9609	0.7947	0.9718	0.97	0.9895
NEF	SGF	0.9982	0.6988	0.9212	0.9061	0.9171
	SIF	0.9862	0.5925	0.8807	0.8514	0.9078

The release of EDR from NEF in SGF and SIF are 100% within 15 and 30 min. There was significant improvement of dissolution EDR release from NEF detected in SIF compared to crude EDR, whereas no dramatic change was witnessed between the dissolution profile of crude EDR and EDR from NEF in SGF except at 5 min. The amorphization, hydrogen bonding interaction and micellization could play a vital role in the improvement of dissolution behavior of EDR from NEF compared to crude EDR. Additionally, the f2 (65) and f1 (3) values confirmed the similar dissolution profiles of EDR in SGF and SIF which suggested less impact of pH on EDR release from NES. Moreover, the first order release kinetic model was best fitted with the dissolutions profiles of NEF. Thus, the rate of EDR release depends on the amount of EDR retained in NEF [361].

4.4.7 Pharmacokinetic study

To study the dose dependant therapeutic effect against the Alzheimer disease, three different doses of NEF were considered for the pharmacokinetic study. The plasma concentration of time and pharmacokinetic parameters are displayed in Fig. 4.4B and Table 4.3. Significant increase in C_{max} was observed at all dose of NEF compared to EDR suspension, while NEF did not show any difference in $T_{max.}$ These results are consistent with the result of dissolution study as NEF displayed quick release in both media similar to EDR suspension release in SGF. Also, NEF showed significantly longer $t_{1/2}$ compared to EDR suspension, which could be due to the inhibitory effect of SOL on EDR glucuronidation. Moreover, NEF exhibited dramatic increment in $AUC_{0\text{-}t}$ and 10.24 (46 µM/kg), 16.08 (138 µM/kg) and 14.78 (414 µM/kg) fold enhancement in relative BA compared to EDR suspension. The solubilise amount of EDR in the vehicle used for pharmacokinetic study might significantly affect the outcome. Thus, determination of solubilised EDR in total 1.5 mL of vehicle used for oral administration in rats, was performed. The dissolved part of EDR in supplied vehicle was 31% and 100% with EDR suspension and NEF, respectively for all doses. The presence of solubilised EDR in greater amount could be one of the reasons for significant improvement of oral BA [342]. Also, improvement in dissolution, metabolism, and permeability could have played a vital role in expectation performance of NEF in the pharmacokinetic study compared to EDR suspension.

Table 4.3 Pharmacokinetic parameters of EDR suspension and NEF with LD, MD, and HD obtained by Phoenix WinNonlin software (mean ± S.D., n = 6)

Parameters	EDR suspension (172 µM/kg)	NEF LD (46 µM/kg)	NEF MD (138 µM/kg)	NEF HD (414 µM/kg)
C_{max} (µg/mL)	3.29 ± 0.51	8.25 ± 2.46	32.13 ± 4.62	86.78 ± 12.96
T_{max} (min)	15.19 ± 1.45	15.42 ± 2.96	15.48 ± 2.12	15.56 ± 2.12
$t_{1/2}$(min)	58.31 ± 3.52	67.85 ± 5.78	73.26 ± 6.81	75.85 ± 4.42
AUC_{0-t} (µg·min/mL)	164.18 ± 35.26	448.5 ± 82.47	2112.52 ± 389.25	5825.47 ± 1086.29
F_{0-t} (%)	100	1024.4 ± 210.42	1608.38 ± 412.73	1478.42 ± 298.69

4.4.8 Behaviour tests

The purpose of the study is to determine the therapeutic potential of NEF against AD, and for that suitable animal model, age, duration of treatment and evaluation tests are the key requirements. The ideal animal model should closely mimic the symptoms and neuropathology of AD disease. APP/PS1 mice model was created by expressing variants of chimeric human amyloid precursor protein and a mutant human presenilin 1 [407]. It is well accepted to investigate the potential therapeutic candidates against AD because it showed key characters such as cognitive dysfunction as a result of pathological changes manifested by senile phaques, neurofibrillary tangles, neuroinflammation and neuronal loss. The potential therapeutic candidates such as EDR [69], docosahexaenoic acid [408], Puerarin [409] and p75NTR ectodomain protein [389] ameliorated the cognitive dysfunction in APP/PS1 mice by improving AD-like pathology. Therefore, the efficacy of NEF against the AD was evaluated based on its potential to improve learning and memory in AD mice. Additionally, the age dependent cognitive decline was observed with APP/PS1 mice models thus selection of suitable age is critical. The 14 months of age for APP/PS1 mice as a starting point because of the fully developed AD-like pathology and behavioral deficits similar to clinical AD were observed in the previous studies [388]. Moreover, due to the chronic nature of AD, three months of the treatment period was selected as an appropriate for efficacy evaluation from the

previous report [69]. As an improvement of learning and memory of APP/PS1 mice used as a marker in evaluating efficacy against AD, a number of behavior tests were selected to assess the motor function (open field), anxiety-related behavior (open field) and cognitive function (NORT, Y-maze, and MWM). APP/PS1 mice showed AD-like behavioral deficits in the open field, NORT, Y-maze and MWM test [69, 389, 410]. A group of C57BL/6 mice (wild type) (Wt) was used as a normal aging control as APP/PS1 mice were genetically modified mice with the background of C57BL/6. One group of APP/PS1 mice at 14 months old was considered as a basal control which had undergone for the behavioral tests at the starting point of treatments. Other groups of mice were used as a negative control without any treatment, blank formulation control (without EDR) and donepezil (DNP) positive control group (for details of grouping designs, see Table 4.1). All behavioral tests were conducted at 17 months similar to NEF treatment groups, except the basal control group which was done at 14 months. The data of control groups such as 17 mo Wt Ctrl, 14 mo Tg Ctrl, 17 mo Tg Ctrl, 17 mo Tg BC, 17 mo Tg DNP are used in other similar projects to reduce the use of an overall number of animals as per the animal ethics guideline.

Daily injection or gavage for three months could affect the behaviors of mice and impact on the outcome as well as a welfare issue. Therefore, mixing of NEF with drinking water was selected as a way of NEF, blank formulation and DNP administration. In animal house facility, acidic drinking water was utilized to avoid the spreading of bacterial infections among the animals in a cage. Thus, evaluating the stability of NEF in acidic drinking water was performed to determine its suitability as an administration technique and frequency of changing the water bottle. The frequency of changing water bottle in our animal house facility was every weekly as per the standard, so stability study was conducted for 7 d. Less than 1% decrease in EDR content with all three doses of NEF were detected in 1 week which confirmed the suitability of mixing NEF with acidic drinking water as a way for administration. The concentration of NEF, SOL, and DNP in acidic drinking water was calculated for appropriate dosing as per the data of average water consumption and weight of the mice mentioned in Table 4.1. The amount of water intake was utilized to calculate the dose for the preparation of drinking water mixed with the different doses of NEF, blank formulation, and DNP.

4.4.8.1 Open field test

The locomotor and exploration activity (measuring total distance traveled and the number of rearing) and anxiety behaviors (% time spent in the central zone, the number of rearing,

grooming, urination and defecation) of all APP/PS1 mice were evaluated by open field test [389]. There was a significant decrease in locomotor and exploration activity as well as high level of anxiety observed at 14 and 17 months of age of APP/PS1 mice without any treatment and with blank formulation treatment compared to Wt control mice. The treatment groups with NEF displayed dose-dependently increase in locomotor activity which was revealed from a statistically significant increase in total distance traveled (Fig. 4.5A) and a number of rearing (Fig. 4.5B). Moreover, mice treated with NEF with MD and HD but not LD spent significantly longer time in the central zone (Fig. 4.5C) which indicated the lowering of anxiety type behavior. Also, NEF treated mice showed decrease but not statistically significant in a number of grooming (Fig. 4.5D), urination (Fig. 4.5E) and defecation (Fig. 4.5F). Besides, the DNP-treated mice showed similar results to the mice treated with NEF LD, but NEF MD and HD treated mice revealed better performance. There was no statistically significant difference in locomotor and exploration activity, and anxiety behaviors of NEF treated mice with normal Wt, suggesting a potential of NEF treatment on the reversal of the behavioral deficits near to the normal level. It is worthy to note that the NEF groups with all dosages performed better than the basal control group at 14 months on the total travel distance, number of rearing, and the time spent in the central zone in the open field test (Fig. 4.5 A, B, C), suggesting the treatment can reverse the mood status of aged AD mice to a much younger age.

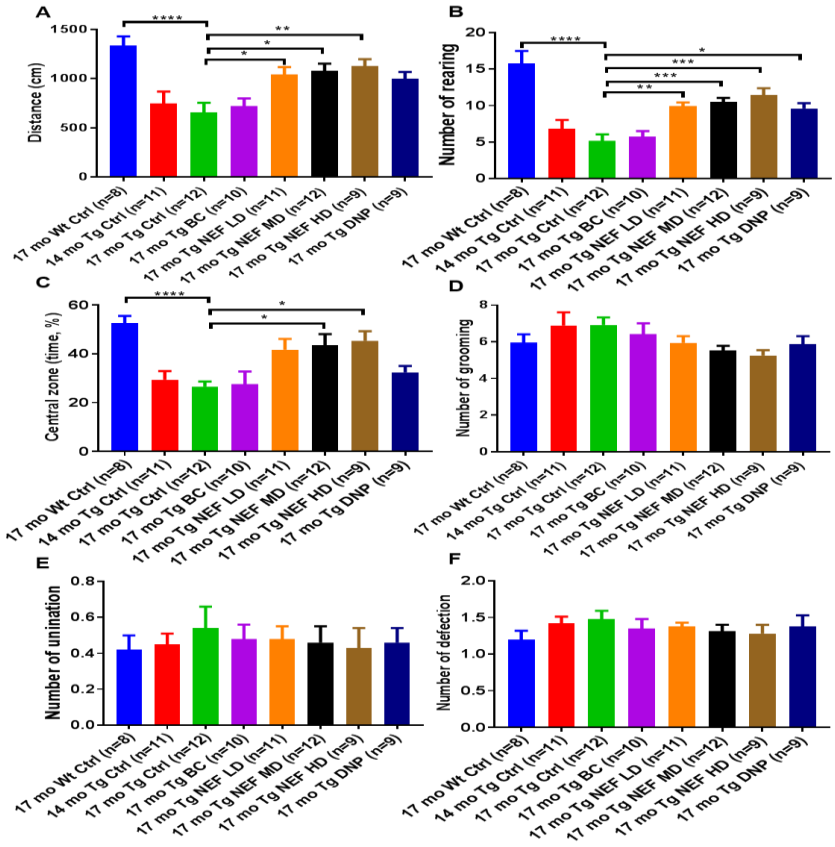

Figure 4.5 Results of the open field test. Total distance traveled (A), number of rearing (B), Time spent in central zone (C), number of grooming (D), number of urination (E) and number of defecation (F). *P < 0.05, **P < 0.01, ***P < 0.001, and ****P < 0.0001 (One-way ANOVA, Tukey' s test) (mean ± SEM)

4.4.8.2 NORT

The NORT reflects the learning and memory of mice based on their natural tenancy of exploring novel object instead of familiar one after exposed to a novel environment [411]. The poor performance of APP/PS1 in NORT made it an ideal study to examine the potential of intervention therapy for AD [412]. All APP/PS1 and Wt mice showed the statistically insignificant difference in recognition index in the phase of familiarization (Fig. 4.6A). In the test phase, the 17 months old APP/PS1 mice without any treatment and with blank formulation treatment showed no tendency to explore the novel object, while NEF treated mice presented significantly higher and dose dependent increase in the discrimination index (Fig. 4.6B and 4.6C). Moreover, NEF treated mice with all doses displayed significantly better performance in a dose dependent manner compared to the basal control at 14 months. DNP-treated mice reflected the improvement of AD-related deficits to the much younger age mice and better than untreated control groups. The performance of NEF treated mice evaluated based on discrimination index in test phase was comparable to Wt normal mice at 17 months and better

than the positive control donepezil group. These results suggest that NEF treatment at all dosages can reverse the cognitive decline to the much younger age of AD mice and the level near Wt normal aging mice.

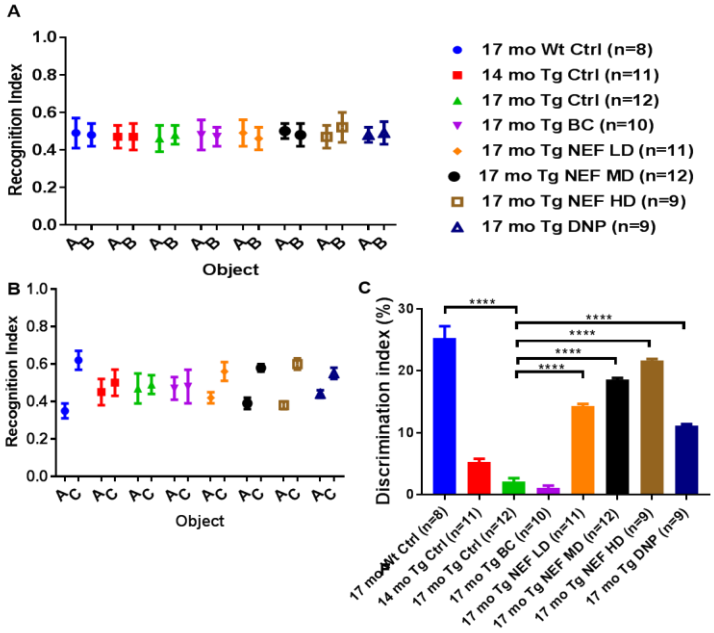

Figure 4.6 The results of NORT. Recognition index in the phase of familiarization (A) and the test phase (B), discrimination index in the test phase (C). ****P < 0.0001 (one-way ANOVA, Tukey's test) (mean ± SEM)

4.4.8.3 Y-maze test

The mouse has natural tendency to explore novel environment, but AD-like cognitive deficits could affect its ability to discriminate between familiar and novel environment [413]. Y-maze test was conducted in 2 phases includes spontaneous alternation and novel arm exploration tests [69, 389]. The performance of APP/PS1 mice without any treatment and treated with blank formulation was poor in both phase compared to Wt control, which indicated AD-like behavioral deficits such as impairment in remembering the already explored arm in spontaneous alternation and the previously blocked arm in novel arm exploration test. The NEF treated mice showed the significantly greater number of alteration (Fig. 4.7A) and entry to each arm (Fig. 4.7B) in dose dependent manner compared to control mice without any treatment or treated with the SOL vehicle. Moreover, significantly higher number of entry (Fig. 4.7C and 4.7D) and time spent (Fig. 4.7E) in the novel arm in comparison to other arms were witnessed in NEF treated mice compared to the mice without any treatment or treated with the vehicle.

All NEF treated mice performed better than the basal control mice at 14 months old, indicating that the NEF treatment can reverse the cognitive status to a much younger age than 14 months, although these basal control younger mice performed slightly better than 17 months old un-treated controls but had no statistical difference. Also, NEF treated mice showed better results but statistically insignificant compared to mice treated with DNP in both phases. Also, most importantly, the performance of NEF treated mice in both phases was not statistically different from that of Wt normal aging control, indicated amendment by NEF at all dosages in AD-like cognitive functions to the normal mice with same age.

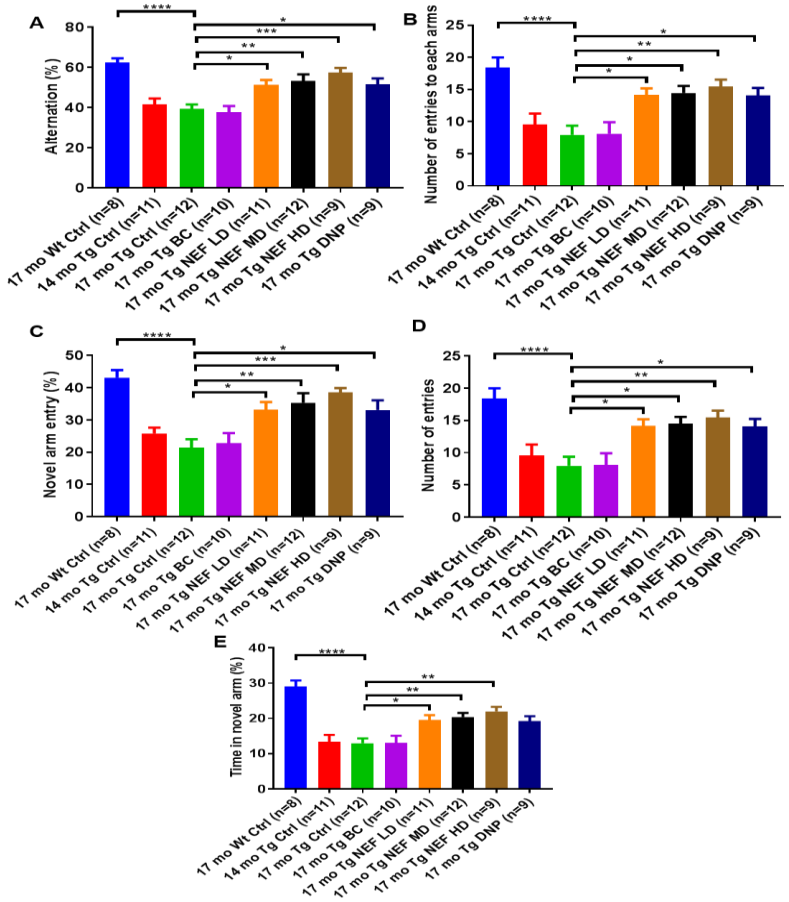

Figure 4.7 The behavioral performances of Tg mice in Y-maze test. % Alternation (A) and numbers of entries in each arm (B) and the spontaneous alternation test, % of total entry in novel arm compared to other arms (C), total number of entry to the novel arm (D) and time (%) (E) in the novel arm test. *P < 0.05, **P < 0.01, ***P < 0.001, and ****P < 0.0001 (one-way ANOVA, Tukey's test) (mean ± SEM)

4.4.8.4 MWM Test

The MWM test is one of the most sensitive tests which represents the AD-like deficits as it examines the function of the hippocampus, the most affected region of the brain in AD. The determination of hippocampal spatial memory deficits was performed by motivating mice to

escape from the water by finding the platform after placing into the water tank [69, 389]. The test was performed in 4 phases include habituation, visible platform, hidden platform and probe test. The performance of all APP/PS1 and Wt mice in first and second phase evaluated by measuring path length (Fig. 4.8A), swimming speed (Fig. 4.8B) and escape latency time, which was not significantly different among groups, which indicated all groups had similar motor and visual capabilities. The learning and memory of all mice were assessed in the third phase by comparing escape latency time (Fig. 4.8C) and forth phase by measuring a number of annulus crossing (Fig. 4.8D) and time spent in target quadrant compared to all other quadrants (Fig. 4.8E) of MWM, respectively. The mice without treatment or treated with the blank formulation in APP/PS1 mice at 14 or 17 months displayed significantly impaired learning compared to Wt mice. NEF treated mice performed significantly better in a dose dependent manner showing a reduction in the escape latency time in the third phase and a higher number of annulus crossing, and longer time spent in the target quadrant in the fourth phase, compared to those of untreated or vehicle treated mice in both phases. Moreover, these mice treated with middle and higher dosages of NEF exhibited better performance than the DNP group. Again, the most important finding is that all mice treated with NEF improved their capacity of learning and memory to the extent comparable to the level of Wt, as no statistical difference was seen between the Wt normal aging control and NEF treated groups.

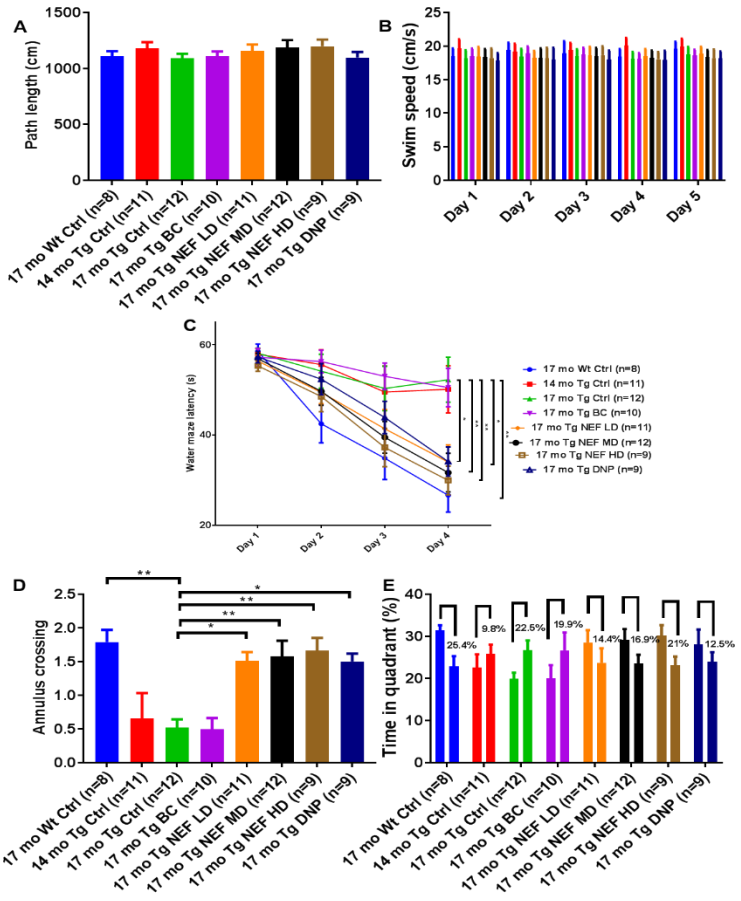

Figure 4.8 The performances of Tg mice in MWM test. Path length (cm) to the platform (A), swim speed (cm/s) during platform trials and probe test (B), escape latency (s) during platform trials and distance travelled on each day of training (C), Number of annulus crossings in probe trial (D), Comparison of time spent in target zone (Q3) (First bar) where platform was located compared to average of all other zones (o.a.) (Second bar) (E). *P < 0.05 and **P < 0.01 (two-way or one-way ANOVA, Tukey's test) (mean ± SEM).

Overall, the performance of untreated or blank formulation treated mice at 17 months showed AD-like deficits behavioral deficits in open-field, NORT, Y-maze and MWM behavior tests compared to Wt control. The basal control group of mice presented slightly better but insignificant than 17 months mice, while blank formulation treatment did not show any improvement compared to 17 months untreated mice. DNP treatment rescues the cognitive deficits of APP/PS1 mice in all behavior tests compared to 17 months untreated mice but only able to match the performance of NEF LD treatment. The NEF MD and HD treated mice revealed exceptional learning and memory ability which were better than DNP-treated, basal control and quite similar to the Wt control mice in all behavior tests. The expressed NEF treatment could not just prevent the deterioration of cognitive functions but also made a reversal of AD-like behavioral deficits in APP/PS1 mice similar to the much younger mice or same age normal mice.

Previously, EDR ameliorates the AD-like memory deficits in APP/PS1 mice by reducing Aβ deposition and alleviates oxidative stress, attenuates the downstream pathologies including Tau hyperphosphorylation, glial activation, neuroinflammation, neuronal loss, synaptic dysfunction [69]. Moreover, it also showed improved streptozotocin-induced cognitive damage by reducing oxidative stress and hyperphosphorylation of tau [196]. Additionally, EDR amended spatial learning and memory deficits in Aβ induced neurotoxicity in rats by lowering 4-Hydroxynonenal level, acetylcholinesterase (AChE) and choline acetyl transferase (ChAT) activities [195]. NEF is a more bioavailable form (>10-fold compared to EDR suspension) of EDR which could not only achieve a higher concentration in systemic circulation but also in the brain as 50-65% of the relative ratio of plasma to the cerebral spinal fluid of EDR was reported previously [414]. The dose dependent therapeutic effect of EDR against AD in *in-vitro* and *in-vivo* studies against amyotrophic lateral sclerosis (ALS) have been already revealed [69, 128, 194]. Therefore, due to the enhancement of oral BA of EDR, NEF could more effectively target multiple pathways of AD pathogenesis and thus rescue the cognitive deficits of a mouse model of AD.

4.4.9 Assessment of long-term repeated dose toxicity

As a result of superior pharmacological properties of EDR against AD and the exceptional performance of NEF, a more bioavailable form or EDR in a behavioral study conducted on APP/PS1 mice, NEF could be developed as a therapeutic agent for AD. The available information on the toxicity of SOL-based preparation is very limited. Thus, as a part of safety assessment, the objective of this study was to evaluate the long-term toxicity study of NEF when supplied for a period of consecutively three months. It could provide guidance for clinical applications of NEF not only for AD but various neurologic and non-neurologic diseases related to organs such as heart, lung, intestine, liver, pancreas, kidney, bladder and testis [212]. The data of 17 mo Tg Ctrl and 17 mo Tg BC control groups are utilized in other similar projects based on SOL based preparations to reduce the use of an overall number of animals as per the animal ethics guideline.

There was no death, or clinical signs noticed related to the treatment in any groups including blank formulation and NEF with all doses. In addition, the insignificant difference was observed in body weight, water and food consumption in NEF treated groups compared to the non-treated group except the first week (Table 4.4). During the first week after initiating the treatment, an increase in water intake and weight gain but a decrease in food intake was noted in both blank formulation, and NEF treated groups than in untreated groups. The preferable

taste of SOL might be the possible reason to explain the higher water intake, which led to a weight gain, and a slight and transient decrease in food intake may not affect the body weight. After one week, the water and food intake, and weight of the mice remained consistent throughout the study.

Table 4.4 Measurement of food and water consumption and body weight of Tg mice (mean ± S.D. n = 5)

Parameter	Time	APP/PS1 mice		
		17 mo Tg Ctrl	**17 mo Tg BC**	**17 mo Tg NEF HD**
Food intake (g/d/10 g body weight)	Before addition (14 months)*	1.34 ± 0.19	1.36 ± 0.26	1.38 ± 0.25
	After addition (14 months)+	-	1.33 ± 0.22	1.33 ± 0.31
	At 17 months	1.22 ± 0.31	1.24 ± 0.22	1.19 ± 0.25
Water intake (g/d/10 g body weight)	Before addition (14 months)*	1.42 ± 0.42	1.41 ± 0.32	1.43 ± 0.32
	After addition (14 months)+	-	1.48 ± 0.24	1.52± 0.34
	At 17 months	1.25 ± 0.20	1.27 ± 0.28	1.23± 0.27
Body weight (g)	Before addition (14 months)*	33.13 ± 3.24	33.9 ± 4.82	32.81 ± 2.59
	After addition (14 months)+	-	34.6 ± 3.45	34.32 ± 2.99

	At 17 months	34.15 ± 3.13	34.24 ± 3.17	34.58 ± 3.12

4.4.9.1 Haematological parameter

The data of hematological parameters of NEF treated mice showed a slight but not significant decrease in most of the parameters except MCH, PLT, monocytes and basophils counts compared to non-treated mice group (Table 4.5). The SOL treatment did not cause any statistically significant increase and decrease in the values of various hematological parameters, compared to non-treated mice groups. The biological significance of the results was further assessed from the study of organ weight and histology of the spleen.

Table 4.5 Analysis of Haematological and Coagulation parameters of Tg mice (mean ± S.D., n = 5)

Parameters	**APP/PS1 mice**		
	17 mo Tg Ctrl	**17 mo Tg BC**	**17 mo Tg NEF HD**
Haematological parameters			
RBC ($x10^{12}$/L)	9.52 ± 0.39	9.38 ± 0.51	9.12 ± 0.47
WBC ($x10^{9}$/L)	7.17 ± 3.28	7.56 ± 3.94	6.95 ± 3.08
HGB (g/dL)	13.64 ± 0.45	13.95 ± 0.61	13.28 ± 0.62
HCT (%)	48.92 ± 1.43	47.67 ± 1.92	46.18 ± 2.42
MCV (fL)	49.81 ± 1.36	48.53 ± 1.89	49.17 ± 2.05
MCH (pg)	14.68 ± 0.82	15.28 ± 0.61	14.80± 0.49
MCHC (g/dL)	29.53 ± 1.16	28.95 ± 1.99	29.18 ± 1.82
PLT ($x10^{9}$/L)	496.81 ± 282.34	521.94 ± 196.05	529.27 ± 297.26
MPV (fL)	6.95 ± 0.14	6.57 ± 0.27	6.58 ± 0.31
PCT (%)	0.23 ± 0.16	0.19 ± 0.11	0.22 ± 0.18
PDW (fL)	8.3 ± 1.62	8.29 ± 1.72	7.96 ± 2.44
Neutrophils (%)	14.35 ± 4.53	12.24 ± 5.25	13.45 ± 4.98

Lympocytes (%)	81.82 ± 5.74	77.56 ± 5.23	76.95 ± 6.29
Monocytes (%)	4.61 ± 2.16	5.25 ± 2.49	4.99 ± 2.46
Eosinophils (%)	1.86 ± 1.65	1.52 ± 1.16	1.79 ± 1.04
Basophils (%)	0.04 ± 0.05	0.05 ± 0.05	0.05 ± 0.03
Coagulation parameters			
PT (s)	10.12 ± 0.62	10.25 ± 1.12	12.21 ± 2.48
APTT (s)	26.67 ± 8.97	28.45 ± 8.12	26.19 ± 9.29

4.4.9.2 Coagulation parameters

There were no statistically significant increase or decrease in the value of PT and APTT detected in the case of the NEF treated mice, and the SOL vehicle-treated mic, compared to non-treated mice (Table 4.5).

4.4.9.3 Blood electrolyte parameters

The results indicated that there were no statistically significant increase or decrease in the values of blood electrolytic parameters between the mice-treated with SOL or NEF and those control mice without any treatment (Table 4.6).

Table 4.6 Analysis of biochemical parameters of Tg mice (mean ± S.D., n = 5)

Parameters	APP/PS1 mice		
	17 mo Tg Ctrl	17 mo Tg BC	17 mo Tg NEF HD
Sodium (mmol/L)	147.66 ± 2.94	143.06 ± 2.98	147.38 ± 2.58
Bicarbonate (mmol/L)	27.16 ± 5.79	27.9 ± 5.02	28.31 ± 5.48
Anion Gap (mmol/L)	22.78 ± 4.70	22.91 ± 5.25	23.46 ± 4.68
Potassium (mmol/L)	11.06 ± 1.52	12.94 ± 1.03	11.00 ± 1.26
Calcium (mmol/L)	2.56 ± 0.19	2.84 ± 0.18	2.58 ± 0.22
Sodium :Potassium ratio	13.6 ± 1.86	13.93 ± 1.92	13.75 ± 1.39

Chloride (mmol/L)	107.71 ± 2.52	109.52 ± 2.91	107.73 ± 2.94
Inorganic phosphorus (mmol/L)	3.08 ± 0.77	3.56 ± 0.99	3.04 ± 0.84
Calcium:Phosphorus ratio	0.83 ± 0.19	0.78 ± 0.14	0.81 ± 0.18
Albumin (g/L)	34.93 ± 2.68	31.16 ± 3.57	33.45 ± 2.48
Total Protein (g/L)	56.69 ± 3.59	54.58 ± 4.56	57.62 ± 3.57
Globulin (g/L)	24.8 ± 2.67	23.4 ± 2.96	22.53 ± 2.48
Total Bilirubin (µmol/L)	0.43 ± 0.05	0.67 ± 0.07	0.46 ± 0.04
Creatinine (µmol/L)	10.84 ± 2.86	12.22 ± 4.76	14.56 ± 3.59
Urea (mmol/L)	7.67 ± 2.12	9.2 ± 3.45	7.24 ± 2.94
Glucose (mmol/L)	15.96 ± 3.15	15.06 ± 3.78	15.64 ± 3.26
Cholesterol (mmol/L)	2.56 ± 0.59	2.51 ± 0.56	2.64 ± 0.61
AST (U/L)	305.07 ± 200.04	326.94 ± 179.35	256.62 ± 127.48
GGT (U/L)	< 0	< 0	< 0
Alkaline phosphatase (U/L)	106.73 ± 31.70	106.44 ± 28.02	115.88 ± 32.14
Lipase (U/L)	98.86 ± 39.77	89.28 ± 35.14	105. 46 ± 45.20
ALT (U/L)	97.01 ± 21.15	99.64 ± 18.04	103.54 ± 23.28
Amylase (U/L)	2181.95 ± 339.34	2295.26 ± 290.25	1944.36 ± 424.28

4.4.9.4 Biochemical parameters

The analysis of serum biochemistry was performed to assess the impact of the treatment of NEF and SOL on the normal function of liver, kidneys, heart, liver and digestive system of mice (Table 4.6). At the end of the treatment period, there was a slight increase in values of creatinine, total bilirubin and urea in NEF and SOL treated groups compared to the untreated controls, these are no statistically significant difference. There was no statistically significant difference in the rest of liver enzymes and metabolites between treated and control mice. These results indicate that the treatment of SO did not display any significant alterations in the serum

biochemistry compared to non-treated groups. The biological significance of the results was further evaluated based on the study of organ weight and histology study.

4.4.9.5 Organ weight

The result of all major organs weight of the mice treated with blank formulations and NEF, and without any treatment are presented in Table 4.7. The NEF treated mice showed a slight increase in weight of all organs but without statistical significance. The average weight of NEF treated mice was higher than the non-treated mice which could explain slight more weights of all major organs. No change in the weight of organs in SOL treated mice compared to untreated mice.

Table 4.7 Analysis of organ weighs of Tg mice (mean ± S.D., n = 5)

Organ (g)	APP/PS1 mice		
	17 mo Tg Ctrl	17 mo Tg BC	17 mo Tg NEF HD
Brain	0.48 ± 0.08	0.49 ± 0.07	0.49 ± 0.08
Liver	1.86 ± 0.48	1.84 ± 0.42	1.89 ± 0.44
Heart	0.22 ± 0.06	0.21 ± 0.08	0.24 ± 0.05
Lung	0.52 ± 0.12	0.55 ± 0.14	0.55 ± 0.10
Spleen	0.13 ± 0.03	0.12 ± 0.04	0.16 ± 0.03
Kidney	0.25 ± 0.04	0.23 ± 0.03	0.27 ± 0.04

4.4.9.6 Histopathology

Histopathological examinations of the all major organs including liver, kidney, brain, heart, spleen, lung, stomach, S.I, and L.I did not reveal any treatment-related changes in NEF or SOL treated mice group compared to non-treated mice group (Fig. 4.9). Therefore, these results are consistent with no statistical significant changes in the results observed in hematological, coagulation, blood electrolytic, and biochemical parameters after the treatment of NEF or SOL for three months. These results together indicate that 1) different dosages of EDA 46, 138 and 414 μM/kg are well tolerated by animals via oral intake for three months; 2) the vehicle SOL adding into the formulation did not alter any organ functions and is also well tolerated in mice fed for three months.

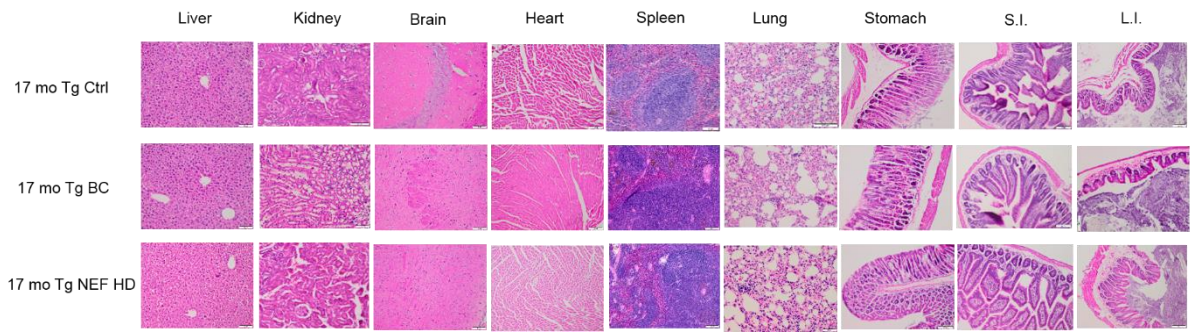

Figure 4.9 Photomicrographs of the sections of the tissues of Tg mice

Previously, the potential of EDR as an intervention therapy for AD was disclosed by targeting multiple key AD pathways including Aβ, Tau phosphorylation, oxidative stress, and neuroinflammation. NEF, the more bioavailable form of EDR, showed exceptional performance by improving AD-like behavioral deficits near the normal level which was better than the already approved drug product (DNP). Additionally, based on the long-term repeated dose toxicity assessment results, the good tolerability of NEF was proven via the oral route of administration. As the oral route of administration is the most preferred route of administration, our study demonstrated NEF as a promising and very safe therapeutic candidate in the current preclinical development.

4.5 Conclusions

The poor oral BA of EDR due to poor aqueous solubility, dissolution and permeability could hamper its optimum use for AD. To improve its BA, EDR loaded NEF was developed using SNMSD based strategy and SOL as a polymer. The significant enhancement of oral BA by improving solubility, dissolution, permeability, brings NEF to the forefront of existing therapeutic agents against the AD. Most importantly, NEF displayed dose dependant rescues of the behavioral deficits of 17-month-old APP/PS1 mice from the open field, NORT, Y-maze and MWM tests after three months of exposure by oral administration. Also, our NEF appeared reserving the cognitive decline of APP/PS1 mice to the cognitive level of wild type normal aging mice and performed better than donepezil. Moreover, the toxicity study data revealed the absence of drug-induced toxicity by oral administration up to 414 µM/kg in the APP/PS1 mice. Thus, NEF could be a promising candidate for the AD treatment. Our data in the present study, together with the earlier prove-of-concept study in 12-month-old APP/PS1 mice, warrants a large scale of clinical trials in mild cognitive impairment, and sporadic and familial AD.

Conflict of Interest

Ankit Parikh, Xin-Fu Zhou, and Sanjay Garg are the named inventors on Chinese patent 200610149832.9. Fujian Kangshimei Co, China owns the intellectual property. There is no other potential conflict of interest relevant to this article.

Contribution

XFZ conceived the project. Ankit Parikh (AP), Krishna Kathawala (KK), Xia Cao (XC), Sanjay Garg (SG) and Xin-Fu Zhou (XFZ) designed the study, AP, KK, Zhengnan Shan (ZS), Chi Chen (CC), Jintao Li (JL), Chun Chuan Tan (CT) and XFZ performed the research, AP, KK, SG and XFZ analysed the data; AP, KK, SG and XFZ wrote the paper.

Acknowledgements

The authors would specially like to acknowledge Fujian Fujian Kangshimei Co, China for the financial support for present research, the University President's Scholarships (UPS) from University of South Australia for Ankit Parikh and Zhengnan Shan for their doctorate study, Vacation Research Scholarships from University of South Australia for Chun Chuan Tan, NHMRC Fellowship for Xin-Fu Zhou, a scholarship under state scholarship fund from China Scholarship Council (CSC) for Jintao Li. The authors would like to acknowledge the technical support provided by Lyn Waterhouse from Adelaide Microscopy, The University of Adelaide for TEM analysis, Dr Andrew C Robinson, Dr Nobuyuki Kawashima and Dr Steve McInnes from Future Industries Institute, the University of South Australia for XRD, SEM and DSC studies, respectively, Rupal Pradhan and Andrew Beck from University of South Australia for hematological, coagulation parameters and histology study, Rebecca Summerton and Dr Ian Beckman from Veterinary Diagnostic Laboratory, the University of Adelaide Serum biochemistry study, H. Md. Morshed Alam (BASF Australia Ltd) for providing samples of SOL, Stephen Philip, a PhD candidate, from School of Pharmacy and Medical Sciences, the University of South Australia for NMR study, Noralyn Manucat-Tan and Chun-Sheng Ruan for behavior tests, Carolyn Streckbein and Deep Pujara for revising the language. The animal welfare officer, Alex Whittaker, and the animal ethics officer, Ruth Brogan and Reid animal house staff members including Jayne Skinner, Alysha Servin, Jess Parken, and Becky Nitschke from the University of South Australia are acknowledged for their generous support in animal work.

Supplementary Information

Novel Edaravone Formulation based on self-nanomicellizing solid dispersion strategy for enhancement of oral bioavailability and reversal of cognitive deficits in Alzheimer's disease model

Author information

Ankit Parikh[1], Krishna Kathawala[1], Zhengnan Shan[1], Chi Chen[1,2], Jintao Li[1,3], Chun Chuan Tan[1], Xia Cao[2], Sanjay Garg[1]*, Xin-Fu Zhou[1]*

[1]School of Pharmacy and Medical Sciences, University of South Australia, Adelaide, SA 5000, Australia.

[2]Central laboratory, Second Affiliated Hospital of Kunming Medical University, Kunming, Yunnan Province 650101, China.

[3]Neuroscience Institute, Kunming Medical University, Kunming, Yunnan Province 650500, China.

*Corresponding author-

E-mail address: Xin-Fu.Zhou@unisa.edu.au, Sanjay.Garg@unisa.edu.au,

Phone: +61 8830 22329, +61 8830 21575

Fax: +61 8830 21087, +61 8830 22389

Table S1 Mathematical models used to describe drug dissolution curves.

Equation	Model	Description
$Q_t = \ln Q_0 + K_1 t$	First order	Q_t: amount of drug dissolved in time t, Q_0: initial amount of drug in the solution, t: time, Q_∞: amount of drug dissolved in time ∞. K_1, K_0, K_C, K_H, K_K are the rate constants for first order, zero order, Hixson–Crowell, Higuchi-matrix and Korsmeyer–Peppas resepctively.
$Q_t = Q_0 + K_0 t$	Zero order	
$Q^{1/3}_0 - Q^{1/3} t = K_C t$	Hixson–Crowell	
$Q_t = K_H t^{1/2}$	Higuchi-matrix	
$Q_t/Q_\infty = K_K t^n$	Korsmeyer–Peppas	
Release profiles comparison		
$f_1 = \frac{\sum_{j=1}^{n} \lvert R_j - T_j \rvert}{\sum_{j=1}^{n} R_j} \times 100$	Dissimilarity factor (f1)	n: sampling number, Rj and Tj: percent dissolved of the reference and test products at each time point j.
$f_2 = 50 \times \log\left\{ \left[1 + (1/n) \sum_{j=1}^{n} \lvert R_j - T_j \rvert^2 \right]^{-0.5} \times 100 \right\}$	Similarity factor (f2)	

Table S2 Protocol for tissue processing in Leica ASP300.

Step	Reagent	Duration (min)	Temp
1	Formalin	5	-
2	Ethanol 70%	45	-
3	Ethanol 90%	60	-
4	Ethanol Absolute	60	-
5	Ethanol Absolute	60	-
6	Ethanol Absolute	90	-
7	Xylene	60	-
8	Xylene	60	-
9	Xylene	90	-
10	Paraffin Wax	60	62
11	Paraffin Wax	60	62
12	Paraffin Wax	60	62

Table S3 Change in the position of chemical shifts of EDR and NEF in 1H NMR spectroscopy.

EDR (chemical shift)	NEF (chemical shift)	Change
11.543	11.459	0.084
7.755	7.706	0.049
7.417	7.422	-0.005
7.195	7.193	0.002
5.381	5.356	0.025
2,136	2.107	0.029

5. Novel Self Nanomicellizing Solid Dispersion Curcumin Formulation for Oral Administration: Development, Optimization, and Assessment in Alzheimer's Disease Models

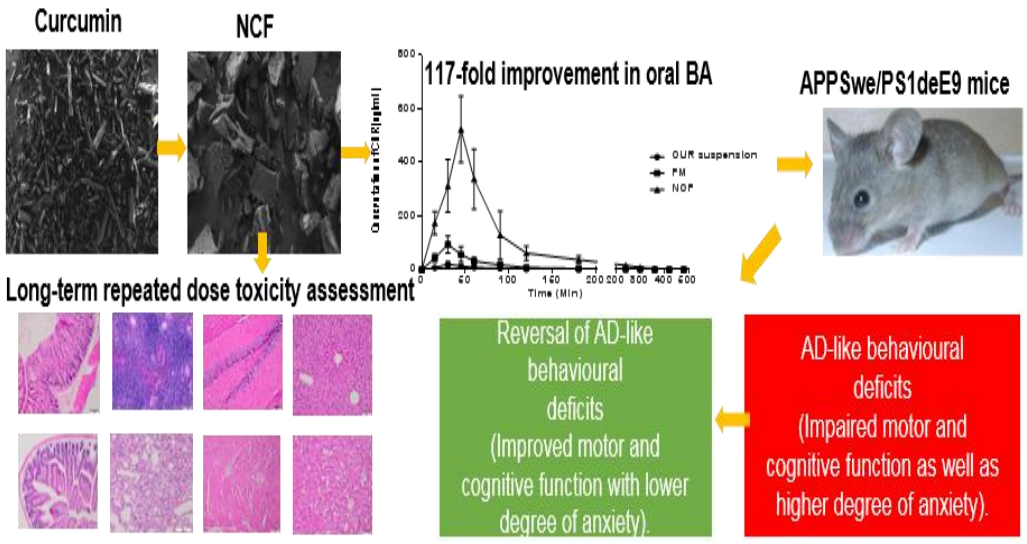

Graphical Abstract

5.1 Abstract

Curcumin (CUR), a natural polyphenolic compound is considered as one of the most potential candidates against Alzheimer disease (AD) by targeting multiple pathologies such as amyloid-beta, tau phosphorylation, and oxidative stress. Poor physicochemical profile and oral bioavailability (BA) are the major contributors to its failure in clinical trials. Lack of success in numerous drug clinical trials for the treatment of AD urges the need of repositioning of CUR. To overcome its limitation and enhance oral BA, Novel CUR formulation (NCF) was developed using self-nanomicellizing solid dispersion strategy. From the initial screening of polymers for their potential to improve the solubility and stability, soluplus was selected. The optimized NCF demonstrated over 20,000-fold improvement in aqueous solubility, a greater stabilizing effect in alkaline pH and light, enhancement of dissolution, and permeability of CUR across everted sacs of rat small intestine. Most importantly, it displayed 117-fold enhancement in oral BA of CUR. Furthermore, its safety and efficacy on mice AD-like behavioral deficits (open field, novel objective recognition, Y-maze and Morris water maze tests) were assessed in transgenic AD (APPSwe/PS1deE9) mice model. The results demonstrated NCF is a safe preparation and rescues the behavioral deficits of mice model. Therefore, NCF has a great potential to pave the way for clinical development for AD.

Keywords: Curcumin, Soluplus, oral bioavailability, APPSwe/PS1deE9 mice, Learning and memory, safety assessment

Chemical compounds: Curcumin (PubChem CID: 969516), Soluplus

5.2 Introduction

Curcumin (CUR) is established as one of the most bioactive molecules ever discovered from nature in the field of medical science. It is chemically 1, 7-bis-(4-hydroxy-3-methoxyphenyl)-hepta-1, 6-diene-3, 5-dione ($C_{21}H_{20}O_6$), extracted commercially from the rhizome of Curcuma longa Linn (turmeric) (family Zingiberaceae) [225]. It has a long history in Ayurveda medicine and been extensively used in countries like India and China for thousands of years [415]. A numerous *in-vitro*, preclinical and clinical studies confirmed its therapeutic potential for diseases including, neurological, cancer, infectious, inflammation and lifestyle associated diseases [246, 416]. Its phenomenal druggability is mainly due to its ability to interact with extra and intracellular targets to manage the cell survival, proliferation, secretion, oxidative stress and inflammation [417, 418]. Moreover, it was designated as a recognised as safe (GRAS) by the regulatory authorities in the countries like USA and Canada [241].

Developing a drug for Alzheimer's disease (AD) remains a holy grail and is one of the most challenging tasks for scientists and clinicians from more than 100 years [15]. Despite the wealth of knowledge available about AD, only a limited of options are currently accessible [419]. Recent repetitive failures of phase II-III AD clinical trials call upon the need for the effective use of therapeutic agents targeting multiple pathways [12, 420]. The significantly less number of AD population in India compared to the USA originates the therapeutic potential of CUR for AD as people in India extensively uses CUR in their food [223]. Later, several *in-vitro* and preclinical studies revealed its potential in targeting the multiple pathologies including amyloid beta (Aβ), oxidative stress, neuroinflammation, neurite degeneration, neuronal loss and tau-hyperphosphorylation [70, 71]. Most importantly, curcumin binds Aβ, inhibit its aggregation and fibrillation and enhance its clearance from the brain of AD mice. It also chelates metals such as copper, zinc, and aluminum which enhance Aβ toxicity and oligomerization [70]. Due to its ability to target the key mechanisms of AD, CUR has been considered as one of the most promising drug candidates that are currently available for further development. The failure in several clinical trials conducted in USA and China made huge disappointment in the field of AD research [384, 385].

The poor oral bioavailability (BA) of CUR (less than 1%) is the major limiting factor in the failure of clinical trials. The level of CUR achieved in plasma after dosing 4000, 6000 and 8000 mg/day for 90 days in 25 patients were 190, 200 and 600 ng/mL, respectively [234]. The poor aqueous solubility, stability, permeability and extensive metabolism are discovered as the potential factors contributing to its poor BA [257]. The hydrophobic nature of CUR because of

the presence of two phenyl domains results into poor water solubility (11 ng/mL in an aqueous solution having pH 5) and dissolution [421]. It also undergoes rapid hydrolysis under physiological and alkaline conditions [422]. The poor intestinal permeability of CUR is owing to intestinal degradation and first-pass metabolism, P-glycoprotein (P-gp) efflux and intracellular accumulation [257]. The rapid and extensive metabolism of CUR in curcumin glucuronide and curcumin sulfate, tetrahydrocurcumin, hexahydrocurcumin, and hexahydrocurcuminol after oral administration is also reported [252]. On account of poor solubility and intestinal permeability, CUR has been classified as a class IV drug as per Biopharmaceutics Classification System (BCS) [257]. To reposition CUR for AD and to achieve desired pharmacological outcome in a preclinical and clinical study, it is necessary to develop a novel formulation to curb the issues that limit in achieving desired concentration at a target site.

Improvement in the solubility and dissolution of CUR are the only majorly focused area in improving oral BA compared to stability and permeability as per current trends in research [252]. The therapeutic activity such as anticancer, anti-inflammatory and antioxidant of CUR metabolites have been reported that is why metabolism was not considered in our study [265]. The limited success at commercial scale was witnessed with drug delivery approaches such as liposome, emulsion, complexation with cyclodextrin, nanosuspension, and nanoparticles. Low encapsulation efficiency, complicated preparation process, poor stability and degradation in the stomach are major factors in the failure of nanotechnology-based systems [297]. The high molecular weight of cyclodextrin, slow process of complexation and the unstable condition of processing media limits its applicability [298]. Targeting multiple issues simultaneously such as solubility, stability, dissolution and permeability in one formulation could be a key step in the development of CUR loaded novel delivery system.

Self-nanomicellizing solid dispersion (SNMSD) is the novel strategy which offers the advantage of the solid dispersion (SD) based strategy and nanotechnology as it forms nanosized micelles upon contact with an aqueous media [323]. It is a mixture of active pharmaceutical ingredient (API) with a single or multiple pharmaceutical carriers. It improves the physicochemical profile of API like solubility, and dissolution by nanosizing, enhancing wettability, and polymorphic changes [324, 325]. Moreover, it could protect the drug against the degradation in a physiological condition. Additionally, it offers a superior loading ability, stability, simple manufacturing and scale-up process, economic, possibility of translating into the conventional oral solid dosage form such as tablets and capsule over other technologies

[326]. Also, its potential for enhancing oral BA was proven with a number of drugs including Cyclosporine A [323], Valsartan [327], and 9-nitrocamptothecin [328]. The selection of the appropriate carrier as per the characteristics of the drug is the key step in achieving the desired outcome. Few studies with limited success were reported based on CUR loaded SD with the polymers Gelucire® 50/13 [329], D-α-Tocopheryl Polyethylene Glycol 1000 Succinate [330] and Eudragit® E PO [331]. For CUR, there is a need of carrier which can offer protection in physiological conditions and enhancement of the intestinal permeability with improving solubility and dissolution. Soluplus® (SOL), a 4th generation novel amphiphilic polymer has successfully improved the BA of drugs having similar characteristics of CUR including Aprepitant [333], Carvedilol [334], Quercetin [335]. It is chemically Polyethyleneglycol–polyvinyl caprolactam– polyvinyl acetate grafted copolymer (PEG 6000/vinylcaprolactam/vinylacetate copolymer, BASF, Germany). It acts as a solubilizer by enhancing wettability and nanosizing, stabilizer by encapsulating the drug in micelles and reducing recrystallization rate of drugs; and permeability enhancer by modulating Pgp efflux pump [328, 332]. To the best of our knowledge, there is no SOL based SNMSD strategy applied to enhance oral BA of CUR.

The lack of suitable animal model is one of the key factor responsible for high failure rate in clinical trials of AD drugs [423]. Genetically modified animal models are most recognized mice models that are used to understand the pathology and to evaluate potential therapeutic interventions [424, 425]. APPSwe/PS1deE9 mice contain human transgenes for both APP bearing the swedish mutation and PSEN1 containing an L166P mutation under the control of the Thy1 promoter [426]. It represents characteristics of AD such as Aβ deposition, global neuron loss, activated microglia around Aβ deposits, dendritic spine loss, cognitive deficits, and therefore widely accepted to assess the often used to study the mechanisms of neuropathology and efficacy of potential therapeutic candidates for AD [69, 389]. The ideal delivery system should not alter the safety profile of CUR and also not produce any unintended toxicity to normal healthy tissues and cells. The information regarding the toxicity of SOL-based preparation is very limited. Therefore, assessment of long-term repeated dose toxicity study of NCF is necessary to provide guidance for its clinical applications.

The aim of this study was to explore NCF based on SNMSD strategy for alleviating the limiting physicochemical factors in the clinical development of CUR against AD. The selection of polymer based on solubility and stability of CUR were evaluated in simulated biological fluids (SBF). The method of preparation and the ratio of drug to polymer for NCF were optimized

based on solubility improvement. The interaction between CUR and SOL were studied by differential scanning calorimetry (DSC), X-ray diffraction (XRD), scanning electron microscopy (SEM), Fourier Transform Infrared Spectroscopy (FTIR), and nuclear magnetic resonance (NMR) spectroscopy. In addition, its self-micellizing properties were assessed after dissolving in water for particle size, zeta potential, loading ability and morphology through transmission electron microscopy (TEM) analysis. Furthermore, the stability of NCF was studied as per ICH guideline. To evaluate the potential of NCF for oral administration, *in-vitro* release kinetics in simulated biological fluids (SBF), permeability across the everted sacs of rat gut and *in-vivo* BA in adult rats were compared against CUR suspension. NCF was further assessed for the long-term (3 months) efficacy of orally administered on mice behavioral deficits (Open field, Novel objective recognition, Y-maze and Morris water maze tests) in transgenic AD mice model (TgAD) (APPSwe/PS1deE9). Moreover, the safety of NCF was investigated by measuring body weights, water, and food consumption, biochemical, coagulation and hematological parameters in blood, determining organ weight, and analyzing histopathology. To exclude the interference of age-associated alterations in tissue morphology or function, the observation of NCF groups were compared to blank NCF (SOL control) and without any treatment group (sham control).

5.3 Materials and Methods

5.3.1 Materials

CUR was bought from Chem-Supply Pty Ltd. (South Australia, Australia), from Tokyo Chemical Industry Co., Ltd. (TCI). SOL was gifted from BASF Australia Ltd (Victoria, Australia). Polyvinylpyrrolidone K 30 (PVPK30), Polyethylene glycol 4000 (PEG 4000), Poloxamer 188, Poloxamer 407, Concentrated HCL, formic acid, disodium hydrogen phosphate, citric acid, Tween 80 and DMSO-d_3 were purchased from Sigma-Aldrich (New South Wales, Australia). Acetic Acid, phosphoric acid, and sodium hydroxide pellets, were obtained from Chem Supply (South Australia, Australia), Boric acid from Optigen Scientific (South Australia, Australia) and saline from Pfizer (New South Wales, Australia). High purity (Milli-Q) water was used throughout the study. All other reagents were of analytical grade. HPLC grade acetonitrile and methanol were purchased from Merck (Melbourne, VIC, Australia).

5.3.2 Analytical methods for CUR

5.3.2.1 High-Performance liquid chromatography (HPLC) method

The HPLC method was utilized with a slight modification of previously reported method [249]. The Ultraviolet-Visible (UV) Spectrophotometers detector coupled with HPLC system was used as per our previous report [342]. A Waters Symmetry™ C18 (3.9*150 mm) analytical column and the mobile phase comprising of acetonitrile (65% v/v) and 1% w/v citric acid buffer (pH 3) (35% v/v) were used at the wavelength of 423 nm. The flow rate was maintained at the rate of 1 mL/min, and sample injection volume was 20 µL. The mean regression equation for CUR for the concentration range of 0.5–100 μgL^{-1} was y = 166659x + 49872 (r = 0.9999, n = 10), where x and y represent the concentration and the peak area of CUR, respectively.

5.3.2.2 Liquid chromatography-tandem mass spectrometry (LC/MS/MS) method

The LC-MS/MS instrument was used as described previously [342]. The samples were diluted in 50:50 methanol and water mixture before introducing into the system. The gradient elution was carried out by using a mobile phase A (MPA) containing 5% methanol, 95% water, and 0.1% formic acid and mobile phase B (MPB) containing 95% methanol, 5% water, and 0.1% formic acid. The gradient method was set up from 10% MPB to 100% MPB in 2 min, set to 100% for further 4 min, followed by 10% for 0.5 min. The chromatographic separation was carried out using a phenomenex Luna C18 (50 mm × 3 mm × 3 µm) column with 0.2 mL/min flow rate and an injection volume of 10 µL. The total run time was 8 min. The electro-spray ionization in negative mode was used here. Identification and quantification of CUR and warfarin as an internal standard was performed using suitable transitions (CUR – 367.1/134.2, Warfarin – 307.2/161.2) in the multiple reaction monitoring modes. The linearity was observed between the concentrations of 1 to 500 ng/mL.

5.3.3 Selection of a suitable carrier for the development of NCF

5.3.3.1 Solubility parameter (SP) analysis

The selection of polymeric carrier is the most important step for the preparation of SDs. The SP analysis was used to determine the miscibility of the drug molecule in the polymeric solution. It was measured by calculating Hansen solubility parameter (HSP) which calculated on the basis of polarity (δp), dispersion (δd), and hydrogen bonding (δh) properties of the compound [332]. These parameters stand for the molecular, atomic, and electron level

interaction. Here, we compared the reported value of CUR with polymers to determine the miscibility as a part of the selection process of a carrier.

5.3.3.2 Miscibility study

In separate glass bottles, 2.5%, 5%, 7.5%, and 10% w/v solutions of different carriers including SOL, PVP K30, PEG 4000, poloxamer 407, and poloxamer 188 were prepared in simulated gastric fluid (SGF, pH 1.2) [390]. The purpose of using SGF is the superior stability of CUR at lower pH [249]. An excess amount of CUR was added to the solutions mentioned above followed by shaking for 24 h at 150 revolutions per minute (rpm), at ambient temperature in a mechanical shaker (Axyos Technologies). After that, each solution was filtered through 0.45 µm polyvinyl difluoride (PVDF) syringe filters, diluted with mobile phase and analyzed in triplicate by using HPLC method.

5.3.3.3 Kinetic Solubility

The SD was prepared by using solvent evaporation (SE) technique. Both the drug and a carrier, at the fixed ratio (1:3) were dissolved in ethanol. The mixture was then evaporated to dryness at 55-60 °C under the vacuum (500-600 mbar). The SDs were further pulverized using a mortar and pestle, passed through 250 µm sieve, covered with aluminum foil to protect from light and stored in a desiccator until use for further studies [391].

An accurately weighed SD equivalent to 10 mg of CUR, crystalline CUR, and amorphous CUR were added to the 2 mL of simulated intestinal fluid (SIF) pH 6.8 [332]. The solubility study was conducted as mentioned in 5.3.3.2. The samples were collected at pre-determined time points and analyzed using HPLC method.

5.3.3.4 Chemical Stability Study

To evaluate the protective effect of polymer due to pH dependent CUR stability profile, pH 1.2, 6.8, and 7.4 buffer systems were used with or without different carriers selected from the miscibility and kinetic solubility study that include SOL (10% w/v) and PVP K30 (10% w/v) and compared with free CUR [249]. Methanol was used to prepare the stock solution of CUR (1000 µg/mL) and then further diluted (up to 100 times) with buffer solutions. The samples were stored at ambient temperature. The aliquots were withdrawn at different time points and analyzed by developed HPLC method.

5.3.4 Formulation development and optimization of NCF

5.3.4.1 Method of Preparation

To optimize the best process for the preparation of SDs using SOL as a carrier, different approaches were investigated with the drug / the polymer ratio 1:3. The best method was selected based on the solubility study.

SE Method

As discussed in section 5.3.3.3.

Melt mixing (MM) method

The SD was prepared by mixing CUR with melted SOL at 130°C (liquid paraffin bath) using a glass rod for 10 min. The mixture was allowed to solidify at room temperature overnight [427]. The SD was further processed as mentioned in section 5.3.3.3.

5.3.4.2 Concentration of Polymer

To study the concentration dependent effect of the polymer, SDs of CUR were prepared at the different drug: polymer ratio including 1:2.5, 1:5, 1:7.5, and 1:10 [249]. The solubility was determined as mentioned in section 5.3.3.2.

5.3.5 Characterization of NCF

5.3.5.1 Loading ability and efficiency

The NCF equivalent to 1 mg of CUR was weighed and dissolved in 1 mL of methanol. The sample was filtered through 0.45-µm PVDF syringe filter and analyzed by HPLC method. The loading ability of NCF was calculated based on the weight ratio of CUR to SOL and loading efficiency with the determination of loaded CUR in NCF after preparation from initial amount [331].

5.3.5.2 Comparison of solubility of physical mixture (PM) and NCF in simulated body fluids

The solubility of NCF against crude CUR, amorphous form of CUR and PM of CUR and SOL (1:10) were investigated. SD and amorphous form of CUR were prepared by SE technique whereas PM was prepared by mixing SOL and CUR using the motor and pestle [330].

5.3.5.3 Determination of interaction between SOL and CUR in NCF

DSC Study

To assess the thermal behavior of CUR, SOL, PM of CUR and SOL, and NCF, DSC was performed using TA Instruments Discovery DSC (Model 2920). Briefly, 2-4 mg of each sample was weighed accurately and placed in the aluminum crucible. The empty crucible was used as a reference. The thermograms were obtained over the temperature range from 40 - 300 °C at the heating rate of 10 °C/min under the nitrogen gas (50 mL/min) [357].

XRD Study

To determine the solid state characteristics of CUR, SOL, PM of CUR and SOL, and NCF, XRD patterns were recorded using an X-ray diffraction instrument (PANalytical, Empyrean X-ray diffractometer). The samples were exposed to the radiation using CuKα radiation (λ = 1.5418 Å), operating at 40 kV and 40 mA. The scanning was performed from 2 to 50°, 2θ at a step size of 0.013° at the scanning rate of 2 °/min [332].

SEM Study

Morphology of CUR, SOL, and NCF were studied by SEM. The samples were mounted on a SEM stub using conductive double-sided adhesive tape prior to analysis. The ultra-high resolution secondary electron microscopy (Zeiss Microscopy Merlin with GEMINI II column) was used to observe the morphological characteristics. The electron images were obtained by operating a microscope at 0.7 kV [332].

FTIR study

FT-IR spectra were recorded using a PerkinElmer Spectrum 400 spectrometer connected with an attenuated total reflectance (ATR, top-plate type) (PerkinElmer) by conventional potassium bromide (KBr) pellet method. The KBr pellet was prepared by taking 2-4 mg of samples and 100-150 mg of KBr into a small agate mortar and grind to a very fine powder using the agate pestle. The fine powder was placed in a die and pressure of 8 tonnes for 10-15 s was applied to make KBr pellet. Each sample was scanned over the range of 400–4,000 cm^{-1} at a resolution of 2 cm^{-1} [391].

^{1}H NMR study

CUR and SD were dissolved in DMSO-d_3 and transferred to a 5 mm diameter tube before the measurement. ^{1}H NMR spectra were obtained with Bruker AVANCE-III 500 at 500 MHz and 125 MHz, respectively and TopSpin 3.2 software was used for data analysis [393].

5.3.6 Preparation and Characterization of self-micellizing properties of NCF

5.3.6.1 Preparation of CUR loaded micellar solution using NCF

The NCF equivalent to 10 mg of CUR was dispersed in 10 mL of water and stirred at 500 rpm with a magnetic stirrer for 3 h. The resultant solution was filtered through 0.45 µm polyvinyl difluoride (PVDF) syringe filter to obtain homogeneous micellar solution [394].

5.3.6.2 Determination of particle size, poly-dispersity index (PDI) and Zeta potential

The particle size, PDI, and zeta potential of micellar solution were analyzed by Malvern Zetasizer Nano ZS.

5.3.6.3 TEM analysis

The tiny drop of micellar solution was spread on copper grids. The copper grid was dried overnight at room temperature and analyzed using Philips CM100 Transmission Electron Microscope equipped with a SIS MegaviewII CCD Camera and analySIS image analysis software.

5.3.6.4 Analysis of photo physical properties

The UV absorbance spectra of both native CUR (dissolved in methanol) and a micellar solution was recorded using HPLC coupled with Photodiode Array (PDA) detector with the specification mentioned in section 5.3.2.1 to determine the impact of encapsulation and binding of CUR with SOL in NCF [428].

5.3.6.5 Stability Study

For micellar formulation, the assessment of stability against hydrolytic, thermal, photolytic and oxidation was evaluated for 24 h [342]. The pH-dependent stability study was also conducted between pH 2-8 to assess its suitability for oral administration. Here, 2 mL of CUR solution was prepared in glass bottles, covered with aluminum foil to protect from light and stored at 25 °C. To assess the thermal stability, the samples were exposed to different stability conditions including 4 ˚C, 25 °C / 60% RH, and 40 °C / 75% RH. To determine the susceptibility to oxidation, the solution was exposed to the 0.03%, and 3% hydrogen peroxide (H_2O_2). For photolytic degradation study, the solution of CUR was kept in the KBF ICH 720 (E2) - constant climate chamber as per ICH guideline. The samples were collected at different time points, filtered and analyzed using UV-HPLC method.

5.3.7 Stability study of NCF as per ICH guideline

The stability of NCF was conducted as per ICH guideline at 4 ˚C, 25 °C / 60% RH, and 40 °C / 75% RH for eight weeks [342]. 1 g of NCF was taken in glass vials, sealed and covered with aluminum foil. The samples were collected at predetermined time intervals and analyzed with HPLC method.

5.3.8 In-vitro release study

In-vitro release study was conducted using USP apparatus type II (paddle) at 37°C and 75 rpm [249]. Briefly, CUR suspension and NCF were placed in the flask containing 900 mL of dissolution media including SGF and SIF (pH 6.8) with 0.01% Tween 80. The samples were collected at different time points of 5, 15, 30, 45, 60, 90, and 120 min and replaced with an equal volume of dissolution media. The samples were then analyzed by HPLC method after appropriate dilution and filtration. To determine the release kinetic of the CUR and NCF, the data obtained from the *in-vitro* release study were fitted into different kinetic models which include First order, Zero order, Hixson Crowell, Higuchi-matrix and Korsmeyer–peppas. The release model was finalized based on the value of the release constant in the equations mentioned above. Moreover, similarity (f_2) factor was used to compare the dissolution profiles of the CUR and NCF. All the equations used for the calculations are mentioned in the Table S1. If f_2 values are in between 50-100, then dissolution profiles are considered to be alike.

5.3.9 Improvement in permeability

Ex vivo absorption of CUR (200 µg/mL) and NCF (equivalent to CUR concentration) were studied using everted sac technique with rat small intestine (S.I) as per previous report [342].

5.3.10 Pharmacokinetic study

5.3.10.1 Animals

The male Sprague-Dawley rats (300 ± 25 g) from laboratory animal services (University of Adelaide, South Australia, Australia) were used in this study as described previously [342]. All the animal experiments were approved by local animal ethics committee of the University of South Australia and by an institutional guideline.

5.3.10.2 Dosing and sampling

The rats were kept on fast for overnight and received CUR suspension, PM, and NCF at an equivalent dose of 47 mg/kg of CUR by oral gavage. The jugular vein blood samples were collected at a pre-determined time interval of 0, 15, 30, 45, 60, 90, 120, 180, 240, 300, 360,

420, and 480 min. A 200 µl of blood sample was collected at each time point, centrifuged at 5000 rpm for 15 min at 4°C to separate the plasma and subsequently stored plasma at-80°C until analyzed.

5.3.10.3 Sample preparation

A 100 µl of the plasma sample was transferred to a 2mL eppendorf tube, after being equilibrated to room temperature. 10µl of 0.1M HCl and 950 µl of methanol were added to the plasma sample followed by vortexing for 20 min. The samples were then centrifuged at 13,000 rpm for 10 min. The supernatant was separated in 1.5 mL eppendorf tube and evaporated to dryness at 50°C. The residue was reconstituted with mobile phase as per the requirement and centrifuged at 13,000 rpm for 3 min. The resultant solution was injected into the LC-MS/MS system for analysis.

5.3.10.4 Pharmacokinetic Parameters

The various pharmacokinetic parameters including maximum plasma concentration (C_{max}), time to achieve maximum plasma concentration (T_{max}), elimination half-life ($t_{1/2}$), area under the concentration–time curve (AUC), and relative BA were determined using Phoenix WinNonlin software and non-compartmental analysis [342].

5.3.11 Behavioral tests with mouse models of Alzheimer disease

5.3.11.1 Animals

APPSwe/PS1deE9 transgenic mice with a C57BL/6 background was obtained from Jackson Laboratory. All mice including C57BL/6 mice bred in the Reid Animal facility of the University of South Australia. The animal facility is occupied with a standardized facility such as 12-h light/12-h dark cycle per day from 7:00 a.m.to 7:00 p.m., temperature 22 ± 1 °C and humidity 52 ± 2%. All breeding procedures were approved by the Animal Ethics Committee of the University of South Australia. Before initiating the treatment, the health of each mouse based on their behavior and appearance was examined to confirm the suitability for the experiment.

5.3.11.2 Stability of NCF in drinking water supplied to animals

The stability study of NCF solution in the water was carried out at the concentration of CUR 300 µg/mL for up to 7 days. 300 mL of the formulation was prepared in the water bottle and kept in the animal cage at the temperature and humidity of 22 ± 1°C and 52 ± 2%, respectively.

The samples were collected at the predetermined time intervals, filtered and analyzed using HPLC method.

5.3.11.3 Average water and food consumption

An average water and food consumption were recorded for one week to finalize the daily dosing. After starting the treatment, all the animals were observed for body weight changes, food, and water consumption on a daily basis up to 1 weeks and then on a monthly basis till the end of the study. From the amount of water consumption before and after the addition of formulation were recorded to finalize the appropriate dosing.

5.3.11.4 Experimental design

APPSwe/PS1deE9 (at the age of 14th months) were randomly divided into six groups/strain: Group 1- basal control (without any treatment) mice were undergone for behavior tests at the age of 14 months and used as a baseline control. Group 2- sham control (without any treatment) mice were administered with normal drinking water for three months. Group 3- blank control (B.C) mice were supplied with blank formulation containing SOL (equivalent amount to the amount used in NCF) in drinking water for 3 months, Group 4- CUR control (C.C) that were administered with PM of CUR and SOL in drinking water for 3 months (equivalent to the amount used in NCF), Group 5- NCF (equivalent to CUR dose of 47 mg/kg) in drinking water for 3 months and Group 6- Donepezil (DNP) (equivalent to dose of 2 mg/kg) in drinking water for 3 months. Aricept® tablets (Pfizer laboratory Limited, Auckland, New Zealand) were crushed using motor and pestle, and the contents were dissolved in drinking water, filtered and supplied to the animals. One group of C57BL/6 mice as a control for APPSwe/PS1deE9 strain was supplied the normal drinking water and subjected to behavior test at the age of 17 months. The detailed about each group, treatment, identity, age, sample size were mentioned in Table S2.

Different behavioral tests including open field, Novel Objective Recognition Test (NORT), Y-maze spontaneous alternation test and Morris water maze (MWM) tests were performed with APPSwe/PS1deE9 and C57BL/6 [69, 389, 429]. These tests were carried out at 23-25°C in the isolated behavior room in the Reid animal house at the University of South Australia. The animals were taken to the behavior room one h before starting the test and allowed them to accustom to the environment. A digital camera was used for the video recording of the animals' behavior. The data were analyzed using the ANY-maze video tracking software (Illinois, USA).

5.3.11.5 Open field test

The open field is a white open arena with the dimensions of 40 cm long, 40 cm wide, and 40 cm height. The video recording using the digital camera was started, and subsequently, the animals were gently placed in the center of the arena and allowed to move for 5 min. At the end of each trial, the arena was cleaned with 70% ethanol. Spontaneous locomotor activity was determined by the distance traveled and % mobility while anxiety-like behavior was evaluated by the % time spent in the middle of the arena (24 × 24 cm). Vertical activity (rearing), grooming, defecation, and urination were also recorded [395].

5.3.11.6 NORT

NORT test was performed in the same arena described in section 5.3.11.4. This test was divided into the three parts: habituation, familiarization, and test phase. In the 1st phase of habituation, the test mice were allowed to accustom to the arena for about 5 min. In the 2nd phase of familiarization, the mice were allowed to familiarize with two identical objects, kept 15 cm apart from each other. In the test phase, one of the identical objects were replaced with a novel object. After 24 h, the mice were again placed into the arena and the time spent in close interaction with a novel object as compared to the time spent closure to the identical objects was recorded to generate the recognition and discrimination index [396].

5.3.11.7 Y-Maze test

Testing was done using a Y-shape maze consisting of 3 opaque arms, 120° angles apart from each other as per previous report [69, 389]. The mice were placed at the end of one arm and allowed to move freely on maze during the 5 min session. The entries to each arm were recorded by visual observation. The alteration was defined as the consecutive entries to each arm of the maze. The % alteration was determined by the ratio of actual alterations to the possible alterations (number of arm entries minus 2), multiplied by 100. For the novel arm exploration, the mice were placed at the one end of the randomly chosen arm and allowed to travel through the maze for about 5 min with a closed novel arm in the 1st phase of training. The mice were then kept in the home cage till the subsequent trial. In the 2nd phase of a trial, the mice were allowed to explore all three arms. The total number of entries and time spent on each arm were recorded for each phase of trials.

5.3.11.8 Morris water maze test

A circular polypropylene pool with the dimensions of 120 cm diameter × 45 cm height was used to carry out the MWM test as per our report [395]. The MWM apparatus was filled with the water (temperature- 23 - 25°C) up to 30 cm depth and made opaque by using a nontoxic white paint before initiating the test. The MWM apparatus was hypothetically divided into four quadrants, and the start positions were selected for each quadrant. Initially, the mice were allowed to freely swim for about 1 min to get adjusted themselves in the testing environment. A white plastic platform with 7.5 cm diameter was kept in the center of one of the four quadrants, and other quadrants were marked as left, right, and opposite. In this test, the mice were trained in two sessions: 1) Visible: the platform was 0.5 cm above the water level and 2) Hidden: the platform was 0.5 cm below the water level. Firstly, the animals were trained to find a visible platform (60 s/trial, 3 trials/day, 1 day) followed by the hidden one (60 s/trial, 3 trials/day, 4 days). In each trial, the animals were allowed to swim in one of the quadrants except the quadrant closer to the platform, for about 60s. If animals could not find the platform by themselves than they were guided towards the platform and left over there for 30 s. Furthermore, the animals were allowed to be on the platform for 30 s even if they find it within 60s. After hidden platform training, probe test (60 s/mice) without platform was performed. In platform trials, swimming distance (path length), speed, and learning curve of escape latency were recorded whereas a number of annulus crossing, the percentage of time spent in the each quadrant, swim speed were recorded.

5.3.12 Assessment of long-term repeated dose toxicity

5.3.12.1 Body Weight

After initiating the treatment, the weight of the mice in each group was recorded daily for two weeks followed by once in a week.

5.3.12.2 Water and food consumption

During the treatment period, food and water consumption (g/day/10 g body weight) were recorded once in a week.

5.3.12.3 General behavior and mortality

All mice were observed daily after initiating the treatment included for mortality or morbidity dull/ruffled coat, hunched posture, reluctant to move, dehydration by skin tent, diarrhoea/abnormal bloating, changes in skin and fur, eyes and mucous membranes and

behavior patterns. The individual mouse was observed daily for its appearance, weight, and behavior, once any abnormality was observed during the treatment period [397].

5.3.12.4 Haematological parameters

Hematological parameters were evaluated by collecting the blood samples at the end of the experiment. There was 5 mice/strain/group. The EDTAK2-coated vials were used to collect the blood samples, and the samples were further analyzed by fully automated 5-part differential hematology analyzer (Sysmex XN550). Here, different hematological parameters including white blood cells (WBC), red blood cells (RBC), hemoglobin (HGB), hematocrit (HCT), mean corpuscular volume (MCV), mean corpuscular hemoglobin (MCH), Mean corpuscular hemoglobin concentration (MCHC), platelets (PLT), mean platelet volume (MPV), platelet haematocrit (PCT), platelet distribution width (PDW), neutrophils, lymphocytes, monocytes, eosinophils, and basophils were analysed [398].

5.3.12.5 Coagulation parameters

Blood plasma was used for manual measurement of coagulation parameters, such as prothrombin time (PT) and activated partial thromboplastin time (APTT) [398]. For determination of PT, Innovin reagent was pre-warmed at 37°C. The plasma sample (100 µL) was taken in glass test tube. 200 µL of Innovin reagent was mixed with plasma sample, and record the time for the fibrin strands at 37°C. For APTT measurement, 0.025M calcium chloride and APTT reagent was pre-warmed at 37°C. 100 µL of plasma sample was taken in a test tube, mixed with 100 µL of APTT reagent and incubated with 180 s in water bath at 37°C. 100 µL of calcium chloride was added to above mixture and time was recorded to the first appearance of fibrin strands at 37°C. The analysis was conducted in triplicate for each sample.

5.3.12.6 Serum biochemistry

The blood biochemical parameters including alanine aminotransferase (ALT), aspartate aminotransferase (AST), alkaline phosphatase (ALP), Amylase, Lipase, gamma-glutamyl transferase (GGT), Sodium, Bicarbonate, Anion Gap, Potassium, Calcium, Sodium :Potassium ratio, Chloride, Inorganic Phosphorus, Calcium: Phosphorus ratio, Albumin, Total Protein, Globulin, Total Bilirubin, Creatinine, urea nitrogen, Glucose, total cholesterol, were determined using an automatic chemistry analyser (Beckman Coulter AU480) [398].

5.3.12.7 Organs weight

At the end of the experiment, the animals were sacrificed by exposing to CO_2 for 5 min and perfused intracardially with cold Phosphate-buffered saline (pH 7.4). Different tissues including brain, liver, heart, lung, spleen and kidney were collected to determine the absolute weight of each tissue [399].

5.3.12.8 Histopathology

The histological examination was carried out on all the collected tissues such as liver, kidney, brain, heart, spleen, lung, stomach, S.I, and large intestine (L.I). The tissues were fixed using 10% formalin followed by processing using protocol describe in Table S3 with Fully Enclosed Tissue Processor (Leica ASP300). The tissues were then embedded in paraffin (Leica EG 1160) and the standard sections were taken using Microm Microtome and histology water bath (Leica HI1210). These sections were examined under the microscope (Olympus CX 41) after staining with a hematoxylin-eosin dye [430].

5.3.13 Statistical analysis

GraphPad Prism 6 was used for statistical analysis. All values were indicated as Mean ± standard deviation (SD) or Mean ± standard error (SEM). The statistical analysis of data was performed by using Student's t-test for two groups, one-way and two-way analysis of variance (ANOVA) for multiple groups. The mean differences were considered significantly valued in all experiments at $P < 0.01$.

5.4 Results and Discussion

5.4.1 Selection of suitable carrier for the development of NCF

Poor aqueous solubility and stability are identified as crucial factors contributing to the poor oral BA of CUR. The selection of polymeric carrier is the key step in developing a successful NCF. Thus, improvement of solubility and stability were monitored for the screening of polymers to develop NCF. The potential of polymer for solubility enhancement depends on the extent of affinity and miscibility towards drugs. Therefore determination of SP value and miscibility study were performed. Furthermore, the short-listed polymers were used to prepare CUR loaded SD to compare their ability to act as a precipitation inhibitor and the duration to maintain the supersaturated condition by kinetic solubility study. The polymer was chosen based on its potential to protect the degradation of CUR in SBF.

5.4.1.1 Solubility parameter (SP) analysis

SP was considered in the initial phase of the selection process of a suitable polymer. From literature, a difference of less than 7 $MPa^{1/2}$ indicates the favorable interaction between drug and polymer, a higher degree of miscibility and lesser chances of recrystallization [332]. The SP value designates the Van der Waals-type interactions. The SP values of CUR and polymers are shown in a Table S4. The ideal range of SP value of polymer should be in the range of 14.4 – 28.4 $MPa^{1/2}$ as 21.4 $MPa^{1/2}$ is the SP value of CUR. The polymer having closure SP value to the CUR SP value could have stronger interaction compared to others. The SP values of selected polymers are in the ideal range of CUR. Poloxamer 407 and poloxamer 188 could be a better choice with the difference of 0.35 and 0.7 $MPa^{1/2}$ compared to CUR, respectively. The difference of SP value of SOL, PEG 4000 and PVP K30 are 2.0, 4.3 and 4.88, respectively. The miscibility study was conducted to evaluate the potential of each polymer for solubilizing CUR.

5.4.1.2 Miscibility Study

Miscibility study was utilized successfully in the polymer selection process for the development of SD system previously [390]. The results are presented in Fig. 5.1A. The aqueous solubility of crystalline CUR was 0.72 ± 0.23 µg/mL. The increment of aqueous solubility of CUR was observed with increasing polymers content from 2.5% to 10% (w/v) as the regression coefficient values for SOL, PVP K30, PEG 4000, poloxamer 188 and poloxamer 407 are 0.9961, 0.9227, 0.7778, 0.972 and 0.9949, respectively. With 10% w/v concentration, SOL and PVP K30 solubility showed 70.93 and 26.02-fold improvement in aqueous solubility of CUR compared crystalline CUR, while poloxamer 407, poloxamer 188 and PEG 4000 presented 6.54, 5.84 and 4.31-fold enhancement, respectively. The greater solubility was observed in a case of SOL and PVP K30 compared to poloxamer 407 and poloxamer 188 despite moderate miscibility predicted by SP. The SP value can predict the miscibility based on Van der Waals-type interactions but does not consider other interaction like hydrogen bonding [332]. A number of reports suggest the improvement of miscibility of water insoluble drug with SOL and PVP K30 because of hydrogen bonding interaction [431, 432]. So, the role of hydrogen bonding interaction in solubility improvement of CUR could have a greater impact.

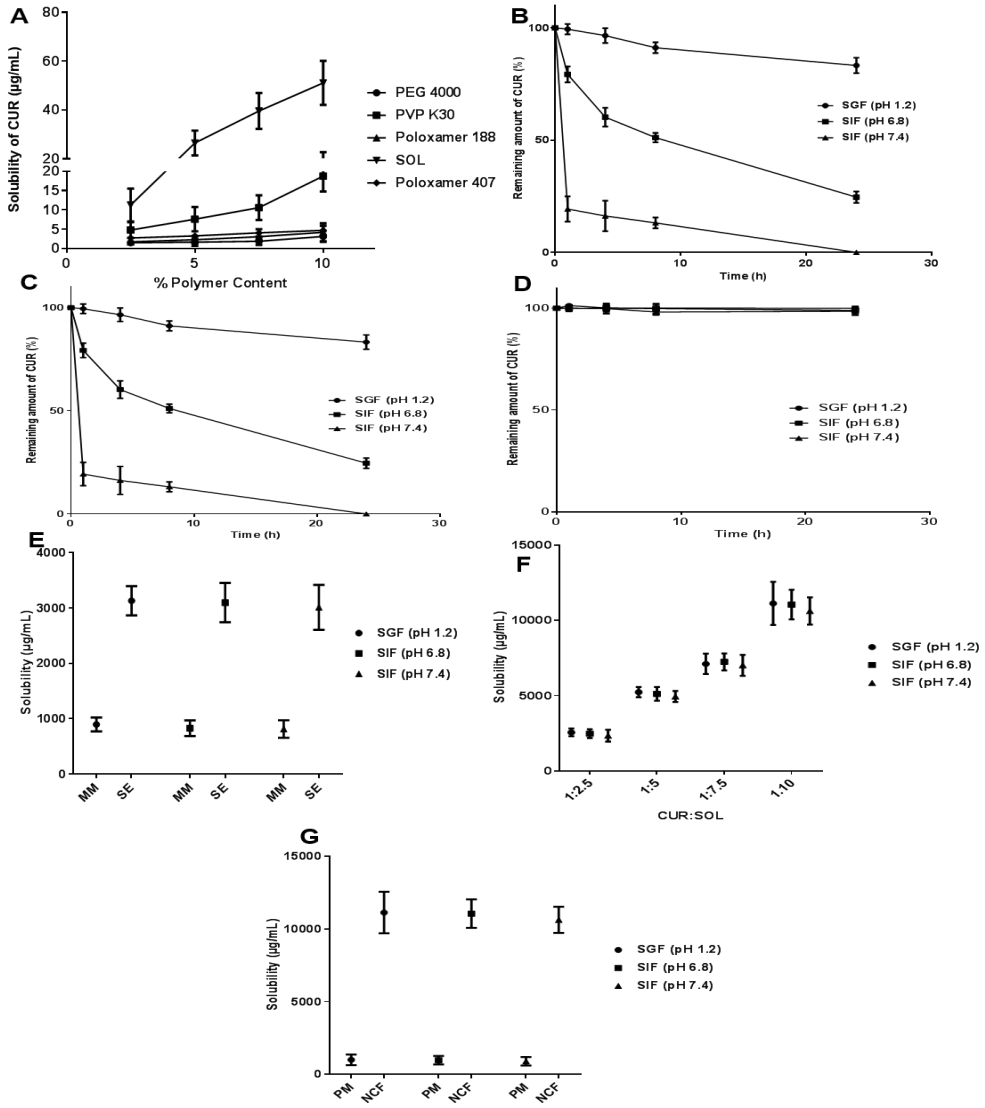

Figure 5.1 Selection of suitable carrier for formulation development and optimization of NCF. Miscibility study of CUR within different polymers (A), chemical stability of CUR in blank buffers (B), buffers containing PVP K30 (C) and 10% (w/v) SOL (D), Solubility of SDs prepared by MM and SE techniques (E), with various CUR and SOL ratios (F), and with optimised ratio compared to PM (G) in SGF (pH 1.2), SIF (pH 6.8 and 7.4) (mean ± S.D., n = 3).

5.4.1.3 Kinetic solubility

From SP and miscibility study, SOL, PVP K30 and poloxamer 407 were considered for kinetic solubility study. SE technique for preparation of SD and CUR to polymer ratio (1:3) were utilized as per our previous study to compare the potential for improvement of CUR solubility. The maximum solubility, time for precipitation and solubility value at 24 h are indicated as S_{max}, Te $_{precipitation}$ and S_{24h}. The equilibrium solubility was the solubility referred at 24 h. The crystalline and amorphous CUR displayed S_{max} value of 0.72 ± 0.23 and 1.89 ± 0.59 µg/mL,

whereas S_{24h} value of 0.54 ± 0.15 and 1.09 ± 0.32, respectively (Table 5.1). The change in the solid state of CUR from crystalline to amorphous showed significant improvement in solubility but did not prevent the precipitation as the time for precipitation were same with both forms. The solubility values of crystalline and amorphous CUR are in good agreement with the previous report. Almost 5800-fold improvement in CUR solubility in the case of SD with SOL compared to the solubility of crystalline CUR, while 801-fold and 225-fold with PVP K30 and poloxamer 407, respectively. Most importantly, SOL completely prevented the precipitation of CUR up to 24 h while PVP K30 (60 min) and Poloxamer 407 (30 min) presented slight improvement in time for precipitation compared to crystalline CUR. Due to greater improvement in solubility and against the precipitation in the presence of SBF, SOL and PVP K30 were short-listed to evaluate their potential for stabilizing CUR.

Table 5.1 Kinetic solubility parameters of CUR and SDs (mean ± S.D., n = 3)

Samples	Ratio	S_{max} (µg/mL)	$T_{precipitation}$ (min)	S_{24h} (µg/mL)	Fold Enhancement*
Crystalline CUR	-	0.72 ± 0.23	5	0.54 ± 0.15	-
Amorphous CUR	-	1.89 ± 0.59	5	1.09 ± 0.32	2.02
CS	1 : 3		-	3131.48 ± 800.87	5799.04
CP30	1 : 3	1232.84 ± 162.42	60	432.84 ± 25.42	801.56
CP407	1 : 3	121.37 ± 18.82	30	121.37 ± 18.82	224.76

*Calculated from S_{24h} of sample/ S_{24h} of crystalline Curcumin

SD with Soluplus (CS), PVP K30 (CP30) and Poloxamer 407 (CP407).

S_{max}: maximum solubility, $Te_{precipitation}$: time for precipitation and S_{24h}: solubility value at 24 h.

5.4.1.4 Chemical stability study

The poor aqueous stability specifically in SBF is another key issue contributed in poor oral BA of CUR. It undergoes hydrolysis upon the attack of OH^- ion to the carbonyl carbon in the keto-enol moiety. The previous report suggested the possibility of stabilization of CUR in SBF after encapsulation in micelles generated from the polymer [249]. To evaluate the potential of SOL and PVP K30 in protection against the hydrolysis, the stability study was conducted with CUR in blank buffers (pH 1.2, 6.8 and 7.4) and buffers are having 10% w/v SOL and 10% w/v PVP K30 for 24 h. CUR undergoes significant hydrolysis with 17%, 76% and 100% degradation in pH 1.2, 6.8 and 7.4, respectively which is close agreement with the previous study (Fig. 5.1B). PVP K30 did not improve the protection against the hydrolysis as 16%, 29% and 100% degradation in pH 1.2, 6.8 and 7.4, respectively (Fig. 5.1C). With SOL, <1.5% degradation was observed with all buffer systems which suggests a possibility of stabilization of CUR in SBF after encapsulation in micelles generated from SOL (Fig. 5.1D). The degradation kinetic of CUR was calculated based on second-order kinetics as mentioned in the literature. There was a significant improvement in the half-lives of CUR in absence and presence of SOL at pH 1.2 (4.88 to 99 days), pH 6.8 (0.32 to 49 days) and pH 7.4 (0.031 to 32.33 days) (Table 5.2). It could be attributed to effective micellar barrier effect of SOL. From superior solubilization and stabilization ability, SOL was finalized for the development of NCF.

Table 5.2 The rate constant and half-lives of CUR in blank buffers of pH 1.2, 6.8 and 7.4, buffers with 10% (w/v) PVP K30 and 10% (w/v) SOL (mean ± S.D., n = 3)

Medium	pH of the medium	Rate Constant (k, h^{-1})	Half-life ($t_{1/2}$, h)	Half-life ($t_{1/2}$, days)	Correlation Coefficient (R^2)
Blank Buffers	1.2	$8.5E^{-05}$	117.18	4.88	0.96
	6.8	0.00132	7.58	0.32	0.83
	7.4	0.01347	0.75	0.031	0.34
Buffers with 10% PVP K30	1.2	$7.4E^{-05}$	136	4.88	0.99
	6.8	0.00102	9.80	0.32	0.86
	7.4	0.00554	1.81	0.03	0.48

Buffers with 10% SOL	1.2	$4.2E^{-06}$	2376	99	0.59
	6.8	$8.5E^{-06}$	1176	49	0.70
	7.4	$1.3E^{-05}$	776	32.33	0.87

5.4.2 Formulation development and optimization of NCF

The complete amorphisation, encapsulation of CUR in SOL, maintenance of supersaturated condition could play a crucial role in the success of NCF. The method of preparation and drug to polymer ratio could affect the characteristics of NCF. Therefore the optimization was performed based on the solubility of CUR in pH 1.2, 6.8 and 7.4 buffers.

5.4.2.1 Method of preparation

To determine the best approach for the preparation at lab scale among SE and MM, the CUR loaded SD with the CUR to SOL ratio of 1:3 were prepared and evaluated based on the solubility of CUR in SBF. The SD prepared from SE technique (nearly 3 mg/mL) showed significant higher solubility ($P<0.0001$) of CUR compared to MM (nearly 0.9 mg/mL) in all buffers (Fig.5.1E). Incomplete transformation in the solid state from amorphous to crystalline could be a potential reason in low solubility of SD prepared from MM and SE. Interestingly, there was no significant difference in solubility of CUR between the different buffer systems which indicate the complete micellar solubilisation independent to the method of preparation. The minimum effect of hydrolysis on solubility could be explained because of effective micellar barrier effect of SOL as mentioned in section 5.4.1.4.

5.4.2.2 Concentration of polymer

The drug to carrier ratio could contribute for amorphisation and maintain supersaturated state, thus, dramatically improvement in the solubility. The optimum amount of carrier could also reduce the particle size of undissolved drug crystals to improve the saturation solubility. With SD made up of CUR and SOL, the saturated solubility of CUR was increased with the increment of a drug to carrier ratio, confirms the significant influence of the amount of carrier on the outcome of SD. The SD of CUR and SOL (1:10) displayed 11.13 mg/mL solubility of CUR in pH 1.2 buffer which is 20613-fold greater compared to crystalline CUR (Fig. 5.1F). The interference of hydrolysis in the solubility of various ratio was insignificant as SD showed almost 11 mg/mL solubility of CUR in all buffer system. We did not consider more than 10 parts of SOL with 1 part of CUR as the viscosity of the aqueous solution was significantly

increase due to a higher amount of SOL [401]. Therefore, SD of CUR and SOL (1:10) was finalized as NCF and to be optimum for further investigations.

5.4.3 Characterization of NCF

5.4.3.1 Loading ability and efficiency

The loading ability and efficiency of NCF were 9.15 ± 0.10 % (w/w) and 98.23 ± 1.62 % (w/w), respectively. The higher amount of loading efficiency designates minimal loss of CUR during the manufacturing process of NCF.

5.4.3.2 Comparison of Solubility of PM and NCF in simulated body fluids

To understand the mechanism of the exceptional property of NCF to solubilisation and stabilization of CUR, the solubility of PM and NCF were investigated in pH 1.2, 6.8 and 7.4 buffers. The SD form (NCF) (almost 11 mg/mL) showed significantly higher solubility (nearly 11-fold) compared to PM (0.9-1 mg/mL) in all buffer systems, but the solubility of CUR was significantly increased with PM compared to crude CUR (Fig. 5.1G). It could be due to partial conversion in the solid state from crystalline to amorphous and micellization property of SOL. SOL could reduce the particle size of undissolved CUR crystals and enhance the solubilisation. It might also keep CUR in the super-saturated state for long period of time. The detailed studies were conducted to uncover the mechanism of interaction between CUR and SOL in NCF.

5.4.3.3 Determination of interaction between SOL and CUR in NCF

Amorphisation, hydrogen bonding interaction between CUR and SOL and micellization property of NCF could be the potential mechanisms contributing to the unique features of NCF. DSC study was carried out to determine any change in solid state characteristics of CUR in NCF. Furthermore, to confirm any conversion of crystalline to the amorphous state of CUR, XRD and SEM studies were conducted. To understand the possibility of hydrogen bond interaction between CUR and SOL, FTIR and ^{1}H NMR studies were performed. Additionally, the micellization property of NCF was evaluated by determining the characteristics of micelles such as particle size, PDI and zeta potential. Moreover, the stability study of NCF in micellar form was assessed for its suitability for the further development.

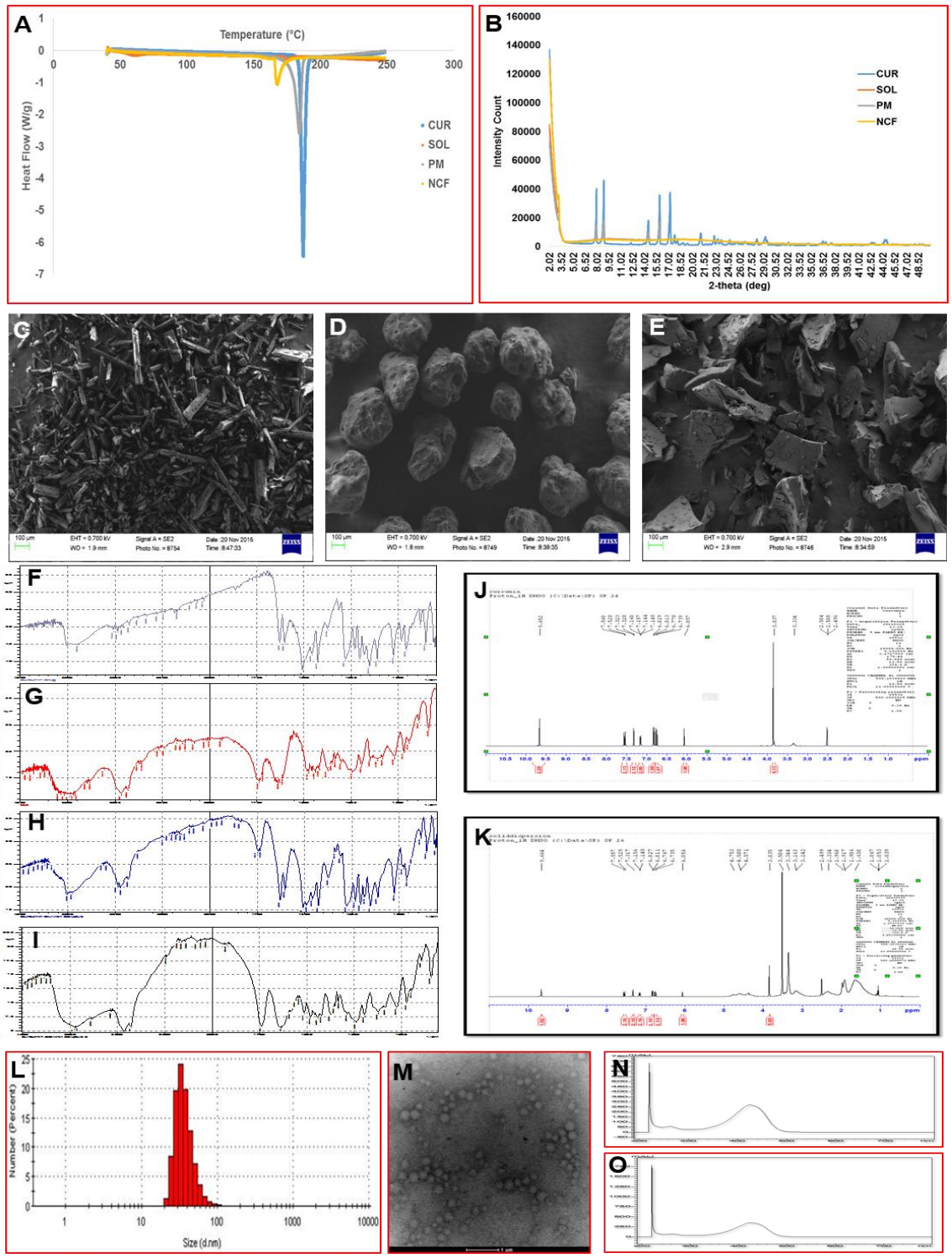

Figure 5.2 *In-vitro* characterization of NCF. DSC thermographs (A) and X-ray diffractograms (B) of CUR, SOL, PM and NCF, SEM photomicrographs of CUR (C), SOL (D) and NCF (E), FTIR spectra of CUR (F), SOL (G), PM (H) and NCF (I), ^{1}H NMR spectra of CUR (J) and NCF (K), Mean particle size of micellar solution of NCF measured by particle size analyzer (L), Transmission electron micrograph images of micellar solution of NCF, (M) UV absorbance spectra of crude CUR (N) and NCF (O).

The solid-state changes in NCF were determined with DSC study by comparing the melting profile of crude CUR, SOL, PM of CUR and SOL (1:10) and NCF. Crystalline CUR showed

a characteristic endothermic peak nearly at 183°C. SOL did not display any thermal event while, PM and SD exhibited a low-intensity peak at 180°C and 167°C, respectively (Fig. 5.2A). The endothermic peak of NCF was not close to the melting point of CUR while PM exhibited near to it, which confirms the complete and incomplete solid state change in NCF and PM, respectively. The shifting of the endothermic peaks could be due to the solvent effect of the SOL [433].

X-ray diffractograms of crude CUR, SOL, PM, and NCF are shown in Fig. 5.2B. As expected, the sharp characteristic peaks were observed at 7.9°, 8.8°, 14.2°, 17.2° and 17.8° 2θ with crude CUR which confirms its crystalline structure before the preparation of NCF. SOL did not show any characteristic peak. The PM of CUR and SOL showed weaker signals at 7.9°, 8.8°, 14.2°, 17.2° and disappearance of other peaks compared to the crude CUR which indicates a partial presence of crystal materials and incomplete amorphization. In contrast, the characteristic peaks of CUR completely disappeared in NCF. The XRD results confirm complete transformation of crystalline to amorphous nature of CUR in NCF which is in good agreement with the DSC results.

The surface morphology of crude CUR, SOL and NCF were studied using SEM analysis. Needle-shaped crystalline forms of drug agglomerates with ordered shape and size were observed in SEM micrograph of crude CUR (Fig. 5.2C), while SOL showed irregularly shaped particles (Fig. 5.2D). However, NCF (Fig. 5.2E) exhibited rough disordered and intact structures without any traces of crystalline CUR, which could aid in solubilization upon the contact with aqueous fluid [433].

The amorphous nature of CUR in NCF was determined from DSC, XRD, and SEM but the exceptional performance of improving solubility and stability could not just relate to amorphization and maintenance of supersaturation state. The hydrogen bonding interaction could be possible between carbonyl and hydroxyl groups present in CUR and SOL structure. It could facilitate the solubilization in aqueous media. Moreover, it could provide the physical stability of NCF by reducing molecular mobility thus inhibiting the drug crystallization [434]. The possibility of hydrogen bond interaction was studied by FT-IR and ^{1}H NMR analysis [331]. The IR spectra of CUR showed characteristic signals nearly 3400, 1627, 1282, 1602 and 1153 of groups hydroxyl (-OH), carbonyl (C=C), enol (C-O), aromatic (C=C) and phenyl mixed with methoxy (C-O-C) groups, respectively (Fig. 5.2F). Two typical peaks were observed at 1735, 2860 and 3469 for carbonyl, aliphatic C–H stretching and hydroxyl groups in case of SOL,

respectively (Fig. 5.2G). No peak shifts/ disappearance of characteristic peaks of CUR and SOL was observed in the spectra of PM (Fig. 5.2H). However, in NCF (Fig. 5.2I), broadening of the peaks at 1286, 1627 and 3510 represent the involvement of carbonyl and hydroxyl in the hydrogen bonding interaction between the SOL and CUR.

The slight shifting of signals of CUR in NCF was observed in the result of ^{1}H NMR spectroscopy compared to crude CUR. It could be a result of a weak interaction between CUR and SOL which might impact their electron density and hydrogen bond interaction [331]. Specifically, there was a dramatic shifting of the chemical signal of a hydroxyl group in the structure of CUR was observed which justify its involvement in the hydrogen-bond formation (Fig. 5.2J and 5.2K, Table S5). The carbonyl group can accept the H atom from hydroxyl group to form the hydrogen bond. CUR and SOL have at least four each hydroxyl and carbonyl groups donate and accept H atoms, respectively, therefore, at least eight hydro-bonding could be possible between them. Therefore, the result of ^{1}H NMR confirms the hydrogen bonding interaction in accordance with the result of FT-IR.

5.4.4 Characterization of self-micellizing properties of NCF

SOL forms the micelles by accommodating polyethylene glycol moiety at wall and vinyl acetate and vinyl caprolactam side chains inside the micelles above its critical micelle concentration (CMC) of 0.0007% w/v at 37°C [332]. Hence, the self-micellizing properties of NCF were investigated. Particle size, PDI and zeta potential are the vital parameters which could influence the performance of micelles. NCF generates the micelles of containing particles size 63.05 ± 5.24 nm (Fig. 5.2L), PDI 0.09 ± 0.04 and zeta potential -4.65 ± 0.92 mV. The morphology characteristics of a freshly prepared micellar solution were examined with TEM analysis. The TEM image (Fig. 5.2M) confirms the spherical shape of micelles with relatively unified size distribution which is consistent with the measurement by zeta sizer. As below 100 nm, particle size is ideal for cellular and nuclear uptake, micelles generated from NCF with small size, narrow size distribution, and higher surface charge, could dramatically increase the intestinal permeability, tissue distribution and cell accumulation of CUR [335]. In addition, no turbidity and precipitation were observed with or without 20-fold dilution with SBF which directs good stability of micelles in the dispersion.

No change in the photo-physical property of CUR was observed after encapsulated in micelles as a distant high absorbance peak was seen at 423 nm with the micellar solution of NCF (Fig. 5.2N) and a methanolic solution of CUR (Fig. 5.2O). It also suggests the successful entrapment

of CUR in micelles [428]. The encapsulation of CUR in micelles could also protect its degradation against the hydrolysis and in the presence of light [331]. Thus, stability study of crude CUR and micellar solution of NCF were conducted. CUR in micellar formulation was remained stable against the hydrolysis, oxidation and photolysis by displaying less than 1% degradation observed in % drug content with no precipitation, whereas crude CUR showed significant degradation due to acid hydrolysis (24.52 ± 6.61 %), base hydrolysis (100 %), oxidation (6.36 ± 2.98 %) and photolysis (64.63 ± 9.59) compared to crude CUR. Further, it protects CUR (<1% degradation) in SGF (pH 1.2) and SIF (6.8 pH) compared to the poor stability of crude CUR mentioned in 5.4.1.4. Moreover, CUR remained stable in micelles form in various buffer systems covering the broad range of pH 2-8 (Fig. 5.3A) which is suitable for oral administration. Thus, with amorphization, hydrogen bonding interaction, and micellization, NCF has a potential to generate superior results after oral administration.

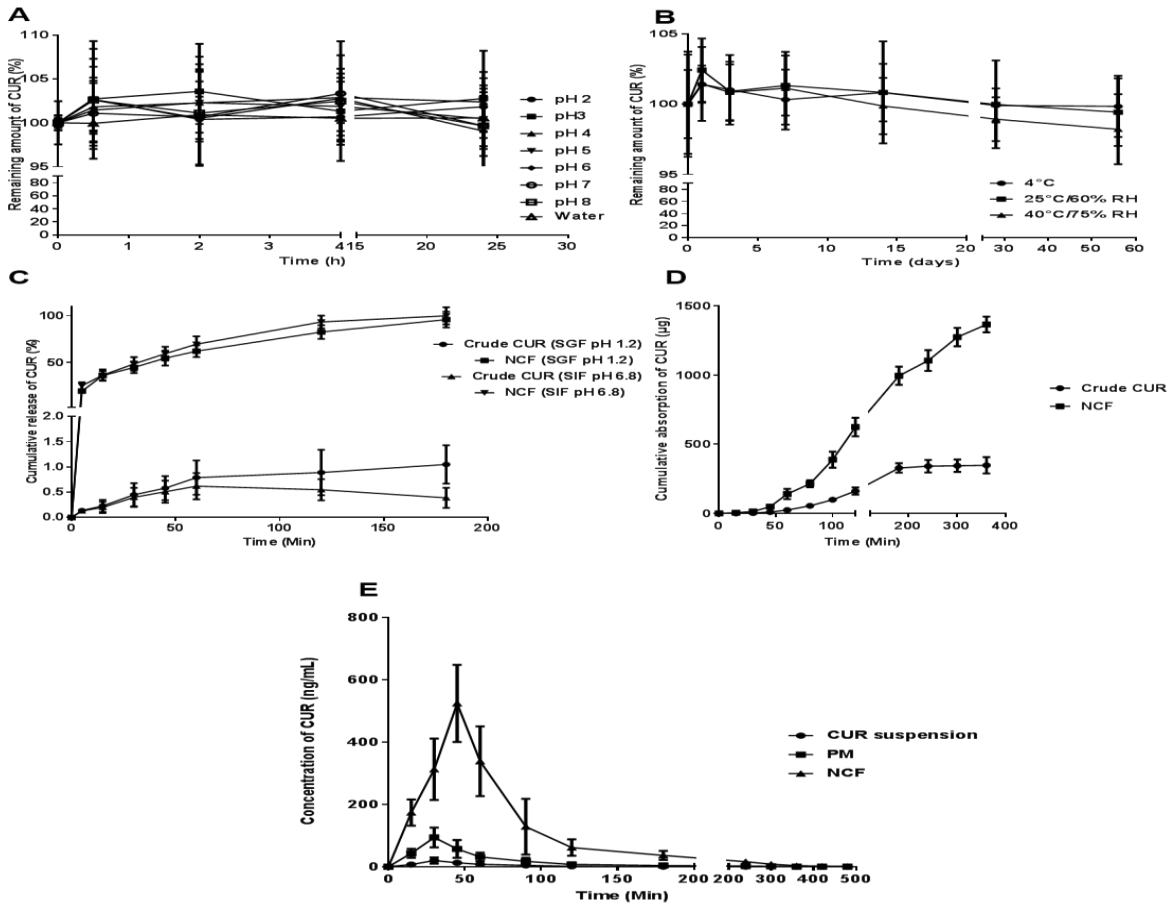

Figure 5.3 Stability profile of NCF at pH dependent stability study (A) and thermal stability as per ICH guideline (B) (mean ± S.D., n = 3), dissolution profiles of crude CUR and NCF in SGF (1.2 pH) and SIF (6.8 pH) (mean ± S.D., n = 3) (C), cumulative absorption of crude CUR and NCF during transportation across everted sacs of rat small intestine (mean ± S.D., n = 3) (D), CUR plasma concentrations upon oral administration of CUR suspension (150 µg/g), PM (47 µg/g) and NCF (47 µg/g) (mean ± S.D., n = 6) (E).

5.4.5 Stability study of NCF as per ICH guideline

The physical stability of NCF was investigated as per the previous study for eight weeks [342]. CUR was found stable in NCF over the period of stability study as no significant degradation (<2% degradation) was witnessed at all the conditions (Fig. 5.3B). Also, no significant difference in solubility of NCF was seen at every time intervals which confirms the lack of recrystallization of CUR within a period of 8 weeks. The strong interaction between SOL and CUR as observed FTIR and ^{1}HNMR study, facilities its effective physical stability, thus increase the shelf life of the dispersion. It could also provide the flexibility to develop a variety of dosage forms and in manufacturing.

5.4.6 In-vitro release test

Fig. 5.3C displays the dissolution profile of crude CUR and NCF in SGF (pH 1.2) and SIF (pH 6.8). The pH dependent solubility profile of CUR was reported previously, so the equilibrium solubility of CUR in SGF and SIF were conducted to evaluate the effect of pH on drug release [330]. The solubility in SIF (26.24 µg/mL) was significantly higher compared to SGF (0.72 µg/mL) which suggests the possibility of the influence of pH on CUR release. The release of crude CUR in SGF and SIF were <1% within 2 h. In SGF, the release kinetic of CUR follows Higuchi-matrix model, whereas, first order kinetic model in SIF (Table 5.3). No significant difference between the dissolution profile of CUR in SGF and SIF was observed. In addition, the determined f_2 value was 95 which indicates no significant influence of pH on CUR release. It could be due to the higher rate of degradation in SIF reported in section 5.4.1.4. Poor aqueous solubility and stability could play a critical role in the poor dissolution profile of CUR. In the case of NCF, nearly 90% and 100% CUR cumulative release were witnessed within 3 h in SGF and SIF, respectively without any significant precipitation. The significant increase in CUR release from NCF in SIF was observed at 2h and 3h compared to SGF. Moreover, the f_2 value of 37 confirms the dissimilarity in dissolution profile as a function of pH. Furthermore, it follows Higuchi-matrix model in both SGF and SIF dissolution medium. Overall, by enhancing solubility and providing protection against the hydrolysis due to amorphization and micellization, NCF showed significant improvement in the dissolution profile of CUR.

Table 5.3 Results of release kinetics of crude CUR and NCF in SGF (pH 1.2) and SIF (pH 6.8) according to various kinetic models including First order, Zero order, Hixson–Crowell, Higuchi-matrix, and Korsmeyer–Peppas

Formulation	Medium	First order	Zero order	Hixson–Crowell	Higuchi-matrix	Korsmeyer–Peppas
CUR Suspension	SGF	0.8497	0.8497	0.8427	0.9567	0.8853
	SIF	0.9761	0.9758	0.967	0.971	0.889
NCF	SGF	0.9825	0.8469	0.9528	0.992	0.9637
	SIF	0.9853	0.8701	0.9845	0.9952	0.9459

5.4.7 Improvement in permeability

The profile of cumulative absorption of CUR suspension and NCF are shown in Fig. 5.3D. Everted intestine sac technique is a well-recognised technique to understand the ex vivo drug absorption [435]. NCF presented the significantly higher amount of CUR absorption after 60 min. (P-0.0097 at 60 min, p-0.0001 at 80 min and $p<0.0001$ after 80 min). The poor stability of CUR in SBF, P-glycoprotein (Pgp)-mediated efflux, and extensive metabolism are determined as major factors which hampered its permeability. The protection of CUR against the degradation in SBF was reported in section 5.4.1.4. Also, the significant inhibitory effect of SOL on Pgp efflux was reported previously [394]. Moreover, the size of micelles generated from NCF is in nano range which could facilitate the transportation of CUR across the intestine membrane through paracellular or transcellular routes [335]. Therefore, enhancement in intestinal permeability of CUR with NCF could be due to stabilization of CUR against the hydrolysis, inhibition of P-gp efflux and/or nano-size micellization.

5.4.8 Pharmacokinetic study

The main purpose of development of NCF was to enhance the oral BA of CUR. The pharmacokinetic study was performed using CUR at the 47 mg/kg for PM and NCF, and 150 mg/kg for CUR suspension by oral administration. The poor oral BA was the reason for using a high dose of CUR suspension [330]. The mean CUR concentration achieved in plasma as a function of time and various pharmacokinetic parameters are mentioned in Fig. 5.3E and Table 5.4. In C_{max} value, 4.75 and 26.54-fold improvement observed with PM and NCF compared to CUR suspension which were statistically significant. The maximum concentration (T_{max}) was not statistically different between the groups though NCF showed a 1.5-fold increase compared

to PM and CUR suspension. The slower release from the micelles due to the strong interaction between the CUR and SOL could be a reason for increasing T_{max} value. PM and NCF revealed significantly longer half-life by 2.5 and 4-fold compared to CUR suspension, respectively. The protection against the hydrolysis due to micellization might be responsible for it. The significant difference between the half-life of NCF and PM could be a result of incomplete encapsulation of CUR in micelles generated from PM. There are 5.43 and 36.79-fold enhancement in AUC of PM and NCF respectively compared to CUR suspension. Overall, PM and NCF are 17 and 117-fold more bioavailable compared to CUS suspension. Because of amorphization, hydrogen bonding interaction and micellization, 100% and 11% of CUR dose used in the pharmacokinetic study for NCF and PM would be present in a dissolved form compared to CUR suspension (0.007%). Therefore, the exceptional results in the pharmacokinetic study could be due to significant enhancement of aqueous solubility, as well as stability, dissolution, and permeability. Similar results were reported previously with TPGS 1000 polymer [330]. Thus, NCF showed a great potential to be developed as a suitable delivery system for conducting *in-vivo* safety and efficacy study in animals before proceeding for the clinical study.

Table 5.4 Pharmacokinetic parameters of CUR suspension, PM and NCF obtained by Phoenix WinNonlin software Unpaired Student's t-test for two groups, (mean ± S.D., n = 6)

Parameters	CUR suspension (150 mg/kg)	PM (47 mg/kg)	NCF (47 mg/kg)	P Value[a]	P Value[b]	P Value[c]
C_{max} (ng/mL)	19.73 ± 9.90	93.62 ± 31.48	523.64 ± 123.53	0.0003	<0.0001	<0.0001
T_{max} (min)	30 ± 15	30 ± 15	45 ± 15	NS	NS	NS
$t_{1/2}$(min)	24.08 ± 8.45	60.27 ± 16.73	96.01 ± 18.57	0.0008	<0.0001	<0.0001
AUC_{0-t} (ng·min/mL)	905.4 ± 412.63	4837.65 ± 1051.37	33310.05 ± 6025.34	<0.0001	<0.0001	<0.0001
F_{0-t} (%)	100	1705.24 ± 812.89	11741.62 ± 4660.30	<0.0001	<0.0001	<0.0001

NS: Non-significant

a: Comparison between CUR suspension and PM

b: Comparison between CUR suspension and NCF

c: Comparison between PM and NCF

5.4.9 Behavioral tests with AD mice model

Cognitive decline is considered as the most predominant and striking sign of AD as a result of neuronal and synapses loss particularly in the hippocampus and other areas of the brain [387]. Well recognized AD mice models including APPSwe/PS1deE9 showed deficits as observed in human AD patients. They showed impairments in learning and memory tasks in various behavioral tests including open field, NORT, Y-maze and MWM tests. The selected age for APPSwe/PS1deE9 mice were 14-17 months for the experiment as the fully developed AD-like pathology, and behavioral deficits were observed in the previous report [436]. Numerous pharmacological agents reversed memory deficits by modulating various pathway contributing to the pathology of AD such as the potential therapeutic candidates such as Edaravone and P75-ECD-FC protein rescues the behavioural deficits occurred in APPSwe/PS1deE9 mice by reducing Aβ deposition, oxidative stress, neuronal loss, synaptic dysfunction, Tau hyperphosphorylation and neuroinflammation [69, 389]. Thus, reversal of cognitive changes used as a marker for the efficacy against AD and the well accepted behavioral tests such as open field, NORT, Y-maze and MWM tests were carried out to assess the efficacy of NCF. The behavioural tests were performed at 17 months of age of APPSwe/PS1deE9 (Tg) and C57BL/6 mice (WT) after 3 months of the treatment except the one group of APPSwe/PS1deE9 (14 mo Tg Ctrl) which was undertaken at 14 months of age before initiating the experiment to use as a basal control, respectively. The DNP-treated group was considered as a positive control for the behavior test as Aricept (donepezil hydrochloride) is approved Food and Drug Administration for the treatment of dementia [437]. As daily gavage or injection would cause stress of the animals and could affect the outcome of in behavior tests, NCF was supplied with drinking water for safety and efficacy study. The key requirement of supplying drug with drinking water is the adequate solubility and stability. Thus, as a control for safety and efficacy study, PM was used because of superior aqueous solubility and stability compare to crude CUR.

Low pH water is used in our animal house facility mainly due to prevent the spread of bacterial disease among laboratory animals through drinking water. Hence, stability was conducted in water supplied to the animals to determine the frequency of changing the water bottles. No

significant difference in the CUR level was observed with NCF and CUR control up to 1 week (Fig. S1). Therefore, the frequency of changing water bottle was kept once in a week for both groups.

To decide the concentration of water to supply to the animals as per the dose of CUR, the daily consumption of water was determined for each cage before initiating the experiment. The results of water consumptions for APPSwe/PS1deE9 mice is shown in Table 5.5. The data were further used to determine the impact of adding drug on routine water consumption of mice as a part of toxicity study.

5.4.9.1 Open field test

The open field test is used to measure the locomotion, anxiety, and exploration. Total traveling distance, a frequency of rearing, grooming, urination, defecation, and duration of time spent in central zone are used as measures of the locomotion, anxiety, and exploration [69, 389]. The results showed that the locomotion activity as reflected by the travel distance and anxiety levels in aged APPSwe/PS1deE9 mice or the same aged mice treated with the blank control was significantly altered, compared with WT control or younger counterparts of basal controls. NCF treated APPSwe/PS1deE9 mice showed significantly longer travel distance (Fig. 5.4A), a higher number of rearing (Fig. 5.4B) and % time spent in the central zone (Fig. 5.4C) compared to without treatment groups. No significant difference in a number of grooming (Fig. 5.4D), urination (Fig. 5.4E) and defecation (Fig. 5.4F) were observed. DNP-treated mice also displayed significant improvement in a number of rearing but the insignificant difference in distance traveled and time spent in the central zone. There was no significant difference between the performances of NCF treated APPSwe/PS1deE9 mice compared to WT mice and dramatic improvement was witnessed compared to basal control group, which indicating NCF treatment could reverse the cognitive deficits to the much lower ages for APPSwe/PS1deE9 mice and better than the currently available treatment option.

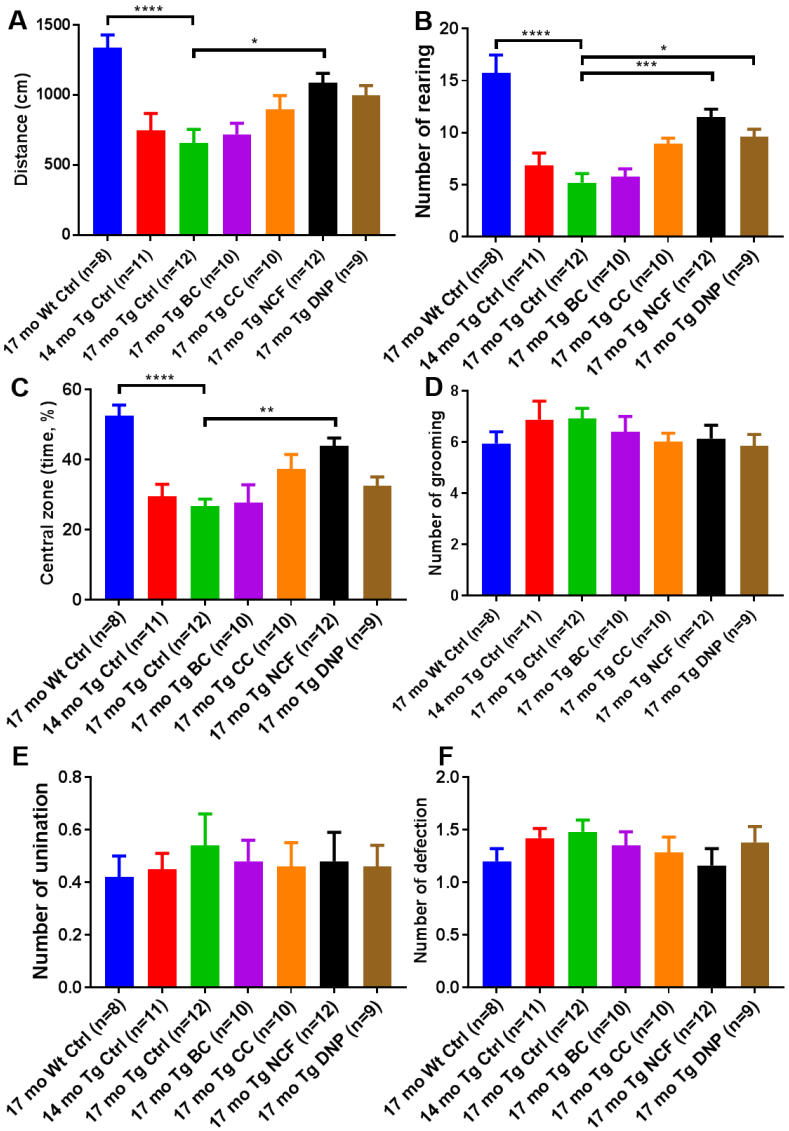

Figure 5.4 NCF improves the behavioral performances of APPSwe/PS1deE9 mice in open filed test. Total distance traveled (A), number of rearing (B), Time spent in central zone (C), number of grooming (D), number of urination (E) and number of defecation (F). *P < 0.05, **P < 0.01, ***P < 0.001, and ****P < 0.0001 (One-way ANOVA, Tukey's test) (mean ± SEM).

5.4.9.2 NORT

The tendency of exploring new objects in NORT test reflects the use of learning and recognition memory processes. Generally, a normal mouse could spend longer time to investigate and explore the novel object compared to the object has already explored [411]. It assesses the short-term memory of remembering the objects. On day 2 of the test, APPSwe/PS1deE9 mice of all groups did not show a significant difference in recognition index which indicates the similar duration of time spent near to each object (Fig. 5.5A). However, NCF treated APPSwe/PS1deE9 revealed the tendency to explore novel object for a longer

duration compared to the familiar object on day 3 (Fig. 5.5B). The significant difference in discrimination index was witnessed in NCF treated group compared to non-treated and basal control groups in both mice models (Fig. 5.5C). The results indicate that NCF treated mice were able to discriminate between the novel and the familiar object. The DNP-treated mice also exhibited significant higher discrimination index compared to non-treated mice group but did not match the performance of NCF. Moreover, there was no significant difference in discrimination Index detected between NCF treated APPSwe/PS1deE9 mice compared to WT mice. It is worth to note that the NCF groups in APPSwe/PS1deE9 at 17 months old performed much better than their younger base line controls (14 months for APPSwe/PS1deE9), suggesting the novel curcumin formulation can reverse the cognitive deficits to the levels of much younger ages and superior to the available treatment preferences.

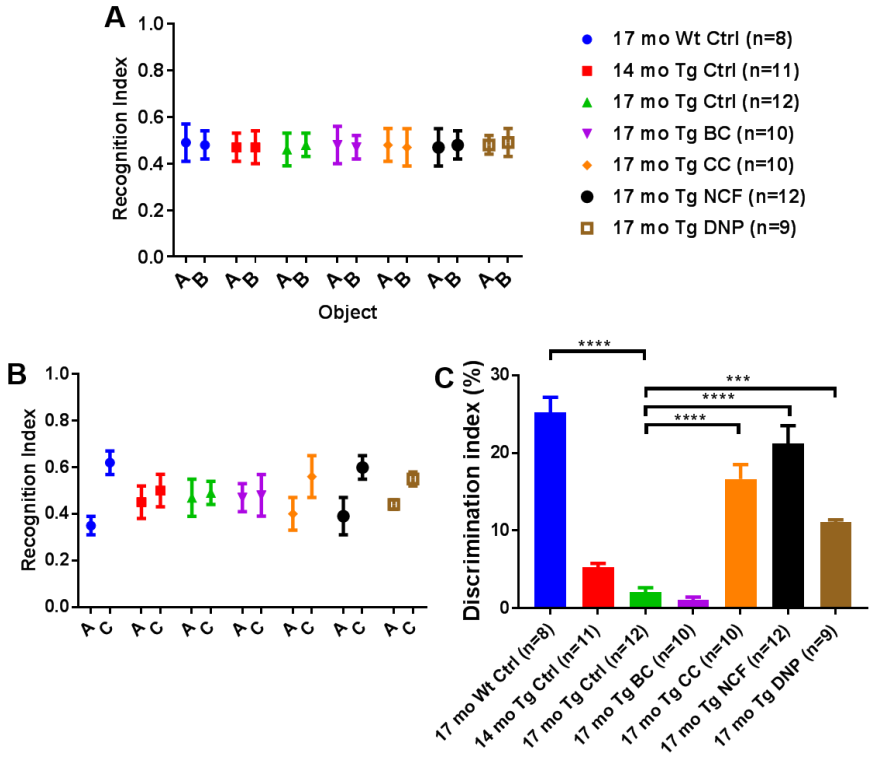

Figure 5.5 NCF improves the behavioral performances of APPSwe/PS1deE9 mice in NORT. The recognition index was calculated as the ratio of time spent exploring to the one object over the total time spent for exploring both objects. The discrimination index was based on the equation [DI = (T_N – T_F)/ (T_N + T_F)] where time spent to explore the novel object (T_N) and familiar object (T_F) [438]. Recognition index in the phase of familiarization (A) and the test phase (B), discrimination index in the test phase (C). ***P < 0.001 and ****P < 0.0001 (one-way ANOVA, Tukey's test) (mean ± SEM).

5.4.9.3 Y-maze test

Y-maze test is based on the inherent preference of mice to explore the new environment [439]. In APPSwe/PS1deE9 mice model, aged sham and SOL blank controls all performed poorer than their three months younger base line controls and WT mice control, being consistent with aging-associated cognitive deficits in these models. In spontaneous alternation test, the high percentage of alteration and a total number of entries to each arm represent the sustained cognition as they remember the arm which they have already explored. NCF treated APPSwe/PS1deE9 mice showed significant improvement in cognitive function by displaying grater % of alteration (Fig. 5.6a) and a higher number of entries to each arm (Fig. 5.6B) compared to the non-treated disease mice models. Moreover, in novel arm exploration tests, mice with a conserved cognitive function would like to remember the previously blocked arm and to explore the novel arm. With NCF treated both mice models, significantly greater % novel arm entry (Fig.5.6C), % time spent in the novel arm (Fig. 5.6D) and a number of entries to the novel arm (Fig. 5.6E) were observed compared to non-treated groups of mice model. The performance of DNP-treated mice was significantly better than the non-treated mice group but consistently, the NCF groups of APPSwe/PS1deE9 mice executed better than DNP treatment, their three months old younger controls, even reaching the level of WT mice. These results suggest that the novel formulation can reverse the cognitive decline of the AD mice.

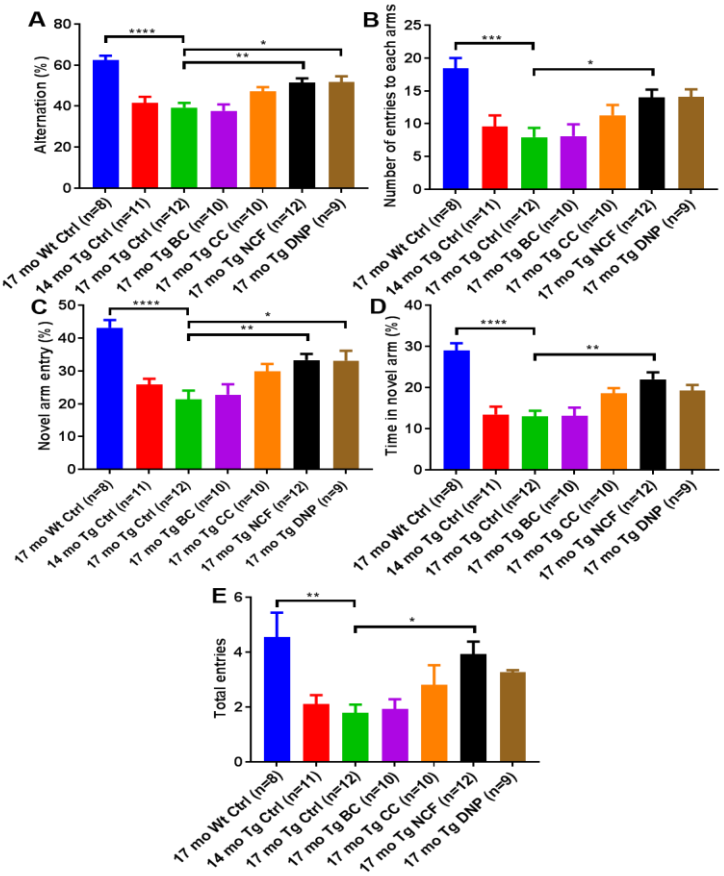

Figure 5.6 NCF improves the behavioral performances of APPSwe/PS1deE9 mice in Y-maze test. % Alternation (A) and numbers of entries in each arm (B) and in the spontaneous alternation test, % of total entry in novel arm compared to other arms (C), time (%) (D) and total number of entry to the novel arm (E) in the novel arm test. *P < 0.05, **P < 0.01, ***P < 0.001, and ****P < 0.0001 (one-way ANOVA, Tukey's test) (mean ± SEM).

5.4.9.4 MWM test

The MWM test has proven as a robust test to determine the hippocampal spatial learning and memory deficits of AD mice models based on their tendency to escape from the water [440]. During the training phase, clues have been provided to indicate the location of the hidden platform. All mice were trained for 4 consecutive days before the probe test. The learning ability was determined from the escape latency time. No significant difference in path length (Fig. 5.7A) and swimming speed (Fig. 5.7B) were also observed compared to non-treated groups, which indicating no interference of swimming ability or the visual ability of mice could be observed in MWM test. Comparing with WT mice at 17 months old, all control AD mice or AD mice treated with the control reagents showed cognitive decline as reflected by increased escaping latency, reduced time in platform quadrant and reduced annulus crossings. APPSwe/PS1deE9 mice treated with NCF showed a significant reduction in the escape latency

time (Fig. 5.7C). The capacity to retrieve the learned tasks was assessed using a probe trial. In probe trial, NCF treated APPSwe/PS1deE9 mice showed a greater number of annulus crossing (Fig. 5.7D), and longer time spent in the quadrant having platform compared to non-treated groups indicate the significant improvement in spatial learning and memory in NCF treated AD mice models (Fig. 5.7E). The results of DNP-treated mice were also superior to non-tarted mice group but did not reach to the NCF performance. APPSwe/PS1deE9 mice at 17 months old treated with the novel curcumin formula performed statistically better on all cognitive parameters in MWM test than their three months younger baseline controls and some parameters even showed no difference from those of WT mice. These results indicate that NCF not only prevents the deterioration of cognitive functions of the aged APPSwe/PS1deE9 mice during aging but also reverses the cognitive functions to their much younger age which is also better than the currently available approved options.

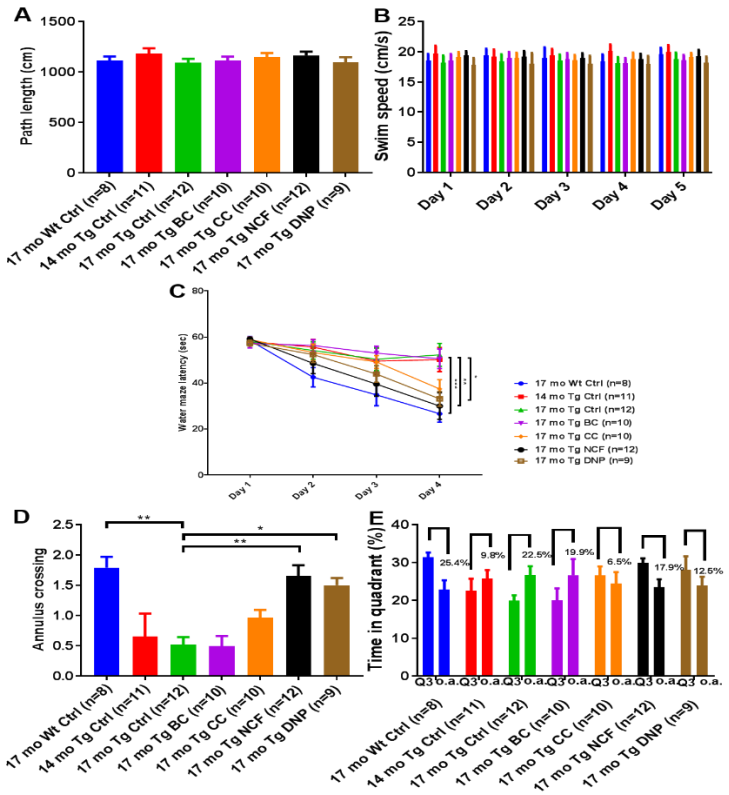

Figure 5.7 NCF improves the behavioral performances of APPSwe/PS1deE9 mice in MWM test. Path length (cm) to the platform on the first day's trial were analysed (A), swim speed (cm/s) calculated by the equation velocity = distance/time during platform trials and probe test (B), escape latency (s) during platform trials and distance travelled on the each day of training (C), Number of crossings over the annulus of the platform in probe trial (D), Comparison of time spent in target zone (Q3) where platform was located compared to average of all other zones (o.a.) (E). *P < 0.05, **P < 0.01, and ***P < 0.001 (two-way or one-way ANOVA, Tukey's test) (mean ± SEM).

The results of open-field, NORT, Y-maze, and MWM test revealed the potential of NCF against the behavioral deficits of APPSwe/PS1deE9 mice. The control group of CUR showed better performance in all behavior tests compared to non-treated groups as 17-fold improvement in oral BA was observed with it. There was no significant difference seen between the basal groups and non-treated groups in all behavior tests. It could be because of the old age of mice at which learning and memory deficits have been already developed. The results of NCF treated APPSwe/PS1deE9 mice are almost similar to those of C57BL/6 controls, suggesting a reversal of the AD-like behavioral deficit to the normal level.

The improvement in behavioural deficit of APPSwe/PS1deE9 mice by CUR is linked as a result of targeting key pathways of the AD pathogenesis such as reducing $A\beta_{40}$ and $A\beta_{42}$ in brain and serum, aggregation of Aβ, microgliosis and astrocytosis, insulin-degrading enzymes, neprilysin, presenilin-2 and inducing neurogenesis [71, 441, 442]. The encouraging results of NCF on the reversal of behavioral deficits of APPSwe/PS1deE9 mice revealed its huge potential against the AD by targeting multiple pathologies. However, a mechanism based further research is necessary to uncover the number of pathologies targeted by NCF to reverse the AD-like behavioral deficit.

5.4.10 Assessment of long-term repeated dose toxicity

The present investigation was carried out to determine the potential toxicity of NCF after long-term exposure via oral administration to the mice used for the efficacy study. The aim of the study was to obtain the information on the safety of SOL-based NCF and to provide the guidance for its future use as a product of CUR as CUR has been proved as a therapeutic agent for the variety of diseases including cancer, neurological, and cardiovascular [252].

There was no significant difference in body weight, water and food consumption witnessed in NCF treated mice compared to other control groups during the experiment (Table 5.5). The increase in water and decrease in food intake in APPSwe/PS1deE9 mice treated with the blank formulation and NCF were observed during the first week of the treatment. It could be because of liking the taste of water containing SOL and the decrease in food intake could be due to increase water intake. In addition, all treatment groups of mice did not show any apparent toxicity related to the treatment during the period of 3 months.

Table 5.5 Measurement of food and water consumption and body weight of APPSwe/PS1deE9 mice (mean ± S.D.)

Parameter	Time	17 mo Tg Ctrl	17 mo Tg BC	17 mo Tg NCF
Food intake (g/day/10 g body weight)	Before addition (14 months)*	1.34 ± 0.19	1.36 ± 0.26	1.37 ± 0.32
	After addition (14 months)+	-	1.33 ± 0.22	1.35 ± 0.33
	At 17 months	1.22 ± 0.31	1.24 ± 0.22	1.23 ± 0.33
Water intake (g/day/10 g body weight)	Before addition (14 months)*	1.42 ± 0.42	1.41 ± 0.32	1.41 ± 0.39
	After addition (14 months)+	-	1.48 ± 0.24	1.50 ± 0.38
	At 17 months	1.25 ± 0.20	1.27 ± 0.28	1.28 ± 0.36
Body weight (g)	Before addition (14 months)*	33.13 ± 3.24	33.9 ± 4.82	31.52 ± 4.61
	After addition (14 months)+	-	34.6 ± 3.45	33.25 ± 3.97
	At 17 months	34.15 ± 3.13	34.24 ± 3.17	31.92 ± 3.17

There were increase and decrease in the number of hematological parameters witnessed with the various treatment groups NCF compared to non-treatment groups, but they were not statistically significant (Table 5.6). Moreover, no abnormities were observed in spleen from

organ weight and histology studies (Fig. 5.8) and other tissues which confirm the non-toxicity of the treatment of NCF on hematological parameters.

Table 5.6 Haematological and Coagulation parameters of APPSwe/PS1deE9 mice after various treatment of 3 months (mean ± S.D., n = 5)

Parameters	17 mo Tg Ctrl	17 mo Tg BC	17 mo Tg NCF
Haematological parameters			
RBC ($x10^{12}$/L)	9.52 ± 0.39	9.38 ± 0.51	9.58 ± 0.28
WBC ($x10^{9}$/L)	7.17 ± 3.28	7.56 ± 3.94	7.04 ± 3.18
HGB (g/dL)	13.64 ± 0.45	13.95 ± 0.61	13.91 ± 0.58
HCT (%)	48.92 ± 1.43	47.67 ± 1.92	48.58 ± 1.18
MCV (fL)	49.81 ± 1.36	48.53 ± 1.89	49.58 ± 1.23
MCH (pg)	14.68 ± 0.82	15.28 ± 0.61	15.32 ± 0.66
MCHC (g/dL)	29.53 ± 1.16	28.95 ± 1.99	30.04 ± 2.12
PLT ($x10^{9}$/L)	496.81 ± 282.34	521.94 ± 196.05	492.13 ± 254.24
MPV (fL)	6.95 ± 0.14	6.57 ± 0.27	6.99 ± 0.11
PCT (%)	0.23 ± 0.16	0.19 ± 0.11	0.25 ± 0.18
PDW (fL)	8.3 ± 1.62	8.29 ± 1.72	8.78 ± 1.49
Neutrophils (%)	14.35 ± 4.53	12.24 ± 5.25	14.94 ± 3.57
Lympocytes (%)	81.82 ± 5.74	77.56 ± 5.23	78.24 ± 3.98
Monocytes (%)	4.61 ± 2.16	5.25 ± 2.49	4.98 ± 1.04
Eosinophils (%)	1.86 ± 1.65	1.52 ± 1.16	1.87 ± 0.93
Basophils (%)	0.04 ± 0.03	0.05 ± 0.02	0.05 ± 0.03
Coagulation parameters			
PT (s)	10.12 ± 0.62	10.25 ± 1.12	27.53 ± 3.14
APTT (s)	26.67 ± 8.97	28.45 ± 8.12	52.95 ± 12.08

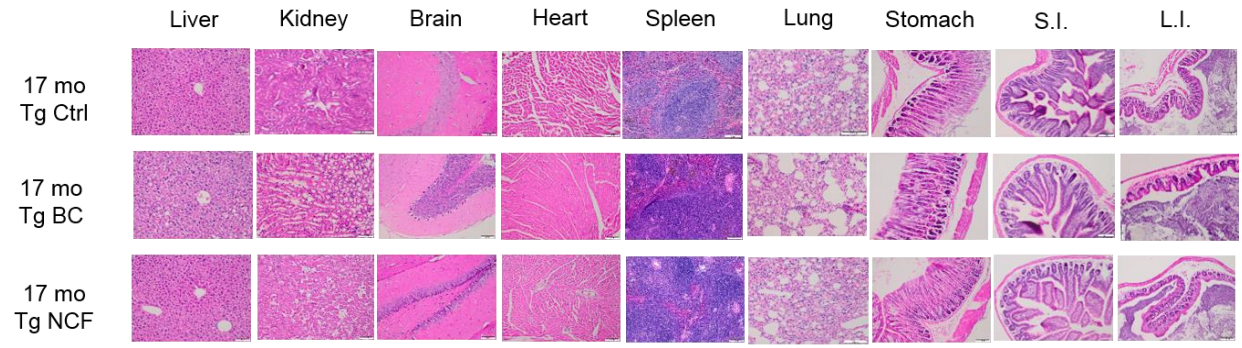

Figure 5.8 Qualitative histopathological evaluation and micrographs of tissues of APPSwe/PS1deE9 mice

The significant alteration in the value of blood coagulation parameters such as PT and APTT in NCF treated groups were detected (Table 5.6). The reason could be the anticoagulant properties of CUR reported previously [443]. Also, no significant difference in coagulation parameters was seen between the non-treated and blank formulation groups.

The analysis of serum biochemistry was performed to assess the impact of the treatment of NCF compared to non-treated and blank formulation on the normal function of liver, kidneys, heart, liver and digestive system. The results revealed no significant alteration in serum biochemistry of any of the treatment groups (Table 5.7). Additionally, the study of organ weight and histology studies of liver, kidney, stomach, brain, heart, liver, S.I and L.I of all treatment groups showed the absence of any gross pathological lesion (Table 5.8).

Table 5.7 Biochemical parameters of APPSwe/PS1deE9 mice after various treatment of 3 months (mean ± S.D., n = 5)

Parameters	17 mo Tg Ctrl	17 mo Tg BC	17 mo Tg NCF
Sodium (mmol/L)	147.66 ± 2.94	143.06 ± 2.98	148.52 ± 3.04
Bicarbonate (mmol/L)	27.16 ± 5.79	27.9 ± 5.02	28.13 ± 4.98
Anion Gap (mmol/L)	22.78 ± 4.70	22.91 ± 5.25	25.73 ± 3.26
Potassium (mmol/L)	11.06 ± 1.52	12.94 ± 1.03	12.52 ± 1.59
Calcium (mmol/L)	2.56 ± 0.19	2.84 ± 0.18	2.18 ± 0.53
Sodium :Potassium ratio	13.6 ± 1.86	13.93 ± 1.92	12.96 ± 2.34
Chloride (mmol/L)	107.71 ± 2.52	109.52 ± 2.91	107.96 ± 3.98

Inorganic phosphorus (mmol/L)	3.08 ± 0.77	3.56 ± 0.99	3.48 ± 0.8
Calcium:Phosphorus ratio	0.83 ± 0.19	0.78 ± 0.14	0.78 ± 0.11
Albumin (g/L)	34.93 ± 2.68	31.16 ± 3.57	30.82 ± 2.07
Total Protein (g/L)	56.69 ± 3.59	54.58 ± 4.56	58.86 ± 3.97
Globulin (g/L)	24.8 ± 2.67	23.4 ± 2.96	23.66 ± 3.14
Total Bilirubin (μmol/L)	0.43 ± 0.05	0.67 ± 0.07	0.47 ± 0.09
Creatinine (μmol/L)	10.84 ± 2.86	12.224 ± 4.76	9.98 ± 3.05
Urea (mmol/L)	7.67 ± 2.12	9.2 ± 3.45	7.34 ± 3.54
Glucose (mmol/L)	15.96 ± 3.15	15.06 ± 3.78	12.72 ± 4.08
Cholesterol (mmol/L)	2.56 ± 0.59	2.51 ± 0.56	2.12 ± 0.58
AST (U/L)	305.07 ± 200.04	326.94 ± 179.35	299.46 ± 200.69
GGT (U/L)	< 0	< 0	< 0
Alkaline phosphatase (U/L)	106.73 ± 31.70	106.44 ± 28.02	101.42 ± 35.51
Lipase (U/L)	98.86 ± 39.77	89.28 ± 35.14	106.20 ± 31.47
ALT (U/L)	97.01 ± 21.15	99.64 ± 18.04	101.54 ± 22.98
Amylase (U/L)	2181.95 ± 339.34	2295.26 ± 290.25	2301.04 ± 289.67

Table 5.8 Organ weights of APPSwe/PS1deE9 mice after various treatment of 3 months (mean ± S.D., n = 5)

Organ (g)	17 mo Tg Ctrl	17 mo Tg BC	17 mo Tg NCF
Brain	0.48 ± 0.08	0.49 ± 0.07	0.51 ± 0.12
Liver	1.86 ± 0.48	1.84 ± 0.42	1.82 ± 0.53
Heart	0.22 ± 0.06	0.21 ± 0.08	0.23 ± 0.08
Lung	0.52 ± 0.12	0.55 ± 0.14	0.54 ± 0.16
Spleen	0.13 ± 0.03	0.12 ± 0.04	0.15 ± 0.05
Kidney	0.25 ± 0.04	0.23 ± 0.03	0.23 ± 0.05

The result of open-field, NORT, Y-maze, and MWM test revealed the therapeutic potential of NCF via oral administration by rescuing the behavioral deficits of APPSwe/PS1deE9 mice. In long-term repeated dose toxicity, NCF was proved as well tolerated with no appearance of any significant toxicity via oral administration. The therapeutic activity of CUR against the AD via targeting key multiple pathologies has been already reported. Thus, our study demonstrates NCF as a promising and very safe therapeutic candidate for AD.

5.5 Conclusions

In conclusion, SOL surpassed among all polymers for CUR by providing superior solubilization and stabilizing effect in SBF. With the ratio 1:10 CUR to SOL and SE method of preparation, NCF demonstrated 20613-fold improvement in solubility which could be attributed to amorphization according to DSC, XRD, and SEM study, the formation of hydrogen bonds between the CUR and SOL found from FTIR and ^{1}H NMR study, and the formation of nanosized micelles on the basis of TEM study. Furthermore, it can be stored at ≤40°C for at least eight weeks which was confirmed from the stability study as per ICH guideline. Additionally, the significant improvement in dissolution and permeability across the S.I were confirmed with NCF compared to crude CUR. As a result of improvement in solubility, stability, dissolution and permeability, the oral pharmacokinetic study in rats displayed 17, and 117-fold enhancement in the case of PM and NCF compared to CUR suspension. The oral administration of NCF for 3 months reversed the behavioral deficit in APPSwe/PS1deE9 mice which were confirmed from the open field, NORT, Y-maze and MWM tests. In addition, it caused no obvious toxicity based on the impact on body weight, food or water consumption, hematology, coagulation, serum biochemistry, organ weight and histology observation. The research outcome demonstrated NCF as a potential candidate to pave the way for clinical development for AD due to its superior safety and efficacy. This study may provide a novel way for repositioning of the potential therapeutic candidates for AD therapy.

Conflict of interest

Ankit Parikh, Xin-Fu Zhou, and Sanjay Garg are the named inventors on Chinese patent 201610267974.5. Fujian Kangshimei Co, China owns the intellectual property. There is no other potential conflict of interest relevant to this article.

Contribution

Ankit Parikh (AP), Krishna Kathawala (KK), Yunmei Song (YS), Xia Cao (XC), Xin-Fu Zhou (XZ) and Sanjay Garg (SG) designed the study, AP, KK, Zhengnan Shan (ZS), Chi Chen (CC), Jintao Li (JL), Chun Chuan Tan (CT) and XZ performed the research, AP, KK, YS, XZ and SG analysed the data; AP, KK, XZ and SG wrote the paper.

Acknowledgements

The authors would like to acknowledge the financial support from Fujian Kangshimei Co, China for the present research. Ankit Parikh and Zhengnan Shan are grateful for the University President's Scholarships (UPS) to support their PhD study. Chun Chuan Tan is also grateful for Vacation Research Scholarships from University of South Australia. Xin-Fu Zhou is grateful for the NHMRC fellowship. Dr Jintao Li is a visiting scholar and grateful for a scholarship under state scholarship fund organized by China Scholarship Council (CSC). The authors would like to express their gratitude towards Lyn Waterhouse from Adelaide Microscopy, The University of Adelaide for the technical support in TEM analysis, Dr Binoy Sarkar from Centre for Environmental Risk Assessment and Remediation, University of South Australia for XRD study, Dr Nobuyuki Kawashima and Dr Steve McInnes from Future Industries Institute, University of South Australia for SEM and DSC analysis, respectively, Rupal Pradhan and Andrew Beck from University of South Australia for technical support in Hematological, coagulation parameters and Histology study, Rebecca Summerton and Dr Ian Beckman from Veterinary Diagnostic Laboratory, the University of Adelaide for providing technical support for Serum biochemistry study, H. Md. Morshed Alam (BASF Australia Ltd) for generously providing SOL, Stephen Philip, a PhD candidate, from School of Pharmacy and Medical Sciences, University of South Australia for NMR study, and Noralyn Manucat-Tan and Chun-Sheng Ruan for behaviour tests. The animal welfare officer, Alex Whittaker and the animal ethics officer, Ruth Brogan and Reid animal house staff members including Jayne Skinner, Alysha Servin, Jess Parken, and Becky Nitschke from University of South Australia are acknowledged for their generous support in animal work.

Supplementary Information

Novel self-nanomicellizing solid dispersion Curcumin formulation for oral administration: Development, optimization and assessment in Alzheimer's disease model

Author information

Ankit Parikh[1], Krishna Kathawala[1], Zhengnan Shan[1], Chi Chen[1,2], Jintao Li[1,3], Chun Chuan Tan[1], Yunmei Song[1], Xia Cao[2], Xin-Fu Zhou[1]*, Sanjay Garg[1]*

[1]School of Pharmacy and Medical Sciences, University of South Australia, Adelaide, SA 5000, Australia.

[2]Central laboratory, Second Affiliated Hospital of Kunming Medical University, Kunming, Yunnan Province 650101, China.

[3]Neuroscience Institute, Kunming Medical University, Kunming, Yunnan Province 650500, China.

*Corresponding author-

E-mail address: Sanjay.Garg@unisa.edu.au, Xin-Fu.Zhou@unisa.edu.au

Phone: +61 8830 21575, +61 8830 22329

Fax: +61 8830 22389, +61 8830 21087

Table S1 Mathematical models used to describe drug dissolution curves.

Mathematical models to determine the release kinetic		
Model	Equation	Description
First order	$Q_t = \ln Q_0 + K_1 t$	Q_t: amount of drug dissolved in time t,
Zero order	$Q_t = Q_0 + K_0 t$	Q_0: initial amount of drug in the solution,
Hixson–Crowell	$Q^{1/3}_0 - Q^{1/3} t = K_C t$	t: time,
Higuchi-matrix	$Q_t = K_H t^{1/2}$	Q_∞: amount of drug dissolved in time ∞.
Korsmeyer–Peppas	$Q_t/Q_\infty = K_K t^n$	K_1, K_0, K_C, K_H, K_K are the rate constants for first order, zero order, Hixson–Crowell, Higuchi-matrix and Korsmeyer–Peppas resepctively.
Release profiles comparison		
Dissimilarity factor (f1)	$f_1 = \frac{\sum_{j=1}^{n} \lvert R_j - T_j \rvert}{\sum_{j=1}^{n} R_j} \times 100$	n: sampling number,
Similarity factor (f2)	$f_2 = 50 \times \log\left\{ \left[1 + (1/n) \sum_{j=1}^{n} \lvert R_j - T_j \rvert^2 \right]^{-0.5} \times 100 \right\}$	Rj and Tj: percent dissolved of the reference and test products at each time point j,

Table S2 Experimental design for behavioural tests with mouse models of Alzheimer disease.

Groups	Treatment	APP/PS1 mice		
		Identity	Age (months)	Sample size (n)
Basal Control	Normal Water	14 mo Tg Ctrl	14	11
Sham control	Normal Water	17 mo Tg Ctrl	17	12
Blank control (B.C)	SOL	17 mo Tg BC	17	10
CUR control	PM	17 mo Tg CC	17	10
NCF Treated	NCF	17 mo Tg NCF	17	12
DNP Treated	DNP	17 mo Tg DNP	17	9

Table S3 Protocol for tissue processing in Leica ASP300.

Step	Reagent	Duration (min)	Temp
1	Formalin	5	-
2	Ethanol 70%	45	-
3	Ethanol 90%	60	-
4	Ethanol Absolute	60	-
5	Ethanol Absolute	60	-
6	Ethanol Absolute	90	-
7	Xylene	60	-
8	Xylene	60	-

9	Xylene	90	-
10	Paraffin Wax	60	62
11	Paraffin Wax	60	62
12	Paraffin Wax	60	62

Table S4 Solubility parameters of CUR and solubilisers

Components	Dispersion (dd) $MPa^{1/2}$	polarity (dp) $MPa^{1/2}$	hydrogen bonding (dh) $MPa^{1/2}$	HSP $MPa^{1/2}$	Difference HSP $MPa^{1/2}$
CUR	17.4	6	10.9	21.4	0.0
SOL [332]	17.4	0.3	8.6	19.4	2.0
Poloxamer 188 [332]	17.49	10.23	8.74	22.10	0.7
Poloxamer 407 [444]	17.36	9.85	8.57	21.75	0.35
PVP K30 [444]	20.44	13.68	9.28	26.28	4.88
PEG 4000 [444]	22.20	11.20	13.20	17.10	4.3

.

Table S5 Change in the position of chemical shifts of CUR and NCF in 1H NMR spectroscopy.

CUR (chemical shift)	NCF (chemical shift)	Change
9.652	9.664	0.012
7.560	7.557	0.003
7.528	7.525	0.003
7.320	7.317	0.003
7.160	7.156	0.004
7.144	7.140	0.003
6.829	6.827	0.002
6.813	6.811	0.002
6.770	6.767	0.003
6.739	6.735	0.004
6.057	6.056	0.001
3.837	3.835	0.002

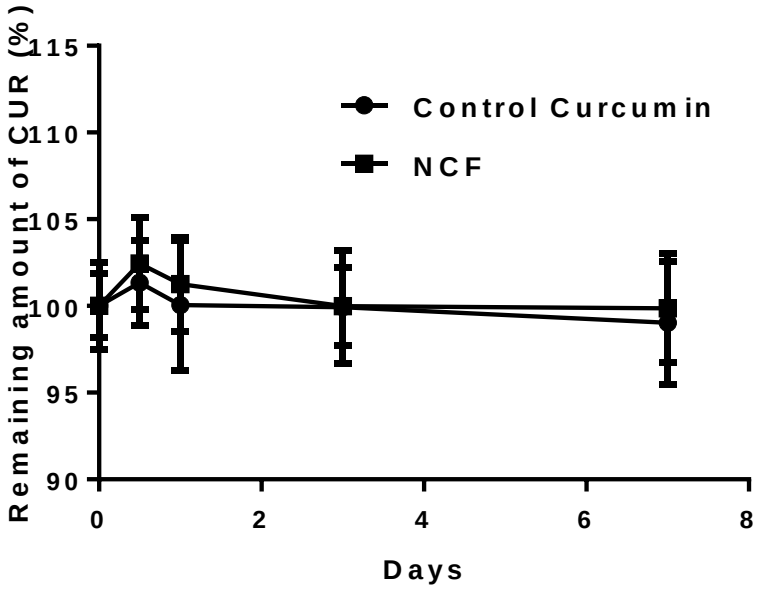

Fig. S1 Stability profile of NCF in the drinking water supplied to the animals (mean ± S.D., n = 3).

6. Summary and Future Directions

6.1 Summary

Alzheimer Disease (AD), the most common cause of dementia, is a chronic neurodegenerative disease linked to the progressive cognitive deficits specifically in elder community with a sufficient severity to compromise an individual's daily function [69]. Even after a century of the discovery of AD, the effective therapy is still not available which could prevent, cure and even stop its progression [14]. The complexity of the disease is the main reason for several failures in clinical trials due to the involvement of multiple pathways in the development and progression of the disease such as oxidative stress, neuroinflammation, mitochondrial dysfunctions, glial activation, synaptic dysfunction, and neurotransmission-related mechanisms. Most of the mechanisms form vicious cycles to accelerate the disease progression. Thus, targeting multiple key pathways of the AD pathogenesis is the key to the successful therapeutic outcome [69, 380]. The therapeutic potential of EDR and CUR for AD have been already proven by targeting multiple pathologies such as Aβ, oxidative stress, Tau hyperphosphorylation, synaptic dysfunction, neuronal loss, neuroinflammation and glial activation. Thus, they were considered as best of the few most promising drug candidates that are currently available for further development [69].

The oral route of administration is the most preferred in terms of compliance and comfort, accurate and flexible dosing, and cost [383]. The poor oral BA was the key reason for the failure of clinical trials of potential candidates against AD such as CUR [384, 385]. Unfortunately, EDR and CUR are designated as class IV compounds as per Biopharmaceutics Classification System (BCS) due to the poor aqueous solubility and permeability [96, 342]. The aim of the current research was to reposition EDR and CUR for AD by developing novel oral delivery systems to enhance their oral bioavailability. In case of EDR, the pre-formulation study was conducted as an initial step, due to limited information on its physicochemical characteristics and unfavorable oral pharmacokinetic profile. Based on the preformulation profile, the strategies including co-solvents (chapter 2), lipid-based preparations (Chapter 3) and SNMED (Chapter 4) were investigated to enhance its oral BA. Due to simplicity and economy of preparation, stability and better oral bioavailability, NEF was considered for *in-vivo* safety and efficacy study. For CUR, SNMED (chapter 5) was identified as a potential strategy to solve the challenges of poor solubility, stability, and permeability. The optimized oral formulations were further assessed for the long-term (three months) efficacy on mice behavioral deficits (Open field, Novel objective recognition, Y-maze and Morris water maze tests) in transgenic AD mice model (TgAD) (APP/PS1). The safety of optimized formulation

was investigated by measuring mice body weights, water, and food consumption, biochemical, coagulation and hematological parameters in blood, organ weight, histopathology and compared with the control groups. The following section critically examines the results obtained and provides suggestions for further development.

6.1.1 Novel Oral Delivery System (NODS) of EDR (Chapter 2)

The NODS of EDR was developed to enhance oral bioavailability based on co-solvents and pH modification approach. From the preformulation study, solubility and stability were identified as key challenges. The requirement of an acidic environment and additional protection against oxidation were also found to be critical. Additionally, based on the literature (REF); poor permeability across the GI tract and extensive metabolism lead to the poor oral bio-availability. The NODS made up of a mixture of Labrasol (LBS) and an acidic aqueous system (pH 4), was optimized on the basis of solubility and stability study. It was stable at 4 °C, 25 °C/60 %RH, and 40 °C/75 %RH for one month revealed from stability study as per ICH guideline. However, stability study needs to be extended for future development. The *in-vitro* drug release from NODS was slow, sustained and significantly better as compared to EDR suspension. Also, LBS showed a significant inhibition of the metabolism as well as enhanced intestinal absorption of EDR with NODS compared to free EDR. The beneficial effect of LBS could be due to its inhibitory activity on UGT enzyme and Pgp efflux transporter. The mechanism-based research would be required in future to confirm the effect of LBS from NODS on Pgp efflux transporter. The enhancement of relative oral bioavailability of NODS was 5.75-fold compared to EDR suspension. The improvement in the oral bioavailability with NODS could be due to a combination effect of improvement in solubility, stability, intestinal permeability and reduction of extensive metabolism of EDR.

6.1.2 NLNS of EDR (Chapter 3)

To achieve better drug loading, facilitate lymphatic uptake allowing enterocyte-based transport to enhance drug uptake, efflux, and deposition; NLNS of EDR based on strategy self-microemulsifying drug delivery system was developed. The components of NLNS including oil, surfactants, and co-surfactants were selected based on their potential to maximize the solubilisation of EDR in gastrointestinal (GI) fluids, reduce its glucuronidation and improve intestinal permeability. The Liquid NLNS (L-NLNS) with Capryol™ PGMC (Oil), Cremophor® RH 40: Labrasol®: TPGS 1000 (1:0.8:0.2) (Surfactant) and Transcutol P® (Co-surfactant) were optimized. It forms a microemulsion after dilution with water, with the droplet

size (16.25 nm), polydispersity index (PDI, 0.039), % Transmittance (99.85%) and self-emulsification time (32 s). It significantly improved the drug loading and intestinal permeability, and reduced metabolism of EDR during the transport across the GI tract. To overcome the possible drawbacks of L-NLNS related to the stability, Aerosil® 200 was used to formulate Solid NLNS (S-NLNS). The concentration of Aerosil® 200 to the L-NLNS was optimized based on flow properties of S-NLNS. The S-NLNS possessed all quality attributes of L-NLNS based on solid-state characterization, morphology, reconstitution ability and stability study. The dissolution rate of EDR was significantly enhanced with L-NLNS and S-NLNS in simulated gastric fluid (SGF), and simulated intestinal fluid (SIF) compared to EDR suspension. The *in-vitro* evaluation of L-NLNS and S-NLNS with the use of biorelevant dissolution media and lipolysis models could indicate fate of EDR during passage through the GI tract. The L-NLNS and S-NLNS showed 10.79-fold and 9.29-fold enhancement of oral BA of EDR, respectively. The mechanism-based studies including the effect of formulation ingredients on the Pgp efflux system and lymphatic uptake would be necessary to examine the contribution of each mechanism to the improvement of oral BA of EDR. Additionally, the stability study as per ICH guideline is required to define the shelf-life of L-NLNS and S-NLNS. Also, *in-vitro/in-vivo* evaluation of safety is recommended.

6.1.3 NEF (Chapter 4)

The NEF was developed using self-nanomicellizing solid dispersion strategy to enhance the oral BA. Soluplus® (SOL) was selected from the screening of polymers based on their potential for improving the solubility of EDR. NEF with EDR and SOL (1:5) showed the highest improvement in aqueous solubility of EDR (17.53-fold) due to amorphization, hydrogen bonding interaction and micellization. Furthermore, the stability of NEF was studied as per ICH guideline. It remained stable at 4 °C, 25 °C/60 %RH, and 40 °C/75 %RH for two months revealed from stability study as per ICH guideline. However, further stability study is recommended as per ICH guideline for an extended period. Moreover, the NEF demonstrated significant improvement in intestinal permeability and dissolution profile of EDR. To investigate the dose-dependent therapeutic effect against the Alzheimer disease, three different doses of NEF were considered for the pharmacokinetic study. The oral BA of NEF showed 10.2, 16.1 and 14.8-fold enhancement compared to EDR suspension at 46, 138 and 414 µM/kg dose, respectively. The mechanistic study is warranted to define the role of inhibition of Pgp efflux transporter in the improvement of oral BA using SOL based formulation. NEF was further assessed for long-term (three months) therapeutic efficacy study on mice behavior

deficits (Open field, Novel objective recognition, Y-maze and Morris water maze tests) and its sub-chronic toxicity with AD mice model APP/PS1 after oral administration. NEF rescued the behavioral deficits of 17-months old APP/PS1 mice dose-dependently. Also, NEF appeared reserving the cognitive decline of APP/PS1 mice to the cognitive level of wild type normal aging mice and performed better than donepezil. Moreover, the toxicity study data showed the absence of drug-induced toxicity by oral administration up to 414 µM/kg in the APP/PS1 mice.

6.1.4 NCF (Chapter 5)

Chapter 5 deals with poor oral bioavailability (BA), the major contributor to the failure of CUR in clinical trials. To enhance oral BA, NCF was developed using self-nanomicellizing solid dispersion strategy. SOL showed better solubilization and stabilizing effect in SBF for CUR among the polymers such as SOL, PVP K30, PEG 4000, poloxamer 407, and poloxamer 188. With the ratio 1:10 CUR to SOL and solvent evaporation as a method of preparation, NCF demonstrated 20613-fold improvement in the aqueous solubility. It could be attributed to amorphization according to DSC, XRD, and SEM study, the formation of hydrogen bonds between the CUR and SOL and the formation of nanosized micelles after dilution with water discovered from FTIR, ^{1}H NMR, and TEM study. Furthermore, it remained stable at 4 °C, 25 °C/60 %RH, and 40 °C/75 %RH for two months revealed from stability study as per ICH guideline. The stability study for an extended period is recommended. Additionally, the significant improvement in dissolution and permeability of CUR across the S.I were confirmed with NCF compared to crude CUR. As a result of improvement in solubility, stability, dissolution and permeability, the oral pharmacokinetic study in rats displayed 17, and 117-fold enhancement of relative oral BA in the case of PM and NCF compared to CUR suspension, respectively. Moreover, the oral administration of NCF for three months reversed the behavioral deficit in APP/PS1 mice which were confirmed from the open field, NORT, Y-maze and MWM tests. Also, it caused no obvious toxicity revealed after examining the impact on body weight, food or water consumption, hematology, coagulation, serum biochemistry, organ weight and histology observation.

6.2 Future Directions

The research outcome demonstrated NEF and NCF as potential candidates for clinical development for AD due to their better safety and efficacy. However, the mechanism-based research would be required to investigate the effect of NEF and NCF treatment on AD including amyloid burden in the brain and blood, inflammation, tau phosphorylation and

expression of BACE1 and presenilin to support the behavior test results. The following sections provide suggestions for future studies.

6.2.1 Mechanism study

After the behavioral test, all AD mice used in safety and efficacy study animal were sacrificed by carbon dioxide inhalation and perfused intracardially with cold phosphate-buffered saline (pH 7.4). Blood, serum, plasma and different organs which include brain were collected. Half of the brain hemisphere was frozen in liquid nitrogen and the other half fixed in 4% formaldehyde. Each sample will be processed for histological and biochemical analysis to answer the following questions as described in our previous publications [70, 445-448].

6.2.1.1 Do NEF and NCF reduce the amyloid burden in the brain and blood of AD mice?

The hemibrain sections of AD mice will be stained by both 6E10 anti-Aβ and congo red for total Aβ and compact Aβ plaques, respectively in a blinded manner. The total plaque area, plaque sizes and a number of plaques will be analyzed and compared between treated and control groups. The other half-brain will be homogenized to measure the levels of Aβ 40 and Aβ 42 in soluble and non-soluble fractions. Aβ 40 and Aβ 42 levels in the serum will also be analyzed by enzyme-linked immunosorbent assay (ELISA).

6.2.1.2 Do NEF and NCF reduce the activation of inflammation in the brain of AD mice?

The microglial and astrocyte staining will be performed on the brain sections from AD mice. The levels of tumor necrosis factor alpha (TNF α), interleukin 1β and interferon γ in the brain homogenates and blood serum will also be assayed with ELISA kits and compared between the treatment and controls groups. Moreover, any suppression of the nuclear factor-κB (NFκB) pathway will be evaluated in brain homogenates by probing with antibodies to NFκB subunits. Additionally, NFκB mRNA will be measured by quantitative reverse transcription-polymerase chain reaction (RT-PCR).

6.2.1.3 Do NEF and NCF reduce Tau phosphorylation and neurofibrillary tangles?

The hemibrain sections will be stained for total and phosphorylated Tau. The intensity and total staining areas will be quantified with Image J software and compared between the treated and control groups. Furthermore, the brain homogenates will be analyzed by western blots on total and activated Glycogen synthase kinase three beta (GSK3β), Cyclin-dependent kinase 5 (CDK5), different subunits of Protein phosphatase 2A and different phosphorylation sites of Tau using different epitope antibodies.

6.2.1.4 Do NEF and NCF inhibit expression of BACE1 and presenilin in vivo?

The levels of Beta-secretase 1 (BACE1) and presenilin will be examined by performing western blot and normalized to β-actin and compared between groups. The levels of mRNA will be quantified by quantitative RT-PCR.

6.2.2 Clinical Studies

Our data in the present study, together with the earlier prove-of-concept study in 12-month-old APP/PS1 mice, warrants a large scale of clinical trials of NEF and NCF in mild cognitive impairment (MCI) or AD patients in the future. In addition to AD, the trial on the EDR (NEF) and CUR (NCF) will also have significance for other diseases, as numerous preclinical and clinical trial reports have shown its effectiveness in chronic diseases ALS, PD and other diseases with oxidative stress [212]. If successful, this study will put in the forefront of dementia research with a disease modifying drug for AD which will provide a significant social and economic impact.

6.2.2.1 Phase I

To establish the PK and tolerability of the oral formula, eight healthy participants (four each male and female) from 20-70 years old with normal liver and kidney functions will be recruited into the study. Before trial, all participants will undergo routine blood examination including liver and kidney functions, health history questionnaire and physical examination. The study will be performed in the same participants in six as treatment groups and two as placebo controls. The first PK trial will be performed with three different drug doses. The collection of blood samples at different time intervals will be followed as per our previous publication [342]. After a seven-day interval, the same participants will take drug formulas or a placebo with the same sampling time points. Before proceeding to a higher dose, participants will be tested for blood routine to investigate for any possible side effects. All blood samples will be processed for drug assay. The oral PK profile generated from this study will be allowed to design dosage and frequency of NEF and NCF in Phase II trials.

6.2.2.2 Phase II:

The double-blind, placebo-controlled, randomized phase II clinical trial of the NEF and NCF will be conducted to evaluate the effects on cognitive as well as AD-related blood, cerebrospinal fluid (CSF) and imaging markers in patients. The trial protocol will be approved by the Human Ethics Committees of all participating sites, and the trial will be registered with the Clinical Trials Registry.

The following inclusion criteria will also be applied: 60-85 years old otherwise healthy individuals with at least one abnormality in biomarkers (either amyloid beta or neurodegeneration or both) at screening phase. Exclusion criteria include Parkinson disease (PD), Huntington's diseases (HD), frontal, temporal dementia, stroke, diabetes, history of schizophrenia, major depression, severe liver and kidney dysfunction, and other age-related diseases affecting cognitive functions. Following the screening and baseline phase, using a computerized program, participants will be randomized into placebo and treatment groups, and the identification numbers (ID) will be passed onto the drug packaging and manufacturing company for allocating the drug or placebo packages. This process will minimize the potential for accidental unbinding by the researchers. The flowchart (Fig. 1) shows the overall design.

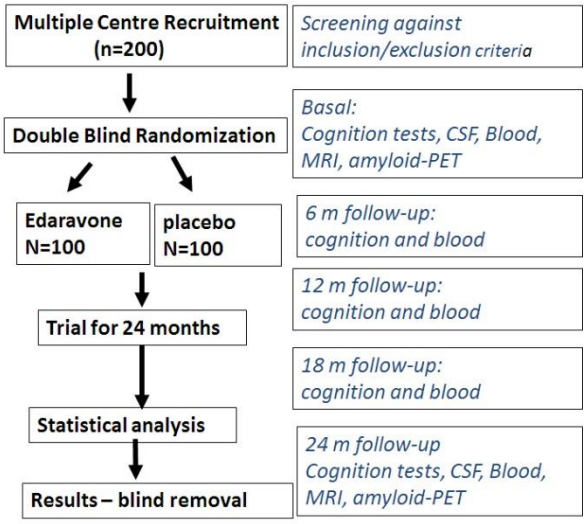

Figure 6.1 A flow chart of the design and trial outlines.

7. References

1. Austin, C.P., *The impact of the completed human genome sequence on the development of novel therapeutics for human disease.* Annu Rev Med, 2004. **55**: p. 1-13.
2. Zwi-Dantsis, L., et al., *Derivation and cardiomyocyte differentiation of induced pluripotent stem cells from heart failure patients.* Eur Heart J, 2013. **34**(21): p. 1575-86.
3. Schwartz, S.D., et al., *Embryonic stem cell trials for macular degeneration: a preliminary report.* Lancet, 2012. **379**(9817): p. 713-20.
4. Levenson, R.W., V.E. Sturm, and C.M. Haase, *Emotional and behavioral symptoms in neurodegenerative disease: a model for studying the neural bases of psychopathology.* Annu Rev Clin Psychol, 2014. **10**: p. 581-606.
5. *Bioactive Nutraceuticals and Dietary Supplements in Neurological and Brain Disease* R.R.W.V. Preedy, Editor. 2014, Academic Press. p. 528-38.
6. Spuch, C., O. Saida, and C. Navarro, *Advances in the treatment of neurodegenerative disorders employing nanoparticles.* Recent Pat Drug Deliv Formul, 2012. **6**(1): p. 2-18.
7. Lopez-Tobon, A., et al., *Silencing of CDK5 as potential therapy for Alzheimer's disease.* Rev Neurosci, 2011. **22**(2): p. 143-52.
8. Jellinger, K.A., *Alzheimer 100--highlights in the history of Alzheimer research.* J Neural Transm, 2006. **113**(11): p. 1603-23.
9. Imtiaz, B., et al., *Future directions in Alzheimer's disease from risk factors to prevention.* Biochem Pharmacol, 2014.
10. Liu, M., H. Du, and G. Zhai, *The Design of Amphiphilic Polymeric Micelles of Curcumin for Cancer Management.* Curr Med Chem, 2015. **22**(38): p. 4398-411.
11. Sood, S., K. Jain, and K. Gowthamarajan, *Intranasal therapeutic strategies for management of Alzheimer's disease.* J Drug Target, 2014.
12. Iqbal, K., F. Liu, and C.X. Gong, *Alzheimer disease therapeutics: Focus on the disease and not just plaques and tangles.* Biochem Pharmacol, 2014.
13. Thies, W., L. Bleiler, and A. Alzheimer's, *2013 Alzheimer's disease facts and figures.* Alzheimers Dement, 2013. **9**(2): p. 208-45.
14. Cipriani, G., et al., *Alzheimer and his disease: a brief history.* Neurol Sci, 2011. **32**(2): p. 275-9.
15. Roberson, E.D. and L. Mucke, *100 years and counting: prospects for defeating Alzheimer's disease.* Science, 2006. **314**(5800): p. 781-4.
16. Liu, L., et al., *Curcumin loaded polymeric micelles inhibit breast tumor growth and spontaneous pulmonary metastasis.* Int J Pharm, 2013. **443**(1-2): p. 175-82.

17. Australia, A.s. *Key facts and statistics 2017*. 2017 [cited 2017 01/03]; Available from: https://www.fightdementia.org.au/statistics.
18. Alzheimer's, A., *2016 Alzheimer's disease facts and figures.* Alzheimers Dement, 2016. **12**(4): p. 459-509.
19. Anand, R., K.D. Gill, and A.A. Mahdi, *Therapeutics of Alzheimer's disease: Past, present and future.* Neuropharmacology, 2014. **76 Pt A**: p. 27-50.
20. Reitz, C. and R. Mayeux, *Alzheimer disease: Epidemiology, diagnostic criteria, risk factors and biomarkers.* Biochem Pharmacol, 2014.
21. Chami, L. and F. Checler, *BACE1 is at the crossroad of a toxic vicious cycle involving cellular stress and beta-amyloid production in Alzheimer's disease.* Molecular neurodegeneration, 2012. **7**: p. 52.
22. Hernandez, F., J.J. Lucas, and J. Avila, *GSK3 and Tau: Two Convergence Points in Alzheimer's Disease.* Journal of Alzheimer's disease : JAD, 2013. **33**(0): p. S141-4.
23. Lopez-Tobon, A., et al., *Silencing of CDK5 as potential therapy for Alzheimer's disease.* Reviews in the neurosciences, 2011. **22**(2): p. 143-52.
24. Ly, P.T., et al., *Inhibition of GSK3beta-mediated BACE1 expression reduces Alzheimer-associated phenotypes.* The Journal of clinical investigation, 2013. **123**(1): p. 224-35.
25. Liu, R. and J.Z. Wang, *Protein phosphatase 2A in Alzheimer's disease.* Pathophysiology : the official journal of the International Society for Pathophysiology / ISP, 2009. **16**(4): p. 273-7.
26. Sontag, E., et al., *Altered expression levels of the protein phosphatase 2A ABalphaC enzyme are associated with Alzheimer disease pathology.* Journal of neuropathology and experimental neurology, 2004. **63**(4): p. 287-301.
27. Ittner, L.M. and J. Gotz, *Amyloid-beta and tau--a toxic pas de deux in Alzheimer's disease.* Nature reviews. Neuroscience, 2011. **12**(2): p. 65-72.
28. Ittner, L.M., et al., *Parkinsonism and impaired axonal transport in a mouse model of frontotemporal dementia.* Proceedings of the National Academy of Sciences of the United States of America, 2008. **105**(41): p. 15997-6002.
29. Tamagno, E., et al., *Oxidative stress increases expression and activity of BACE in NT2 neurons.* Neurobiology of disease, 2002. **10**(3): p. 279-88.
30. Tamagno, E., et al., *Beta-site APP cleaving enzyme up-regulation induced by 4-hydroxynonenal is mediated by stress-activated protein kinases pathways.* Journal of neurochemistry, 2005. **92**(3): p. 628-36.

31. Tong, Y., et al., *Oxidative stress potentiates BACE1 gene expression and Abeta generation.* Journal of neural transmission, 2005. **112**(3): p. 455-69.
32. Borghi, R., et al., *The increased activity of BACE1 correlates with oxidative stress in Alzheimer's disease.* Neurobiology of aging, 2007. **28**(7): p. 1009-14.
33. Ayton, S., P. Lei, and A.I. Bush, *Metallostasis in Alzheimer disease.* Free radical biology & medicine, 2012.
34. Greenough, M.A., J. Camakaris, and A.I. Bush, *Metal dyshomeostasis and oxidative stress in Alzheimer's disease.* Neurochemistry international, 2012.
35. Tabner, B.J., et al., *Protein aggregation, metals and oxidative stress in neurodegenerative diseases.* Biochemical Society transactions, 2005. **33**(Pt 5): p. 1082-6.
36. Nunomura, A., et al., *Oxidative damage is the earliest event in Alzheimer disease.* Journal of neuropathology and experimental neurology, 2001. **60**(8): p. 759-67.
37. Cutler, R.G., et al., *Involvement of oxidative stress-induced abnormalities in ceramide and cholesterol metabolism in brain aging and Alzheimer's disease.* Proceedings of the National Academy of Sciences of the United States of America, 2004. **101**(7): p. 2070-5.
38. Perry, G., et al., *Oxidative damage in Alzheimer's disease: the metabolic dimension.* International journal of developmental neuroscience : the official journal of the International Society for Developmental Neuroscience, 2000. **18**(4-5): p. 417-21.
39. Tabner, B.J., et al., *Hydrogen peroxide is generated during the very early stages of aggregation of the amyloid peptides implicated in Alzheimer disease and familial British dementia.* The Journal of biological chemistry, 2005. **280**(43): p. 35789-92.
40. Mark, R.J., et al., *Amyloid beta-peptide impairs glucose transport in hippocampal and cortical neurons: involvement of membrane lipid peroxidation.* The Journal of neuroscience : the official journal of the Society for Neuroscience, 1997. **17**(3): p. 1046-54.
41. Murakami, K., et al., *Formation and stabilization model of the 42-mer Abeta radical: implications for the long-lasting oxidative stress in Alzheimer's disease.* Journal of the American Chemical Society, 2005. **127**(43): p. 15168-74.
42. Paola, D., et al., *Oxidative stress induces increase in intracellular amyloid beta-protein production and selective activation of betaI and betaII PKCs in NT2 cells.* Biochemical and biophysical research communications, 2000. **268**(2): p. 642-6.

43. Mazzitelli, S., et al., *The loss of c-Jun N-terminal protein kinase activity prevents the amyloidogenic cleavage of amyloid precursor protein and the formation of amyloid plaques in vivo.* The Journal of neuroscience : the official journal of the Society for Neuroscience, 2011. **31**(47): p. 16969-76.
44. Buggia-Prevot, V., et al., *NFkappaB-dependent control of BACE1 promoter transactivation by Abeta42.* The Journal of biological chemistry, 2008. **283**(15): p. 10037-47.
45. Chami, L., et al., *Nuclear factor-kappaB regulates betaAPP and beta- and gamma-secretases differently at physiological and supraphysiological Abeta concentrations.* The Journal of biological chemistry, 2012. **287**(29): p. 24573-84.
46. Mangialasche, F., et al., *Alzheimer's disease: clinical trials and drug development.* Lancet neurology, 2010. **9**(7): p. 702-16.
47. Chami, L. and F. Checler, *BACE1 is at the crossroad of a toxic vicious cycle involving cellular stress and beta-amyloid production in Alzheimer's disease.* Mol Neurodegener, 2012. **7**: p. 52.
48. Colovic, M.B., et al., *Acetylcholinesterase inhibitors: pharmacology and toxicology.* Curr Neuropharmacol, 2013. **11**(3): p. 315-35.
49. Danysz, W. and C.G. Parsons, *Alzheimer's disease, beta-amyloid, glutamate, NMDA receptors and memantine--searching for the connections.* Br J Pharmacol, 2012. **167**(2): p. 324-52.
50. Frisardi, V., F. Panza, and A.A. Farooqui, *Late-life depression and Alzheimer's disease: the glutamatergic system inside of this mirror relationship.* Brain Res Rev, 2011. **67**(1-2): p. 344-55.
51. Schon, E.A. and E. Area-Gomez, *Mitochondria-associated ER membranes in Alzheimer disease.* Mol Cell Neurosci, 2013. **55**: p. 26-36.
52. Eckert, A., K. Schmitt, and J. Gotz, *Mitochondrial dysfunction - the beginning of the end in Alzheimer's disease? Separate and synergistic modes of tau and amyloid-beta toxicity.* Alzheimer's research & therapy, 2011. **3**(2): p. 15.
53. Eckert, A., et al., *Convergence of amyloid-beta and tau pathologies on mitochondria in vivo.* Molecular neurobiology, 2010. **41**(2-3): p. 107-14.
54. Hirai, K., et al., *Mitochondrial abnormalities in Alzheimer's disease.* The Journal of neuroscience : the official journal of the Society for Neuroscience, 2001. **21**(9): p. 3017-23.

55. Gibson, G.E., K.F. Sheu, and J.P. Blass, *Abnormalities of mitochondrial enzymes in Alzheimer disease.* Journal of neural transmission, 1998. **105**(8-9): p. 855-70.
56. Aksenov, M.Y., et al., *Amyloid beta-peptide (1-40)-mediated oxidative stress in cultured hippocampal neurons. Protein carbonyl formation, CK BB expression, and the level of Cu, Zn, and Mn SOD mRNA.* Journal of molecular neuroscience : MN, 1998. **10**(3): p. 181-92.
57. Casley, C.S., et al., *Beta-amyloid fragment 25-35 causes mitochondrial dysfunction in primary cortical neurons.* Neurobiology of disease, 2002. **10**(3): p. 258-67.
58. Casley, C.S., et al., *Beta-amyloid inhibits integrated mitochondrial respiration and key enzyme activities.* Journal of neurochemistry, 2002. **80**(1): p. 91-100.
59. Melov, S., et al., *Mitochondrial oxidative stress causes hyperphosphorylation of tau.* PLoS One, 2007. **2**(6): p. e536.
60. Webber, K.M., et al., *Steroidogenic acute regulatory protein (StAR): evidence of gonadotropin-induced steroidogenesis in Alzheimer disease.* Mol Neurodegener, 2006. **1**: p. 14.
61. Sultana, R., M. Perluigi, and D. Allan Butterfield, *Lipid peroxidation triggers neurodegeneration: a redox proteomics view into the Alzheimer disease brain.* Free Radic Biol Med, 2013. **62**: p. 157-69.
62. Association, A.s. *Alzheimer's & Dementia: Global Resources*. 2017 [cited 2017 01/03]; Available from: https://alz.org/global/.
63. Ho, M., et al., *Effect of Metal Chelators on gamma-Secretase Indicates That Calcium and Magnesium Ions Facilitate Cleavage of Alzheimer Amyloid Precursor Substrate.* Int J Alzheimers Dis, 2010: p. 950932.
64. Liu, G., et al., *Nanoparticle iron chelators: a new therapeutic approach in Alzheimer disease and other neurologic disorders associated with trace metal imbalance.* Neurosci Lett, 2006. **406**(3): p. 189-93.
65. Scarpa, S., et al., *Gene silencing through methylation: an epigenetic intervention on Alzheimer disease.* J Alzheimers Dis, 2006. **9**(4): p. 407-14.
66. Facchinetti, P., et al., *SET translocation is associated with increase in caspase cleaved amyloid precursor protein in CA1 of Alzheimer and Down syndrome patients.* Neurobiol Aging, 2014. **35**(5): p. 958-68.
67. Aliev, G., et al., *Link between cancer and Alzheimer disease via oxidative stress induced by nitric oxide-dependent mitochondrial DNA overproliferation and deletion.* Oxid Med Cell Longev, 2013: p. 962984.

68. Holtzman, D.M., J.C. Morris, and A.M. Goate, *Alzheimer's disease: the challenge of the second century.* Science translational medicine, 2011. **3**(77): p. 77sr1.
69. Jiao, S.S., et al., *Edaravone alleviates Alzheimer's disease-type pathologies and cognitive deficits.* Proc Natl Acad Sci U S A, 2015. **112**(16): p. 5225-30.
70. Wang, Y.J., et al., *Consumption of grape seed extract prevents amyloid-beta deposition and attenuates inflammation in brain of an Alzheimer's disease mouse.* Neurotox Res, 2009. **15**(1): p. 3-14.
71. Zeng, Y.Q., Y.J. Wang, and X.F. Zhou, *Effects of (-)Epicatechin on the Pathology of APP/PS1 Transgenic Mice.* Front Neurol, 2014. **5**: p. 1-10.
72. Sano, Y., et al., *1-(3'-[125I]Iodophenyl)-3-methy-2-pyrazolin-5-one: preparation, solution stability, and biodistribution in normal mice.* Chem Pharm Bull (Tokyo), 2010. **58**(8): p. 1020-5.
73. Linn, M., et al., *Soluplus(R) as an effective absorption enhancer of poorly soluble drugs in vitro and in vivo.* Eur J Pharm Sci, 2012. **45**(3): p. 336-43.
74. Hori, K., et al., *Protective effect of edaravone for tourniquet-induced ischemia-reperfusion injury on skeletal muscle in murine hindlimb.* BMC Musculoskelet Disord, 2013. **14**: p. 113.
75. Kikuchi, K., et al., *Potential of edaravone for neuroprotection in neurologic diseases that do not involve cerebral infarction.* Exp Ther Med, 2011. **2**(5): p. 771-775.
76. Kikuchi, K., et al., *Beyond neurological disease: new targets for edaravone (Review).* Int J Mol Med, 2011. **28**(6): p. 899-906.
77. Anonymous. *Information for Approved Products*. 2015 [cited 2016 01/08]; Available from: http://www.pmda.go.jp/english/review-services/reviews/approved-information/drugs/0001.html.
78. Lapchak, P.A., *A critical assessment of edaravone acute ischemic stroke efficacy trials: is edaravone an effective neuroprotective therapy?* Expert Opin Pharmacother, 2010. **11**(10): p. 1753-63.
79. Kikuchi, K., et al., *The efficacy of edaravone (radicut), a free radical scavenger, for cardiovascular disease.* Int J Mol Sci, 2013. **14**(7): p. 13909-30.
80. Watanabe, T., M. Tahara, and S. Todo, *The novel antioxidant edaravone: from bench to bedside.* Cardiovasc Ther, 2008. **26**(2): p. 101-14.
81. Yang, J., et al., *Edaravone for acute stroke: Meta-analyses of data from randomized controlled trials.* Dev Neurorehabil, 2013.

82. Anonymous. *Public summary of opinion on orphan designation: Edaravone for the treatment of amyotrophic lateral sclerosis*. 2015 [cited 2016 12/08]; Available from: http://www.ema.europa.eu/ema/index.jsp?curl=pages/medicines/human/orphans/2015/02/human_orphan_001489.jsp&mid=WC0b01ac058001d12b.
83. Anonymous. *Orphan Drug Designations and Approvals*. 2015 [cited 2017 01/06]; Available from: https://www.accessdata.fda.gov/scripts/opdlisting/oopd/detailedIndex.cfm?cfgridkey=465514.
84. Tabrizchi, R., *Edaravone Mitsubishi-Tokyo.* Curr Opin Investig Drugs, 2000. **1**(3): p. 347-54.
85. Watanabe, K., et al., *Structure-activity relationship of 3-methyl-1-phenyl-2-pyrazolin-5-one (edaravone).* Redox Rep, 2003. **8**(3): p. 151-5.
86. Brewer, M.S., *Natural Antioxidants: Sources, Compounds, Mechanisms of Action, and Potential Applications.* ComprehensiveReviewsinFoodScienceandFoodSafety, 2011. **10**: p. 211-247.
87. Yamamoto, T., et al., *Delayed neuronal death prevented by inhibition of increased hydroxyl radical formation in a transient cerebral ischemia.* Brain Res, 1997. **762**(1-2): p. 240-2.
88. Kikuchi, K., et al., *Edaravone (Radicut), a free radical scavenger, is a potentially useful addition to thrombolytic therapy in patients with acute ischemic stroke.* Biomed Rep, 2013. **1**(1): p. 7-12.
89. Yoshida, H., et al., *Neuroprotective effects of edaravone: a novel free radical scavenger in cerebrovascular injury.* CNS Drug Rev, 2006. **12**(1): p. 9-20.
90. Inokuchi, Y., et al., *Edaravone, a free radical scavenger, protects against retinal damage in vitro and in vivo.* J Pharmacol Exp Ther, 2009. **329**(2): p. 687-98.
91. Sommani, P., et al., *Effects of edaravone on singlet oxygen released from activated human neutrophils.* J Pharmacol Sci, 2007. **103**(1): p. 117-20.
92. Watanabe, T., et al., *Protective effects of MCI-186 on cerebral ischemia: possible involvement of free radical scavenging and antioxidant actions.* J Pharmacol Exp Ther, 1994. **268**(3): p. 1597-604.
93. Higashi, Y., et al., *Edaravone (3-methyl-1-phenyl-2-pyrazolin-5-one), a novel free radical scavenger, for treatment of cardiovascular diseases.* Recent Pat Cardiovasc Drug Discov, 2006. **1**(1): p. 85-93.

94. Yamamoto, Y., et al., *Antioxidant activity of 3-methyl-1-phenyl-2-pyrazolin-5-one`*. Redox Report 1996. **2**(5): p. 333-338.
95. Jian Zenga, Y.R., Chengliang Zhoua, Shuqin Yua, Wen-Hua Chenb, *Preparation and physicochemical characteristics of the complex of edaravone with hydroxypropyl- -cyclodextrin.* Carbohydrate Polymers, 2010. **83**: p. 5.
96. Rong, W.T., et al., *Hydroxypropyl-sulfobutyl-beta-cyclodextrin improves the oral bioavailability of edaravone by modulating drug efflux pump of enterocytes.* J Pharm Sci, 2014. **103**(2): p. 730-42.
97. Lapchak, P.A., *Emerging Therapies: Pleiotropic Multi-target Drugs to Treat Stroke Victims.* Transl Stroke Res, 2011. **2**(2): p. 129-35.
98. Holdings, J.B.-P. *Timing for profit jump*. 2010 [cited 2017 15/03]; Available from: http://www.sbichinacapital.com/research/pdf/2327HQ043010.pdf.
99. Simcere. *Edaravone Injection*. 2015 [cited 2017 12/01]; Available from: http://www.yaopinnet.com/h/h80/H20050280.htm.
100. Ltd., S.P.I. *Annual Report 2007 - 08: New Product*. 2008 [cited 2016 24/12]; Available from: http://www.sunpharma.com/Html%20version%203/newproductlist.htm.
101. MedGuideIndia. *Brands of Edaravone*. 2010 [cited 2016 21/10]; Available from: http://www.medguideindia.com/find_brand_bygeneric.php?gen_mask=,2881,.
102. Ltd., U.I. *Fraseda® (Edaravone)*. 2015 [cited 2016 05/12]; Available from: http://www.ucb.co.in/products/Product/CNS/Fraseda®.
103. Drug-info.in. *Nuravon (1.5 mg)- 1 ml- Edaravone*. 2014 [cited 2016 24/12]; Available from: http://drug-info.in/indian-medicines/nuravon-injection-1-5-piramal-edaravone.
104. Ltd., C.B.S.P. *Edarabid*. 2013 [cited 2016 24/12]; Available from: http://www.medclik.com/General/pages/Drugmanual/BrandSearch/EDARABID.asp.
105. Ltd, C.B.S.P. *Carevon*. 2013 [[cited 2016 24/12]; Available from: http://www.medclik.com/General/pages/Drugmanual/BrandSearch/CAREVON.asp.
106. Catalog.md. *Radicut Drug Information*. 2015 [cited 2016 24/12]; Available from: http://www.catalog.md/drugs/radicut.html.
107. Feng, S., et al., *Edaravone for acute ischaemic stroke.* Cochrane Database Syst Rev, 2011(12): p. CD007230.
108. Ishibashi, A., Y. Yoshitake, and H. Adachi, *Investigation of Effect of Edaravone on Ischemic Stroke.* Kurume Med J, 2013.
109. Kikuchi, K., et al., *Edaravone: a new therapeutic approach for the treatment of acute stroke.* Med Hypotheses, 2010. **75**(6): p. 583-5.

110. Kimura, K., et al., *Administration of edaravone, a free radical scavenger, during t-PA infusion can enhance early recanalization in acute stroke patients--a preliminary study.* J Neurol Sci, 2012. **313**(1-2): p. 132-6.
111. Kitagawa, Y., *Edaravone in acute ischemic stroke.* Intern Med, 2006. **45**(5): p. 225-6.
112. Unno, Y., M. Katayama, and H. Shimizu, *Does functional outcome in acute ischaemic stroke patients correlate with the amount of free-radical scavenger treatment? A retrospective study of edaravone therapy.* Clin Drug Investig, 2010. **30**(3): p. 143-55.
113. Abe, T., et al., *A new free radical scavenger, edaravone, ameliorates oxidative liver damage due to ischemia-reperfusion in vitro and in vivo.* J Gastrointest Surg, 2004. **8**(5): p. 604-15.
114. Hirano, M., *Clinical evaluation of liver injury in patients with acute ischemic brain stroke treated with edaravone.* Hepatol Res, 2011. **41**(2): p. 142-50.
115. Kobayashi, Y., et al., *Signaling pathway on the effect of oxygenated warm perfusion prior to cold preservation of the liver grafts from non-heart-beating donors, and the additive effect of edaravone.* Transplant Proc, 2009. **41**(1): p. 49-51.
116. Kono, H., et al., *Edaravone, a novel free radical scavenger, prevents liver injury and mortality in rats administered endotoxin.* J Pharmacol Exp Ther, 2003. **307**(1): p. 74-82.
117. Nakamoto, N., et al., *A free radical scavenger, edaravone, attenuates steatosis and cell death via reducing inflammatory cytokine production in rat acute liver injury.* Free Radic Res, 2003. **37**(8): p. 849-59.
118. Nakamura, A., et al., *A free radical scavenger, edaravone, prevents ischemia-reperfusion injury in liver grafts from non-heart-beating donors.* Transplant Proc, 2008. **40**(7): p. 2171-4.
119. Okatani, Y., et al., *Edaravone protects against ischemia/reperfusion-induced oxidative damage to mitochondria in rat liver.* Eur J Pharmacol, 2003. **465**(1-2): p. 163-70.
120. Tada, S., et al., *Clinical usefulness of edaravone for acute liver injury.* J Gastroenterol Hepatol, 2003. **18**(7): p. 851-7.
121. Tanaka, H., et al., *Antifibrotic effect of edaravone in rat liver cirrhosis induced by dimethylnitrosamine.* Clin Exp Med, 2009. **9**(3): p. 229-33.
122. Taniguchi, M., et al., *Edaravone reduces ischemia-reperfusion injury mediators in rat liver.* J Surg Res, 2007. **137**(1): p. 69-74.
123. Tsuji, K., et al., *Free radical scavenger (edaravone) prevents endotoxin-induced liver injury after partial hepatectomy in rats.* J Hepatol, 2005. **42**(1): p. 94-101.

124. Zong, L., et al., *Edaravone protects endotoxin-induced liver injury by inhibiting apoptosis and reducing proinflammatory cytokines.* Braz J Med Biol Res, 2014. **47**(3): p. 231-6.

125. Aoki, T., et al., *Reactive oxygen species modulate growth of cerebral aneurysms: a study using the free radical scavenger edaravone and p47phox(-/-) mice.* Lab Invest, 2009. **89**(7): p. 730-41.

126. Yoshino, H. and A. Kimura, *Investigation of the therapeutic effects of edaravone, a free radical scavenger, on amyotrophic lateral sclerosis (Phase II study).* Amyotroph Lateral Scler, 2006. **7**(4): p. 241-5.

127. Aoki, M., et al., *Feasibility study for functional test battery of SOD transgenic rat (H46R) and evaluation of edaravone, a free radical scavenger.* Brain Res, 2011. **1382**: p. 321-5.

128. Ito, H., et al., *Treatment with edaravone, initiated at symptom onset, slows motor decline and decreases SOD1 deposition in ALS mice.* Exp Neurol, 2008. **213**(2): p. 448-55.

129. Anzai, K., et al., *In vivo radioprotection of mice by 3-methyl-1-phenyl-2-pyrazolin-5-one (edaravone; Radicut), a clinical drug.* J Radiat Res, 2004. **45**(2): p. 319-23.

130. Aoyama, T., et al., *Edaravone (MCI-186) scavenges reactive oxygen species and ameliorates tissue damage in the murine spinal cord injury model.* Neurol Med Chir (Tokyo), 2008. **48**(12): p. 539-45; discussion 545.

131. Hamaishi, M., et al., *Low-dose edaravone injection into the clamped aorta prevents ischemic spinal cord injury.* Ann Vasc Surg, 2009. **23**(1): p. 128-35.

132. Ohta, S., et al., *Neuroprotection and enhanced recovery with edaravone after acute spinal cord injury in rats.* Spine (Phila Pa 1976), 2005. **30**(10): p. 1154-8.

133. Ozgiray, E., et al., *Protective effects of edaravone on experimental spinal cord injury in rats.* Pediatr Neurosurg, 2011. **47**(4): p. 254-60.

134. Suzuki, K., et al., *Experimental study on the protective effects of edaravone against ischemic spinal cord injury.* J Thorac Cardiovasc Surg, 2005. **130**(6): p. 1586-92.

135. Araki, Y., A. Andoh, and Y. Fujiyama, *The free radical scavenger edaravone suppresses experimental dextran sulfate sodium-induced colitis in rats.* Int J Mol Med, 2003. **12**(1): p. 125-9.

136. Araki, Y., H. Sugihara, and T. Hattori, *The free radical scavengers edaravone and tempol suppress experimental dextran sulfate sodium-induced colitis in mice.* Int J Mol Med, 2006. **17**(2): p. 331-4.

137. Arii, K., et al., *Edaravone inhibits the disease activity in rheumatoid arthritis.* J Clin Pharm Ther, 2006. **31**(2): p. 197-9.
138. Arii, K., et al., *Edaravone inhibits rheumatoid synovial cell proliferation and migration.* Free Radic Res, 2006. **40**(2): p. 121-5.
139. Arii, K., et al., *Edaravone inhibits collagen-induced arthritis possibly through suppression of nuclear factor-kappa B.* Mol Immunol, 2008. **45**(2): p. 463-9.
140. Arumugam, S., et al., *Beneficial effects of edaravone, a novel antioxidant, in rats with dilated cardiomyopathy.* J Cell Mol Med, 2012. **16**(9): p. 2176-85.
141. Fukuda, A., et al., *Cardioprotective effect of edaravone against ischaemia-reperfusion injury in the rabbit heart before, during and after reperfusion treatment.* J Int Med Res, 2006. **34**(5): p. 475-84.
142. Yagi, H., S. Horinaka, and H. Matsuoka, *Edaravone prevented deteriorated cardiac function after myocardial ischemia-reperfusion via inhibiting lipid peroxidation in rat.* J Cardiovasc Pharmacol, 2005. **46**(1): p. 46-51.
143. Zhang, W., et al., *Effects of edaravone on the expression of beta-defensin-2 mRNA in lung tissue of rats with myocardial ischemia reperfusion.* Mol Med Rep, 2013. **7**(5): p. 1683-7.
144. Zhang, Y.M., et al., *[Cardioprotective effect of edaravone pharmacological postconditioning on acute myocardial ischemia/reperfusion injury: experiment with rats]*. Zhonghua Yi Xue Za Zhi, 2008. **88**(36): p. 2558-61.
145. Sueishi, K., et al., *Protection by a radical scavenger edaravone against cisplatin-induced nephrotoxicity in rats.* Eur J Pharmacol, 2002. **451**(2): p. 203-8.
146. Hishida, A., *Determinants for the prognosis of acute renal disorders that developed during or after treatment with edaravone.* Clin Exp Nephrol, 2009. **13**(2): p. 118-22.
147. Iguchi, T., et al., *Edaravone inhibits acute renal injury and cyst formation in cisplatin-treated rat kidney.* Free Radic Res, 2004. **38**(4): p. 333-41.
148. Li, Y., A.Z. Xia, and S.H. Xing, *Protective effect of edaravone against renal ischemia/reperfusion injury and compared with ischemic postconditioning in rats.* Yao Xue Xue Bao, 2010. **45**(7): p. 840-8.
149. Matsuyama, M., et al., *Treatment with edaravone improves the survival rate in renal warm ischemia-reperfusion injury using rat model.* Transplant Proc, 2006. **38**(7): p. 2199-200.

150. Tahara, M., et al., *A radical scavenger, edaravone, protects canine kidneys from ischemia-reperfusion injury after 72 hours of cold preservation and autotransplantation.* Transplantation, 2005. **80**(2): p. 213-21.

151. Tsukamoto, Y., et al., *Effect of edaravone on the estimated glomerular filtration rate in patients with acute ischemic stroke and chronic kidney disease.* J Stroke Cerebrovasc Dis, 2011. **20**(2): p. 111-6.

152. Zhang, G., Q.P. Xu, and H.Y. Huang, *[Protective effects of edaravone on renal ischemia-reperfusion injury in rats]*. Zhejiang Da Xue Xue Bao Yi Xue Ban, 2008. **37**(3): p. 308-11.

153. Itoh, T., et al., *The novel free radical scavenger, edaravone, increases neural stem cell number around the area of damage following rat traumatic brain injury.* Neurotox Res, 2009. **16**(4): p. 378-89.

154. Miyamoto, K., et al., *Therapeutic time window for edaravone treatment of traumatic brain injury in mice.* Biomed Res Int, 2013. **2013**: p. 379206.

155. Ohta, M., et al., *Attenuation of axonal injury and oxidative stress by edaravone protects against cognitive impairments after traumatic brain injury.* Brain Res, 2013. **1490**: p. 184-92.

156. Wang, G.H., et al., *Free-radical scavenger edaravone treatment confers neuroprotection against traumatic brain injury in rats.* J Neurotrauma, 2011. **28**(10): p. 2123-34.

157. Zhao, Y.N., et al., *[Effect of edaravone on extracellular signal-regulated kinase 1/2 pathway following severe traumatic brain injury in rats]*. Zhongguo Wei Zhong Bing Ji Jiu Yi Xue, 2010. **22**(4): p. 230-3.

158. Fukudome, D., et al., *The radical scavenger edaravone counteracts diabetes in multiple low-dose streptozotocin-treated mice.* Eur J Pharmacol, 2008. **583**(1): p. 164-9.

159. Hayashi, T., et al., *Efficacy of edaravone, a free radical scavenger, on left ventricular function and structure in diabetes mellitus.* J Cardiovasc Pharmacol, 2003. **41**(6): p. 923-9.

160. Srinivasan, K. and S.S. Sharma, *Edaravone Offers Neuroprotection in a Diabetic Stroke Model via Inhibition of Endoplasmic Reticulum Stress.* Basic Clin Pharmacol Toxicol, 2011.

161. Tsounapi, P., et al., *Antioxidant treatment with edaravone or taurine ameliorates diabetes-induced testicular dysfunction in the rat.* Mol Cell Biochem, 2012. **369**(1-2): p. 195-204.

162. Li, B., D. Yu, and Z. Xu, *Edaravone prevents neurotoxicity of mutant L166P DJ-1 in Parkinson's disease.* J Mol Neurosci, 2013. **51**(2): p. 539-49.
163. Xiong, N., et al., *Edaravone guards dopamine neurons in a rotenone model for Parkinson's disease.* PLoS One, 2011. **6**(6): p. e20677.
164. Yuan, W.J., et al., *Neuroprotective effects of edaravone-administration on 6-OHDA-treated dopaminergic neurons.* BMC Neurosci, 2008. **9**: p. 75.
165. Imai, S., et al., *Systemic administration of a free radical scavenger, edaravone, protects against light-induced photoreceptor degeneration in the mouse retina.* Eur J Pharmacol, 2010. **642**(1-3): p. 77-85.
166. Kamida, T., et al., *Edaravone, a free radical scavenger, retards the development of amygdala kindling in rats.* Neurosci Lett, 2009. **461**(3): p. 298-301.
167. Wang, H.P., X.L. Deng, and G.Q. Li, *[Effects of edaravone on the expression of interleukin-1beta, nuclear factor-kappaB and neuron apoptosis in juvenile rat hippocampus after status convulsion]*. Zhonghua Er Ke Za Zhi, 2009. **47**(8): p. 575-80.
168. Asai, T., et al., *The specific free radical scavenger edaravone suppresses bleomycin-induced acute pulmonary injury in rabbits.* Clin Exp Pharmacol Physiol, 2007. **34**(1-2): p. 22-6.
169. Ito, K., H. Ozasa, and S. Horikawa, *Edaravone protects against lung injury induced by intestinal ischemia/reperfusion in rat.* Free Radic Biol Med, 2005. **38**(3): p. 369-74.
170. Tajima, S., et al., *Effects of edaravone, a free-radical scavenger, on bleomycin-induced lung injury in mice.* Eur Respir J, 2008. **32**(5): p. 1337-43.
171. Tajima, S., et al., *Preventive effects of edaravone, a free radical scavenger, on lipopolysaccharide-induced lung injury in mice.* Respirology, 2008. **13**(5): p. 646-53.
172. Wang, C., et al., *Targeting reactive oxygen species by edaravone inhalation in a rat hyperoxic lung injury model: role of inflammasome.* Undersea Hyperb Med, 2013. **40**(6): p. 505-11.
173. Zhi, Q., et al., *Edaravone, a novel antidote against lung injury and pulmonary fibrosis induced by paraquat?* Int Immunopharmacol, 2011. **11**(1): p. 96-102.
174. Kara, M., et al., *The effect of edaravone on ischemia-reperfusion injury in rat ovary.* Eur J Obstet Gynecol Reprod Biol, 2012. **162**(2): p. 197-202.
175. Koizumi, T., et al., *The therapeutic efficacy of edaravone in extensively burned rats.* Arch Surg, 2006. **141**(10): p. 992-5.
176. Li, G.Y., et al., *Edaravone, a novel free radical scavenger, prevents steroid-induced osteonecrosis in rabbits.* Rheumatology (Oxford), 2013. **52**(3): p. 438-47.

177. Gao, G., et al., *[Edaravone protects hearing from acute acoustic trauma in guinea pigs]*. Zhonghua Er Bi Yan Hou Tou Jing Wai Ke Za Zhi, 2009. **44**(2): p. 150-3.
178. Inoue, Y., et al., *Effect of edaravone on acute brainstem-cerebellar infarction with vertigo and sudden hearing loss.* Auris Nasus Larynx, 2013.
179. Asplund, M.S., et al., *Protective effect of edaravone against tobramycin-induced ototoxicity.* Acta Otolaryngol, 2009. **129**(1): p. 8-13.
180. Maekawa, H., et al., *Therapeutic effect of edaravone on inner ear barotrauma in the guinea pig.* Neurochem Int, 2009. **54**(8): p. 513-8.
181. Sano, H., et al., *Edaravone, a free radical scavenger, in the treatment of idiopathic sudden sensorineural hearing loss with profound hearing loss.* Auris Nasus Larynx, 2010. **37**(1): p. 42-6.
182. Takumida, M. and M. Anniko, *Protective effect of edaravone against the ototoxicity of Pseudomonas aeruginosa exotoxin A.* Acta Otolaryngol, 2006. **126**(1): p. 15-9.
183. Hong, S.J., et al., *Protective effects of edaravone against cisplatin-induced hair cell damage in zebrafish.* Int J Pediatr Otorhinolaryngol, 2013. **77**(6): p. 1025-31.
184. Takeda, T., et al., *Protective effects of edaravone against ischemia-induced facial palsy.* Auris Nasus Larynx, 2008. **35**(3): p. 321-7.
185. Horiike, O., et al., *Protective effect of edaravone against streptomycin-induced vestibulotoxicity in the guinea pig.* Eur J Pharmacol, 2003. **464**(1): p. 75-8.
186. Yoshida, H., et al., *Edaravone, a novel radical scavenger, inhibits oxidative modification of low-density lipoprotein (LDL) and reverses oxidized LDL-mediated reduction in the expression of endothelial nitric oxide synthase.* Atherosclerosis, 2005. **179**(1): p. 97-102.
187. Xiao, B., et al., *Edaravone neuroprotection effected by suppressing the gene expression of the Fas signal pathway following transient focal ischemia in rats.* Neurotoxicity research, 2007. **12**(3): p. 155-62.
188. Yan, Y., et al., *Protective effect of edaravone against Alzheimer's disease-relevant insults in neuroblastoma N2a cells.* Neuroscience letters, 2012. **531**(2): p. 160-5.
189. Wen, J., et al., *Edaravone inhibits JNK-c-Jun pathway and restores anti-oxidative defense after ischemia-reperfusion injury in aged rats.* Biological & pharmaceutical bulletin, 2006. **29**(4): p. 713-8.
190. Yoshino, H. and A. Kimura, *Investigation of the therapeutic effects of edaravone, a free radical scavenger, on amyotrophic lateral sclerosis (Phase II study).* Amyotrophic

lateral sclerosis : official publication of the World Federation of Neurology Research Group on Motor Neuron Diseases, 2006. **7**(4): p. 241-5.

191. Kikuchi, K., et al., *Beyond free radical scavenging: Beneficial effects of edaravone (Radicut) in various diseases (Review).* Experimental and therapeutic medicine, 2012. **3**(1): p. 3-8.
192. Yuan, W.J., et al., *Neuroprotective effects of edaravone-administration on 6-OHDA-treated dopaminergic neurons.* BMC neuroscience, 2008. **9**: p. 75.
193. Yan, Y., et al., *Protective effect of edaravone against Alzheimer's disease-relevant insults in neuroblastoma N2a cells.* Neurosci Lett, 2012. **531**(2): p. 160-5.
194. Shen, Y.E., et al., *Effects of edaravone on amyloid-beta precursor protein processing in SY5Y-APP695 cells.* Neurotox Res, 2013. **24**(2): p. 139-47.
195. He, F., et al., *Inhibitory effects of edaravone in beta-amyloid-induced neurotoxicity in rats.* Biomed Res Int, 2014. **2014**: p. 370368.
196. Zhou, S., et al., *Neuroprotective effects of edaravone on cognitive deficit, oxidative stress and tau hyperphosphorylation induced by intracerebroventricular streptozotocin in rats.* Neurotoxicology, 2013. **38**: p. 136-45.
197. Yang, R., et al., *Edaravone injection ameliorates cognitive deficits in rat model of Alzheimer's disease.* Neurol Sci, 2015. **36**(11): p. 2067-72.
198. Iwase, T., et al., *Thirty-day intravenous toxicity study of MCI-186 in beagle dogs.* JPN PHARMACOL THER, 1997. **25**(7): p. 39-56.
199. Dalgard, D.W., et al., *Twenty six-week intravenous toxicity study of MCI-186 in beagle dogs with a recovery period of 5-week.* JPN PHARMACOL THER, 1997. **25**(7): p. 79-104.
200. Iwase, T. and H. Inoue, *Reproductive and developmental toxicity study of MCI-186 (I) - A study on intravenous administration of MCI-186 prior to and in the early stages of pregnancy in rats.* . JPN PHARMACOL THER, 1997. **25**(7): p. 105-114.
201. Ishida, S., M. Ikeya, and T. Iwase, *Reproductive and developmental toxicity study of MCI-186 (II) - A study on intravenous administration of MCI-186 during the period of organogenesis in rats.* JPN PHARMACOL THER, 1997. **25**(7): p. 115-130.
202. Iwase, T., I. Toyonaga, and H. Inoue, *Reproductive and developmental toxicity study of MCI-186 (III) - A study on intravenous administration of MCI-186 during the period of organogenesis in rabbits.* JPN PHARMACOL THER, 1997. **25**(7): p. 131-137.
203. Iwase, Y., et al., *Mutagenicity study on MCI-186.* . JPN PHARMACOL THER, 1997 **25**(7): p. 173-180.

204. Bicun Product Detail. 2009, Simcere: China.
205. Kawaguchi, H., N. Tsutsui, and H. Inoue, *Antigenicity study on MCI-186.* . JPN PHARMACOL THER, 1997 **25**(7): p. 163-172.
206. Baba, N. and M. Miura, *The single dose toxicity study of MCI-186.* JPN PHARMACOL THER, 1997. **25 Suppl. 7** p. 7-20.
207. Abe, K., et al., *Confirmatory double-blind, parallel-group, placebo-controlled study of efficacy and safety of edaravone (MCI-186) in amyotrophic lateral sclerosis patients.* Amyotroph Lateral Scler Frontotemporal Degener, 2014. **15**(7-8): p. 610-7.
208. RADICUT Injection 30mg Package Insert. 2013, Mitsubishi Tanabe Pharma Corporation: Japan.
209. Otomo, E., et al., *Clinical efficacy of a free radical scavenger, MCI-186 on acute cerebral infarction - Early phase II clinical trial.* THER RES, 1998. **19**(4): p. 531-552.
210. Watanabe T, T.M.a.T.S., *The Novel Antioxidant Edaravone: From Bench to Bedside.* Cardiovascular Therapeutics, 2008. **26**(2): p. 101–114.
211. Bala, V., et al., *Enabling Oral SN38-Based Chemotherapy with a Combined Lipophilic Prodrug and Self-Microemulsifying Drug Delivery System.* Mol Pharm, 2016. **13**(10): 3518-25.
212. Kikuchi, K., et al., *Beyond free radical scavenging: Beneficial effects of edaravone (Radicut) in various diseases (Review).* Exp Ther Med, 2012. **3**(1): p. 3-8.
213. Jian Zeng, Y.R., Chengliang Zhou, Shuqin Yu, Wen-Hua Chen, *Preparation and physicochemical characteristics of the complex of edaravone with hydroxypropyl-b-cyclodextrin.* Carbohydrate Polymers, 2011. **83**: p. 5.
214. Ma, L., et al., *Glucuronidation of edaravone by human liver and kidney microsomes: biphasic kinetics and identification of UGT1A9 as the major UDP-glucuronosyltransferase isoform.* Drug Metab Dispos, 2012. **40**(4): p. 734-41.
215. Li, H., et al., *Phase I clinical study of edaravone in healthy Chinese volunteers: safety and pharmacokinetics of single or multiple intravenous infusions.* Drugs R D, 2012. **12**(2): p. 65-70.
216. Aggarwal., S.P.a.B.B., *Chapter 13 Turmeric, the Golden Spice: From Traditional Medicine to Modern Medicine,* in *Herbal Medicine: Biomolecular and Clinical Aspects*, W.-G.S. Benzie IFF, Editor. 2011, CRC Press/Taylor & Francis.
217. Gupta, S.C., et al., *Multitargeting by turmeric, the golden spice: From kitchen to clinic.* Mol Nutr Food Res, 2013. **57**(9): p. 1510-28.

218. Andrew M. Anderson, M.S.M., and Ram S. Mohan, *Isolation of Curcumin from Turmeric.* Journal of chemical education, 2000. **77**(3): p. 359.
219. Priyadarsini, K.I., *The chemistry of curcumin: from extraction to therapeutic agent.* Molecules, 2014. **19**(12): p. 20091-112.
220. Trujillo, J., et al., *Renoprotective effect of the antioxidant curcumin: Recent findings.* Redox Biol, 2013. **1**: p. 448-56.
221. Douglass, B.J. and D.L. Clouatre, *Beyond Yellow Curry: Assessing Commercial Curcumin Absorption Technologies.* J Am Coll Nutr, 2015. **34**(4): p. 347-58.
222. Panahi, Y., et al., *Short-term Curcuminoid Supplementation for Chronic Pulmonary Complications due to Sulfur Mustard Intoxication: Positive Results of a Randomized Double-blind Placebo-controlled Trial.* Drug Res (Stuttg), 2015. **65**(11): p. 567-73.
223. Mishra, S. and K. Palanivelu, *The effect of curcumin (turmeric) on Alzheimer's disease: An overview.* Ann Indian Acad Neurol, 2008. **11**(1): p. 13-9.
224. Gupta, S.C., et al., *Discovery of curcumin, a component of golden spice, and its miraculous biological activities.* Clin Exp Pharmacol Physiol, 2012. **39**(3): p. 283-99.
225. Prasad, S., et al., *Curcumin, a component of golden spice: from bedside to bench and back.* Biotechnol Adv, 2014. **32**(6): p. 1053-64.
226. Ghalandarlaki, N., A.M. Alizadeh, and S. Ashkani-Esfahani, *Nanotechnology-applied curcumin for different diseases therapy.* Biomed Res Int, 2014. **2014**: p. 394264.
227. Bose, S., et al., *Curcumin and tumor immune-editing: resurrecting the immune system.* Cell Div, 2015. **10**: p. 6.
228. Jitoe-Masuda, A., A. Fujimoto, and T. Masuda, *Curcumin: from chemistry to chemistry-based functions.* Curr Pharm Des, 2013. **19**(11): p. 2084-92.
229. Subash C. Gupta, S.P., Ji Hye Kim, Sridevi Patchva, Lauren J. Webb, Indira K. Priyadarsini, and Bharat B. Aggarwala, *Multitargeting by curcumin as revealed by molecular interaction studies.* Natural Product Reports, 2011. **28**(12): p. 1937–1955.
230. Lee, W.H., et al., *Curcumin and its derivatives: their application in neuropharmacology and neuroscience in the 21st century.* Curr Neuropharmacol, 2013. **11**(4): p. 338-78.
231. Zhou, H., C.S. Beevers, and S. Huang, *The targets of curcumin.* Curr Drug Targets, 2011. **12**(3): p. 332-47.
232. Sa, G. and T. Das, *Anti cancer effects of curcumin: cycle of life and death.* Cell Div, 2008. **3**: p. 14.

233. Orlando, R.A., et al., *A chemical analog of curcumin as an improved inhibitor of amyloid Abeta oligomerization.* PLoS One, 2012. **7**(3): p. e31869.
234. Gupta, S.C., S. Patchva, and B.B. Aggarwal, *Therapeutic roles of curcumin: lessons learned from clinical trials.* AAPS J, 2013. **15**(1): p. 195-218.
235. Thapa, A., S.D. Jett, and E.Y. Chi, *Curcumin Attenuates Amyloid-beta Aggregate Toxicity and Modulates Amyloid-beta Aggregation Pathway.* ACS Chem Neurosci, 2016. **7**(1): p. 56-68.
236. Yang, F., et al., *Curcumin inhibits formation of amyloid beta oligomers and fibrils, binds plaques, and reduces amyloid in vivo.* J Biol Chem, 2005. **280**(7): p. 5892-901.
237. Cole, G.M., B. Teter, and S.A. Frautschy, *Neuroprotective effects of curcumin.* Adv Exp Med Biol, 2007. **595**: p. 197-212.
238. Hamaguchi, T., K. Ono, and M. Yamada, *REVIEW: Curcumin and Alzheimer's disease.* CNS Neurosci Ther, 2010. **16**(5): p. 285-97.
239. Ahmed, T. and A.H. Gilani, *Inhibitory effect of curcuminoids on acetylcholinesterase activity and attenuation of scopolamine-induced amnesia may explain medicinal use of turmeric in Alzheimer's disease.* Pharmacol Biochem Behav, 2009. **91**(4): p. 554-9.
240. Akinyemi, A.J., et al., *Anti-amnestic Effect of Curcumin in Combination with Donepezil, an Anticholinesterase Drug: Involvement of Cholinergic System.* Neurotox Res, 2017.
241. Ringman, J.M., et al., *A potential role of the curry spice curcumin in Alzheimer's disease.* Curr Alzheimer Res, 2005. **2**(2): p. 131-6.
242. Begum, A.N., et al., *Curcumin structure-function, bioavailability, and efficacy in models of neuroinflammation and Alzheimer's disease.* J Pharmacol Exp Ther, 2008. **326**(1): p. 196-208.
243. He, Y., et al., *Curcumin, inflammation, and chronic diseases: how are they linked?* Molecules, 2015. **20**(5): p. 9183-213.
244. Basnet, P. and N. Skalko-Basnet, *Curcumin: an anti-inflammatory molecule from a curry spice on the path to cancer treatment.* Molecules, 2011. **16**(6): p. 4567-98.
245. Velusami, C.C., et al., *Safety evaluation of turmeric polysaccharide extract: assessment of mutagenicity and acute oral toxicity.* Biomed Res Int, 2013. **2013**: p. 158348.
246. Aggarwal, B.B. and K.B. Harikumar, *Potential therapeutic effects of curcumin, the anti-inflammatory agent, against neurodegenerative, cardiovascular, pulmonary, metabolic, autoimmune and neoplastic diseases.* Int J Biochem Cell Biol, 2009. **41**(1): p. 40-59.

247. Hamid Reza Rahimi, M.R.J., Amir Hooshang Mohammadpour, Khalil Abnous, Majid Ghayour-Mobarhan, Elahe Ramezanzadeh, Fateme Mousavi, Reza Kazemi Oskuee, *Curcumin: Reintroduced Therapeutic Agent from Traditional Medicine for Alcoholic Liver Disease* Asia pacific journal of medical toxicology, 2015. **4**(1): p. 25-30.

248. Bae, Y.H. and K. Park, *Targeted drug delivery to tumors: myths, reality and possibility.* J Control Release, 2011. **153**(3): p. 198-205.

249. Seo, S.W., et al., *Preparation and pharmacokinetic evaluation of curcumin solid dispersion using Solutol(R) HS15 as a carrier.* Int J Pharm, 2012. **424**(1-2): p. 18-25.

250. Vaage, J., et al., *Tissue distribution and therapeutic effect of intravenous free or encapsulated liposomal doxorubicin on human prostate carcinoma xenografts.* Cancer, 1994. **73**(5): p. 1478-84.

251. Bischoff, S.C., et al., *Intestinal permeability--a new target for disease prevention and therapy.* BMC Gastroenterol, 2014. **14**: p. 189.

252. Anand, P., et al., *Bioavailability of curcumin: problems and promises.* Mol Pharm, 2007. **4**(6): p. 807-18.

253. Tonnesen, H.H., M. Masson, and T. Loftsson, *Studies of curcumin and curcuminoids. XXVII. Cyclodextrin complexation: solubility, chemical and photochemical stability.* Int J Pharm, 2002. **244**(1-2): p. 127-35.

254. Schneider, C., et al., *Degradation of Curcumin: From Mechanism to Biological Implications.* J Agric Food Chem, 2015. **63**(35): p. 7606-14.

255. Hu, L., et al., *Enhancement of Oral Bioavailability of Curcumin by a Novel Solid Dispersion System.* AAPS PharmSciTech, 2015. **16**(6): p. 1327-34.

256. Grynkiewicz, G. and P. Slifirski, *Curcumin and curcuminoids in quest for medicinal status.* Acta Biochim Pol, 2012. **59**(2): p. 201-12.

257. Wahlang, B., Y.B. Pawar, and A.K. Bansal, *Identification of permeability-related hurdles in oral delivery of curcumin using the Caco-2 cell model.* Eur J Pharm Biopharm, 2011. **77**(2): p. 275-82.

258. Thangavel, S., et al., *Redox nanoparticles inhibit curcumin oxidative degradation and enhance its therapeutic effect on prostate cancer.* J Control Release, 2015. **209**: p. 110-9.

259. Suresh D.Kumavat, Y.S.C., Priyanka Borole, Preetesh Mishra, Khusbu Shenghani, Pallavi Duvvuri, *Degradation studies of curcumin.* International Journal of Pharmacy Review & Research, 2013. **3**(2): p. 50-55.

260. Wang, Y.J., et al., *Stability of curcumin in buffer solutions and characterization of its degradation products.* J Pharm Biomed Anal, 1997. **15**(12): p. 1867-76.

261. Loganathan Palanikumar, N.P., *Curcumin: A putative chemopreventive agent.* Journal of Life Sciences, 2009. **3**(5): p. 47-53.

262. Zebib, B., Z. Mouloungui, and V. Noirot, *Stabilization of curcumin by complexation with divalent cations in glycerol/water system.* Bioinorg Chem Appl, 2010: p. 292760.

263. Shen, L. and H.F. Ji, *The pharmacology of curcumin: is it the degradation products?* Trends Mol Med, 2012. **18**(3): p. 138-44.

264. Min-Hsiung Pan, T.-M.H., and Jen-Kun Lin, *Biotransformation of curcumin through reduction and glucuronidation in mice.* Drug metabolism and disposition, 1999. **27**(1): p. 486-494.

265. Prasad, S., A.K. Tyagi, and B.B. Aggarwal, *Recent developments in delivery, bioavailability, absorption and metabolism of curcumin: the golden pigment from golden spice.* Cancer Res Treat, 2014. **46**(1): p. 2-18.

266. Grill, A.E., B. Koniar, and J. Panyam, *Co-delivery of natural metabolic inhibitors in a self-microemulsifying drug delivery system for improved oral bioavailability of curcumin.* Drug Deliv Transl Res, 2014. **4**(4): p. 344-52.

267. Sharma, R.A., et al., *Pharmacodynamic and pharmacokinetic study of oral Curcuma extract in patients with colorectal cancer.* Clin Cancer Res, 2001. **7**(7): p. 1894-900.

268. Lao, C.D., et al., *Dose escalation of a curcuminoid formulation.* BMC Complement Altern Med, 2006. **6**: p. 10.

269. Farooqui, A.A., *Therapeutic Potentials of Curcumin for Alzheimer Disease*. 2016, Springer International Publishing: Switzerland. p. XIX, 402.

270. Judy Gopal, M.M.a.S.-C.C., *One-step, ultrasonication-mobilized, solvent-free extraction/synthesis of nanocurcumin from turmeric*. RSC Advances, 2015. **5**: p. 48391-48398.

271. Sharma, R.A., et al., *Phase I clinical trial of oral curcumin: biomarkers of systemic activity and compliance.* Clin Cancer Res, 2004. **10**(20): p. 6847-54.

272. RevGenetics. *MetaCurcumin: Super Curcumin*. 2016 [cited 2016 10 June]; Available from: https://www.revgenetics.com/store/c-1-metacurcumin-super-curcumin.aspx.

273. LLC, M.H.T. *NovaSOL® Curcumin*. 2014 [cited 2016 1 June]; Available from: http://novasolcurcumin.com/.

274. Tonics, N. *What is Curcumin*. 2014 [cited 2016 2 June]; Available from: http://nanolifetonics.com/curcusome/what-is-curcumin.

275. Health, S. *Optimal Liposomal Curcumin - 6 oz*. 2014 [cited 2016 2 June 2016]; Available from: http://www.seekinghealth.com/optimal-liposomal-curcumin-6-oz.html.
276. Zealand, B.N. *Liposomal Turmeric Complex*. 2016 [cited 2016 2 June 2016]; Available from: http://www.biobalance.co.nz/product/liposomal-turmeric-complex/.
277. Labs, E. *Liposomal curcumin/resveratrol*. 2016; Available from: http://www.empirical-labs.com/vitamins-supplements/liposomal-curcumin-resveratrol/.
278. Items, H. *Liposomal curcumin 16 fluid ounces*. 2007; Available from: http://www.healthyitems.com/curcumin-p/607.htm.
279. Indena. *Meriva® Bioavailable curcumin*. 2014 [cited 2016 5 June]; Available from: http://www.meriva.info/en/.
280. Corporation, T. *Theracurmin® — Our unique form of curcumin with markedly improved absorptivity*. 2015 [cited 2016 2 June]; Available from: http://theravalues.com/english/2015/10/21/theracurmin-highly-bioavailable-curcumin/.
281. Nutrition, O.P. *Nano Curcusorb – Powerful Natural Anti-inflammatory & Pain Reliever from Curcumin*. [cited 2016 5 June]; Available from: https://oneplanetnutrition.com/product/nano-curcusorb-variations/.
282. Asia, N.C. *Nano Curcumin Elixir*. 2016 [cited 2016 10 June]; Available from: http://www.nanocurcumin.asia/.
283. Sciences, V. *Longvida® Optimized Curcumin*. 2016 [cited 2016 5 June]; Available from: http://www.longvida.com/.
284. Inc, S. *Full Spectrum Curcumin*. 2016 [cited 2016 2 June]; Available from: http://www.solgar.com/SolgarProducts/Full-Spectrum-Curcumin.htm.
285. Technologies, O.H. *CurcuWIN*. 2016 [cited 2016 2 June]; Available from: http://omniactives.com/curcuwin.
286. AG, W.C. *Highly bioavailable curcumin*. 2016 [cited 2016 2 June]; Available from: http://www.wacker.com/cms/en/industries/food/curcumin.jsp.
287. Feng, Y. and X. Wang, *Antioxidant therapies for Alzheimer's disease.* Oxid Med Cell Longev, 2012. **2012**: p. 472932.
288. Galasko, D.R., et al., *Antioxidants for Alzheimer disease: a randomized clinical trial with cerebrospinal fluid biomarker measures.* Arch Neurol, 2012. **69**(7): p. 836-41.

289. Bharate, S.S. and R.A. Vishwakarma, *Impact of preformulation on drug development.* Expert Opin Drug Deliv, 2013. **10**(9): p. 1239-57.

290. Allen, L.V., Jr., *Dosage form design and development.* Clin Ther, 2008. **30**(11): p. 2102-11.

291. R.Gopinath and R.A.S. Naidu, *Pharmaceutical Preformulation Studies – Current Review.* International Journal of Pharmaceutical & Biological Archives, 2011. **2**(5): p. 1391-1400.

292. Amita Tilak, et al., *Significance of preformulation studies in designing, fabricating for pharmaceutical dosage forms.* Journal of Biomedical and Pharmaceutical Research, 2015. **4**(6): p. 35-45.

293. Ayad, M.H., et al., *Amorphous solid dispersion successfully improved oral exposure of ADX71943 in support of toxicology studies.* Drug Dev Ind Pharm, 2013. **39**(9): p. 1300-5.

294. Kawakami, K., *Modification of physicochemical characteristics of active pharmaceutical ingredients and application of supersaturatable dosage forms for improving bioavailability of poorly absorbed drugs.* Adv Drug Deliv Rev, 2012. **64**(6): p. 480-95.

295. Sato, T., K. Mizuno, and F. Ishii, *A novel administration route of edaravone--II: mucosal absorption of edaravone from edaravone/hydroxypropyl-beta-cyclodextrin complex solution including L-cysteine and sodium hydrogen sulfite.* Pharmacology, 2010. **85**(2): p. 88-94.

296. Sato, T., K. Mizuno, and F. Ishii, *A novel administration route for edaravone: I. Effects of metabolic inhibitors on skin permeability of edaravone.* Int J Pharm, 2009. **372**(1-2): p. 33-8.

297. Chuah, A.M., et al., *Enhanced bioavailability and bioefficacy of an amorphous solid dispersion of curcumin.* Food Chem, 2014. **156**: p. 227-33.

298. Paradkar, A., et al., *Characterization of curcumin-PVP solid dispersion obtained by spray drying.* Int J Pharm, 2004. **271**(1-2): p. 281-6.

299. Panigrahi, A.K.N.a.P.P., *Solubility Enhancement of Etoricoxib by Cosolvency Approach.* ISRN Physical Chemistry, 2012. **2012**: p. 5.

300. Liu, F., et al., *Patient-centred pharmaceutical design to improve acceptability of medicines: similarities and differences in paediatric and geriatric populations.* Drugs, 2014. **74**(16): p. 1871-89.

301. Fatouros, D.G., et al., *Clinical studies with oral lipid based formulations of poorly soluble compounds.* Ther Clin Risk Manag, 2007. **3**(4): p. 591-604.
302. Y.V. Rama Prasad, S.P.P., Sudarat Eaimtrakarn, Makoto Ishida, Yukako Yoshikawa, Nobuhito Shibata, Kanji Takada, *Enhanced intestinal absorption of vancomycin with Labrasol and D-a-tocopheryl PEG 1000 succinate in rats.* International Journal of Pharmaceutics, 2003. **250**: p. 10.
303. Rama Prasad, Y.V., et al., *In situ intestinal absorption studies on low molecular weight heparin in rats using Labrasol as absorption enhancer.* International Journal of Pharmaceutics, 2004. **271**(1-2): p. 225-232.
304. Rama Prasad, Y.V., et al., *Evaluation of oral formulations of gentamicin containing labrasol in beagle dogs.* International Journal of Pharmaceutics, 2003. **268**(1-2): p. 13-21.
305. Ma, L., et al., *Effects of Pluronic F68 and Labrasol on the intestinal absorption and pharmacokinetics of rifampicin in rats.* Arch Pharm Res, 2011. **34**(11): p. 1939-43.
306. Zhou, J., et al., *Involvement of the inhibition of intestinal glucuronidation in enhancing the oral bioavailability of resveratrol by labrasol containing nanoemulsions.* Mol Pharm, 2015. **12**(4): p. 1084-95.
307. Koga, K., et al., *Enhancing mechanism of Labrasol on intestinal membrane permeability of the hydrophilic drug gentamicin sulfate.* Eur J Pharm Biopharm, 2006. **64**(1): p. 82-91.
308. Shah, S.M., et al., *Preclinical formulations: insight, strategies, and practical considerations.* AAPS PharmSciTech, 2014. **15**(5): p. 1307-23.
309. Strickley, R.G., *Solubilizing Excipients in Oral and Injectable Formulations.* Pharmaceutical Research, 2004. **21**(2): p. 30.
310. Dixit, A.R., S.J. Rajput, and S.G. Patel, *Preparation and bioavailability assessment of SMEDDS containing valsartan.* AAPS PharmSciTech, 2010. **11**(1): p. 314-21.
311. Wu, L., et al., *A Self-microemulsifying Drug Delivery System (SMEDDS) for a Novel Medicative Compound Against Depression: a Preparation and Bioavailability Study in Rats.* AAPS PharmSciTech, 2015. **16**(5): p. 1051-8.
312. Yeom, D.W., et al., *Development and optimization of a self-microemulsifying drug delivery system for atorvastatin calcium by using D-optimal mixture design.* Int J Nanomedicine, 2015. **10**: p. 3865-77.

313. Bi, X., et al., *Improved Oral Bioavailability Using a Solid Self-Microemulsifying Drug Delivery System Containing a Multicomponent Mixture Extracted from Salvia miltiorrhiza.* Molecules, 2016. **21**(4): p. 456.
314. Yeom, D.W., et al., *Development of a solidified self-microemulsifying drug delivery system (S-SMEDDS) for atorvastatin calcium with improved dissolution and bioavailability.* Int J Pharm, 2016. **506**(1-2): p. 302-11.
315. Oh, D.H., et al., *Comparison of solid self-microemulsifying drug delivery system (solid SMEDDS) prepared with hydrophilic and hydrophobic solid carrier.* Int J Pharm, 2011. **420**(2): p. 412-8.
316. Hoosain, F.G., et al., *Bypassing P-Glycoprotein Drug Efflux Mechanisms: Possible Applications in Pharmacoresistant Schizophrenia Therapy.* Biomed Res Int, 2015. **2015**: p. 484963.
317. Zhang, W., et al., *The Effects of Pharmaceutical Excipients on Gastrointestinal Tract Metabolic Enzymes and Transporters-an Update.* AAPS J, 2016. **18**(4): p. 830-43.
318. Singh, A.K., et al., *Oral bioavailability enhancement of exemestane from self-microemulsifying drug delivery system (SMEDDS).* AAPS PharmSciTech, 2009. **10**(3): p. 906-16.
319. Balakrishnan, P., et al., *Enhanced oral bioavailability of Coenzyme Q10 by self-emulsifying drug delivery systems.* Int J Pharm, 2009. **374**(1-2): p. 66-72.
320. Kim, G.G., et al., *Enhancement of oral bioavailability of fenofibrate by solid self-microemulsifying drug delivery systems.* Drug Dev Ind Pharm, 2013. **39**(9): p. 1431-8.
321. Wais, U., et al., *Nanoformulation and encapsulation approaches for poorly water-soluble drug nanoparticles.* Nanoscale, 2016. **8**(4): p. 1746-69.
322. Huang, Y. and W.G. Dai, *Fundamental aspects of solid dispersion technology for poorly soluble drugs.* Acta Pharm Sin B, 2014. **4**(1): p. 18-25.
323. Onoue, S., et al., *Self-micellizing solid dispersion of cyclosporine A with improved dissolution and oral bioavailability.* Eur J Pharm Sci, 2014. **62**: p. 16-22.
324. Mendonca, L.M., et al., *Comparative study of curcumin and curcumin formulated in a solid dispersion: Evaluation of their antigenotoxic effects.* Genet Mol Biol, 2015. **38**(4): p. 490-8.
325. Vo, C.L., C. Park, and B.J. Lee, *Current trends and future perspectives of solid dispersions containing poorly water-soluble drugs.* Eur J Pharm Biopharm, 2013. **85**(3 Pt B): p. 799-813.

326. Singh, A. and G. Van den Mooter, *Spray drying formulation of amorphous solid dispersions.* Adv Drug Deliv Rev, 2016. **100**: p. 27-50.

327. Lee, J.Y., et al., *Soluplus(R)/TPGS-based solid dispersions prepared by hot-melt extrusion equipped with twin-screw systems for enhancing oral bioavailability of valsartan.* Drug Des Devel Ther, 2015. **9**: p. 2745-56.

328. Lian, X., et al., *Soluplus((R)) based 9-nitrocamptothecin solid dispersion for peroral administration: preparation, characterization, in vitro and in vivo evaluation.* Int J Pharm, 2014. **477**(1-2): p. 399-407.

329. Teixeira, C.C., et al., *Microparticles Containing Curcumin Solid Dispersion: Stability, Bioavailability and Anti-Inflammatory Activity.* AAPS PharmSciTech, 2016. **17**(2): p. 252-61.

330. Song, I.S., J.S. Cha, and M.K. Choi, *Characterization, in Vivo and in Vitro Evaluation of Solid Dispersion of Curcumin Containing d-alpha-Tocopheryl Polyethylene Glycol 1000 Succinate and Mannitol.* Molecules, 2016. **21**(10).

331. Li, J., et al., *Curcumin-Eudragit(R) E PO solid dispersion: A simple and potent method to solve the problems of curcumin.* Eur J Pharm Biopharm, 2015. **94**: p. 322-32.

332. Lim, S.M., et al., *Enhancement of docetaxel solubility using binary and ternary solid dispersion systems.* Drug Dev Ind Pharm, 2015. **41**(11): p. 1847-55.

333. Liu, J., et al., *Characterization and Pharmacokinetic Study of Aprepitant Solid Dispersions with Soluplus(R).* Molecules, 2015. **20**(6): p. 11345-56.

334. Wegmann, M., et al., *Novel carvedilol paediatric nanomicelle formulation: in-vitro characterization and in-vivo evaluation.* J Pharm Pharmacol, 2016.

335. Dian, L., et al., *Enhancing oral bioavailability of quercetin using novel soluplus polymeric micelles.* Nanoscale Res Lett, 2014. **9**(1): p. 2406.

336. Valko, M., et al., *Free radicals and antioxidants in normal physiological functions and human disease.* Int J Biochem Cell Biol, 2007. **39**(1): p. 44-84.

337. Lien Ai Pham-Huy, Hua He, and C. Pham-Huy, *Free Radicals, Antioxidants in Disease and Health.* International Journal of Biomedical Science, 2008. **4**(2): p. 89-96.

338. Rahman, K., *Studies on free radicals, antioxidants, and co-factors.* Clin Interv Aging, 2007. **2**(2): p. 219-36.

339. MK Sinha, et al., *Edaravone in acute ischemic stroke, An Indian experience.* Neurology Asia, 2009. **14**: p. 7-10.

340. Hudson, J.S., D.S. Hoyne, and D.M. Hasan, *Inflammation and human cerebral aneurysms: current and future treatment prospects.* Future Neurol, 2013. **8**(6).

341. Borges, R.S., et al., *Density functional theory (DFT) study of edaravone derivatives as antioxidants.* Int J Mol Sci, 2012. **13**(6): p. 7594-606.

342. Parikh, A., et al., *Development of a novel oral delivery system of edaravone for enhancing bioavailability.* Int J Pharm, 2016. **515**(1-2): p. 490-500.

343. Ali Khan, A., et al., *Advanced drug delivery to the lymphatic system: lipid-based nanoformulations.* Int J Nanomedicine, 2013. **8**: p. 2733-44.

344. Sandeep Kalepu, Mohanvarma Manthina, and V. Padavala, *Oral lipid-based drug delivery systems – an overview* Acta Pharmaceutica Sinica B, 2013. **3**(6): p. 361-372.

345. Dokania, S. and A.K. Joshi, *Self-microemulsifying drug delivery system (SMEDDS)--challenges and road ahead.* Drug Deliv, 2015. **22**(6): p. 675-90.

346. Jain, A.K., K. Thanki, and S. Jain, *Solidified self-nanoemulsifying formulation for oral delivery of combinatorial therapeutic regimen: part I. Formulation development, statistical optimization, and in vitro characterization.* Pharm Res, 2014. **31**(4): p. 923-45.

347. Dangre, P., R. Gilhotra, and S. Dhole, *Formulation and statistical optimization of self-microemulsifying drug delivery system of eprosartan mesylate for improvement of oral bioavailability.* Drug Deliv Transl Res, 2016. **6**(5): p. 610-21.

348. Kanaujia, P., W.K. Ng, and R.B. Tan, *Solid self-emulsifying drug delivery system (S-SEDDS) for improved dissolution rate of fenofibrate.* J Microencapsul, 2014. **31**(3): p. 293-8.

349. Monica R.P. Rao , Ghanshyam S. Munjapara, and I.A. Khole, *Preparation and Evaluation of Self-Microemulsifying Drug Delivery System of Carvedilol.* Latin American Journal of Pharmacy, 2011. **30**(5): p. 837-843.

350. Borhade, V., H. Nair, and D. Hegde, *Design and evaluation of self-microemulsifying drug delivery system (SMEDDS) of tacrolimus.* AAPS PharmSciTech, 2008. **9**(1): p. 13-21.

351. Wei, L., et al., *Preparation and evaluation of SEDDS and SMEDDS containing carvedilol.* Drug Dev Ind Pharm, 2005. **31**(8): p. 785-94.

352. Zhang, P., et al., *Preparation and evaluation of self-microemulsifying drug delivery system of oridonin.* Int J Pharm, 2008. **355**(1-2): p. 269-76.

353. Singh, A.K., et al., *Exemestane loaded self-microemulsifying drug delivery system (SMEDDS): development and optimization.* AAPS PharmSciTech, 2008. **9**(2): p. 628-34.

354. Sung-Eun Park, et al., *Preparation of pH-sensitive poly(vinyl alcohol-g-methacrylic acid) and poly(vinyl alcohol-g-acrylic acid) hydrogels by gamma ray irradiation and their insulin release behavior.* Journal of Applied Polymer Science, 2003. **91**: p. 636-643.

355. Pankaj Laddha, V.S., Shital Butani, *Development and optimization of self microemulsifying drug delivery of domperidone.* Brazilian Journal of Pharmaceutical Sciences, 2014. **50**(1): p. 10.

356. Anonymous, *Powder Flow*. 2012, The United States Pharmacopeial Convention: United States. p. 801-804.

357. Cerpnjak, K., et al., *Characterization of naproxen-loaded solid SMEDDSs prepared by spray drying: the effect of the polysaccharide carrier and naproxen concentration.* Int J Pharm, 2015. **485**(1-2): p. 215-28.

358. Kuntsche, J., J.C. Horst, and H. Bunjes, *Cryogenic transmission electron microscopy (cryo-TEM) for studying the morphology of colloidal drug delivery systems.* Int J Pharm, 2011. **417**(1-2): p. 120-37.

359. Kamboj, S. and V. Rana, *Quality-by-design based development of a self-microemulsifying drug delivery system to reduce the effect of food on Nelfinavir mesylate.* Int J Pharm, 2016. **501**(1-2): p. 311-25.

360. Jaiswal, P., et al., *Development of self-microemulsifying drug delivery system and solid-self-microemulsifying drug delivery system of telmisartan.* International Journal of Pharmaceutical Investigation, 2014. **4**(4): p. 195-2016.

361. Costa, P. and J.M. Sousa Lobo, *Modeling and comparison of dissolution profiles.* Eur J Pharm Sci, 2001. **13**(2): p. 123-33.

362. Gupta, S., R. Kesarla, and A. Omri, *Formulation strategies to improve the bioavailability of poorly absorbed drugs with special emphasis on self-emulsifying systems.* ISRN Pharm, 2013. **2013**: p. 848043.

363. Anonymous. *Capryol™ PGMC* 2010 [cited 2016 30 Jan]; Available from: http://www.gattefosse.com/en/applications/capryol-pgmc.html.

364. Verma;, A., M.K. Singh;, and B. Kumar, *Development and Characterization of Flutamide Containing Self-Microemulsifying Drug Delivery System (SMEDDS).* International Journal of Pharmacy and Pharmaceutical Sciences, 2011. **3**: p. 60-65.

365. Christiansen, A., et al., *Effects of non-ionic surfactants on cytochrome P450-mediated metabolism in vitro.* Eur J Pharm Biopharm, 2011. **78**(1): p. 166-72.

366. Collnot, E.M., et al., *Mechanism of inhibition of P-glycoprotein mediated efflux by vitamin E TPGS: influence on ATPase activity and membrane fluidity.* Mol Pharm, 2007. **4**(3): p. 465-74.

367. Prasad, Y.V., et al., *Enhanced intestinal absorption of vancomycin with Labrasol and D-alpha-tocopheryl PEG 1000 succinate in rats.* Int J Pharm, 2003. **250**(1): p. 181-90.

368. Ilem-Ozdemir, D., et al., *Comparative permeability studies with radioactive and nonradioactive risedronate sodium from self-microemulsifying drug delivery system and solution.* Drug Dev Ind Pharm, 2015. **41**(9): p. 1493-8.

369. Ishak, R.A. and R. Osman, *Lecithin/TPGS-based spray-dried self-microemulsifying drug delivery systems: In vitro pulmonary deposition and cytotoxicity.* Int J Pharm, 2015. **485**(1-2): p. 249-60.

370. Raymond C Rowe, Paul J Sheskey, and M.E. Quinn, *Handbook of Pharmaceutical Excipient*. 2009, Pharmaceutical Press and American Pharmacists Association: UK and USA. p. 1-917.

371. Deshmukh, A. and S. Kulkarni, *Solid self-microemulsifying drug delivery system of ritonavir.* Drug Dev Ind Pharm, 2014. **40**(4): p. 477-87.

372. Grove, M., et al., *Bioavailability of seocalcitol II: development and characterisation of self-microemulsifying drug delivery systems (SMEDDS) for oral administration containing medium and long chain triglycerides.* Eur J Pharm Sci, 2006. **28**(3): p. 233-42.

373. Cirri, M., P. Mura, and P.C. Mora, *Liquid spray formulations of xibornol by using self-microemulsifying drug delivery systems.* Int J Pharm, 2007. **340**(1-2): p. 84-91.

374. Mohsin, K., et al., *Development of self-nanoemulsifying drug delivery systems for the enhancement of solubility and oral bioavailability of fenofibrate, a poorly water-soluble drug.* Int J Nanomedicine, 2016. **11**: p. 2829-38.

375. Sallam, M.A. and M.T. Marin Bosca, *Optimization, ex vivo permeation, and stability study of lipid nanocarrier loaded gelatin capsules for treatment of intermittent claudication.* Int J Nanomedicine, 2015. **10**: p. 4459-78.

376. Sheikh Shafiq-un-Nabi, et al., *Formulation Development and Optimization Using Nanoemulsion Technique: A Technical Note.* AAPS PharmSciTech, 2007. **8**(2): p. E1-E6.

377. Krstic, M., et al., *Influence of Solid Drug Delivery System Formulation on Poorly Water-Soluble Drug Dissolution and Permeability.* Molecules, 2015. **20**(8): p. 14684-98.

378. Centers for Disease, C. and Prevention, *Trends in aging--United States and worldwide.* MMWR Morb Mortal Wkly Rep, 2003. **52**(6): p. 101-4, 106.

379. McGeer, P.L. and E.G. McGeer, *The amyloid cascade-inflammatory hypothesis of Alzheimer disease: implications for therapy.* Acta Neuropathol, 2013. **126**(4): p. 479-97.

380. Bu, X.L., et al., *Perspectives on the Tertiary Prevention Strategy for Alzheimer's Disease.* Curr Alzheimer Res, 2016. **13**(3): p. 307-16.

381. Watanabe, T. and M. Egawa, *Effects of an antistroke agent MCl-186 on cerebral arachidonate cascade.* J Pharmacol Exp Ther, 1994. **271**(3): p. 1624-9.

382. Ikeda, T., et al., *Effect of the free radical scavenger, 3-methyl-1-phenyl-2-pyrazolin-5-one (MCI-186), on hypoxia-ischemia-induced brain injury in neonatal rats.* Neurosci Lett, 2002. **329**(1): p. 33-6.

383. Aleksovski, A., et al., *Mini-tablets: a contemporary system for oral drug delivery in targeted patient groups.* Expert Opin Drug Deliv, 2015. **12**(1): p. 65-84.

384. Ringman, J.M., et al., *Oral curcumin for Alzheimer's disease: tolerability and efficacy in a 24-week randomized, double blind, placebo-controlled study.* Alzheimers Res Ther, 2012. **4**(5): p. 43.

385. Mecocci, P. and M.C. Polidori, *Antioxidant clinical trials in mild cognitive impairment and Alzheimer's disease.* Biochim Biophys Acta, 2012. **1822**(5): p. 631-8.

386. Sinha, S., et al., *Solid dispersion as an approach for bioavailability enhancement of poorly water-soluble drug ritonavir.* AAPS PharmSciTech, 2010. **11**(2): p. 518-27.

387. West, M.J., *Regionally specific loss of neurons in the aging human hippocampus.* Neurobiol Aging, 1993. **14**(4): p. 287-93.

388. Gary W. Arendash, et al., *Progressive, age-related behavioral impairments in transgenic mice carrying both mutant amyloid precursor protein and presenilin-1 transgenes.* Brain Research, 2001. **891**: p. 42-53.

389. Yao, X.Q., et al., *p75NTR ectodomain is a physiological neuroprotective molecule against amyloid-beta toxicity in the brain of Alzheimer's disease.* Mol Psychiatry, 2015. **20**(11): p. 1301-10.

390. Kyaw Oo, M., U.K. Mandal, and B. Chatterjee, *Polymeric behavior evaluation of PVP K30-poloxamer binary carrier for solid dispersed nisoldipine by experimental design.* Pharm Dev Technol, 2015: p. 1-11.
391. Wang, W., et al., *Development of intramammary delivery systems containing lasalocid for the treatment of bovine mastitis: impact of solubility improvement on safety, efficacy, and milk distribution in dairy cattle.* Drug Des Devel Ther, 2015. **9**: p. 631-42.
392. Leonardi, D. and C.J. Salomon, *Unexpected performance of physical mixtures over solid dispersions on the dissolution behavior of benznidazole from tablets.* J Pharm Sci, 2013. **102**(3): p. 1016-23.
393. Bala, V., et al., *Lipophilic Prodrugs of SN38: Synthesis and in Vitro Characterization toward Oral Chemotherapy.* Mol Pharm, 2016. **13**(1): p. 287-94.
394. Yu, H., et al., *Supersaturated polymeric micelles for oral cyclosporine A delivery.* Eur J Pharm Biopharm, 2013. **85**(3 Pt B): p. 1325-36.
395. Ruan, C.S., et al., *Mice with Sort1 deficiency display normal cognition but elevated anxiety-like behavior.* Exp Neurol, 2016. **281**: p. 99-108.
396. Zhang, Q., et al., *Impaired Dendritic Development and Memory in Sorbs2 Knock-Out Mice.* J Neurosci, 2016. **36**(7): p. 2247-60.
397. Bakoma, B., et al., *Acute and sub-chronic (28days) oral toxicity evaluation of hydroethanolic extract of Bridelia ferruginea Benth root bark in male rodent animals.* Food Chem Toxicol, 2013. **52**: p. 176-9.
398. Zhang, Q., et al., *Acute and sub-chronic toxicity studies of honokiol microemulsion.* Regul Toxicol Pharmacol, 2014. **71**(3): p. 428-436.
399. Wang, L., et al., *Acute and sub-chronic oral toxicity profiles of the aqueous extract of Cortex Dictamni in mice and rats.* J Ethnopharmacol, 2014. **158 Pt A**: p. 207-15.
400. Bahl, D. and R.H. Bogner, *Amorphization of Indomethacin by Co-Grinding with Neusilin US2: amorphization kinetics, physical stability and mechanism.* Pharm Res, 2006. **23**(10): p. 2317-25.
401. Shi, N.Q., et al., *On the inherent properties of Soluplus and its application in ibuprofen solid dispersions generated by microwave-quench cooling technology.* Pharm Dev Technol, 2016: p. 1-14.
402. Fule, R.A., et al., *Artemether-Soluplus Hot-Melt Extrudate Solid Dispersion Systems for Solubility and Dissolution Rate Enhancement with Amorphous State Characteristics.* J Pharm (Cairo), 2013. **2013**: p. 151432.

403. Yuan, X., et al., *Hydrogen Bonding Interactions in Amorphous Indomethacin and Its Amorphous Solid Dispersions with Poly(vinylpyrrolidone) and Poly(vinylpyrrolidone-co-vinyl acetate) Studied Using (13)C Solid-State NMR.* Mol Pharm, 2015. **12**(12): p. 4518-28.

404. Jin, X., et al., *Soluplus((R)) micelles as a potential drug delivery system for reversal of resistant tumor.* Biomed Pharmacother, 2015. **69**: p. 388-95.

405. Alvarez-Rivera, F., et al., *alpha-Lipoic Acid in Soluplus((R)) Polymeric Nanomicelles for Ocular Treatment of Diabetes-Associated Corneal Diseases.* J Pharm Sci, 2016. **105**(9): p. 2855-63.

406. Lu, Y. and K. Park, *Polymeric micelles and alternative nanonized delivery vehicles for poorly soluble drugs.* Int J Pharm, 2013. **453**(1): p. 198-214.

407. Ashe, K.H., *Learning and memory in transgenic mice modeling Alzheimer's disease.* Learn Mem, 2001. **8**(6): p. 301-8.

408. Perez, S.E., et al., *DHA diet reduces AD pathology in young APPswe/PS1 Delta E9 transgenic mice: possible gender effects.* J Neurosci Res, 2010. **88**(5): p. 1026-40.

409. Zhou, Y., et al., *Puerarin alleviates cognitive impairment and oxidative stress in APP/PS1 transgenic mice.* Int J Neuropsychopharmacol, 2014. **17**(4): p. 635-44.

410. Guo, H.B., et al., *Donepezil improves learning and memory deficits in APP/PS1 mice by inhibition of microglial activation.* Neuroscience, 2015. **290**: p. 530-42.

411. Antunes, M. and G. Biala, *The novel object recognition memory: neurobiology, test procedure, and its modifications.* Cogn Process, 2012. **13**(2): p. 93-110.

412. Cheng, D., et al., *Chronic cannabidiol treatment improves social and object recognition in double transgenic APPswe/PS1E9 mice.* Psychopharmacology (Berl), 2014. **231**(15): p. 3009-17.

413. Kim, H.Y., et al., *Rapid and sustained cognitive recovery in APP/PS1 transgenic mice by co-administration of EPPS and donepezil.* Sci Rep, 2016. **6**: p. 34165.

414. Tabrizchi, R., *Edaravone Mitsubishi-Tokyo.* Current Opinion in Investigational Drugs, 2000. **1**(3): p. 347-354.

415. Goel, A., A.B. Kunnumakkara, and B.B. Aggarwal, *Curcumin as "Curecumin": from kitchen to clinic.* Biochem Pharmacol, 2008. **75**(4): p. 787-809.

416. Ravindran, J., S. Prasad, and B.B. Aggarwal, *Curcumin and cancer cells: how many ways can curry kill tumor cells selectively?* AAPS J, 2009. **11**(3): p. 495-510.

417. Ramassamy, C., *Emerging role of polyphenolic compounds in the treatment of neurodegenerative diseases: a review of their intracellular targets.* Eur J Pharmacol, 2006. **545**(1): p. 51-64.
418. Thangapazham, R.L., A. Sharma, and R.K. Maheshwari, *Multiple molecular targets in cancer chemoprevention by curcumin.* AAPS J, 2006. **8**(3): p. E443-9.
419. Mangialasche, F., et al., *Alzheimer's disease: clinical trials and drug development.* Lancet Neurol, 2010. **9**(7): p. 702-16.
420. Schneider, L.S., et al., *Clinical trials and late-stage drug development for Alzheimer's disease: an appraisal from 1984 to 2014.* J Intern Med, 2014. **275**(3): p. 251-83.
421. Song, Z., et al., *Curcumin-loaded PLGA-PEG-PLGA triblock copolymeric micelles: Preparation, pharmacokinetics and distribution in vivo.* J Colloid Interface Sci, 2011. **354**(1): p. 116-23.
422. Tomren, M.A., et al., *Studies on curcumin and curcuminoids XXXI. Symmetric and asymmetric curcuminoids: stability, activity and complexation with cyclodextrin.* Int J Pharm, 2007. **338**(1-2): p. 27-34.
423. Buckholtz, N.S., et al., *NIA commentary: translational issues in Alzheimer's disease drug development.* Neuropsychopharmacology, 2012. **37**(1): p. 284-6.
424. LaFerla, F.M. and K.N. Green, *Animal models of Alzheimer disease.* Cold Spring Harb Perspect Med, 2012. **2**(11).
425. Saraceno, C., et al., *Modeling Alzheimer's disease: from past to future.* Front Pharmacol, 2013. **4**: p. 77.
426. Russo, P., et al., *New Drugs from Marine Organisms in Alzheimer's Disease.* Mar Drugs, 2015. **14**(1): p. 5.
427. Homayouni, A., et al., *Preparation and characterization of celecoxib dispersions in soluplus((R)): comparison of spray drying and conventional methods.* Iran J Pharm Res, 2015. **14**(1): p. 35-50.
428. Mohanty, C. and S.K. Sahoo, *The in vitro stability and in vivo pharmacokinetics of curcumin prepared as an aqueous nanoparticulate formulation.* Biomaterials, 2010. **31**(25): p. 6597-611.
429. Christakis, D.A., J.S. Ramirez, and J.M. Ramirez, *Overstimulation of newborn mice leads to behavioral differences and deficits in cognitive performance.* Sci Rep, 2012. **2**: p. 546.

430. Arjo, G., et al., *Mice fed on a diet enriched with genetically engineered multivitamin corn show no sub-acute toxic effects and no sub-chronic toxicity.* Plant Biotechnol J, 2012. **10**(9): p. 1026-34.
431. Thakral, N.K., et al., *Soluplus--solubilized citrated camptothecin--a potential drug delivery strategy in colon cancer.* AAPS PharmSciTech, 2012. **13**(1): p. 59-66.
432. Wen, H., K.R. Morris, and K. Park, *Study on the interactions between polyvinylpyrrolidone (PVP) and acetaminophen crystals: partial dissolution pattern change.* J Pharm Sci, 2005. **94**(10): p. 2166-74.
433. Ritesh Fule and P. Amin, *Development and evaluation of lafutidine solid dispersion via hot melt extrusion: Investigating drug-polymer miscibility with advanced characterisation* Asian Journal of Pharmaceutical Sciences, 2014. **9**(2): p. 92–106.
434. Kothari, K., V. Ragoonanan, and R. Suryanarayanan, *The role of drug-polymer hydrogen bonding interactions on the molecular mobility and physical stability of nifedipine solid dispersions.* Mol Pharm, 2015. **12**(1): p. 162-70.
435. Gupta, N.K. and V.K. Dixit, *Bioavailability enhancement of curcumin by complexation with phosphatidyl choline.* J Pharm Sci, 2011. **100**(5): p. 1987-95.
436. Gary W. Arendash, et al., *Progressive, age-related behavioral impairments in transgenic mice carrying both mutant amyloid precursor protein and presenilin-1 transgenes.* Brain Research, 2001. **891**: p. 42-53.
437. Francis, P.T., A. Nordberg, and S.E. Arnold, *A preclinical view of cholinesterase inhibitors in neuroprotection: do they provide more than symptomatic benefits in Alzheimer's disease?* Trends Pharmacol Sci, 2005. **26**(2): p. 104-11.
438. Hebert-Chatelain, E., et al., *A cannabinoid link between mitochondria and memory.* Nature, 2016. **539**(7630): p. 555-559.
439. Wolf, A., et al., *A Comprehensive Behavioral Test Battery to Assess Learning and Memory in 129S6/Tg2576 Mice.* PLoS One, 2016. **11**(1): p. e0147733.
440. Vorhees, C.V. and M.T. Williams, *Morris water maze: procedures for assessing spatial and related forms of learning and memory.* Nat Protoc, 2006. **1**(2): p. 848-58.
441. Wang, P., et al., *Mechanisms and effects of curcumin on spatial learning and memory improvement in APPswe/PS1dE9 mice.* J Neurosci Res, 2014. **92**(2): p. 218-31.
442. Tiwari, S.K., et al., *Curcumin-loaded nanoparticles potently induce adult neurogenesis and reverse cognitive deficits in Alzheimer's disease model via canonical Wnt/beta-catenin pathway.* ACS Nano, 2014. **8**(1): p. 76-103.

443. Kim, D.C., S.K. Ku, and J.S. Bae, *Anticoagulant activities of curcumin and its derivative.* BMB Rep, 2012. **45**(4): p. 221-6.

444. Hansen, C.M., *Hansen Solubility Parameters: A User's Handbook*. 2007, CRC Press: Boca Raton, Florida. p. 1-546.

445. Wang, Y.J., et al., *Intramuscular delivery of a single chain antibody gene prevents brain Abeta deposition and cognitive impairment in a mouse model of Alzheimer's disease.* Brain, behavior, and immunity, 2010. **24**(8): p. 1281-93.

446. Wang, Y.J., et al., *Intramuscular delivery of a single chain antibody gene reduces brain Abeta burden in a mouse model of Alzheimer's disease.* Neurobiol Aging, 2009. **30**(3): p. 364-76.

447. Wang, Y.J., et al., *p75NTR regulates Abeta deposition by increasing Abeta production but inhibiting Abeta aggregation with its extracellular domain.* J Neurosci. **31**(6): p. 2292-304.

448. Thomas, P., et al., *Grape seed polyphenols and curcumin reduce genomic instability events in a transgenic mouse model for Alzheimer's disease.* Mutation research, 2009. **661**(1-2): p. 25-34.